Effects of land management and climate change on soil microbial communities in Appalachian forest ecosystems

Ernest Daniel Osburn

Dissertation submitted to the faculty of the Virginia Polytechnic Institute and State University in partial fulfillment of the requirements for the degree of

Doctor of Philosophy
In
Biological Sciences

John E. Barrett
Frank O Aylward
Brian D Strahm
Brian D Badgley

March 12, 2021
Blacksburg, VA

Keywords: soil, forest, microbial community, bacteria, fungi, carbon, nitrogen, ecosystem

Effects of land management and climate change on soil microbial communities in Appalachian forest ecosystems

Ernest Daniel Osburn

ABSTRACT

In terrestrial ecosystems, microorganisms are the dominant drivers of virtually all ecosystem processes, particularly cycling of carbon (C), nitrogen (N), and phosphorus (P). These microbial functions are critical for promoting ecosystem services that support human well-being, such as provisioning of clean drinking water, nitrogen retention, and carbon storage. In forests of the Appalachian region of the eastern US, these ecosystem services are threatened by multiple anthropogenic influences, including present and past land use activities (e.g., logging, conversion to agriculture) and climate change (e.g., intensifying droughts). However, despite the central importance of microbial communities in promoting ecosystem functions, impacts of land management and climate change on soil microorganisms remain poorly understood in the region. This dissertation seeks to address the following questions: 1) How does a new forest management practice, *Rhododendron* understory removal, influence the ecosystem functions of soil microbial communities? 2) Do historical land management activities have long-term legacy effects on the structure and ecosystem functions of soil microbial communities? And 3) Does historical land use influence responses of soil microbial communities to intensifying drought? In chapter 2, I show that experimental *Rhododendron* understory removal increased soil C and N availability, thereby promoting increased total microbial biomass. This increased microbial biomass resulted in elevated production of microbial extracellular enzymes, which increased rates of C and N cycling in soils following *Rhododendron* removal. In chapter 3, I examined soils across several historically

disturbed and adjacent undisturbed reference forests and show that historical management activities, e.g., logging, conversion to agriculture, have long-term effects on soil microbial communities 4-8 decades after management activities occurred. These effects included increased bacterial diversity, increased relative abundance of r-selected bacterial taxa, and increased abundance of arbuscular mycorrhizal fungi. In chapter 4, I show that key soil biogeochemical processes, i.e., C mineralization, N mineralization, and nitrification, exhibit generally higher rates in historically disturbed forests relative to adjacent reference forests. Further, I attributed these changes in ecosystem process rates to changes in key aspects of microbial communities, including microbial biomass, extracellular enzyme activities, and bacterial r- vs K-selection. In chapter 5, I conducted a drought-rewetting experiment and show wide-ranging effects of experimental drought on soil microbial communities, including altered diversity, community composition, and shifts in the relative abundances of several specific taxa. Further, drought responses were particularly evident in soils from historically disturbed forests, indicating influences of land management on responses of soil communities to climate change. Finally, in chapter 6, I show that the experimental drought also influenced several ecosystem-scale properties of soils, including increased soil N pools and increased respiratory C loss. Overall, my dissertation reveals wide-ranging effects of anthropogenic activities on soil microorganisms and shows that microbial communities will influence forest responses to global change at the ecosystem scale.

Effects of land management and climate change on soil microbial communities in Appalachian forest ecosystems

Ernest Daniel Osburn

GENERAL AUDIENCE ABSTRACT

Forest ecosystems of the southern Appalachian region provide numerous services that support human well-being, including provisioning of clean drinking water and the retention of nutrients and carbon (C). These ecosystem services are dependent on several processes that occur in soil, including the C and nitrogen (N) cycles. These cycles, in turn, are carried out primarily by microorganisms (bacteria and fungi) that live in soil. The ecosystem services provided by these forests are being threatened in the Appalachian region by a variety of land use activities such as logging and conversion of forests to agriculture and are also being threatened by climate change. However, despite the critical role of microorganisms in supporting ecosystem services, effects of land use activities and climate change on soil microorganisms are largely unknown in the Appalachian region. The goal of this dissertation is to answer the following questions: 1) How does *Rhododendron* understory removal, a new land management practice, influence soil microbial communities? 2) What are the long-term effects of historical land use activities, such as logging and conversion to agriculture, on soil microbial communities? And 3) In what ways will intensifying droughts influence soil microorganisms in Appalachian forests? I used a variety of approaches to answer these questions, including experiments and observational approaches. In chapter 2, I show that experimental *Rhododendron* understory removal increased the overall size of microbial communities (i.e., more microbial biomass) due to greater availability of soil resources (i.e., C and N). These larger microbial communities produced more enzymes involved in C and N metabolism,

thereby increasing rates of C and N cycling in soils. In chapter 3, I surveyed soils from several forests that were disturbed by humans ~40-80 years previously (i.e., logged, converted to agriculture) and showed that these historical human activities have many long-term effects on soil bacteria and fungi. Specifically, in historically disturbed soils, I observed higher diversity of bacteria, higher abundance of rapidly growing (i.e., r-selected) bacteria and higher abundance of some groups of fungi that associate with plant roots and aid in acquiring nutrients for plants (i.e., mycorrhizal fungi). In chapter 4, I show that these historically disturbed soils also had altered rates of C and N cycling and that these altered cycling rates were associated with changes in several properties of microbial communities, including microbial enzymes, microbial biomass, and growth rates of bacteria (i.e., r-selection). In chapter 5, I conducted an experimental drought in these soils and show that drought has wide-ranging effects on many aspects of microbial communities, including effects on diversity, species composition, and abundances of many specific microbial taxonomic groups. Further, responses of microbial communities were larger in soils from historically disturbed forests, showing that past management will influence microbial responses to future climate change. In chapter 6, I show that many aspects of the soil ecosystems as a whole were also impacted by the experimental drought. In particular, soils exposed to drought released more CO_2 over the course of the experiment and had higher N concentrations than control soils. Overall, my dissertation identifies many influences of land management and climate change on soil microbial communities and shows that these microorganisms will influence forest responses to global change at the ecosystem scale.

DEDICATION

This dissertation is dedicated to my dog, Charlie, who endured considerable boredom waiting for me to finish writing this thing.

ACKNOWLEDGEMENTS

First, I would like to acknowledge my committee, chaired by Jeb Barrett and including Frank Aylward, Brian Strahm, and Brian Badgley. Each of my committee members was supportive of me throughout my graduate studies and each made significant and unique contributions to the work described herein. I also thank my collaborators at the USDA Forest Service Coweeta Hydrologic Lab, Jennifer Knoepp, Chelcy Miniat and Kitty Elliot, who also provided support and advice throughout my dissertation research. I also express my gratitude to my fellow graduate students within the IGC program, the Biological Sciences Department, and the VT Stream Team for their support, friendship, and contributions to my work. I also thank Bobbie Niederlehner, who displayed remarkable patience in training me how to use analytical instruments. I also want to thank the many undergraduate students who worked with me and contributed to my studies, including Fahd Mohammed, Cameron Hughes, Angela, Weisel, and Julia Simpson. Special thank goes to my dog, Charlie, who hopes to go on more walks now that my dissertation is finally complete. Finally, I want to thank my family, who have supported me though my decision to change careers and pursue yet another degree.

Table of Contents

CHAPTER 1 - INTRODUCTION

From Microbes to Ecosystems

Ecosystems provide essential services that support human well-being, including provisioning of food and clean drinking water and storage of carbon (C) (Millenium Ecosystem Assessment 2005). Underlying these ecosystem services are key ecosystem processes such as primary productivity, organic matter decomposition, and nutrient transformations, all of which, in turn, are facilitated by biota present in the ecosystem. The clear importance of biota to ecosystem functioning has led to multiple decades of ecological research investigating relationships between biological communities and the processes they facilitate (Duffy 2009, Tilman et al. 2014). These relationships are often investigated within a 'biodiversity-ecosystem function' (BEF) framework, as species extinctions have led to concerns that ecosystem services may be diminished in a more species-poor world (Cardinale et al. 2012). After three decades of investigation, BEF research now spans hundreds of published studies, finding significant BEF relationships across multiple trophic levels in both terrestrial and aquatic ecosystems (Hooper et al. 2005, Cardinale et al. 2012, Tilman et al. 2014), including positive effects of plant diversity on ecosystem productivity (Tilman et al. 2001), fish diversity on carbon cycling rates (Taylor et al. 2006), and predator diversity on plant biomass (Otto et al. 2008).

Though most published BEF studies involve macroorganisms (i.e., plants and animals), nearly all ecosystem processes are facilitated by or are conducted exclusively by microorganisms (Hall et al. 2018). For example, microorganisms (i.e., bacteria, archaea, and fungi) are the primary decomposers of organic matter (Fierer 2017), and all biochemical steps of the N cycle are carried out exclusively by microorganisms (Canfield

et al. 2010). However, despite the critical role of microorganisms in promoting ecosystem functions, relationships between microorganisms at the community scale and processes at the ecosystem scale remain poorly characterized. Indeed, identification of microbial community-ecosystem function relationships has proven to be exceptionally challenging, in part because microbial diversity is orders of magnitude higher than it is for large organisms (e.g., plants), especially in soil (Torsvik et al. 2002). Further, the presence and/or strength of microbial community-ecosystem function relationships likely varies among ecosystem processes depending on the phylogenetic breadth of microorganisms capable of facilitating specific processes (Schimel 1995, Nannipieri et al. 2003, Bardgett and van der Putten 2014). These complexities and challenges in identifying community-ecosystem relationships for microbial-mediated processes are reflected by the rarity of published microbial BEF studies - to my knowledge, BEF relationships have only been rigorously tested for two functions: denitrification (Philippot et al. 2013) and ecosystem multifunctionality (Delgado-Baquerizo et al. 2020).

This notable dearth of identified microbial community-ecosystem function relationships contrasts with the abundance of literature that has emerged in recent decades utilizing -omics technologies (e.g., amplicon sequencing, metagenomics) to provide detailed descriptions of microbial community structure and function. Often, these studies are justified under the premise that microbial -omics information will improve understanding of the ecosystem-scale processes that microorganisms facilitate (Hall et al. 2018). However, in practice, relationships between microbial communities and ecosystem functioning are rarely directly tested, and even when tested are often not found (Rocca et al. 2015, Bier et al. 2015, Graham et al. 2016), leading to uncertainty regarding the

importance of microbial community information in improving understanding of ecosystem-scale processes.

Identification of microbial community-ecosystem function relationships is further complicated by the fact that microbial communities are continually altered by global change drivers such as land use change and climate change (Fierer 2017). Indeed, land use change has modified ~75% of earth's land surface (Ellis 2011) and these land uses (e.g., logging, conversion to agriculture) have well-established impacts on soil microbial communities (e.g., Jangid et al. 2011, Zhou et al. 2018). Climate change drivers influencing microorganisms include drought, increased temperature, and increased CO_2 concentrations, all of which can alter microbial communities (Rillig et al. 2019, Jansson and Hofmockel 2020). In particular, drought represents a significant physiological stressor for microbial taxa and has altered the structure and functioning of soil microbial communities in many ecosystems (Schimel 2018, Jansson and Hofmockel 2020). However, despite the clear potential for soil microorganisms to respond to global change drivers, relationships among anthropogenic influences, microbial communities, and ecosystem functioning remain poorly understood.

Environmental Context: Forests of Appalachia

This dissertation investigates relationships among land use, vegetation history, climate change, microbial communities, and ecosystem functions within the context of southern Appalachian forests of the eastern US. Southern Appalachia, typically defined as the region between north Georgia's Blue Ridge Mountains and the New River Divide in southwestern Virginia (Gragson and Bolstad 2006), is an ecoregion of astounding biodiversity. Indeed, southern Appalachia hosts North America's highest diversity of

amphibians, birds, crayfish, mollusks, fish, fungi, and trees (Sheldon 1988, Neves et al. 1997, Kozak and Wiens 2010, Jetz et al. 2012). This extraordinary biodiversity is due in part to the high productivity of these ecosystems (Belote et al. 2011) and also due to geologic age – the Appalachian mountains date back to the Caledonian Orogeny more than 480 million years ago, making the Appalachians the oldest mountains in the world (Williams 1995). The majority of land cover in the region is forested (~70%) (Simon et al. 2005) and the tens of thousands of headwater streams that drain the forested watersheds of the region ultimately supply larger water bodies upon which the large populations centers of the eastern US are reliant. Indeed, southern Appalachia has been referred to as "the water tower of the South." (Webster et al. 2012). However, this and other ecosystem services of southern Appalachia are increasingly threatened by accelerating anthropogenic impacts due to climate change and past and present land use change in the region (Gragson and Bolstad 2006).

Human impacts on southern Appalachian ecosystems trace back more than a millennium to the Mississippian culture, which arrived in the region around 900 AD (Davis 2011). The Mississippians, as well as the Cherokees that replaced them centuries later, exerted influence on the Appalachian environment by clearing forests in valley-bottom areas for cultivation of maize and other North American crops (Davis 2011). Expansion of European settlements in the region in the 18th Century intensified environmental impacts in southern Appalachia, including clearing of high elevation areas for livestock grazing, introductions of Old World crops (e.g., barley, wheat, apples) and wild plants and animals (e.g., clover, privet, dandelion, honeybees), and the beginnings of extractive industries in the region, including timber harvesting, and mining of gold, salt,

copper, and coal (Davis 2011). Human impacts further accelerated in the decades of the late 19th and early 20th Centuries, which were characterized by widespread industrial logging of Appalachian forests, with environmental impacts such as stream sedimentation, soil erosion, and flooding (Davis 2011). This industrialization of southern Appalachia was also accompanied by the eventual widespread abandonment of subsistence agriculture in the region (Davis 2011). An additional notable human impact during this time period was the introduction of the fungal pathogen Chestnut blight (*Cryphonectria parasitica*) from Asia, which drove once-dominant Chestnut trees to functional extinction (Davis 2011).

Overall, southern Appalachia is a region with a long history of anthropogenic impacts and ecosystems in the region are still recovering from relatively recent 20th Century impacts of invasive species (i.e., chestnut blight), industrial logging, and agricultural abandonment. These historical impacts are compounded by a more recent 'exurbanization' phenomenon in southern Appalachia, which is characterized by accelerating residential development as people from urban centers in-migrate to take advantage of rural natural amenities in the region (Gragson and Bolstad 2006). An additional recent impact is the appearance of invasive hemlock wooly adelgid beetles (*Adelges tsugae*), resulting in widespread declines in eastern hemlock (*Tsuga canadensis*) in forests of the region (Ford et al. 2012). Hemlock declines, in turn, have promoted expansion of *Rhododendron maximum*, an understory shrub that reduces soil nutrient availability and inhibits forest tree recruitment (Ford et al. 2012). Further, in addition to past and present land use change, southern Appalachian ecosystems are experiencing impacts from climate change, which has increased the frequency and duration of droughts

in the region (Laseter et al. 2012, Burt et al. 2018). Some of these anthropogenic influences have well described impacts on Appalachian ecosystems – for example, forest disturbance (e.g., logging, conversion to agriculture) results in increased soil nitrification rates and increased watershed-scale N export over long time scales in the region (Swank and Vose 1997, Keiser et al. 2016, Norman and Barrett 2016, Webster et al. 2016). However, impacts of anthropogenic disturbance and climate change are largely unknown for the smallest but arguably most important residents of southern Appalachian forests: soil microorganisms.

Dissertation Goals

This dissertation aims to elucidate relationships among land use change, climate change, soil microbial communities, and ecosystem functioning in southern Appalachian forests by answering the following questions: 1) How does *Rhododendron maximum* removal, a new forest management practice, influence the ecosystem functions of soil microbial communities in riparian forests of southern Appalachia? 2) Does historical disturbance (e.g., logging, conversion to agriculture) have long-term legacy effects on the structure and ecosystem functions of soil microbial communities? And 3) Does historical land use influence the responses of soil microbial communities to drought? I predict that *R. maximum* removal will increase availability of soil C and N, which will stimulate microbial activity and increase rates of biogeochemical cycling in soils. I further predict that soils from historically disturbed forests will exhibit long-term changes in microbial communities that are consistent with ecosystem-scale observations (i.e., increased N-cycling rates), including increased abundance of nitrifying bacteria. Finally, I predict that compositional differences in soil microbial communities as a result of past forest

disturbance will result in distinct microbial drought responses among differing historical land management regimes. Overall, this work provides key insights into anthropogenic influences on soil microorganisms and associated ecosystem functions, thereby representing significant contributions to both ecology in general and Appalachian forest management specifically.

References

Bardgett, R. D., and W. H. van der Putten. 2014. Belowground biodiversity and ecosystem functioning. Nature 515:505–511.

Belote, R. T., S. Prisley, R. H. Jones, M. Fitzpatrick, and K. de Beurs. 2011. Forest productivity and tree diversity relationships depend on ecological context within mid-Atlantic and Appalachian forests (USA). Forest Ecology and Management 261:1315–1324.

Bier, R. L., E. S. Bernhardt, C. M. Boot, E. B. Graham, E. K. Hall, et al. 2015. Linking microbial community structure and microbial processes: an empirical and conceptual overview. FEMS Microbiology Ecology 91.

Burt, T. P., C. Ford Miniat, S. H. Laseter, and W. T. Swank. 2018. Changing patterns of daily precipitation totals at the Coweeta Hydrologic Laboratory, North Carolina, USA. International Journal of Climatology 38:94–104.

Canfield, D. E., A. N. Glazer, and P. G. Falkowski. 2010. The Evolution and Future of Earth's Nitrogen Cycle. Science 330:192–196.

Cardinale, B. J., J. E. Duffy, A. Gonzalez, D. U. Hooper, C. Perrings, et al. 2012. Biodiversity loss and its impact on humanity. Nature 486:59–67.

Davis, D. E. 2011. Where There Are Mountains: An Environmental History of the Southern Appalachians. University of Georgia Press.

Delgado-Baquerizo, M., P. B. Reich, C. Trivedi, D. J. Eldridge, S. Abades, et al. 2020. Multiple elements of soil biodiversity drive ecosystem functions across biomes. Nature Ecology & Evolution 4:210–220.

Duffy, J. E. 2009. Why biodiversity is important to the functioning of real-world ecosystems. Frontiers in Ecology and the Environment 7:437–444.

Ellis, E. C. 2011. Anthropogenic transformation of the terrestrial biosphere. Philosophical Transactions of the Royal Society a-Mathematical Physical and Engineering Sciences 369:1010–1035.

Fierer, N. 2017. Embracing the unknown: disentangling the complexities of the soil microbiome. Nature Reviews Microbiology 15:579–590.

Ford, C. R., K. J. Elliott, B. D. Clinton, B. D. Kloeppel, and J. M. Vose. 2012. Forest dynamics following eastern hemlock mortality in the southern Appalachians. Oikos 121:523–536.

Gragson, T. L., and P. V. Bolstad. 2006. Land Use Legacies and the Future of Southern Appalachia. Society & Natural Resources 19:175–190.

Graham, E. B., J. E. Knelman, A. Schindlbacher, S. Siciliano, M. Breulmann, et al. 2016. Microbes as Engines of Ecosystem Function: When Does Community Structure Enhance Predictions of Ecosystem Processes? Frontiers in Microbiology 7.
Hall, E. K., E. S. Bernhardt, R. L. Bier, M. A. Bradford, C. M. Boot, et al. 2018. Understanding how microbiomes influence the systems they inhabit. Nature Microbiology 3:977–982.
Hooper, D. U., F. S. Chapin, J. J. Ewel, A. Hector, P. Inchausti, et al. 2005. Effects of Biodiversity on Ecosystem Functioning: A Consensus of Current Knowledge. Ecological Monographs 75:3–35.
Jangid, K., M. A. Williams, A. J. Franzluebbers, T. M. Schmidt, D. C. Coleman, et al. 2011. Land-use history has a stronger impact on soil microbial community composition than aboveground vegetation and soil properties. Soil Biology and Biochemistry 43:2184–2193.
Jansson, J. K., and K. S. Hofmockel. 2020. Soil microbiomes and climate change. Nature Reviews Microbiology 18:35–46.
Jetz, W., G. H. Thomas, J. B. Joy, K. Hartmann, and A. O. Mooers. 2012. The global diversity of birds in space and time. Nature 491:444–448.
Keiser, A. D., J. D. Knoepp, and M. A. Bradford. 2016. Disturbance Decouples Biogeochemical Cycles Across Forests of the Southeastern US. Ecosystems 19:50–61.
Kozak, K. H., and J. J. Wiens. 2010. Niche Conservatism Drives Elevational Diversity Patterns in Appalachian Salamanders. The American Naturalist 176:40–54.
Laseter, S. H., C. R. Ford, J. M. Vose, and L. W. Swift. 2012. Long-term temperature and precipitation trends at the Coweeta Hydrologic Laboratory, Otto, North Carolina, USA. Hydrology Research 43:890–901.
Millenium Ecosystem Assessment. 2005. Ecosystems and Human Well Being: Synthesis. Island Press, Washington, DC.
Nannipieri, P., J. Ascher, M. T. Ceccherini, L. Landi, G. Pietramellara, et al. 2003. Microbial diversity and soil functions. European Journal of Soil Science 54:655–670.
Neves, R. J., A. E. Bogan, J. D. Williams, S. A. Ahlstedt, and P. D. Hartfield. 1997. Status of aquatic mollusks in the southeastern United States: a downward spiral of diversity.
Norman, J. S., and J. E. Barrett. 2016. Substrate availability drives spatial patterns in richness of ammonia-oxidizing bacteria and archaea in temperate forest soils. Soil Biology & Biochemistry 94:169–172.
Otto, S. B., E. L. Berlow, N. E. Rank, J. Smiley, and U. Brose. 2008. Predator Diversity and Identity Drive Interaction Strength and Trophic Cascades in a Food Web. Ecology 89:134–144.
Philippot, L., A. Spor, C. Hénault, D. Bru, F. Bizouard, et al. 2013. Loss in microbial diversity affects nitrogen cycling in soil. The ISME Journal 7:1609–1619.
Rillig, M. C., M. Ryo, A. Lehmann, C. A. Aguilar-Trigueros, S. Buchert, et al. 2019. The role of multiple global change factors in driving soil functions and microbial biodiversity. Science 366:886–890.
Rocca, J. D., E. K. Hall, J. T. Lennon, S. E. Evans, M. P. Waldrop, et al. 2015. Relationships between protein-encoding gene abundance and corresponding

process are commonly assumed yet rarely observed. The ISME Journal 9:1693–1699.
Schimel, J. 1995. Ecosystem Consequences of Microbial Diversity and Community Structure. Pages 239–254 *in* F. S. Chapin and C. Körner, editors. Arctic and Alpine Biodiversity: Patterns, Causes and Ecosystem Consequences. Springer Berlin Heidelberg, Berlin, Heidelberg.
Schimel, J. P. 2018. Life in Dry Soils: Effects of Drought on Soil Microbial Communities and Processes. Annual Review of Ecology, Evolution, and Systematics 49:409–432.
Sheldon, A. L. 1988. Conservation of Stream Fishes: Patterns of Diversity, Rarity, and Risk. Conservation Biology 2:149–156.
Simon, S. A., T. K. Collins, G. L. Kauffman, W. H. McNab, and C. J. Ulrey. 2005. Ecological zones in the southern Appalachians: first approximation. USDA Forest Service, Asheville, NC.
Swank, W. T., and J. M. Vose. 1997. Long-term nitrogen dynamics of Coweeta forested watersheds in the southeastern United States of America. Global Biogeochemical Cycles 11:657–671.
Taylor, B. W., A. S. Flecker, and R. O. Hall. 2006. Loss of a harvested fish species disrupts carbon flow in a diverse tropical river. Science 313:833–836.
Tilman, D., F. Isbell, and J. M. Cowles. 2014. Biodiversity and Ecosystem Functioning. Annual Review of Ecology, Evolution, and Systematics 45:471–493.
Tilman, D., P. B. Reich, J. Knops, D. Wedin, T. Mielke, et al. 2001. Diversity and Productivity in a Long-Term Grassland Experiment. Science 294:843–845.
Webster, J. R. (n.d.). River Conservation and Management. First edition. John Wiley & Sons, Ltd.
Webster, J. R., J. D. Knoepp, W. T. Swank, and C. F. Miniat. 2016. Evidence for a Regime Shift in Nitrogen Export from a Forested Watershed. Ecosystems 19:881–895.
Williams, H. 1995. Geology of the Appalachian—Caledonian Orogen in Canada and Greenland. Geological Society of America.
Zhou, Z., C. Wang, and Y. Luo. 2018. Effects of forest degradation on microbial communities and soil carbon cycling: A global meta-analysis. Global Ecology and Biogeography 27:110–124.

CHAPTER 2 - Soil microbial response to Rhododendron understory removal in southern Appalachian forests: effects on extracellular enzymes

Authors:

Ernest D Osburn, Katherine J Elliottt, Jennifer D Knoepp, Chelcy F Miniat, J E Barrett

Published in *Soil Biology and Biochemistry*:

Osburn, E. D., K. J. Elliottt, J. D. Knoepp, C. F. Miniat, and J. E. Barrett. 2018. Soil microbial response to Rhododendron understory removal in southern Appalachian forests: Effects on extracellular enzymes. *Soil Biology and Biochemistry* 127:50 -59.

Abstract

Rhododendron maximum is a native evergreen shrub that has expanded in Appalachian forests following declines of american chestnut (*Castanea dentata*) and eastern hemlock (*Tsuga canadensis*). *R. maximum* is of concern to forest managers because it suppresses hardwood tree establishment by limiting light and soil nutrient availability. We are testing *R. maximum* removal as a management strategy to promote recovery of Appalachian forests. We hypothesized that *R. maximum* removal would increase soil nitrogen (N) availability, resulting in increased microbial C-demand (i.e. increased C-acquiring enzyme activity) and a shift towards bacterial-dominated microbial communities. *R. maximum* removal treatments were applied in a 2 x 2 factorial design, with two *R. maximum* canopy removal levels (removed vs not) combined with two O-horizon removal levels (burned vs unburned). Following removals, we sampled soils and found that dissolved organic carbon (DOC), N (TDN, NO_3, NH_4), and microbial biomass all increased with *R. maximum* canopy + O-horizon removal. Additionally, we observed increases in C-acquisition enzymes involved in degrading cellulose (β-glucosidase) and

hemicellulose (β-xylosidase) with canopy + O-horizon removal. We did not see treatment effects on bacterial dominance, though F:B ratios from all treatments increased from spring to summer. Our results show that *R. maximum* removal stimulates microbial activity by increasing soil C and N availability, which may influence recovery of forests in the Appalachian region.

Introduction

In terrestrial ecosystems, plant-soil interactions regulate the structure of aboveground and belowground communities as well as rates of biogeochemical processes (Wardle et al. 2004, Ehrenfeld et al. 2005, Berg and Smalla 2009). Plants influence soil microbial communities through their carbon (C) inputs via litterfall and root exudation (Wardle et al. 2006, Berg and Smalla 2009, Chapman and Newman 2010), while soil microorganisms influence plant productivity by mobilizing nutrients such as nitrogen (N), highlighting the potential for complex feedbacks between plants and belowground communities (van der Heijden et al., 2008). Such feedbacks are common in forest ecosystems, where different tree species are associated with distinct microbial communities that exhibit significant functional differences in terms of extracellular enzyme production and nutrient cycling (Weand et al. 2010, Ribbons et al. 2016). Similarly, forest understory shrubs and herbaceous vegetation can influence microbial community structure and function, even within the same forest type (Wurzburger and Hendrick 2007, Burke et al. 2011, Fu et al. 2015, Shen et al. 2018).

In moist cove and riparian habitats in southern Appalachian forests of the eastern US, the dominant understory species is rosebay rhododendron (*Rhododendron maximum* L.), a native evergreen shrub. *R. maximum* dominates plant-soil interactions in these forests

by suppressing decomposition rates (Hunter et al. 2003, Ball et al. 2008, Strickland et al. 2009) and immobilizing N and other nutrients in complex organic compounds that are preferentially utilized by *R. maximum's* own mycorrhizal symbionts (Wurzburger and Hendrick 2007, 2009). This immobilization of nutrients, along with attenuation of light, inhibits recruitment of hardwood tree seedlings, thereby influencing forest dynamics (Beckage et al. 2000, Nilsen et al. 2001, Clinton 2003). Further, in the past century *R. maximum* has experienced a habitat expansion, due to the die-off of American chestnut (*Castanea dentata* (Marsh) Borkh) in the early 20th century (Elliottt and Vose, 2012), and more recently it has increased its growth following the decline of eastern hemlock (*Tsuga canadensis* (L.) Carrière) due to hemlock wooly adelgid (*Adelges tsugae* Annand) infestation (Ford et al. 2012). Landscape-level studies also show that where *R. maximum* is present in the understory, forest trees are on average 6 m shorter than where it is absent (Bolstad et al. 2018). These studies suggest that riparian forest structure may be fundamentally altered in the wake of eastern hemlock decline. This has prompted forest managers to suggest aggressive management strategies involving the removal of *R. maximum* from areas impacted by hemlock die-off in order to promote forest recovery (Vose et al. 2013).

Proposed *R. maximum* management strategies include mechanical removal of the *R. maximum* understory and subsequent use of herbicides to suppress stump sprouting (Vose et al. 2013). Soil responses to understory vegetation removal are challenging to predict, with prior studies reporting positive, negative, and neutral responses of soil C and N, microbial biomass, fungal:bacterial (F:B) ratios, and extracellular enzyme activities in response to forest understory removal (Giai and Boerner 2007, Boerner et al. 2008, Zhao

et al. 2011, Wu et al. 2011, Shen et al. 2018). A prior *R. maximum* removal study in the southern Appalachian region showed modest increases in soil inorganic N with no evident effects on soil microbial biomass or invertebrate communities (Wright and Coleman 2002, Yeakley et al. 2003). Though that study was not replicated and was confounded by a large disturbance event (hurricane) that affected the reference plot, it suggests that *R. maximum* canopy removal alone may not affect soil communities and processes in the short term.

Proposed *R. maximum* management strategies also involve the use of low-intensity prescribed fire to remove the thick soil O-horizon that develops in *R. maximum* thickets (Vose et al. 2013). Soil responses to prescribed fire in forests generally depend on vegetation type, fire frequency, and fire intensity (Certini 2005). Though soil organic matter (SOM) often decreases following fires (González-Pérez et al. 2004, Certini 2005), low intensity burns can increase SOM decomposability by heat-altering carbon polymers (Knicker 2007), resulting in increased C available to soil microorganisms. Additionally, low-intensity burns can increase soil N availability by converting organic N to inorganic forms (Certini 2005, Hernández and Hobbie 2008). In southern Appalachian forests, low intensity prescribed fires have not significantly affected soil C and N stocks (Hubbard et al. 2004, Knoepp et al. 2004, 2009), but have increased inorganic-N transformation rates in some cases (Knoepp et al. 2004). In other forested regions, prescribed burns have resulted in increased N availability and altered activities of microbial extracellular enzymes (Boerner et al. 2008, Rietl and Jackson 2012, Taylor and Midgley 2018). Studies addressing the combined effects of forest understory removal and prescribed burns in eastern US forests are rare, though increased bacterial activity and altered fungal

and bacterial catabolic function have been reported when understory removal and prescribed burning were combined (Giai and Boerner 2007).

The objective of this study was to examine soil responses to *R. maximum* understory removal in combination with soil O-horizon removal via prescribed burning at the Coweeta Hydrologic Laboratory in the southern Appalachian mountains of North Carolina. We focused on responses of soil C and N pools, fungal vs bacterial dominance, and extracellular enzyme production by microbial communities following *R. maximum* removal. We hypothesized that (1) *R. maximum* + O-horizon removal would mobilize organic matter from recalcitrant *R. maximum* leaf litter, resulting in increased DOC and N availability in mineral soils and a shift towards bacterial-dominated microbial communities; (2) that increased N availability would increase microbial C demand, resulting in elevated production of extracellular enzymes associated with C acquisition; and (3) that reductions in lignin-rich *R. maximum* leaf litter in the O-horizon following burning would result in reduced activities of lignolytic enzymes.

Materials and Methods

Site description

We conducted this study at the Coweeta Hydrologic Laboratory (CWT, latitude 35º03' N, longitude 83º25' W), a U.S. Forest Service experimental forest located in the Nantahala Mountains of western North Carolina within the Blue Ridge physiographic province in the southern Appalachians. Soils are deep sandy loams underlain by folded schist and gneiss. Two soil orders are found within the study sites, Inceptisols and Ultisols in the Cullasaja-Tuckasegee and Edneyville-Chestnut complexes, respectively

(Thomas 1996). Soils are characterized by high organic matter in the A horizon, a clay accumulating B horizon, and depth to saprolite of 80 to 100 cm.

We selected areas within the Coweeta Basin in mesic, riparian areas with low-to-moderate slopes (<30 %) and elevations ranging from 760 to 1060 m. All study areas had high abundance of *R. maximum*. Mean annual temperature at Coweeta is 12.6 ºC and seasonally ranges from 3.3 to 21.6 ºC. While annual rainfall is usually abundant in this region, averaging ca. 1800 mm, drought years are becoming increasingly common (Laseter et al. 2012).

Experimental design and sample collection

We applied four *R. maximum* removal treatments to sixteen 20 m x 20 m (0.04 ha) plots located in the Coweeta Basin. Six of the sixteen plots have been monitored for vegetation dynamics, carbon and nutrient pools and fluxes, and soil solution chemistry since 2004 (Nuckolls et al. 2009, Knoepp et al. 2011, Ford et al. 2012). We established ten additional plots with similar characteristics, and then randomly selected among the sixteen plots to assign treatments, resulting in four replicates of each treatment. The four treatments were designed to remove the *R. maximum* canopy (hereafter, CR), remove the soil O-horizon (hereafter, FF), remove the *R. maximum* canopy and soil O-horizon (hereafter, CFFR), and no removal (hereafter, REF). The CR and CFFR treatments included cutting *R. maximum*, immediately followed by application of herbicide on cut stumps (Romancier 1971, Eşen and Zedaker 2004, Harrell 2006). The herbicide was a triclopyr amine (Garlon 3A®, DOW Agrosciences) formulation with an aquatic label (50% triclopyr amine/50% water) to prevent stump sprouting. *R. maximum* cutting (CR, CFFR) occurred in March-May 2015. O-horizon removal in the FF and CFFR treatments

involved low intensity prescribed fires, which temporarily removed the Oi (leaf litter) layer but did not consume the Oe+Oa layers (Elliott and Miniat 2018). Fires were implemented in plots in March 2016 and were performed according to the USDA Forest Service, Nantahala National Forest Prescribed Burning Plan (USDA 2011).

In April and July 2017, two years following *R. maximum* canopy removal and one year following partial O-horizon removal (Oi only), we took three A-horizon (0-10 cm depth) soil cores from each plot and composited samples by plot. We transported soils to the lab on ice and stored samples at 4°C until analysis.

Soil pH, soil C and N, microbial biomass C and N

Gravimetric soil water content was determined by mass loss after drying at 105° C for 24 hours. Soil pH was measured in a soil:water slurry, 1:1 by volume, using a Hach Sension+ pH meter (Hach company, Loveland, CO, USA). Microbial biomass C and N were determined using a modified chloroform fumigation extraction procedure described by Fierer and Schimel (2003). Extracts were measured for extractable dissolved organic carbon (DOC), total extractable nitrogen (TDN), microbial biomass carbon (MBC) and microbial biomass nitrogen (MBN) on an Elementar vario cube TOC/TN (Elementar Americas Inc, Mt. Laurel, NJ, USA). Extracts were analyzed for extractable NH_4 and NO_3 on a Lachat QuikChem flow injection analyzer (Hach Company, Loveland, CO, USA). Dissolved organic nitrogen (DON) was calculated as TDN – (NH_4 + NO_3).

Extracellular enzyme assays

We measured activities of eight extracellular enzymes involved in C, N, and phosphorus (P) cycling in sampled soils. For the hydrolytic enzymes (AP, LAP, NAG, BG, CHB, XYL) (Table 2.1), we performed fluorometric enzyme assays modified from

Saiya-Cork et al. (2002). Briefly, we homogenized ~0.25 g of fresh soil in 125 ml of pH-adjusted 50 mM sodium acetate buffer and stirred homogenate continuously while 200 µl aliquots were added to a 96-well microplate containing substrates fluorescently labelled with 7-amino-4-methylcoumarin (AMC) or 4-methylumbelliferone (MUB). AMC-linked substrates were used to measure LAP activity while MUB-linked substrates were used for all other hydrolytic enzymes. We used a single concentration (10 µM) AMC or MUB standard on each plate, and each plate contained eight analytical replicates of each assay. We measured fluorescence using a Tecan infinite M200 microplate reader (Tecan Group ltd, Mannedorf, Switzerland) with excitation and emission wavelengths of 365 nm and 450 nm, respectively.

We also measured potential enzyme activity of two oxidative enzymes, POX and PER (Table 2.1), using colorimetric microplate assays (Saiya-Cork et al. 2002). Oxidative enzyme activities were determined by measuring color change associated with the breakdown of the substrate 3,4-dihydroxy-L-phenylalanine (L-DOPA). We measured absorbance of microplate wells at 460 nm using a Tecan infinite M200 microplate reader (Tecan Group ltd, Mannedorf, Switzerland).

Activities of extracellular enzymes were corrected for dry soil mass and for microbial biomass C. Prior to multivariate statistical analysis (see below), enzyme activities were relativized based on the maximum observed activity for each respective enzyme in the data set. Ratios of C and N cycling enzymes were calculated as BG:(NAG + LAP) while ratios of C and P cycling enzymes were calculated as BG:AP. These ratios are commonly employed as metrics of relative microbial nutrient demand (Sinsabaugh et al. 2008).

DNA extraction and qPCR

DNA was extracted from ~0.25 g of fresh soil using the DNeasy PowerSoil kit (Qiagen, Valencia, CA, USA) and extracts were quantified using a Qubit fluorometer (Thermo Fisher Inc., Waltham, MA, USA). Total bacterial abundance and total fungal abundance were estimated via qPCR amplification of the 16s rRNA gene and the internal transcriber spacer (ITS) region, respectively. For 16s rRNA gene amplification, we used the primer set EUB 518 and EUB 338, while for ITS amplification we used the primers ITS1f and 5.8s (Fierer et al. 2005). Each qPCR reaction contained 10 µl Quantitect SYBR green master mix (Qiagen, Valencia, CA, USA), 0.5 µm forward and reverse primer, 3 ng DNA template, and nuclease-free H_2O to 20 µl. For both 16s and ITS, thermal cycling conditions were 15 min at 95°C followed by 40 cycles of 15 s at 94°C, 30 s at 55°C and 30 s at 72°C. Standard curves were generated by amplifying serial dilutions of plasmids containing cloned copies of the target sequences. All qPCR reactions were performed in triplicate. Amplification efficiencies ranged from 80.4 – 89.2% with R^2 values > 0.99. Amplification specificity was determined using melt curve analysis. 16s and ITS gene abundances were normalized per gram dry soil and F:B ratios were calculated for each sample by calculating ratios of ITS to 16s gene copies (Fierer et al. 2005).

Statistical Analysis

All statistical analyses were performed in R (R Core Development Team, 2017). We used principal components analysis (PCA) to visualize multivariate extracellular enzyme profiles across treatments (*princomp* function, *vegan* package). Treatment effects on multivariate enzyme profiles were determined with permutational analysis of

variance (PERMANOVA) using Euclidean distance matrices. We used a nested PERMANOVA, which allowed us to account for non-independence of enzyme measurements from the same plot across sample dates (*nested.pmanova* function, *biodiversityR* package). Prior to PERMANOVA, we tested for multivariate dispersion effects using the *betadisper* function in the *vegan* package. Effects of treatment and sampling date on soil chemistry variables, individual enzymes, C:N and C:P enzyme ratios, and fungal/bacterial abundance were tested with linear mixed effects models using the *lme4* package. Treatment and sample date were considered fixed effects in the models while plot was considered a random effect. We compared models with treatment as the only fixed effect to models containing both treatment and sampling date as fixed effects using AIC_c and selected the model with the highest AIC_c weight. Model selection results are presented in Tables 2.S1-S4. Pairwise comparisons between treatments were made with Tukey's HSD using the *lsmeans* package. Relationships between F:B ratios and C:N and C:P enzyme ratios were determined with linear regression, while relationships between fungal and bacterial abundance and individual enzymes were determined using Pearson correlation. Where necessary, values were log transformed in order to meet assumptions of normality of residuals. For visualization purposes, log-transformed values were back-transformed. Where sampling date was not included in the best-supported mixed effects model, we only show treatment comparisons to illustrate effects of *R. maximum* removal.

Results

Soil pH, C and N pools, and microbial biomass C and N

For all soil variables except for TDN and DON, the best-supported mixed effects models had treatment as the only fixed effect (Table 2.S1). Soil pH was not different among treatments, while DOC, MBC, MBN, NH_4, and NO_3, were all significantly different among treatments (Table 2.2). DOC was higher in CFFR plots relative to CR plots (~50% higher, $P = 0.025$) and was marginally higher in CFFR plots relative to REF plots (~33% higher, $P = 0.089$). MBC was higher in CFFR plots than in REF plots only (~125% higher, $P = 0.008$). MBN, NH_4, and NO_3 were all higher in CFFR plots than in all other treatments (all $P < 0.05$). MBN increased ~125%, NH_4 increased ~100%, and NO_3 increased ~230% in CFFR plots relative to REF plots (Table 2.2).

The best-supported model for TDN had both treatment and sampling date as fixed effects (Table 2.S1) and had a significant treatment x date interaction term, where CFFR plots had approximately 100% higher TDN than REF ($P = 0.015$) and FF ($P = 0.021$) plots only in the July sampling (Figure 2.1). Across all samples, DON comprised > 90% of TDN, resulting in identical patterns across sampling dates and treatments for DON (data not shown).

Extracellular enzyme activities

There were no multivariate dispersion effects on extracellular enzyme activities across treatments ($P > 0.05$), indicating that PERMANOVA was able to reliably identify treatment effects. PERMANOVA showed that soil mass-corrected enzyme profiles were significantly different among treatments (Figure 2.2A), while microbial biomass-corrected enzyme profiles were not (Figure 2.2B).

For individual enzyme activities corrected for soil mass, all best-supported mixed models had treatment as the only fixed effect (Table 2.S2). BG, CHB, XYL, and AP were significantly different among treatments, LAP was marginally different among treatments, and NAG, POX, and PER were not different among treatments (Figure 2.3). BG activity was higher in CFFR plots than in CR plots (~100% higher, $P = 0.02$) and was marginally higher in CFFR than in both REF ($P = 0.053$) and FF plots ($P = 0.059$, Figure 3A). CHB activity was higher in CFFR than in CR plots only (~150% higher, $P = 0.039$, Figure 2.3B). XYL activity was higher in CFFR than in all other treatments (~100-175% higher, all $P < 0.05$, Figure 2.3C). AP activity was higher in CFFR than in CR plots only (~130% higher, $P = 0.009$, Figure 2.3D) while LAP activity was marginally higher in CFFR than in CR plots (~60% higher, $P = 0.073$, Figure 2.3E).

The best-supported mixed models for all microbial biomass-corrected enzyme activities had treatment as the only fixed effect (Table 2.S3). There were no significant effects of treatment on biomass-corrected activities of any of the eight extracellular enzymes (all $P > 0.05$, Figure 2.S1).

Best-supported models for C:N and C:P enzyme ratios had both treatment and sampling date as fixed effects (Table 2.S4). For C:N enzyme ratios, there was a significant treatment x date interaction, where CFFR plots had marginally higher C:N enzyme ratios than REF plots ($P = 0.065$) and CR plots ($P = 0.077$) only in the April sampling (Figure 2.4A). For C:P enzyme ratios, there was a significant effect of sampling date and a marginal treatment x date interaction, though no pairwise comparisons between treatments within sampling dates were significant (Figure 2.4B).

Bacterial and fungal abundance

Best-supported models for bacterial abundance, fungal abundance, and F:B ratios had both treatment and sampling date as fixed effects (Table 2.S4). Bacterial abundance was marginally higher in CFFR plots relative to CR plots in July (~50% higher, P = 0.097) and was overall higher in the April sampling than in the July sampling (~70% higher, $P < 0.001$, Figure 2.5A). Bacterial abundance was significantly positively correlated with the C-acquiring enzymes BG, CHB, and XYL (Table 2.3). Fungal abundance was higher in the July sampling than in the April sampling (~80% higher, $P <$ 0.001), and there were no differences in fungal abundance between treatments (Figure 2.5B). There were significant positive correlations between fungal abundance and the N-acquiring enzyme NAG and the P-acquiring enzyme AP and a marginal negative correlation between fungal abundance and the lignolytic enzyme POX (Table 2.3).

The observed fungal and bacterial abundance patterns resulted in F:B ratios that were not significantly different among treatments, but were higher in the July sampling than in the April sampling (~200% higher, $P < 0.001$, Figure 2.5C). There was a significant negative relationship between F:B ratios and C:N enzyme ratios (Figure 2.5D) and a marginal negative relationship between F:B ratios and C:P enzyme ratios (Figure 2.5E).

Discussion

Rhododendron maximum promotes a soil N feedback in Appalachian forests, in which soil N availability is limited by the preferential immobilization of N from *R. maximum* leaf litter by the plant's own mycorrhizal symbionts (Wurzburger and Hendrick 2009). We predicted that the combination of *R. maximum* canopy and soil O-horizon removal

would disrupt this feedback, resulting in increased soil N availability. Our results are generally consistent with this prediction, as TDN was higher in canopy + O-horizon removal plots compared with reference plots in our summer sampling (Figure 2.1). We also observed increased DOC availability in canopy + O-horizon removal plots relative to reference plots (Table 2.2). The DOC and TDN responses may be explained by increased availability of C and N following prescribed burns. A parallel study to this one found that burning in the O-horizon removal plots and canopy + O-horizon removal plots resulted in temporary removal of the leaf litter (Oi) layer, which was replaced by litter fall the next year, with no apparent effects on Oe/a layers (Elliott and Miniat 2018). However, even a single low-intensity burn event may have generated the C and N responses we observed, as heat-alteration of organic compounds during low-intensity burns can promote microbial colonization of residues (Knicker 2007), potentially mobilizing organic C and N from heat-altered *R. maximum* leaf litter. Similar responses of DOC and TDN in A-horizon soils in response to prescribed fire have been recently reported in other forested regions (Näthe et al. 2018). We also saw significantly higher TDN in canopy + O-horizon removal plots compared with O-horizon removal plots in our summer samples (Figure 2.1). The lack of increase in TDN in O-horizon removal plots following burning may be due to continued N uptake by *R. maximum* roots and associated mycorrhizae, which were still active in O-horizon removal plots, or may be due to incomplete O-horizon removal in these plots (Elliott and Miniat 2018). The lack of treatment differences in TDN in our spring samples may have been due to delayed soil N response to removal treatments or due to N immobilization by soil bacteria, which were 70% more abundant in spring than

summer and were more abundant in canopy + O-horizon removal plots than in other treatments (Figure 2.5A), potentially dampening any treatment effects on TDN.

We also observed increases in inorganic N (NH_4, NO_3) in canopy + O-horizon removal plots compared with all other treatments (Table 2.2). This may be explained by direct conversion of organic N to inorganic N by combustion (Certini 2005) or increased inorganic-N transformation rates following burns, as has been observed at other southern Appalachian sites (Knoepp et al. 2004). These effects, in combination with reduced inorganic N uptake by roots and mycorrhizae following *R. maximum* canopy removal, could have produced the observed trend, where both canopy removal and prescribed fire were necessary to increase concentrations of soil inorganic N.

The observed increases in soil N and DOC were associated with an apparent increase in microbial C-demand, as two C-acquiring enzymes (BG, XYL) were elevated in canopy + O-horizon removal plots relative to all other treatments (Figure 2.3). Similar responses of C-acquiring enzymes to increased N availability have been observed in earlier studies in different regions (Allison and Vitousek 2005, Geisseler and Horwath 2009). Increased N availability can also result in reduced N-acquisition enzyme activity (Sinsabaugh et al. 2002, Allison and Vitousek 2005, Ramirez et al. 2012), which is often explained using a resource allocation framework. Within this framework, microorganisms increase production of enzymes for acquiring scarce resources and reduce production of enzymes when resources are abundant (Allison et al. 2010). Our results appear to be inconsistent with this framework, as activity of all hydrolytic enzymes, including N-acquiring enzymes, were generally higher with *R. maximum* removal (Figures 2.2A, 2.3). This response was likely driven by increases in microbial biomass, evidenced by the lack of

treatment differences in biomass-corrected enzyme activities (Figures 2.2B, 2.S1). This points to nutrient supply-driven enzyme production (i.e. biomass effects) as opposed to nutrient demand-driven enzyme production (i.e. resource allocation) in our soils, though the particularly strong response of C-acquiring enzymes to increased N suggest that some resource allocation may have occurred.

Interestingly, the largest observed differences in DOC and all hydrolytic enzyme activities were between the canopy + O-horizon removal and canopy removal only treatments (Table 2.2, Figure 2.3). This may be explained by reduced root exudation of DOC following *R. maximum* cutting, which likely resulted in significant root die-back. Root exudation is known to stimulate microbial production of extracellular enzymes in rhizosphere soils (Brzostek et al. 2013), potentially accounting for the consistent responses of DOC and enzyme activities in this study. Though root die-back also likely occurred in canopy + O-horizon removal plots, DOC and TDN mobilized by prescribed fire may have compensated for reductions in root exudation.

Prior studies examining *R. maximum* effects on extracellular enzyme activities found elevated activities of phenol oxidase (POX) in O-horizon soils under *R. maximum* thickets (Wurzburger and Hendrick 2007), leading us to predict that O-horizon removal via prescribed burns would reduce lignolytic enzyme (POX, PER) production. Our results show no treatment effects on POX or PER activity (Figure 2.3), likely because POX activity differences were previously shown in O-horizon soils of *R. maximum* thickets, while we measured enzyme activities only in A-horizon soils. The lack of treatment differences in POX and PER may also be due to incomplete O-horizon removal by fire, potentially resulting in similar availability of lignin-rich substrates across treatments.

Because bacteria are generally associated with higher growth rates and more copiotrophic lifestyles relative to fungi (Strickland and Rousk 2010), we predicted that increases in DOC and N following *R. maximum* removal would stimulate bacterial growth and lead to bacterial-dominated microbial communities. Our results do not support this prediction; removal treatments did not result in differences in F:B ratios (Figure 2.5C). Though our results do not show treatment effects on microbial community structure at this coarse scale, studies using more sophisticated molecular tools (i.e. 16s and ITS sequencing) have shown changes in bacterial and fungal communities following forest management practices (i.e. Bastida et al., 2017), highlighting the need for similar tools to be used in future studies to determine effects of *R. maximum* removal on microbial community structure. Though treatments did not affect F:B ratios in our study, we did observe a clear shift towards higher F:B ratios from spring to summer (Figure 2.5C), which was due to simultaneous declines in bacterial abundance and increases in fungal abundance (Figure 2.5A, B). The bacterial decline was likely linked to declines in soil moisture from spring to summer (Elliott and Miniat 2018), while fungi are less susceptible to soil drying (Schimel et al. 2007). The increase in fungal abundance may be linked to seasonal increases in root C inputs to mineral soil, as has been shown in other forested regions (Voříšková et al. 2014). Seasonal increases in plant productivity may also have promoted growth of mycorrhizal fungi, potentially contributing to the high fungal abundance we observed in summer. This possibility is supported by the positive correlations between fungal abundance and N- and P-acquiring enzymes (Table 2.3), which are known to be produced by mycorrhizae (Burke et al., 2011). Additionally, we found a negative correlation between fungal abundance and the lignolytic enzyme POX

(Table 2.3), contrary to prior research on the lignolytic capabilities of soil fungi (Strickland and Rousk 2010). Other studies have reported similar negative correlations between lignolytic enzymes and soil fungi in forests (Brockett et al. 2012), and many mycorrhizal taxa may not be capable of producing lignolytic enzymes (Smith and Read 2010), further supporting the possibility that many of the fungi we detected were mycorrhizae. We also observed significant positive correlations between bacterial abundance and C-acquiring enzymes (BG, CHB, and XYL) (Table 2.3), similar to previous reports (Brockett et al. 2012). Overall, the observed relationships between bacteria, fungi, and enzyme activities suggest functional differences between microbial communities with different F:B ratios. Prior studies report conflicting results regarding functional characteristics of communities with different F:B ratios, with some studies reporting functional differences (i.e. Blagodatskaya and Anderson, 1998; Malik et al., 2016), and others reporting no functional differences (i.e. Rousk and Frey, 2015; Thiet et al., 2006). Our results, which show clear associations between bacteria and fungi and specific extracellular enzymes, suggest that such functional differences may indeed exist.

The observed correlations between extracellular enzymes and bacterial vs fungal abundance (Table 2.3) resulted in C:N enzyme activity ratios that were negatively correlated with F:B ratios (Figure 2.5D). Prior studies have shown low C- vs N-acquiring enzyme activity in arbuscular mycorrhizal (AM) fungi (Burke et al. 2011), potentially accounting for the negative F:B vs C:N enzyme relationship we observed if AM fungi are in fact abundant in our plots. Future studies should evaluate the hypothesis that abundance of mycorrhizal fungi can significantly affect patterns of extracellular enzyme activities measured in forest soils. In addition to relationships with F:B ratios, we

observed treatment differences in C:N enzyme activity ratios that were dependent on sample date, with higher relative C-acquiring enzyme activity in canopy + O-horizon removal plots relative to O-horizon removal and reference plots only in the spring (Figure 2.4A). These results suggest that extracellular enzyme responses to *R. maximum* removal are potentially dependent upon both season and the resident microbial community. Because microbial communities and associated extracellular enzyme activities differ among tree species in eastern US forests (Weand et al. 2010), we may also expect enzyme responses to *R. maximum* understory removal to depend upon the tree species composition of the remaining forest.

Conclusions

Overall, our results show that the combination of *R. maximum* canopy + Oi layer removal by burning increases soil C and N availability, resulting in increased microbial biomass and increased production of key microbial extracellular enzymes, while individual removal treatments had much smaller effects. Enzymes associated with C-acquisition show particularly strong responses, suggesting that soil C dynamics were altered with *R. maximum* removal. Further, responses to *R. maximum* removal were different between seasons, with a shift from relatively higher microbial C-acquiring enzyme activity in spring to relatively higher N-acquisition enzyme activity in summer, which was associated with increased F:B ratios. The observed increases in soil nutrients and microbial enzyme activity will potentially influence recovery rates of Appalachian forests, at least in the short term. Medium- and long-term microbial responses to *R. maximum* removal are difficult to predict; microbial activity may return to baseline levels after recovering from disturbances associated with removal treatments or may remain

persistently higher due to continued absence of *R. maximum*. Regardless, these ecosystems should be continually monitored to further inform the use of *R. maximum* removal to achieve forest management goals.

Acknowledgements

We thank Bobbie Niederlehner for help with soil chemistry analyses and the VT Stream Team for their helpful comments on this work. This project was supported by the Coweeta LTER, funded by National Science Foundation grant DEB-1440485. We also thank the Coweeta Hydrologic Laboratory, Southern Research Station, USDA Forest Service for support and the USDA Forest Service Nantahala Ranger District staff, Nantahala National Forest, for executing the treatments. Finally, we thank two anonymous reviewers, whose feedback greatly improved this manuscript. The use of trade or firm names in this publication is for reader information and does not imply endorsement by the U.S. Department of Agriculture of any product or service.

References

Allison, S.D., Vitousek, P.M., 2005. Responses of extracellular enzymes to simple and complex nutrient inputs. Soil Biology and Biochemistry 37, 937–944. doi:10.1016/j.soilbio.2004.09.014

Allison, S.D., Weintraub, M.N., Gartner, T.B., Waldrop, M.P., 2010. Evolutionary-Economic Principles as Regulators of Soil Enzyme Production and Ecosystem Function, in: Soil Enzymology, Soil Biology. Springer, Berlin, Heidelberg, pp. 229–243. doi:10.1007/978-3-642-14225-3_12

Ball, B.A., Hunter, M.D., Kominoski, J.S., Swan, C.M., Bradford, M.A., 2008. Consequences of non-random species loss for decomposition dynamics: experimental evidence for additive and non-additive effects. Journal of Ecology 96, 303–313. doi:10.1111/j.1365-2745.2007.01346.x

Bastida, F., Torres, I.F., Andrés-Abellán, M., Baldrian, P., López-Mondéjar, R., Větrovský, T., Richnow, H.H., Starke, R., Ondoño, S., García, C., López-Serrano, F.R., Jehmlich, N., 2017. Differential sensitivity of total and active soil microbial communities to drought and forest management. Global Change Biology 1–19. doi:10.1111/gcb.13790

Beckage, B., Clark, J.S., Clinton, B.D., Haines, B.L., 2000. A long-term study of tree seedling recruitment in southern Appalachian forests: the effects of canopy gaps

and shrub understories. Canadian Journal of Forest Research 30, 1617–1631. doi:10.1139/cjfr-30-10-1617
Berg, G., Smalla, K., 2009. Plant species and soil type cooperatively shape the structure and function of microbial communities in the rhizosphere. FEMS Microbiology Ecology 68, 1–13. doi:10.1111/j.1574-6941.2009.00654.x
Blagodatskaya, E.V., Anderson, T.-H., 1998. Interactive effects of pH and substrate quality on the fungal-to-bacterial ratio and qCO2 of microbial communities in forest soils. Soil Biology and Biochemistry 30, 1269–1274. doi:10.1016/S0038-0717(98)00050-9
Boerner, R.E.J., Giai, C., Huang, J., Miesel, J.R., 2008. Initial effects of fire and mechanical thinning on soil enzyme activity and nitrogen transformations in eight North American forest ecosystems. Soil Biology and Biochemistry 40, 3076–3085. doi:10.1016/j.soilbio.2008.09.008
Bolstad, P.V., Elliot, K.J., Miniat, C.F., 2018. Forests, shrubs, and terrain: top-down and bottom-up controls on forest structure. Ecosphere 9, e02185. doi:10.1002/ecs2.2185
Brockett, B.F.T., Prescott, C.E., Grayston, S.J., 2012. Soil moisture is the major factor influencing microbial community structure and enzyme activities across seven biogeoclimatic zones in western Canada. Soil Biology and Biochemistry 44, 9–20. doi:10.1016/j.soilbio.2011.09.003
Brzostek, E.R., Greco, A., Drake, J.E., Finzi, A.C., 2013. Root carbon inputs to the rhizosphere stimulate extracellular enzyme activity and increase nitrogen availability in temperate forest soils. Biogeochemistry 115, 65–76. doi:10.1007/s10533-012-9818-9
Burke, D.J., Weintraub, M.N., Hewins, C.R., Kalisz, S., 2011. Relationship between soil enzyme activities, nutrient cycling and soil fungal communities in a northern hardwood forest. Soil Biology and Biochemistry 43, 795–803. doi:10.1016/j.soilbio.2010.12.014
Certini, G., 2005. Effects of fire on properties of forest soils: a review. Oecologia 143, 1–10. doi:10.1007/s00442-004-1788-8
Chapman, S.K., Newman, G.S., 2010. Biodiversity at the plant–soil interface: microbial abundance and community structure respond to litter mixing. Oecologia 162, 763–769. doi:10.1007/s00442-009-1498-3
Clinton, B.D., 2003. Light, temperature, and soil moisture responses to elevation, evergreen understory, and small canopy gaps in the southern Appalachians. Forest Ecology and Management 186, 243–255. doi:10.1016/S0378-1127(03)00277-9
Ehrenfeld, J.G., Ravit, B., Elgersma, K., 2005. Feedback in the Plant-Soil System. Annual Review of Environment and Resources 30, 75–115. doi:10.1146/annurev.energy.30.050504.144212
Elliott, K.J., Miniat, C.F., 2018. Herbaceous-layer diversity and tree seedling recruitment are enhanced following Rhododendron maximum shrub removal. Forest Ecology and Management 430, 403–412. doi:10.1016/j.foreco.2018.08.016
Elliott, K.J., Vose, J.M., 2012. Age and distribution of an evergreen clonal shrub in the Coweeta Basin: Rhododendron maximum L. The Journal of the Torrey Botanical Society 139, 149–166.

Eşen, D., Zedaker, S.M., 2004. Control of rhododendron (Rhododendron ponticum and R. flavum) in the eastern beech Fagus orientalis) forests of Turkey. New Forests 27, 69–79. doi:10.1023/A:1025072105849

Fierer, N., Jackson, J.A., Vilgalys, R., Jackson, R.B., 2005. Assessment of Soil Microbial Community Structure by Use of Taxon-Specific Quantitative PCR Assays. Applied and Environmental Microbiology 71, 4117–4120. doi:10.1128/AEM.71.7.4117-4120.2005

Fierer, N., Schimel, J.P., 2003. A Proposed Mechanism for the Pulse in Carbon Dioxide Production Commonly Observed Following the Rapid Rewetting of a Dry Soil. Soil Science Society of America Journal 67, 798–805. doi:10.2136/sssaj2003.7980

Ford, C.R., Elliott, K.J., Clinton, B.D., Kloeppel, B.D., Vose, J.M., 2012. Forest dynamics following eastern hemlock mortality in the southern Appalachians. Oikos 121, 523–536. doi:10.1111/j.1600-0706.2011.19622.x

Fu, X., Yang, F., Wang, J., Di, Y., Dai, X., Zhang, X., Wang, H., 2015. Understory vegetation leads to changes in soil acidity and in microbial communities 27 years after reforestation. Science of the Total Environment 502, 280–286. doi:10.1016/j.scitotenv.2014.09.018

Geisseler, D., Horwath, W.R., 2009. Relationship between carbon and nitrogen availability and extracellular enzyme activities in soil. Pedobiologia 53, 87–98. doi:10.1016/j.pedobi.2009.06.002

Giai, C., Boerner, R.E.J., 2007. Effects of ecological restoration on microbial activity, microbial functional diversity, and soil organic matter in mixed-oak forests of southern Ohio, USA. Applied Soil Ecology 35, 281–290. doi:10.1016/j.apsoil.2006.08.003

González-Pérez, J.A., González-Vila, F.J., Almendros, G., Knicker, H., 2004. The effect of fire on soil organic matter—a review. Environment International 30, 855–870. doi:10.1016/j.envint.2004.02.003

Harrell, C.W., 2006. Effects of prescribed burning, mechanical and chemical treatments to curtail rhododendron dominance and reduce wildfire fuel loads (Thesis). Virginia Tech.

Hernández, D.L., Hobbie, S.E., 2008. Effects of fire frequency on oak litter decomposition and nitrogen dynamics. Oecologia 158, 535–543. doi:10.1007/s00442-008-1162-3

Hubbard, R.M., Vose, J.M., Clinton, B.D., Elliott, K.J., Knoepp, J.D., 2004. Stand restoration burning in oak–pine forests in the southern Appalachians: effects on aboveground biomass and carbon and nitrogen cycling. Forest Ecology and Management 190, 311–321. doi:10.1016/j.foreco.2003.10.021

Hunter, M.D., Adl, S., Pringle, C.M., Coleman, D.C., 2003. Relative effects of macroinvertebrates and habitat on the chemistry of litter during decomposition. Pedobiologia 47, 101–115. doi:10.1078/0031-4056-00174

Knicker, H., 2007. How does fire affect the nature and stability of soil organic nitrogen and carbon? A review. Biogeochemistry 85, 91–118. doi:10.1007/s10533-007-9104-4

Knoepp, J.D., Elliott, K.J., Clinton, B.D., Vose, J.M., 2009. Effects of prescribed fire in mixed oak forests of the southern Appalachians: forest floor, soil, and soil

solution nitrogen responses. Journal of the Torrey Botanical Society 136, 380–391. doi:10.3159/08-RA-052.1

Knoepp, J.D., Vose, J.M., Clinton, B.D., Hunter, M.D., 2011. Hemlock Infestation and Mortality: Impacts on Nutrient Pools and Cycling in Appalachian Forests. Soil Science Society of America Journal 75, 1935–1945. doi:10.2136/sssaj2010.0409

Knoepp, J.D., Vose, J.M., Swank, W.T., 2004. Long-Term Soil Responses to Site Preparation Burning in the Southern Appalachians. Forest Science 50, 540–550. doi:10.1093/forestscience/50.4.540

Laseter, S.H., Ford, C.R., Vose, J.M., Swift, L.W., 2012. Long-term temperature and precipitation trends at the Coweeta Hydrologic Laboratory, Otto, North Carolina, USA. Hydrology Research 43, 890–901. doi:10.2166/nh.2012.067

Malik, A.A., Chowdhury, S., Schlager, V., Oliver, A., Puissant, J., Vazquez, P.G.M., Jehmlich, N., von Bergen, M., Griffiths, R.I., Gleixner, G., 2016. Soil Fungal:Bacterial Ratios Are Linked to Altered Carbon Cycling. Frontiers in Microbiology 7. doi:10.3389/fmicb.2016.01247

Näthe, K., Levia, D.F., Tischer, A., Michalzik, B., 2018. Low-intensity surface fire effects on carbon and nitrogen cycling in soil and soil solution of a Scots pine forest in central Germany. CATENA 162, 360–375. doi:10.1016/j.catena.2017.10.026

Nilsen, E.T., Clinton, B.D., Lei, T.T., Miller, O.K., Semones, S.W., Walker, J.F., 2001. Does Rhododendron maximum L. (Ericaceae) Reduce the Availability of Resources Above and Belowground for Canopy Tree Seedlings? The American Midland Naturalist 145, 325–343. doi:10.1674/0003-0031(2001)145[0325:DRMLER]2.0.CO;2

Nuckolls, A.E., Wurzburger, N., Ford, C.R., Hendrick, R.L., Vose, J.M., Kloeppel, B.D., 2009. Hemlock Declines Rapidly with Hemlock Woolly Adelgid Infestation: Impacts on the Carbon Cycle of Southern Appalachian Forests. Ecosystems 12, 179–190. doi:10.1007/s10021-008-9215-3

R Core Development Team, 2017. R: A Language and Environment for Statistical Computing. R Foundation for Statistical Computing, Vienna, Austria.

Ramirez, K.S., Craine, J.M., Fierer, N., 2012. Consistent effects of nitrogen amendments on soil microbial communities and processes across biomes. Global Change Biology 18, 1918–1927. doi:10.1111/j.1365-2486.2012.02639.x

Ribbons, R.R., Levy-Booth, D.J., Masse, J., Grayston, S.J., McDonald, M.A., Vesterdal, L., Prescott, C.E., 2016. Linking microbial communities, functional genes and nitrogen-cycling processes in forest floors under four tree species. Soil Biology & Biochemistry 103, 181–191. doi:10.1016/j.soilbio.2016.07.024

Rietl, A.J., Jackson, C.R., 2012. Effects of the ecological restoration practices of prescribed burning and mechanical thinning on soil microbial enzyme activities and leaf litter decomposition. Soil Biology & Biochemistry 50, 47–57. doi:10.1016/j.soilbio.2012.03.008

Romancier, R.M., 1971. Combining Fire and Chemicals For the Control of Rhododendron Thickets. Res. Pap. SE-149. Asheville, NC: U.S. Department of Agriculture, Forest Service, Southeastern Forest Experiment Station. 7 P. 149.

Rousk, J., Frey, S.D., 2015. Revisiting the hypothesis that fungal-to-bacterial dominance characterizes turnover of soil organic matter and nutrients. Ecological Monographs 85, 457–472. doi:10.1890/14-1796.1

Saiya-Cork, K.R., Sinsabaugh, R.L., Zak, D.R., 2002. The effects of long term nitrogen deposition on extracellular enzyme activity in an Acer saccharum forest soil. Soil Biology and Biochemistry 34, 1309–1315. doi:10.1016/S0038-0717(02)00074-3

Schimel, J., Balser, T.C., Wallenstein, M., 2007. Microbial stress-response physiology and its implications for ecosystem function. Ecology 88, 1386–1394.

Shen, Y., Cheng, R., Xiao, W., Yang, S., Guo, Y., Wang, N., Zeng, L., Lei, L., Wang, X., 2018. Labile organic carbon pools and enzyme activities of Pinus massoniana plantation soil as affected by understory vegetation removal and thinning. Scientific Reports 8, 573. doi:10.1038/s41598-017-18812-x

Sinsabaugh, R.L., Carreiro, M.M., Repert, D.A., 2002. Allocation of Extracellular Enzymatic Activity in Relation to Litter Composition, N Deposition, and Mass Loss. Biogeochemistry 60, 1–24. doi:10.2307/1469657

Sinsabaugh, R.L., Lauber, C.L., Weintraub, M.N., Ahmed, B., Allison, S.D., Crenshaw, C., Contosta, A.R., Cusack, D., Frey, S., Gallo, M.E., Gartner, T.B., Hobbie, S.E., Holland, K., Keeler, B.L., Powers, J.S., Stursova, M., Takacs-Vesbach, C., Waldrop, M.P., Wallenstein, M.D., Zak, D.R., Zeglin, L.H., 2008. Stoichiometry of soil enzyme activity at global scale. Ecology Letters 11, 1252–1264. doi:10.1111/j.1461-0248.2008.01245.x

Smith, S.E., Read, D.J., 2010. Mycorrhizal Symbiosis. Academic Press.

Strickland, M.S., Osburn, E.D., Lauber, C., Fierer, N., Bradford, M.A., 2009. Litter quality is in the eye of the beholder: initial decomposition rates as a function of inoculum characteristics. Functional Ecology 23, 627–636. doi:10.1111/j.1365-2435.2008.01515.x

Strickland, M.S., Rousk, J., 2010. Considering fungal:bacterial dominance in soils – Methods, controls, and ecosystem implications. Soil Biology and Biochemistry 42, 1385–1395. doi:10.1016/j.soilbio.2010.05.007

Taylor, Q.A., Midgley, M.G., 2018. Prescription side effects: Long-term, high-frequency controlled burning enhances nitrogen availability in an Illinois oak-dominated forest. Forest Ecology and Management 411, 82–89. doi:10.1016/j.foreco.2017.12.041

Thiet, R.K., Frey, S.D., Six, J., 2006. Do growth yield efficiencies differ between soil microbial communities differing in fungal:bacterial ratios? Reality check and methodological issues. Soil Biology and Biochemistry 38, 837–844. doi:10.1016/j.soilbio.2005.07.010

Thomas, D., 1996. Soil Survey of Macon County, North Carolina. USDA, Natural Resources Conservation Service, Washington, DC, USA.

USDA, 2011. Nantahala Pisgah NF Forest Plan Amendments: Prescribed fire amendment 26 [WWW Document]. URL https://www.fs.usda.gov/Internet/FSE_DOCUMENTS/stelprdb5346291.pdf (accessed 4.30.18).

van der Heijden, M.G.A., Bardgett, R.D., Straalen, N.M.V., 2008. The unseen majority: soil microbes as drivers of plant diversity and productivity in terrestrial ecosystems. Ecology Letters 11, 296–310. doi:10.1111/j.1461-0248.2007.01139.x

Voříšková, J., Brabcová, V., Cajthaml, T., Baldrian, P., 2014. Seasonal dynamics of fungal communities in a temperate oak forest soil. New Phytologist 201, 269–278. doi:10.1111/nph.12481

Vose, J.M., Wear, D.N., Mayfield, A.E., Dana Nelson, C., 2013. Hemlock woolly adelgid in the southern Appalachians: Control strategies, ecological impacts, and potential management responses. Forest Ecology and Management 291, 209–219. doi:10.1016/j.foreco.2012.11.002

Wardle, D., Yeates, G., Barker, G., Bonner, K., 2006. The influence of plant litter diversity on decomposer abundance and diversity. Soil Biology and Biochemistry 38, 1052–1062. doi:10.1016/j.soilbio.2005.09.003

Wardle, D.A., Bardgett, R.D., Klironomos, J.N., Setälä, H., Putten, W.H. van der, Wall, D.H., 2004. Ecological Linkages Between Aboveground and Belowground Biota. Science 304, 1629–1633. doi:10.1126/science.1094875

Weand, M.P., Arthur, M.A., Lovett, G.M., McCulley, R.L., Weathers, K.C., 2010. Effects of tree species and N additions on forest floor microbial communities and extracellular enzyme activities. Soil Biology and Biochemistry 42, 2161–2173. doi:10.1016/j.soilbio.2010.08.012

Wright, C.J., Coleman, D.C., 2002. Responses of soil microbial biomass, nematode trophic groups, N-mineralization, and litter decomposition to disturbance events in the southern Appalachians. Soil Biology & Biochemistry 34, 13–25. doi:10.1016/S0038-0717(01)00128-6

Wu, J., Liu, Z., Wang, X., Sun, Y., Zhou, L., Lin, Y., Fu, S., 2011. Effects of understory removal and tree girdling on soil microbial community composition and litter decomposition in two Eucalyptus plantations in South China. Functional Ecology 25, 921–931. doi:10.1111/j.1365-2435.2011.01845.x

Wurzburger, N., Hendrick, R.L., 2009. Plant litter chemistry and mycorrhizal roots promote a nitrogen feedback in a temperate forest. Journal of Ecology 97, 528–536. doi:10.1111/j.1365-2745.2009.01487.x

Wurzburger, N., Hendrick, R.L., 2007. Rhododendron thickets alter N cycling and soil extracellular enzyme activities in southern Appalachian hardwood forests. Pedobiologia 50, 563–576. doi:10.1016/j.pedobi.2006.10.001

Yeakley, J.A., Coleman, D.C., Haines, B.L., Kloeppel, B.D., Meyer, J.L., Swank, W.T., Argo, B.W., Deal, J.M., Taylor, S.F., 2003. Hillslope nutrient dynamics following upland riparian vegetation disturbance. Ecosystems 6, 154–167. doi:10.1007/s10021-002-0116-6

Zhao, J., Wang, X., Shao, Y., Xu, G., Fu, S., 2011. Effects of vegetation removal on soil properties and decomposer organisms. Soil Biology and Biochemistry 43, 954–960. doi:10.1016/j.soilbio.2011.01.010

Figures

Figure 2.1

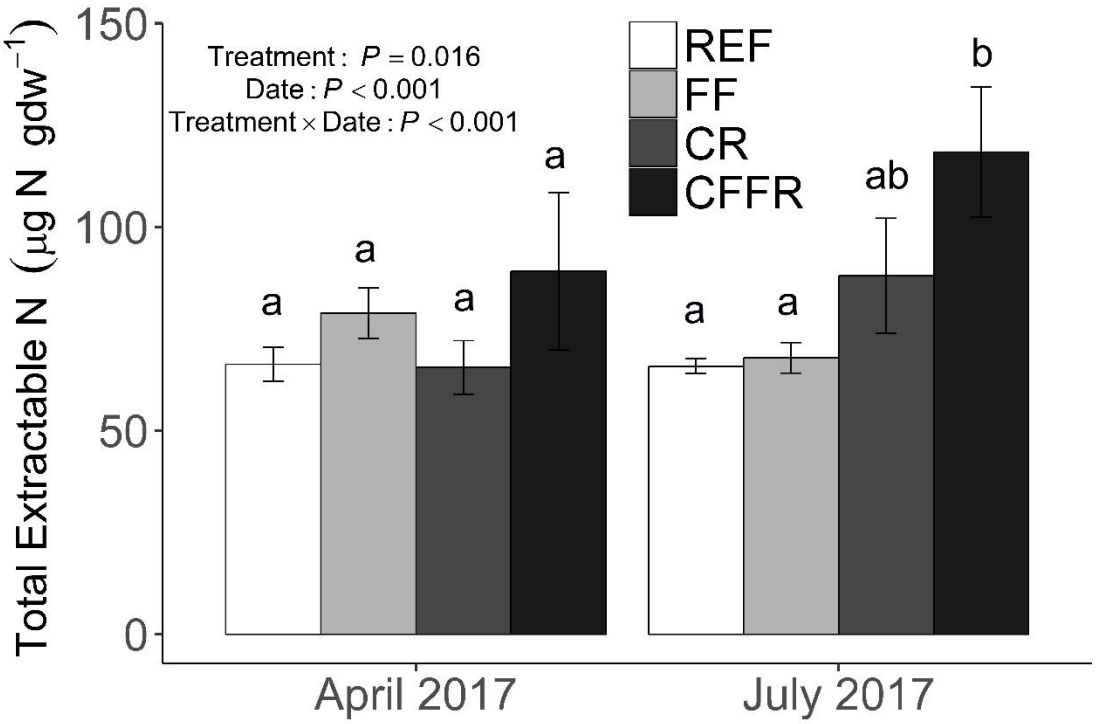

Figure 2.1: Total extractable N (TDN) across treatments and sampling dates. Bars represent means while error bars are ± one standard error. *P*-values presented are linear mixed model effects of treatment, sampling date, and treatment x date interactions. Different letters represent significant pairwise differences between treatments within a sampling date ($P < 0.05$). Treatment abbreviations are as follows: reference (REF), O-horizon removal (FF), canopy removal (CR), and canopy + O-horizon removal (CFFR).

Figure 2.2

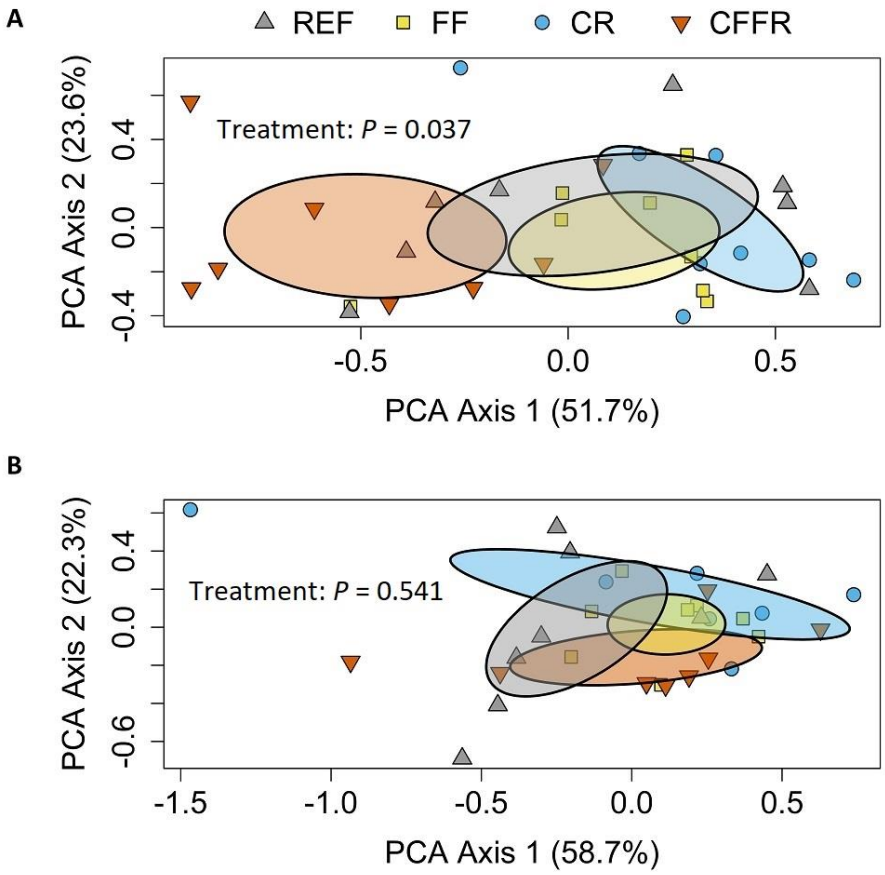

Figure 2.2: Principal components analysis (PCA) of extracellular enzyme activities corrected for dry soil mass **(A)**. PCA axis 1 is negatively correlated with all hydrolytic enzymes (BG, CHB, XYL, AP, LAP, NAG) while PCA axis 2 is positively correlated with oxidative enzymes (POX, PER). PCA of extracellular enzyme activities corrected for microbial biomass **(B)**. PCA axis 1 is negatively correlated with all eight enzymes while PCA axis 2 is negatively correlated with XYL and CHB and positively correlated with POX and PER. *P*-values presented are treatment effects from nested PERMANOVA. Ellipses are 95% confidence intervals around the centroid of each treatment. Treatment abbreviations are as follows: reference (REF), O-horizon removal (FF), canopy removal (CR), and canopy + O-horizon removal (CFFR).

Figure 2.3

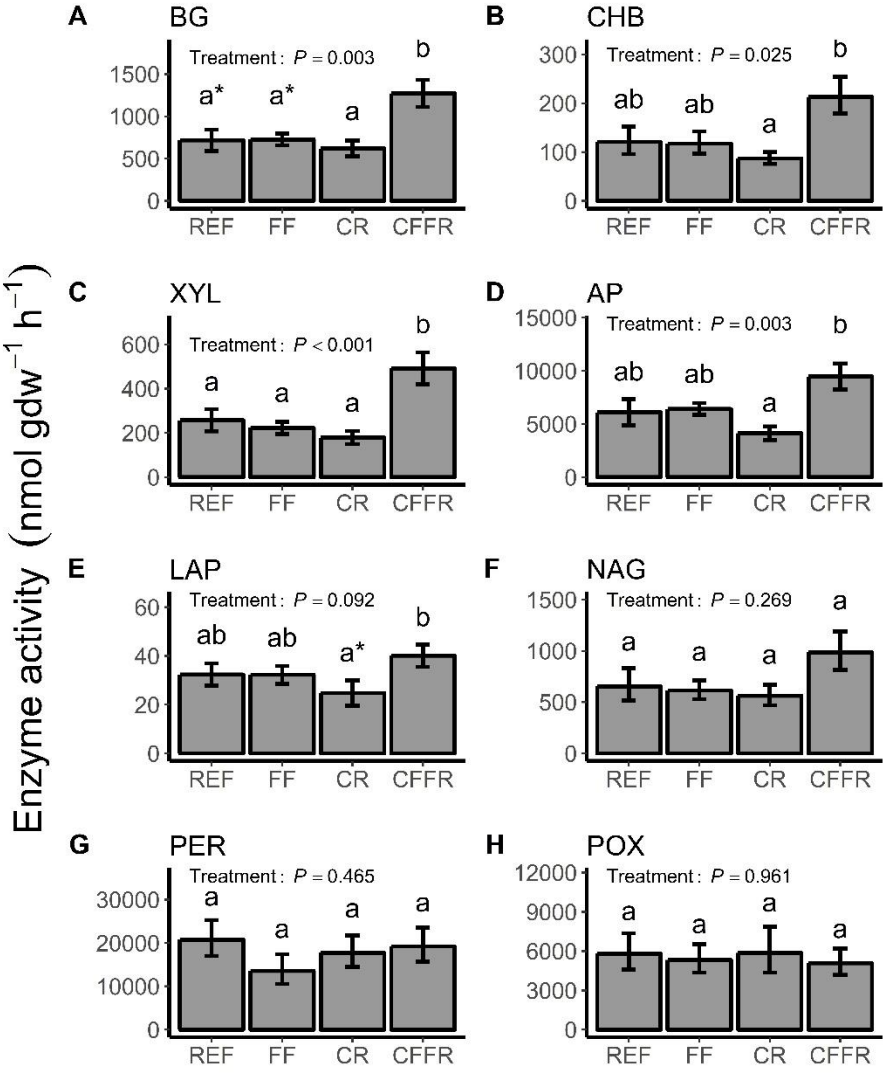

Figure 2.3: Individual extracellular enzyme activities corrected for dry soil mass across treatments: BG **(A)**, CHB **(B)**, XYL **(C)**, AP **(D)**, LAP **(E)**, NAG **(F)**, POX **(G)**, and PER **(H)**. Bars represent means while error bars are ± one standard error. *P*-values presented are linear mixed model effects of treatment. Different letters represent significant differences ($P < 0.05$), while asterisks represent marginally significant differences ($P < 0.1$). Treatment abbreviations are as follows: reference (REF), O-horizon removal (FF), canopy removal (CR), and canopy + O-horizon removal (CFFR).

Figure 2.4

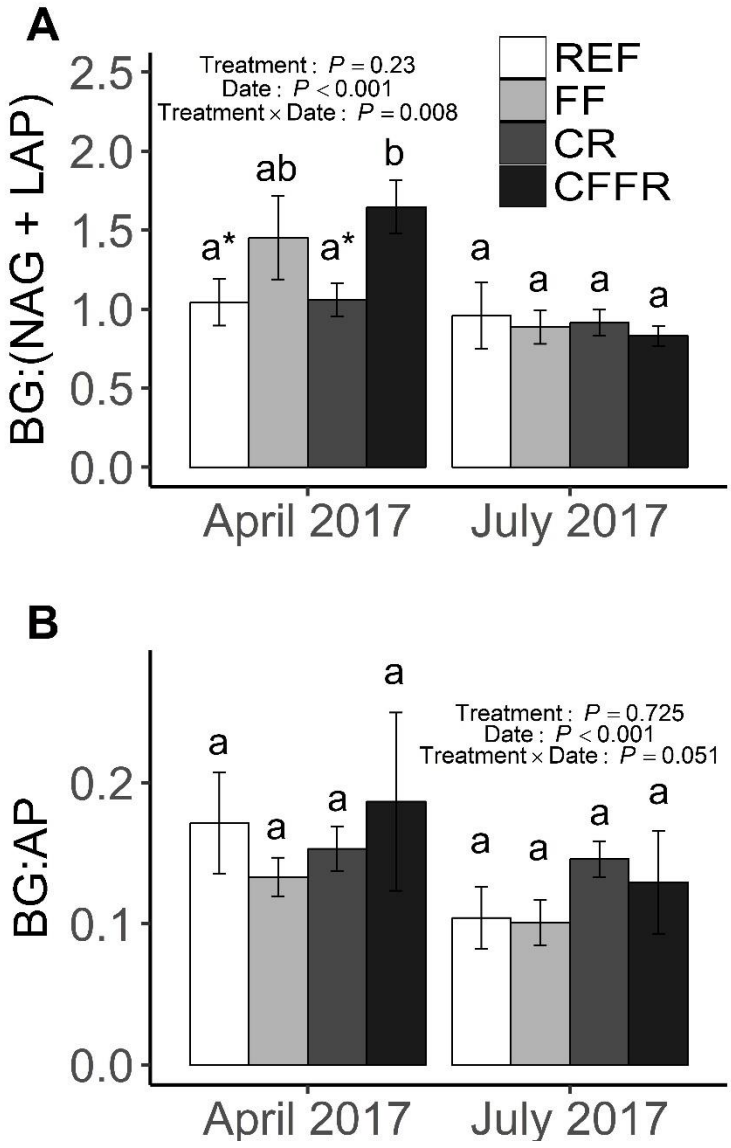

Figure 2.4: C:N enzyme ratios **(A)** and C:P enzyme ratios **(B)** across treatments and sample dates. *P*-values presented are linear mixed model effects of treatment, sampling date, and treatment x date interactions. Different letters represent significant differences between treatments within a sampling date ($P < 0.05$), while asterisks represent marginally significant differences ($P < 0.1$). Treatment abbreviations are as follows: reference (REF), O-horizon removal (FF), canopy removal (CR), and canopy + O-horizon removal (CFFR).

Figure 2.5

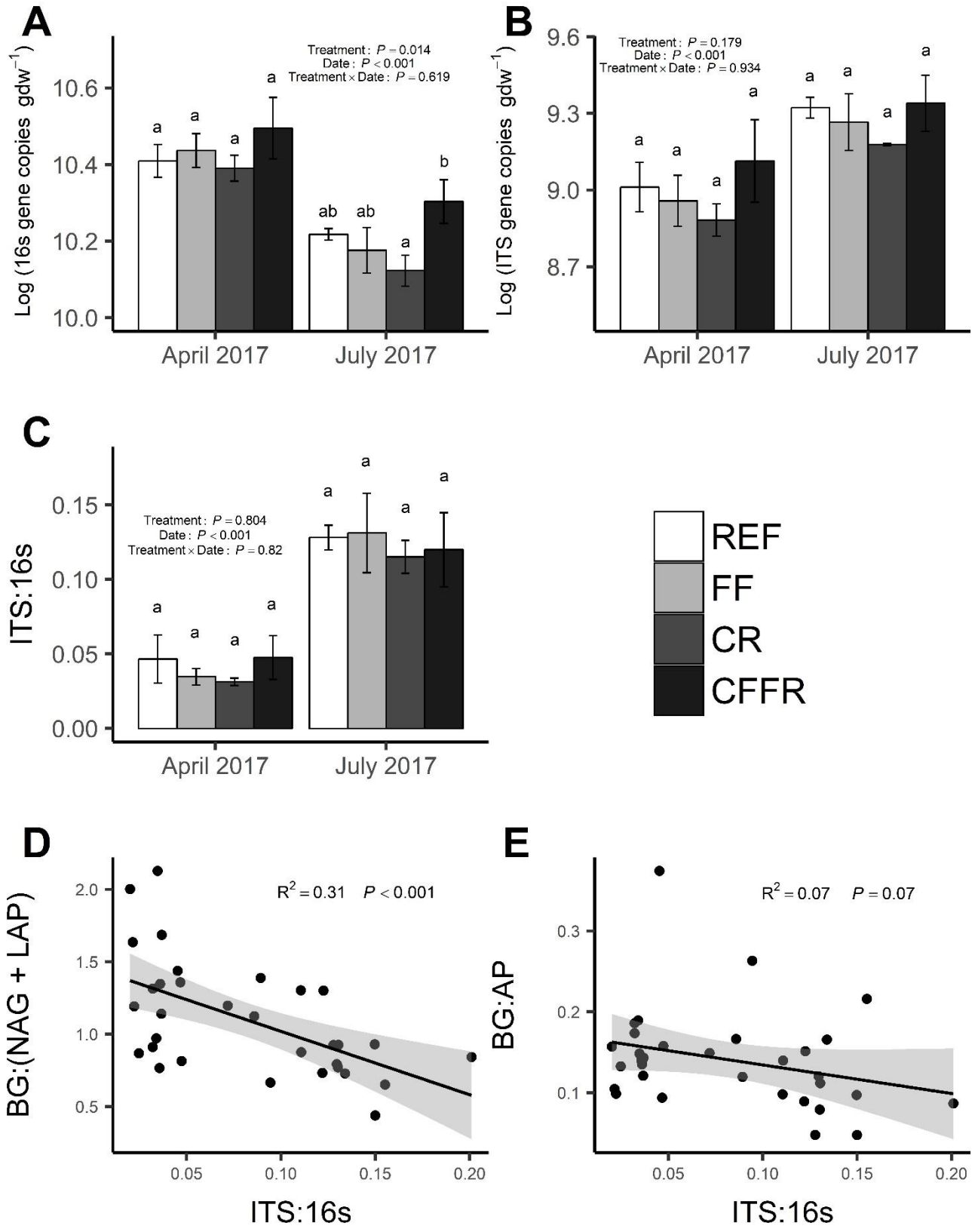
A
Log (16s gene copies gdw^{-1})
Treatment: $P = 0.014$
Date: $P < 0.001$
Treatment × Date: $P = 0.619$
10.6
10.4
10.2
10.0
a a a a ab ab a b
April 2017
July 2017
B
Log (ITS gene copies gdw^{-1})
Treatment: $P = 0.179$
Date: $P < 0.001$
Treatment × Date: $P = 0.934$
9.6
9.3
9.0
8.7
a a a a a a a a
April 2017
July 2017
C
ITS:16s
Treatment: $P = 0.804$
Date: $P < 0.001$
Treatment × Date: $P = 0.82$
0.15
0.10
0.05
0.00
a a a a a a a a
April 2017
July 2017
REF
FF
CR
CFFR
D
BG:(NAG + LAP)
$R^2 = 0.31$ $P < 0.001$
2.0
1.5
1.0
0.5
0.05 0.10 0.15 0.20
ITS:16s
E
BG:AP
$R^2 = 0.07$ $P = 0.07$
0.3
0.2
0.1
0.05 0.10 0.15 0.20
ITS:16s

Figure 2.5: Bacterial (16s) abundance **(A)**, fungal (ITS) abundance **(B)**, and F:B ratios **(C)** across treatments and sample dates. Also shown are relationships between C:N enzyme ratios and F:B ratios **(D)** and relationships between C:P enzyme ratios and F:B ratios **(E)**. Bars represent means while error bars are ± one standard error. *P*-values presented are linear mixed model effects of treatment, sampling date, and treatment x date interactions. Different letters represent significant differences between treatments within a sampling date ($P < 0.05$). Treatment abbreviations are as follows: reference (REF), O-horizon removal (FF), canopy removal (CR), and canopy + O-horizon removal (CFFR).

Tables

Table 2.1

Enzyme	Abbreviation	Enzyme Function
β-glucosidase	BG	Cellulose degradation
β-xylosidase	XYL	Hemicellulose degradation
β-D-cellubiosidase	CHB	Cellulose degradation
Acid Phosphatase	AP	Phosphorus mineralization
Leucine aminopeptidase	LAP	Protein depolymerization
N-acetyl-β-glucosaminidase	NAG	Chitin degradation
Phenol oxidase	POX	Lignin degradation
Peroxidase	PER	Lignin degradation

Table 2.1: Extracellular enzymes assayed in this study, their abbreviations, and their functions.

Table 2.2

Treatment	DOC	MBC	MBN	NH_4	NO_3	pH
REF	697^{a*} (55.8)	240^{a} (21.6)	42.7^{a} (4.61)	3.70^{a} (0.672)	0.042^{a} (0.014)	4.86 (0.111)
FF	721^{ab} (59.9)	306^{ab} (35.7)	53.8^{a} (7.96)	3.25^{a} (0.526)	0.031^{a} (0.011)	4.89 (0.274)
CR	635^{a} (31.3)	315^{ab} (45.9)	55.9^{a} (6.93)	3.19^{a} (0.228)	0.041^{a} (0.039)	4.97 (0.272)
CFFR	932^{b} (89.9)	530^{b} (126)	96.9^{b} (13.9)	6.54^{b} (0.978)	0.139^{b} (0.035)	4.75 (0.249)
	Linear Mixed Models					
Effects						
Treatment	**0.008**	**0.005**	**<0.001**	**0.001**	**<0.001**	0.438

Table 2.2: DOC, MBC, MBN, TDN, NH_4, NO_3, and pH across treatments. Means followed by one standard error are presented. Units for DOC and MBC are μg C g $soil^{-1}$ while units for MBN, NH_4, and NO_3 are μg N g $soil^{-1}$. Different superscript letters indicate significant pairwise differences ($P < 0.05$), while asterisks indicate marginally significant differences ($P < 0.1$). Linear mixed models with significant effects ($P < 0.05$) are presented in bold. Treatment abbreviations are as follows: reference (REF), O-horizon removal (FF), canopy removal (CR), and canopy + O-horizon removal (CFFR).

Table 2.3

	BG	CHB	XYL	AP	LAP	NAG	POX	PER
16s	**0.381**	**0.500**	**0.394**	0.224	0.161	0.029	0.009	0.059
Abundance	0.032	0.004	0.026	0.218	0.378	0.876	0.962	0.505
ITS	0.117	0.062	0.288	**0.358**	0.264	**0.391**	-0.343	0.122
Abundance	0.523	0.736	0.110	0.044	0.144	0.027	0.055	0.574

Table 2.3: Pearson correlation coefficients between 16s (bacterial) abundance, ITS (fungal) abundance, and eight extracellular enzymes. Values represent correlation coefficients (upper lines) and *P* values (lower lines). Correlation coefficients in bold represent significant relationships between variables ($P < 0.05$).

Supplementary Figures

Figure 2.S1

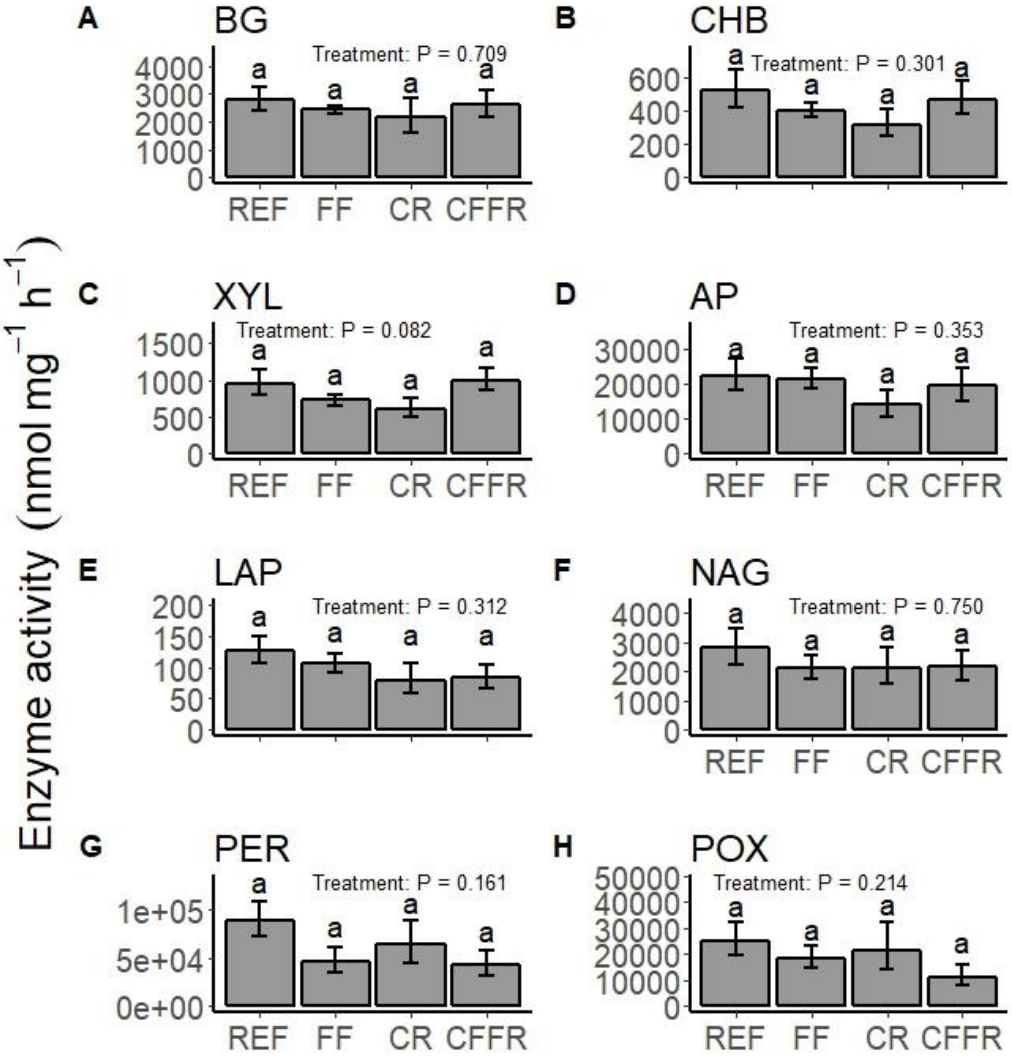

Figure 2.S1: Individual extracellular enzyme activities corrected for microbial biomass across treatments: **(A)** BG, **(B)** CHB, **(C)** XYL, **(D)** AP, **(E)** LAP, **(F)** NAG, **(G)** POX, and **(H)** PER. Bars represent means while error bars are ± one standard error. P-values presented are linear mixed model effects of treatment. Different letters represent significant differences between treatments ($P < 0.05$). Treatment abbreviations are as follows: reference (REF), forest floor removal (FF), canopy removal (CR), and canopy + forest floor removal (CFFR).

Supplementary Tables

Table 2.S1

Response Variable	Model	ΔAICc	AICc Weight	Best Supported Model
TDN	~Treatment	5.11	0.07	~Treatment x Date
	~Treatment x Date	0.00	0.93	
DOC	~Treatment	0.00	0.98	~Treatment
	~Treatment x Date	7.98	0.02	
MBC	~Treatment	0.00	0.99	~Treatment
	~Treatment x Date	8.76	0.01	
MBN	~Treatment	0.00	0.91	~Treatment
	~Treatment x Date	4.60	0.09	
NO_3	~Treatment	0.00	0.98	~Treatment
	~Treatment x Date	8.11	0.02	
NH_4	~Treatment	0.00	0.90	~Treatment
	~Treatment x Date	4.30	0.10	
pH	~Treatment	0.00	0.99	~Treatment
	~Treatment x Date	9.29	0.01	

Table 2.S1: AIC model selection output for soil chemistry and microbial biomass variables

Table 2.S2

Response Variable	Model	ΔAICc	AICc Weight	Best Supported Model
BG	~Treatment	0.00	0.99	~Treatment
	~Treatment x Date	9.00	0.01	
CHB	~Treatment	0.00	0.73	~Treatment
	~Treatment x Date	2.03	0.27	
XYL	~Treatment	0.00	1.00	~Treatment
	~Treatment x Date	11.58	0.00	
AP	~Treatment	0.00	0.97	~Treatment
	~Treatment x Date	7.02	0.03	
LAP	~Treatment	0.00	0.99	~Treatment
	~Treatment x Date	9.72	0.01	
NAG	~Treatment	0.00	0.98	~Treatment
	~Treatment x Date	8.24	0.02	
POX	~Treatment	0.00	1.00	~Treatment
	~Treatment x Date	12.35	0.00	
PER	~Treatment	0.00	1.00	~Treatment
	~Treatment x Date	12.21	0.00	

Table 2.S2: AIC model selection output for dry soil mass-corrected extracellular enzyme activities

Table 2.S3

Response Variable	Model	ΔAICc	AICc Weight	Best Supported Model
BG	~Treatment	0.00	0.99	~Treatment
	~Treatment x Date	10.26	0.01	
CHB	~Treatment	0.00	1.00	~Treatment
	~Treatment x Date	14.27	0.00	
XYL	~Treatment	0.00	0.96	~Treatment
	~Treatment x Date	6.41	0.04	
AP	~Treatment	0.00	0.95	~Treatment
	~Treatment x Date	5.81	0.05	
LAP	~Treatment	0.00	0.94	~Treatment
	~Treatment x Date	5.62	0.06	
NAG	~Treatment	0.00	0.92	~Treatment
	~Treatment x Date	4.98	0.08	
POX	~Treatment	0.00	1.00	~Treatment
	~Treatment x Date	13.67	0.00	
PER	~Treatment	0.00	1.00	~Treatment
	~Treatment x Date	11.38	0.00	

Table 2.S3: AIC model selection output for microbial biomass-corrected extracellular enzyme activities

Table 2.S4

Response Variable	Model	ΔAICc	AICc Weight	Best Supported Model
C:N	~Treatment	5.17	0.07	~Treatment x Date
	~Treatment x Date	0.00	0.93	
C:P	~Treatment	2.81	0.20	~Treatment x Date
	~Treatment x Date	0.00	0.80	
16s	~Treatment	17.55	0.00	~Treatment x Date
	~Treatment x Date	0.00	1.00	
ITS	~Treatment	3.14	0.17	~Treatment x Date
	~Treatment x Date	0.00	0.83	
ITS:16s	~Treatment	23.62	0.00	~Treatment x Date
	~Treatment x Date	0.00	1.00	

Table 2.S4: AIC model selection output for C:N and C:P enzyme ratios, Bacterial (16s) and Fungal (ITS) abundance, and Fungal:Bacterial ratios (ITS:16s).

CHAPTER 3 - Soil bacterial and fungal communities exhibit distinct long-term responses to disturbance in temperate forests

Authors:

Ernest D Osburn, Steven G McBride, Frank O Aylward, Brian D Badgley, Brian D Strahm, Jennifer D Knoepp, J E Barrett

Published in *Frontiers in Microbiology*:

Osburn, E. D., McBride, S.G., Aylward, F.O., Badgley, B.D, J. D. Knoepp, Strahm, B.D., and J. E. Barrett. 2019. Soil bacterial and fungal communities exhibit distinct long-term responses to disturbance in temperate forests. *Frontiers in Microbiology* 10:2872.

Abstract

In Appalachian ecosystems, forest disturbance has long-term effects on microbially-driven biogeochemical processes such as nitrogen (N) cycling. However, little is known regarding long-term responses of forest soil microbial communities to disturbance in the region. We used 16S and ITS sequencing to characterize soil bacterial (16S) and fungal (ITS) communities across forested watersheds with a range of past disturbance regimes and adjacent reference forests at the Coweeta Hydrologic Laboratory in the Appalachian mountains of North Carolina. Bacterial communities in previously disturbed forests exhibited consistent responses, including increased alpha diversity and increased abundance of copiotrophic (e.g., Proteobacteria) and N-cycling (e.g., Nitrospirae) bacterial phyla. Fungal community composition also showed disturbance effects, particularly in mycorrhizal taxa. However disturbance did not affect fungal alpha diversity, and disturbance effects were not consistent at the fungal class level. Co-occurrence networks constructed for bacteria and fungi showed that disturbed communities were characterized by more connected and tightly clustered network topologies, indicating that disturbance alters not only community composition but also

potential ecological interactions among taxa. Though bacteria and fungi displayed different long-term responses to forest disturbance, our results demonstrate clear responses of important bacterial and fungal functional groups (e.g., nitrifying bacteria and mycorrhizal fungi), and suggest that both microbial groups play key roles in the long-term alterations to biogeochemical processes observed following forest disturbance in the region.

Introduction

Globally, land use change has modified 75% of ice-free terrestrial ecosystems (Ellis 2011), with conversion of forests to managed states (e.g., agriculture, timber plantations) being one of earth's dominant land conversions (Vitousek et al. 1997, Foley et al. 2005, Rudel et al. 2005). Though ~50% of Earth's land surface was forested in prehistoric times, approximately 40% of that forest cover has been lost and much of the remaining forest subjected to various forms of disturbance, especially within the past two centuries (Millenium Ecosystem Assessment 2005). The extent of anthropogenic forest conversion continues to accelerate in the 21st Century (Drummond and Loveland 2010, Hansen et al. 2010, Watson et al. 2014), highlighting the need to characterize impacts of forest disturbance on terrestrial biodiversity and ecosystem functions. Understanding these impacts is particularly critical from a biogeochemical perspective, as forested ecosystems are central components of Earth's elemental cycles and provide ecosystem services that support human well-being, including storage of carbon (C), regulation of nutrient cycles, and provisioning of clean drinking water (Millenium Ecosystem Assessment 2005). These biogeochemical processes and associated ecosystem services are primarily driven by soil microorganisms, which perform a variety of essential functions including litter

decomposition and several C- and nitrogen (N)-cycling processes (Fierer 2017), thus emphasizing the need for studies investigating effects of forest disturbance on soil microbial communities.

Forest disturbances influence multiple factors that can affect terrestrial microorganisms, including vegetation characteristics (i.e., plant biomass, species composition) as well as several soil physicochemical properties. For example, disturbance alters forest soil C and N stocks (Guo and Gifford 2002, Foote et al. 2015, James and Harrison 2016), both of which are known drivers of microbial community structure (e.g., Eilers et al., 2010; Ramirez et al., 2012). Several previous studies have directly assessed effects of forest disturbances on soil microbial communities: timber harvest (Kohout et al. 2018, Mushinski et al. 2018b, 2018a), conversion to agriculture (Jangid et al. 2011, Rodrigues et al. 2013, Zhou et al. 2018), and prescribed fire (Oliver et al. 2015, Shen et al. 2016) can all alter bacterial and/or fungal communities. Additionally, a recent global meta-analysis showed consistent bacterial community changes in previously disturbed forests, including increased relative abundance of r-selected bacterial phyla (e.g., Proteobacteria) with past disturbance (Zhou et al. 2018). Though these prior studies suggest that forest soil microbial community shifts in response to disturbance are likely to occur, no studies to our knowledge have fully characterized long-term (i.e., several decades) responses of both soil bacterial and fungal communities to several different past disturbances (e.g., timber harvest, agricultural conversion, timber plantation conversion) simultaneously in temperate forests.

Understanding disturbance responses of soil microbial communities is particularly important in forests of the Appalachian region of the Eastern US, where approximately

70% of land area is forested (Simon et al. 2005) and nearly all forested ecosystems in the region have experienced past disturbances from human activities, including commercial logging and/or conversion to agriculture (Gragson and Bolstad 2006). Further, forest disturbance is known to have long-term effects on biogeochemical cycling in these ecosystems; previous studies from the region have shown impacts of disturbance on watershed-scale N-cycling (Vitousek et al. 1979, Peterjohn et al. 1996, Swank and Vose 1997), with previously disturbed forested watersheds often exporting N at elevated rates for several decades following disturbance (Webster et al. 2016). Some prior studies in the region assessed long-term effects of disturbance on soil microbial N-cycle functions, finding elevated nitrification rates (Montagnini et al. 1986, Keiser et al. 2016) and elevated abundance of nitrifying microorganisms (Lin et al. 2017) in previously disturbed forests. However, though one previous study documented effects of previous logging and conversion to agriculture on PLFA-determined soil microbial community structure in the Appalachians (Fraterrigo et al. 2006), relatively little is known regarding long-term disturbance impacts on bacterial and fungal communities in the region.

To address questions of long-term soil microbial responses to past forest disturbance, we characterized soil bacterial and fungal communities from four previously disturbed forested watersheds as well as adjacent reference forests at the Coweeta Hydrologic Laboratory in the Appalachian mountains of North Carolina. Because bacterial community structure is driven primarily by soil physicochemical variables (Fierer and Jackson 2006) and because these variables (e.g., soil NO_3^-) respond similarly to different disturbances in the region (e.g., Keiser et al., 2016), we predicted that bacterial communities would display generally consistent responses across different past

disturbances. More specifically, we predicted higher relative abundance of bacterial taxa associated with N-cycling processes in previously disturbed forests (i.e., nitrifiers) and that elevated soil inorganic-N in disturbed forests would promote higher relative abundance of r-selected (i.e., copiotrophic) soil bacterial taxa. In contrast, because fungal communities are often closely coupled to plant communities (Bonfante and Anca 2009, Peay et al. 2013), and because different forest conversions have unique effects on plant communities, we predicted fungal responses to be site-specific. For example, we predicted pine conversion to increase abundance of ectomycorrhizal (ECM) fungi, while disturbances that promote arbuscular mycorrhizal (AM) hosts (e.g. red maple, tulip poplar) to increase abundance of AM fungi.

Materials and Methods

Site Description and Soil Sampling

We conducted this study at the Coweeta Hydrologic Laboratory, a USDA Forest Service experimental forest located in the Blue Ridge physiographic province in the Appalachian Mountains of southwestern North Carolina (latitude 35°03′ N, longitude 83°25′ W). Within the Coweeta Basin, we selected four forested watersheds that experienced whole-watershed disturbances associated with forest management experiments conducted by the USDA Forest Service at different times during the 20th Century. All disturbed watersheds are currently forested and have not been manipulated since disturbances occurred ~4-8 decades ago (Table 3.1). Previous disturbances included clear-cutting, commercial clear cut-cable logging, conversion to pasture, and conversion to pine monoculture (Table 3.1, Figure 3.1). Adjacent to each previously disturbed watershed is a reference watershed (Figure 3.1) that has not been disturbed since the time

period 1919-1923, when ~20% of the basal area of the entire Coweeta Basin was cut and harvested (Elliott and Vose 2011). Detailed information, including size, aspect, and dominant vegetation of each watershed can be found on Supplementary Table 3.S1. Within each of the eight watersheds, we established six 4 m x 4 m plots (48 plots total) at 40 m intervals along a 200 m stretch of the main stream channel. All plots were located 5 m upslope from the stream itself. We sampled near-stream environments because these areas support high rates of microbial biogeochemical processes (Knoepp and Clinton 2009) and because spatially consistent sampling across watersheds of varying sizes (Supplementary Table 3.S1) enabled cross-watershed comparisons. In June 2018, at the height of the growing season, we surveyed all woody vegetation and sampled five soil cores (from four plot corners and plot center) from each plot. Soil samples included the top 10 cm of mineral soil and did not include O-horizon material. This sampling depth generally includes the entire A horizon in low elevation watersheds (Knoepp and Swank 1994) and coincides with the depth of sampling in many research studies in the Coweeta Basin (e.g., Knoepp et al., 2018; Osburn et al., 2018). We composited samples by plot, sieved composited samples (4 mm), and stored subsamples at -20°C (for DNA extraction) or 4°C (for measurement of soil properties) until further processing.

Soil Properties

Soil pH was measured in a 1:1 soil:DI H_2O mixture using a Hach Sension+ pH meter (Hach Company, Loveland, CO, USA). Soils were extracted for one hour with 2M KCl (1:5 soil:solution ratio) and extracts were analyzed for NH_4^+ and NO_3^- using a Lachat QuikChem flow injection analyzer (Hach Company, Loveland, CO, USA). Microbial Biomass C and N were determined using a modified chloroform extraction

method (Fierer and Schimel 2003a) and extracts were measured for dissolved organic carbon (DOC), total dissolved N, and microbial biomass C and N on an Elementar vario cube TOC/TN (Elementar Americas Inc, Mt. Laurel, NJ, USA). Soil subsamples were air dried, milled, and analyzed for total C and total N using an Elementar vario MAX cube (Elementar Americas Inc, Mt. Laurel, NJ, USA). Microbial activity was assessed via substrate-induced respiration (SIR) (Bradford et al. 2008). Gravimetric water content was measured by mass loss after oven drying at 105° C for 24 hours and all soil properties are presented on an oven-dried basis.

DNA Extraction and qPCR

DNA was extracted from ~0.25g fresh soil using the Qiagen DNeasy PowerSoil kit (Qiagen, Valencia, CA, USA) and extracts were quantified using a Qubit 2.0 fluorometer (Thermo Fisher Inc, Waltham, MA, USA). We estimated bacterial and fungal abundance by qPCR amplifying the 16S rRNA and ITS regions, respectively. For 16S rRNA qPCR we used the EUB 338/515 primer set while for ITS qPCR we used the ITS1f/5.8s primers (Fierer et al. 2005). Each qPCR reaction contained 10 µl Quantitect SYBR green master mix (Qiagen, Valencia, CA, USA), 2 µl of 1:10 diluted DNA template (~1-4 ng DNA), 0.25 µM forward and reverse primers, and nuclease-free H_2O to 20 µl. For both genes, thermal cycling conditions were as follows: 15 min at 95°C followed by 40 cycles of 15s at 94°C, 30s at 55°C, and 30s at 72°C. Standard curves were generated by amplifying serial dilutions of the target regions cloned into plasmids, with amplification efficiencies ranging from 87 to 92% and R^2 values >0.99. All amplifications were performed in triplicate and amplification specificity was assessed using melt curve analysis. 16S and ITS gene copy numbers were corrected for dry soil mass and fungal:bacterial ratios

(ITS:16S) were calculated by dividing fungal gene copy numbers by bacterial gene copy numbers (Fierer et al. 2005).

16S and ITS Sequencing and Bioinformatic Analysis

We characterized bacterial and fungal communities by amplifying and sequencing the V4 16S rRNA region and the ITS1 region, respectively. We amplified the V4 region using the 515F/806R primer pair (Apprill et al. 2015, Parada et al. 2016) and the ITS region using the ITS1F/ITS2 primer pair (Bellemain et al. 2010). We amplified samples in triplicate and PCR reactions contained 10 µl Thermo Fisher Platinum II Hot Start PCR Master Mix (Thermo Fisher Inc, Waltham, MA, USA), 1 µl undiluted DNA template (~5-20 ng DNA), 0.2 µM forward and reverse primer, and nuclease-free H_2O to 25 µl. We also amplified negative controls for each barcoded PCR primer to detect possible contamination. Thermal cycling conditions for 16S amplification were 2 min at 94°C followed by 35 cycles of 45 s at 94°C, 60 s at 50°C and 90 s at 72°C, with a 10 min final extension at 72°C. Conditions for ITS amplification were 2 min at 94°C followed by 35 cycles of 30 s at 94°C, 30 s at 52°C and 30 s at 68°C, with a 10 min final extension at 68°C. After amplification, we pooled triplicate PCR amplicons, visualized amplicons and negative controls on an agarose gel, and purified them using the Qiagen QIAquick PCR Purification Kit (Qiagen, Valencia, CA, USA). We quantified purified amplicons (see above) and pooled 16S and ITS amplicons separately in equimolar ratios. Amplicons were sequenced on the Illumina MiSeq platform using 250 bp paired-end reads. Due to poor quality scores for the ITS forward reads, we only processed and analyzed the reverse reads. Raw sequence reads were deposited in NCBI's BioProject database under accession number PRJNA548911.

We processed raw sequence reads using the QIIME2 pipeline (Bolyen et al. 2018). After demultiplexing, we joined paired-ends (16S only), denoised sequences, and removed chimeras using DADA2 (Callahan et al. 2016). We then used VSEARCH (Rognes et al. 2016) to cluster processed sequences into 97% OTUs and removed OTUs only appearing in one sample. After processing, we retained 2,511,186 sequences and 794,909 sequences for 16S and ITS, respectively. For downstream statistical analyses, we randomly selected 12,754 16S sequences and 7,038 ITS sequences from each sample to account for differences in sequencing depth. One sample was excluded from ITS sequence analysis due to insufficient sequencing depth. After random sampling, we retained 2,560 16S OTUs and 1,419 ITS OTUs for further analysis.

We assigned taxonomy to sequences using a naïve-bayes classifier (Pedregosa et al. 2011) trained on the Greengenes and UNITE databases for 16S and ITS, respectively (Abarenkov et al. 2010, McDonald et al. 2012). To assess potential bacterial life history shifts induced by disturbance, we categorized bacterial phyla as copiotrophic (i.e., r-selected, Proteobacteria + Bacteroidetes) or oligotrophic (i.e., K-selected, Acidobacteria + Actinobacteria) similar to the approach used by Zhou et al. (2018), and calculated copiotroph:oligotroph ratios for each sample. For functional analysis of fungal communities, we parsed fungal OTUs into functional guilds using FUNGuild (Nguyen et al. 2016). Similar to previous studies (e.g., Veach et al., 2017), we only analyzed sequences assigned to a single guild with a confidence of ‘probable’ or ‘highly probable.’

Statistical Analysis

All statistical analyses were performed in R (R Core Development Team 2019) using the ‘phyloseq’, ‘vegan’, ‘emmeans’, and ‘MASS’ packages (McMurdie and

Holmes 2013, Oksanen et al. 2019, Lenth et al. 2019, Ripley et al. 2019). For all statistical analyses, $P < 0.05$ was considered statistically significant while $P < 0.1$ was considered marginally significant, and all plots were considered independent replicates. We determined 16S and ITS alpha (i.e., Shannon) diversity using the 'estimate_richness' function in the phyloseq package and identified differentially abundant OTUs across disturbed and reference forests using the 'exactTest' function in the edgeR package (Robinson et al. 2010). To determine disturbance effects on Shannon diversity, copiotroph:oligotroph ratios, and relative abundance of phyla/classes/guilds, we used two-way ANOVAs with disturbance and watershed pair as factors in the models. Though we focus on main effects of disturbance from the ANOVAs, using watershed pair as a factor allowed us to determine pairwise differences between watersheds within each disturbed-reference pair using the emmeans package ('emmeans' and 'contrast' functions), though these pairwise differences should be interpreted with caution, as individual disturbances were not replicated. Where necessary, we log-transformed variables in order to meet assumptions of normality of residuals. When log transformation failed to normalize residuals, we verified ANOVA results using generalized linear models ('glm' function with gamma distribution and log-link function, MASS package).

We visualized 16S and ITS community structure using Non-Metric Multidimensional Scaling (i.e., NMDS, 'metaMDS' function, vegan package) with Bray-Curtis distance matrices (untransformed) and added key soil variables to the ordinations using the 'envfit' function (vegan package). We determined effects of disturbance on 16S and ITS community structure using PERMANOVA ('adonis2' function, vegan package).

We also used PERMANOVA to determine pairwise differences between watersheds in each disturbed-reference pair, with *P*-values adjusted using the Benjamini-Hochberg method to control for false discovery rate (Benjamini and Hochberg 1995). We used variation partitioning (Peres-Neto et al. 2006) to determine relationships between microbial communities, soil properties, and vegetation communities, and used distance-based redundancy analysis ('dbrda' function, Bray-Curtis distances, vegan package) to test the statistical significance of each partition.

To investigate responses of potential microbial community interactions to disturbance, we constructed bacterial and fungal co-occurrence networks for reference and disturbed forests separately by grouping communities from all 24 samples from each treatment. Similar to Shi et al. (2016), to ensure robustness of correlations used to construct networks, we only included OTUs that occurred in a minimum of 10 samples for each treatment. Spearman's rank correlations were used to calculate interaction strength among OTUs and network metrics were calculated using all significant OTU correlations ($P < 0.01$ and $|\rho| > 0.5$). For visualization purposes, we constructed random networks using code modified from Williams et al. (2014) available at https://github.com/ryanjw/co-occurrence. We then used the igraph package (Csardi and Nepusz 2006) to calculate degree centrality, closeness centrality, and betweenness centrality, all of which were normalized for each respective network. We also used igraph to calculate clustering coefficients for each node in each network. We identified differences in network topology (degree centrality, closeness centrality, betweenness centrality, and clustering coefficients) between disturbed and reference communities using Kruskal-Wallis tests, similar to the approach taken by Ma et al. (2016), while

proportion of negative edges was compared using Z-tests. Although statistical comparisons were performed on the full networks including all significant correlations, for purposes of visualization, our bacterial network diagrams only include correlations with $|\rho| > 0.7$.

Results

Soil Properties and Plant Communities

Disturbed forest soils were characterized by ~41% higher NH_4^+ concentrations, ~12% higher SIR, significantly higher pH, and ~900% higher NO_3^- concentration relative to reference forest soils (all ANOVA $P < 0.05$, Supplementary Table 3.S2). In contrast, reference soils had ~29% higher DOC concentrations, ~18% higher Microbial Biomass C, ~11% higher C:N ratios and ~19% higher DOC:TDN ratios (all ANOVA $P < 0.05$, Supplementary Table 3.S2) relative to disturbed soils. Vegetation surveys revealed distinct plant communities between reference and disturbed forests and also showed a significant disturbance x watershed pair interaction (both PERMANOVA $P < 0.001$, Supplementary Figure 3.S1), indicating unique effects of particular disturbance history on forest vegetation communities. In general, our vegetation analysis reflects known disturbance effects on woody vegetation previously described from Coweeta (i.e. increased abundance of species such as red maple and tulip poplar, see Supplementary Table 3.S1) (Elliott and Vose 2011).

Bacterial and Fungal Abundance, copiotroph:oligotroph ratios, and α Diversity

Bacterial (16S) gene copy abundance was marginally higher in disturbed watersheds (ANOVA $P = 0.07$, Supplementary Figure 3.S2A), while fungal (ITS) gene copy abundance was not affected by disturbance (ANOVA $P = 0.54$, Supplementary

Figure 3.S2B). ITS:16S gene copy ratios were ~23% higher in reference than in disturbed soils (ANOVA $P < 0.001$, Figure 3.2A), which was driven primarily by large differences between reference and disturbed forests in the pasture conversion and pine conversion watershed pairs (Supplementary Figure 3.S2C). ITS:16S gene copy ratios were negatively correlated with soil pH and positively correlated with soil DOC (Figure 3.2E). Disturbed soils had ~29% higher bacterial copiotroph:oligotroph ratios than reference soils (ANOVA $P < 0.001$, Figure 3.2B), a pattern that was consistent across all four disturbed-reference watershed pairs (Supplementary Figure 3.S3). Copiotroph:oligotroph ratios were positively correlated with soil pH, NO_3^-, and NH_4^+, and negatively correlated with soil C:N ratios (Figure 3.2E).

Bacterial Shannon diversity was significantly higher in disturbed forest soils (ANOVA $P < 0.001$, Figure 3.2C), which was generally consistent across all four past disturbances, but was most prominent in the pasture conversion disturbed-reference pair (Supplementary Figure 3.S4A). Bacterial Shannon diversity was positively correlated with soil pH, NO_3^-, and NH_4^+, and negatively correlated with soil DOC and C:N ratios (Figure 3.2E). Fungal Shannon diversity was not significantly different between disturbed and reference forest soils (ANOVA $P = 0.24$, Figure 3.2D, Supplementary Figure 3.S4B) but was positively correlated with soil pH (Figure 3.2E).

Bacterial and Fungal β Diversity Patterns

NMDS visualization of bacterial communities using Bray-Curtis distances showed clear, statistically significant separation of communities based on past forest disturbance (Figure 3.3A, PERMANOVA $P = 0.001$). Additionally, all pairwise comparisons between disturbed-reference watershed pairs were significant (PERMANOVA, all

adjusted $P < 0.05$). NMDS axis 1 was negatively correlated with soil C:N and DOC and positively correlated with soil NO_3^-, NH_4^+, and pH (Figure 3.3A). Variation partitioning showed soil chemistry accounting for 37% of observed variation in bacterial communities, 29% of which was independent of vegetation communities (Figure 3.3C). Vegetation communities accounted for 16% of observed variation in bacterial communities, 8% of which was independent of soil chemistry (Figure 3.3C). All partitions were statistically significant (distance-based redundancy analysis, all $P < 0.01$).

Similar to bacteria, NMDS visualization of fungal communities using Bray-Curtis distances showed statistically significant separation of communities based on past disturbance (Figure 3.3B, PERMANOVA $P = 0.001$). Pairwise comparisons were significant for the clear-cut, pine conversion, and pasture conversion watershed pairs (PERMANOVA, all adjusted $P < 0.05$), while the cable-logged watershed and its reference were marginally different (PERMANOVA adjusted $P = 0.065$). Similar to bacteria, fungal NMDS axis 1 was negatively correlated with soil C:N and DOC and positively correlated with soil NO_3^-, NH_4^+, and pH (Figure 3.3B). Variation partitioning for fungal communities showed soil chemistry accounting for 11% of observed fungal community variation and vegetation accounting for 9% of observed variation (Figure 3.3D) and all partitions were statistically significant (distance-based redundancy analysis, all $P < 0.001$).

Bacterial Phyla, Fungal Classes and Fungal Guilds

Aggregated across all samples, bacterial communities were dominated by the phyla Acidobacteria and Proteobacteria, which accounted for ~65% of sequences (Figure 3.4A). Relative abundance of several bacterial phyla displayed disturbance effects, with

Acidobacteria and Planctomycetes ~20% and ~12% higher in reference soils, respectively (ANOVA, both $P < 0.01$, Figure 3.4B). In contrast, Proteobacteria, Chloroflexi, Actinobacteria, and Nitrospirae had ~11%, ~23%, ~39%, and ~280% higher relative abundance in disturbed soils, respectively (ANOVA, all $P < 0.05$, Figure 3.4B). Pairwise comparisons within disturbed-reference watershed pairs indicated that these patterns were consistent across all disturbances for Acidobacteria, Proteobacteria, and Nitrospirae (Supplementary Table 3.S3). In contrast, disturbance effects for Planctomycetes and Chloroflexi were driven primarily by large differences in the pine conversion watershed pair, while effects for Actinobacteria were driven primarily by the clear-cut watershed pair (Supplementary Table 3.S3).

Fungal communities were dominated by class Agaricomycetes, which had marginally higher relative abundance in reference forest soils (~17% higher, ANOVA $P = 0.07$, Figure 3.4D) and comprised > 63% of sequences (Figure 3.4C). Other fungal classes with significant disturbance effects include Geminibasidiomycetes and Mucoromycotina, which had 73% and 85% higher relative abundance in reference soils, respectively, while Sordariomycetes and Eurotiomycetes had 67% and 150% higher relative abundances in disturbed soils, respectively (ANOVA, all $P < 0.05$, Figure 3.4D). However, pairwise comparisons within disturbed-watershed pairs revealed that disturbance effects for each class were driven primarily by only one watershed pair, with differences in Agaricomycetes, Sordariomycetes, and Eurotiomycetes driven by large differences in the pasture conversion pair (Supplementary Table 3.S4) and differences in Mucoromycotina and Geminibasidiomycetes driven by large differences in the cable-logged pair (Supplementary Table 3.S4).

Analysis of fungal sequences using FUNGuild resulted in ~46% of sequences confidently identified to a single functional guild (Figure 3.4E). Sequences identified as Arbuscular Mycorrhizae had ~83% higher relative abundance in disturbed soils, while Ectomycorrhizae had ~52% higher relative abundance in reference soils (ANOVA, both $P < 0.05$, Figure 3.4F). Pairwise comparisons within disturbed-reference watershed pairs showed this pattern was consistent for both groups of mycorrhizae across all disturbances except for pine conversion, which showed the reverse patterns (i.e., higher Ectomycorrhizae and lower Arbuscular mycorrhizae with pine conversion, Supplementary Table 3.S5). Additionally, animal pathogens showed higher relative abundance with pasture conversion while endophytes showed higher relative abundance with pine conversion (ANOVA, both $P < 0.05$, Figure 3.4F, Supplementary Table 3.S5)

Differentially abundant OTUs

EdgeR identified 298 bacterial OTUs as differentially abundant between disturbed and reference sites, ~69% of which belonged to Acidobacteria and Proteobacteria (Figure 3.5A). Phylum-level analysis of these OTUs showed largely the same pattern as the full OTU dataset (Figure 3.4B, Figure 3.5C), but disturbance effects for all phyla were significant (ANOVA, all $P < 0.01$, Figure 3.5C), indicating that differentially abundant bacterial taxa exhibit generally consistent disturbance responses at the phylum level. Additionally, though the pasture conversion and clear cut watershed pairs showed the largest pairwise differences, patterns of relative abundance were consistent across all watershed pairs for all phyla (Supplementary Table 3.S6), indicating consistent phylum-level responses to different past disturbances.

EdgeR identified 196 fungal OTUs as differentially abundant between disturbed and reference sites, ~90% of which belonged to class Agaricomycetes (Figure 3.5B). Class-level analysis of these OTUs showed that only Agaricomycetes, Sordariomycetes, Eurotiomycetes, and Motierellomycetes had significant disturbance effects (all $P < 0.05$, Figure 3.5D), and similar to the full OTU dataset, effects for each respective class were driven primarily by a single watershed pair (Supplementary Table 3.S7), indicating that fungal disturbance responses were not consistent at the class level or across different past disturbances.

Co-occurrence Networks

Network analysis of bacterial communities showed distinct network topologies between reference and disturbed forest soils (Figure 3.6A,B). The disturbed network had more nodes (546 vs 451) and edges (14,174 vs 6,216) compared with reference communities (Figure 3.6A,B, Table 3.2), while the reference network had a higher proportion of negative edges than the disturbed network (0.15 vs 0.09, Z-test $P < 0.001$, Table 3.2). The disturbed network had more connections per node (65% higher degree centrality), nodes that were closer on average to all other nodes in the network (10% higher closeness centrality), and nodes that were more tightly clustered together (20% higher clustering coefficient) than nodes in the reference network (all Kruskal-Wallis $P < 0.001$, Table 3.2). Also, the disturbed network had 28% lower betweenness centrality (Kruskal-Wallis $P < 0.001$, Table 3.2), indicating that nodes are less likely to bridge the shortest path between two nodes than nodes in the reference network.

Topologies were also distinct between reference and disturbed communities for fungal co-occurrence networks (Figure 3.6C,D). Similar to the bacterial networks, the

disturbed fungal network had more nodes (61 vs 55) and edges (279 vs 95) than the reference network (Table 3.2). However, there was no difference in the proportion of negative edges between the disturbed and reference networks (Z-test, $P = 0.45$, Table 3.2) for fungi. Also similar to the bacterial networks, the disturbed fungal network had more connections per node (305% higher degree centrality), nodes that were closer to other nodes in the network (676% higher closeness centrality), and nodes that were more tightly clustered than in the reference network (all Kruskal-Wallis $P < 0.05$, Table 3.2). However, unlike the bacterial networks, the disturbed fungal network had 531% higher betweenness centrality (Kruskal-Wallis, $P = 0.034$, Table 3.2), indicating that nodes are more likely to bridge the shortest path between two nodes than nodes in the reference network.

Discussion

Bacterial responses are consistent across different disturbance histories

Disturbance alters forest soil properties (e.g., increases NO_3^- and pH, Supplementary Table 3.S2) and processes (e.g., increases N-cycling rates) (Keiser et al. 2016), which we predicted would be associated with consistent long-term responses of soil bacterial communities across several different past disturbances. Our results are consistent with this prediction, as reference and disturbed bacterial communities were distinct in terms of community composition (Figure 3.3A), Shannon diversity (Figure 3.2B), copiotroph:oligotroph ratios (Figure 3.2C), and ITS:16S ratios (Figure 3.2A). Similar results were presented in a recent global meta-analysis of bacterial response to forest degradation (Zhou et al. 2018). Additionally, bacteria exhibited clear disturbance responses at high taxonomic levels, (Figure 3.4B), and taxonomic analysis of

differentially abundant OTUs revealed consistent patterns, with all dominant bacterial phyla (> 1% of sequences) showing significant disturbance effects (Figure 3.5C, Supplementary Table 3.S6). Importantly, the phylum Nitrospirae, a bacterial group involved in N-cycling processes (nitrite-oxidation, commamox), displayed particularly strong disturbance responses, with nearly three-fold higher relative abundance in disturbed soils (Figure 3.4B). Bacterial co-occurrence networks also showed clear disturbance responses, with the disturbed network exhibiting more clustering, more connections among OTUs, and a lower proportion of negative correlations among OTUs (Figure 3.6A,B, Table 3.2) relative to the reference network. Thus, our network analyses suggest that disturbance affects not only the taxa present in soil bacterial communities but also alters potential ecological interactions among bacterial taxa. For example, reductions in negative correlations in the disturbed network may reflect fewer competitive interactions between bacterial taxa due to relaxation of nutrient limitation with increased inorganic-N availability. Overall, our results suggest that disturbance of forests in the Appalachian region fundamentally alters bacterial community structure and ecological interactions over decadal time scales and that these changes are consistent across a range of disturbance types, including agricultural conversion, conversion to timber plantation, and commercial clear-cutting.

The observed bacterial community metrics were strongly correlated with several soil properties (e.g., pH, inorganic-N, C:N ratios, Figure 3.2E), with soil chemistry accounting for 37% of observed variation in bacterial community structure (Figure 3.3C), consistent with previous studies demonstrating that soil physicochemical properties are the primary drivers of soil bacterial communities (e.g., Fierer and Jackson, 2006; Lauber

et al., 2008, 2009). The differences in soil properties observed in this study are likely linked to vegetation changes that occur during forest succession following disturbance. Early successional forests in this region are often dominated by N-fixing black locust (*Robinia pseudoacacia*) (Elliott and Vose 2011), which likely contributed to increased inorganic-N levels and lower soil C:N in disturbed watersheds. Vegetation differences may also be responsible for soil pH shifts, as previously disturbed watersheds in this study were associated with reduced abundance of species with acidic leaf litter such as rosebay rhododendron (*Rhododendron maximum*) and oaks (*Quercus spp.*) and increased abundance of species with higher pH litter such as red maple (*Acer rubrum*) and tulip poplar *(Liriodendron tulipifera*) (Supplementary Figure 3.S1), which over long time scales may have contributed to increased soil pH. In addition to vegetation changes, the pasture conversion watershed was limed in 1959, likely explaining the relatively high soil pH (~5.75) and clear disturbance effects on bacterial communities we observed for this site, including the highest observed bacterial Shannon diversity of all examined watersheds (Figure 3.2B).

Though bacterial responses to disturbance were largely consistent, we also observed some responses that varied among watersheds with different past disturbances. For example, changes in Chloroflexi and Planctomycetes were only observed in the pine conversion pair, while changes in Actinobacteria were only observed in the clear-cut pair (Figure 3.4B). These context-dependent effects may be related to unique effects of specific disturbances on plant communities observed in this study (e.g., conversion to pine monoculture, Supplementary Figure 3.S1), as vegetation accounted for a significant proportion of variation in bacterial communities, 8% of which was independent of soil

chemistry (Figure 3.3C). Though some prior studies have not found strong correlations between vegetation and soil bacterial communities (e.g., Fierer and Jackson, 2006; Jangid et al., 2011), our results suggest that these relationships may indeed exist and therefore vegetation should be considered when assessing responses of soil bacteria to environmental change.

Fungal responses vary among different disturbance histories

Fungal communities also showed evidence of long-term responses to past forest disturbance, with distinct fungal community composition between reference and disturbed soils (Figure 3.3B). Similar to bacteria, disturbed and reference fungal communities displayed distinct co-occurrence patterns, with the disturbed network displaying higher clustering and more connections among fungal OTUs (Figure 3.6C,D, Table 3.2). However, other fungal community metrics did not have consistent disturbance responses; fungal Shannon diversity was not different between reference and disturbed soils and disturbance responses were not consistent at the class level for the full OTU dataset (Figure 3.4C, Supplementary Table 3.S4) or for differentially abundant OTUs (Figure 3.5D, Supplementary Table 3.S7). The inconsistent responses we observed for fungi at the class level likely reflects the diversity of life strategies that occur within fungal classes. Another potential explanation for the observed responses is that fungal communities have high fidelity to plant communities (Bonfante and Anca 2009, Peay et al. 2013), and watersheds with different past disturbances sampled for this study displayed unique plant communities (Supplementary Figure 3.S1). Indeed, vegetation communities accounted for a significant proportion (9%) of observed variation in fungal communities (Figure 3.3D) and other studies in temperate forests have also noted the

importance of vegetation in structuring fungal communities (e.g., Goldmann et al., 2015). Analysis of fungal functional guilds also reflects the importance of vegetation in structuring fungal communities; our disturbed sites had lower abundance of tree species that host ectomycorrhizal fungi (ECM) such as oaks (i.e., *Quercus montana*, Supplementary Figure 3.S1), and our disturbed fungal communities indeed displayed lower relative abundance of ECM fungi (Figure 3.4F), with the exception of conversion to white pine (*Pinus strobus*) (Figure 3.4F), which is a known ECM host. Additionally, tree species that host arbuscular mycorrhizae (AM), such as red maple (*Acer rubrum*) and tulip poplar (*Liriodendron tulipifera*), were more abundant in our previously disturbed sites, and these communities featured higher relative abundance of AM fungi (Figure 3.4F), with the exception of conversion to pine (Figure 3.4F).

Soil properties also likely played a role in structuring fungal communities; soil chemistry accounted for a significant proportion of variation (11%) in fungal community composition (Figure 3.3D), and previous studies have found nutrient status (e.g., soil C:N) to be an important driver of soil fungal communities (Lauber et al. 2008). Though it is likely that both soil physicochemical properties and vegetation are important in structuring fungal communities, we were able to explain much less variation in fungal communities (~20% of variation explained, Figure 3.3C) relative to bacterial communities (~45% of variation explained, Figure 3.3D), suggesting that factors we did not consider, such as soil phosphorus, herbaceous vegetation, and elevation may be important in determining fungal community structure, as has been shown in other studies from temperate forests in the Appalachian region (Veach et al. 2017). Additionally, variation partitioning analysis of fungal guilds increased the proportion of explained

variation in fungal communities (~40% of variation explained, Supplementary Figure 3.S5), highlighting the potential usefulness of trait-based approaches for describing fungal communities in addition to taxonomy-based approaches.

Community shifts contribute to altered N-cycling after disturbance

In addition to documenting community shifts, our results cast new light on the role of soil microbial communities in long-term biogeochemical responses to disturbances that have been observed in Appalachian forests (e.g., Webster et al., 2016). Existing frameworks such as the mycorrhizal-associated nutrient economy (MANE) (Phillips et al., 2013) have been used to predict temperate forest N-cycling rates using known tree-mycorrhizal associations (ECM vs AM), informed by differences in nutrient acquisition pathways of ECM vs AM fungi. This framework predicts that forests dominated by trees with AM symbionts (e.g., maple, tulip poplar) will feature rapid N-cycling rates and soil N pools dominated by inorganic-N. These predictions are generally consistent with our results for mycorrhizal fungi (Figure 3.4F) and vegetation communities (Supplementary Figure 3.S1), and with previous studies on soil N-cycling (e.g., Keiser et al., 2016) from the region. However, our results suggest that the MANE framework and associated trees/mycorrhizae are part of a complex system of feedbacks in Appalachian forests that also includes land use history, forest successional dynamics, and soil bacterial communities. In these ecosystems, N-fixing black locust often dominates plant communities following disturbance (Elliott and Vose 2011), increasing soil inorganic-N and likely promoting increased abundance of copiotrophic bacterial taxa (Ramirez et al., 2012) (Figure 3.2B). Some bacterial copiotrophs have been linked to elevated N-mineralization rates in soil (Fierer et al. 2007), which may contribute to

persistently elevated inorganic-N pools even after successional declines of N-fixers. Higher inorganic-N facilitates N-acquisition by AM fungi, potentially promoting dominance of their maple and poplar hosts in disturbed sites, and the high pH litter of these tree species likely leads to higher pH in disturbed soils over long time scales. Increased soil pH further alters soil bacterial communities, including increased abundance of bacterial nitrifiers such as ammonia-oxidizers (Stempfhuber et al. 2015, Lin et al. 2017) and nitrite oxidizers (i.e., Nitrospirae, Figure 3.4B), likely resulting in elevated nitrification rates in soil (Norman and Barrett 2014, Keiser et al. 2016) and persistently increased rates of nitrate export from these previously disturbed watersheds (Swank and Vose 1997, Webster et al. 2016). The long-term responses we observed may not be universal across temperate forests, as other studies have reported different long-term forest N-cycle disturbance responses; for example, a previously disturbed forest in the northern Appalachians displayed reduced N-cycling rates relative to a reference forest (Goodale and Aber 2001). However, similar N-cycle responses to forest disturbance have been documented in several forests across the continental US (Vitousek et al., 1979), suggesting that similar microbial community responses may be expected across temperate forest ecosystems, at least in the short term.

Conclusions

Overall, our results show different long-term responses of bacterial and fungal communities to forest disturbance in Appalachian forests of the eastern US. A similar study from the region also showed distinct responses of bacteria and fungi along a forest recovery chronosequence following mine reclamation (Sun et al. 2017), further suggesting that different microbial groups will respond differently to environmental

change. Additionally, we noted striking differences in co-occurrence network characteristics between both bacterial and fungal communities in reference and disturbed soils. For both groups, disturbed communities showed more connected, clustered, and overall more complex networks (Figure 3.6, Table 3.2). Though co-occurrence patterns do not necessarily imply ecological relationships (Faust and Raes 2012), our networks suggest the possibility of fundamentally altered microbial community interactions following disturbance. For example, the more complex networks observed in disturbed soils suggest these soils are potentially characterized by more microbial interactions and overall higher biological activity (Karimi et al. 2017), which is supported by direct assays of microbial activity from these sites (i.e., higher SIR for disturbed soils, Supplementary Table 3.S2). Additionally, our networks show more potential negative interactions for fungi vs bacteria and for reference bacteria vs disturbed bacteria. Previous studies have suggested that negative ecological interactions (i.e., competition) increase microbial community stability under environmental change (Coyte et al. 2015), suggesting that fungal communities will be more resilient to perturbations (i.e., drought, warming) than bacterial communities, similar to observations in a grassland ecosystem (De Vries et al. 2018), and that reference bacterial communities will be more resilient than disturbed bacterial communities. Evaluating these hypotheses should be a priority for future research, as temperate forests are already experiencing stresses associated with climate change (i.e., increased drought frequency and severity) (Burt et al. 2018), likely altering the structure and biogeochemical functions of soil microbial communities and potentially threatening the critical ecosystem services they provide for the region.

Acknowledgements

We thank the Coweeta Hydrologic Laboratory, Southern Research Station, USDA Forest Service for support and Angela Wiesel for assistance with field soil sampling and laboratory analyses. We also thank Bobbie Niederlehner for help with analytical chemistry. Finally, we thank our reviewers, whose helpful comments greatly improved this manuscript. The use of trade or firm names in this publication is for reader information and does not imply endorsement by the U.S. Department of Agriculture of any product or service.

References

Abarenkov, K., Nilsson, R. H., Larsson, K.-H., Alexander, I. J., Eberhardt, U., Erland, S., et al. (2010). The UNITE database for molecular identification of fungi – recent updates and future perspectives. *New Phytol.* 186, 281–285.

Apprill, A., McNally, S., Parsons, R., and Weber, L. (2015). Minor revision to V4 region SSU rRNA 806R gene primer greatly increases detection of SAR11 bacterioplankton. *Aquat. Microb. Ecol.* 75, 129–137. doi:10.3354/ame01753.

Bellemain, E., Carlsen, T., Brochmann, C., Coissac, E., Taberlet, P., and Kauserud, H. (2010). ITS as an environmental DNA barcode for fungi: an in silico approach reveals potential PCR biases. *BMC Microbiol.* 10, 189. doi:10.1186/1471-2180-10-189.

Benjamini, Y., and Hochberg, Y. (1995). Controlling the False Discovery Rate: A Practical and Powerful Approach to Multiple Testing. *J. Royal Stat. Soc.* 57, 289–300. doi:10.1111/j.2517-6161.1995.tb02031.x.

Bolyen, E., Rideout, J. R., Dillon, M. R., Bokulich, N. A., Abnet, C., Al-Ghalith, G. A., et al. (2018). QIIME 2: Reproducible, interactive, scalable, and extensible microbiome data science. *PeerJ*. doi:10.7287/peerj.preprints.27295v2.

Bonfante, P., and Anca, I.-A. (2009). Plants, Mycorrhizal Fungi, and Bacteria: A Network of Interactions. *Annu. Rev. Microbiol.* 63, 363–383. doi:10.1146/annurev.micro.091208.073504.

Bradford, M. A., Fierer, N., and Reynolds, J. F. (2008). Soil carbon stocks in experimental mesocosms are dependent on the rate of labile carbon, nitrogen and phosphorus inputs to soils. *Funct Ecol.* 22, 964–974. doi:10.1111/j.1365-2435.2008.01404.x.

Burt, T. P., Ford Miniat, C., Laseter, S. H., and Swank, W. T. (2018). Changing patterns of daily precipitation totals at the Coweeta Hydrologic Laboratory, North Carolina, USA. *Int J Climatol* 38, 94–104. doi:10.1002/joc.5163.

Callahan, B. J., McMurdie, P. J., Rosen, M. J., Han, A. W., Johnson, A. J. A., and Holmes, S. P. (2016). DADA2: High-resolution sample inference from Illumina amplicon data. *Nat. Methods* 13, 581–583. doi:10.1038/nmeth.3869.

Coyte, K. Z., Schluter, J., and Foster, K. R. (2015). The ecology of the microbiome: Networks, competition, and stability. *Science* 350, 663–666. doi:10.1126/science.aad2602.

Csardi, G., and Nepusz, T. (2006). The igraph software package for complex network research. *InterJournal* Complex Systems, 1695. doi:http://igraph.org.

De Vries, F. T., Griffiths, R. I., Bailey, M., Craig, H., Girlanda, M., Gweon, H. S., et al. (2018). Soil bacterial networks are less stable under drought than fungal networks. *Nat. Commun.* 9, 3033. doi:10.1038/s41467-018-05516-7.

Drummond, M. A., and Loveland, T. R. (2010). Land-use Pressure and a Transition to Forest-cover Loss in the Eastern United States. *BioScience* 60, 286–298. doi:10.1525/bio.2010.60.4.7.

Eilers, K. G., Lauber, C. L., Knight, R., and Fierer, N. (2010). Shifts in bacterial community structure associated with inputs of low molecular weight carbon compounds to soil. *Soil Biol. Biochem.* 42, 896–903. doi:10.1016/j.soilbio.2010.02.003.

Elliott, K. J., and Vose, J. M. (2011). The contribution of the Coweeta Hydrologic Laboratory to developing an understanding of long-term (1934-2008) changes in managed and unmanaged forests. *For. Ecol. Manag.* 261, 900–910. doi:10.1016/j.foreco.2010.03.010.

Ellis, E. C. (2011). Anthropogenic transformation of the terrestrial biosphere. *Philos. Trans. R. Soc. A-Math. Phys. Eng. Sci.* 369, 1010–1035. doi:10.1098/rsta.2010.0331.

Faust, K., and Raes, J. (2012). Microbial interactions: from networks to models. *Nat. Rev. Microbiol.* 10, 538–550. doi:10.1038/nrmicro2832.

Fierer, N. (2017). Embracing the unknown: disentangling the complexities of the soil microbiome. *Nat. Rev. Microbiol.* 15, 579–590. doi:10.1038/nrmicro.2017.87.

Fierer, N., Bradford, M. A., and Jackson, R. B. (2007). Toward an ecological classification of soil bacteria. *Ecology* 88, 1354–1364.

Fierer, N., Jackson, J. A., Vilgalys, R., and Jackson, R. B. (2005). Assessment of Soil Microbial Community Structure by Use of Taxon-Specific Quantitative PCR Assays. *Appl. Environ. Microbiol.* 71, 4117–4120. doi:10.1128/AEM.71.7.4117-4120.2005.

Fierer, N., and Jackson, R. B. (2006). The diversity and biogeography of soil bacterial communities. *Proc. Natl. Acad. Sci. U.S.A.* 103, 626–631. doi:10.1073/pnas.0507535103.

Fierer, N., and Schimel, J. P. (2003). A Proposed Mechanism for the Pulse in Carbon Dioxide Production Commonly Observed Following the Rapid Rewetting of a Dry Soil. *Soil Sci. Soc. Am. J.* 67, 798. doi:10.2136/sssaj2003.0798.

Foley, J. A., DeFries, R., Asner, G. P., Barford, C., Bonan, G., Carpenter, S. R., et al. (2005). Global Consequences of Land Use. *Science* 309, 570–574. doi:10.1126/science.1111772.

Foote, J. A., Boutton, T. W., and Scott, D. A. (2015). Soil C and N storage and microbial biomass in US southern pine forests: Influence of forest management. *For. Ecol. Manag.* 355, 48–57. doi:10.1016/j.foreco.2015.03.036.

Fraterrigo, J. M., Balser, T. C., and Turner, M. G. (2006). Microbial community variation and its relationship with nitrogen mineralization in historically altered forests. *Ecology* 87, 570–579. doi:10.1890/05-0638.

Goldmann, K., Schöning, I., Buscot, F., and Wubet, T. (2015). Forest Management Type Influences Diversity and Community Composition of Soil Fungi across Temperate Forest Ecosystems. *Front. Microbiol.* 6. doi:10.3389/fmicb.2015.01300.

Goodale, C. L., and Aber, J. D. (2001). The Long-Term Effects of Land-Use History on Nitrogen Cycling in Northern Hardwood Forests. *Ecological Applications* 11, 253–267. doi:10.1890/1051-0761(2001)011[0253:TLTEOL]2.0.CO;2.

Gragson, T. L., and Bolstad, P. V. (2006). Land Use Legacies and the Future of Southern Appalachia. *Soc. Nat. Resour.* 19, 175–190. doi:10.1080/08941920500394857.

Guo, L. B., and Gifford, R. M. (2002). Soil carbon stocks and land use change: a meta analysis. *Glob. Change Biol.* 8, 345–360. doi:10.1046/j.1354-1013.2002.00486.x.

Hansen, M. C., Stehman, S. V., and Potapov, P. V. (2010). Quantification of global gross forest cover loss. *Proc. Natl. Acad. Sci. U.S.A.* 107, 8650–8655. doi:10.1073/pnas.0912668107.

James, J., and Harrison, R. (2016). The Effect of Harvest on Forest Soil Carbon: A Meta-Analysis. *Forests* 7, 308. doi:10.3390/f7120308.

Jangid, K., Williams, M. A., Franzluebbers, A. J., Schmidt, T. M., Coleman, D. C., and Whitman, W. B. (2011). Land-use history has a stronger impact on soil microbial community composition than aboveground vegetation and soil properties. *Soil Biol. Biochem.* 43, 2184–2193. doi:10.1016/j.soilbio.2011.06.022.

Karimi, B., Maron, P. A., Chemidlin-Prevost Boure, N., Bernard, N., Gilbert, D., and Ranjard, L. (2017). Microbial diversity and ecological networks as indicators of environmental quality. *Environ. Chem. Lett.* 15, 265–281. doi:10.1007/s10311-017-0614-6.

Keiser, A. D., Knoepp, J. D., and Bradford, M. A. (2016). Disturbance Decouples Biogeochemical Cycles Across Forests of the Southeastern US. *Ecosystems* 19, 50–61. doi:10.1007/s10021-015-9917-2.

Knoepp, J. D., and Clinton, B. D. (2009). Riparian zones in southern Appalachian headwater catchments: Carbon and nitrogen responses to forest cutting. *For. Ecol. Manag.* 258, 2282–2293. doi:10.1016/j.foreco.2009.04.006.

Knoepp, J. D., See, C. R., Vose, J. M., Miniat, C. F., and Clark, J. S. (2018). Total C and N Pools and Fluxes Vary with Time, Soil Temperature, and Moisture Along an Elevation, Precipitation, and Vegetation Gradient in Southern Appalachian Forests. *Ecosystems* 21, 1623–1638. doi:10.1007/s10021-018-0244-2.

Knoepp, J. D., and Swank, W. T. (1994). Long-Term Soil Chemistry Changes in Aggrading Forest Ecosystems. *Soil Sci. Soc. Am. J.* 58, 325. doi:10.2136/sssaj1994.03615995005800020010x.

Kohout, P., Charvátová, M., Štursová, M., Mašínová, T., Tomšovský, M., and Baldrian, P. (2018). Clearcutting alters decomposition processes and initiates complex

restructuring of fungal communities in soil and tree roots. *ISME J* 12, 692–703. doi:10.1038/s41396-017-0027-3.

Lauber, C. L., Hamady, M., Knight, R., and Fierer, N. (2009). Pyrosequencing-Based Assessment of Soil pH as a Predictor of Soil Bacterial Community Structure at the Continental Scale. *Appl. Environ. Microbiol.* 75, 5111–5120. doi:10.1128/AEM.00335-09.

Lauber, C. L., Strickland, M. S., Bradford, M. A., and Fierer, N. (2008). The influence of soil properties on the structure of bacterial and fungal communities across land-use types. *Soil Biol. Biochem.* 40, 2407–2415. doi:10.1016/j.soilbio.2008.05.021.

Lenth, R., Singmann, H., Love, J., Buerkner, P., and Herve, M. (2019). *emmeans: Estimated Marginal Means, aka Least-Squares Means*. Available at: https://CRAN.R-project.org/package=emmeans [Accessed May 3, 2019].

Lin, L., Norman, J. S., and Barrett, J. E. (2017). Ammonia-uptake kinetics and domain-level contributions of bacteria and archaea to nitrification in temperate forest soils. *Ecol. Modell.* 362, 111–119. doi:10.1016/j.ecolmodel.2017.08.016.

Ma, B., Wang, H., Dsouza, M., Lou, J., He, Y., Dai, Z., et al. (2016). Geographic patterns of co-occurrence network topological features for soil microbiota at continental scale in eastern China. *ISME J* 10, 1891–1901. doi:10.1038/ismej.2015.261.

McDonald, D., Price, M. N., Goodrich, J., Nawrocki, E. P., DeSantis, T. Z., Probst, A., et al. (2012). An improved Greengenes taxonomy with explicit ranks for ecological and evolutionary analyses of bacteria and archaea. *ISME J* 6, 610–618. doi:10.1038/ismej.2011.139.

McMurdie, P. J., and Holmes, S. (2013). phyloseq: An R Package for Reproducible Interactive Analysis and Graphics of Microbiome Census Data. *PLOS ONE* 8, e61217. doi:10.1371/journal.pone.0061217.

Millenium Ecosystem Assessment (2005). *Ecosystems and Human Well Being: Synthesis*. Washington, DC: Island Press.

Montagnini, F., Haines, B., Boring, L., and Swank, W. (1986). Nitrification potentials in early successional black locust and in mixed hardwood forest stands in the southern Appalachians, USA. *Biogeochemistry* 2, 197–210. doi:10.1007/BF02180195.

Mushinski, R. M., Gentry, T. J., and Boutton, T. W. (2018a). Organic matter removal associated with forest harvest leads to decade scale alterations in soil fungal communities and functional guilds. *Soil Biol. Biochem.* doi:10.1016/j.soilbio.2018.09.019.

Mushinski, R. M., Zhou, Y., Gentry, T. J., and Boutton, T. W. (2018b). Bacterial metataxonomic profile and putative functional behavior associated with C and N cycle processes remain altered for decades after forest harvest. *Soil Biol. Biochem.* 119, 184–193. doi:10.1016/j.soilbio.2018.01.008.

Nguyen, N. H., Song, Z., Bates, S. T., Branco, S., Tedersoo, L., Menke, J., et al. (2016). FUNGuild: An open annotation tool for parsing fungal community datasets by ecological guild. *Fungal Ecol.* 20, 241–248. doi:10.1016/j.funeco.2015.06.006.

Norman, J. S., and Barrett, J. E. (2014). Substrate and nutrient limitation of ammonia-oxidizing bacteria and archaea in temperate forest soil. *Soil Biol. Biochem.* 69, 141–146. doi:10.1016/j.soilbio.2013.11.003.

Oksanen, J., Blanchet, F. G., Friendly, M., Kindt, R., Legendre, P., McGlinn, D., et al. (2019). *vegan: Community Ecology Package*. Available at: https://CRAN.R-project.org/package=vegan [Accessed May 3, 2019].

Oliver, A. K., Callaham, M. A., and Jumpponen, A. (2015). Soil fungal communities respond compositionally to recurring frequent prescribed burning in a managed southeastern US forest ecosystem. *For. Ecol. Manag.* 345, 1–9. doi:10.1016/j.foreco.2015.02.020.

Osburn, E. D., Elliottt, K. J., Knoepp, J. D., Miniat, C. F., and Barrett, J. E. (2018). Soil microbial response to Rhododendron understory removal in southern Appalachian forests: Effects on extracellular enzymes. *Soil Biol. Biochem.* 127, 50–59. doi:10.1016/j.soilbio.2018.09.008.

Parada, A. E., Needham, D. M., and Fuhrman, J. A. (2016). Every base matters: assessing small subunit rRNA primers for marine microbiomes with mock communities, time series and global field samples. *Environ. Microbiol.* 18, 1403–1414. doi:10.1111/1462-2920.13023.

Peay, K. G., Baraloto, C., and Fine, P. V. (2013). Strong coupling of plant and fungal community structure across western Amazonian rainforests. *ISME J* 7, 1852–1861. doi:10.1038/ismej.2013.66.

Pedregosa, F., Varoquaux, G., Gramfort, A., Michel, V., Thirion, B., Grisel, O., et al. (2011). Scikit-learn: Machine Learning in Python. *J. Mach. Learn. Res.* 12, 2825–2830.

Peres-Neto, P. R., Legendre, P., Dray, S., and Borcard, D. (2006). Variation Partitioning of Species Data Matrices: Estimation and Comparison of Fractions. *Ecology* 87, 2614–2625. doi:10.1890/0012-9658(2006)87[2614:VPOSDM]2.0.CO;2.

Peterjohn, W. T., Adams, M. B., and Gilliam, F. S. (1996). Symptoms of nitrogen saturation in two central Appalachian hardwood forest ecosystems. *Biogeochemistry* 35, 507–522. doi:10.1007/BF02183038.

Phillips, R. P., Brzostek, E., and Midgley, M. G. (2013). The mycorrhizal-associated nutrient economy: a new framework for predicting carbon-nutrient couplings in temperate forests. *New Phytol.* 199, 41–51. doi:10.1111/nph.12221.

R Core Development Team (2017). *R: A Language and Environment for Statistical Computing*. Vienna, Austria: R Foundation for Statistical Computing Available at: http://www.R-project.org.

Ramirez, K. S., Craine, J. M., and Fierer, N. (2012). Consistent effects of nitrogen amendments on soil microbial communities and processes across biomes. *Glob. Change Biol.* 18, 1918–1927. doi:10.1111/j.1365-2486.2012.02639.x.

Ripley, B., Venables, B., Bates, D. M., ca 1998), K. H. (partial port, ca 1998), A. G. (partial port, and Firth, D. (2019). *MASS: Support Functions and Datasets for Venables and Ripley's MASS*. Available at: https://CRAN.R-project.org/package=MASS [Accessed May 3, 2019].

Robinson, M. D., McCarthy, D. J., and Smyth, G. K. (2010). edgeR: a Bioconductor package for differential expression analysis of digital gene expression data. *Bioinformatics* 26, 139–140. doi:10.1093/bioinformatics/btp616.

Rodrigues, J. L. M., Pellizari, V. H., Mueller, R., Baek, K., Jesus, E. da C., Paula, F. S., et al. (2013). Conversion of the Amazon rainforest to agriculture results in biotic

homogenization of soil bacterial communities. *Proc. Natl. Acad. Sci. U.S.A.* 110, 988–993. doi:10.1073/pnas.1220608110.
Rognes, T., Flouri, T., Nichols, B., Quince, C., and Mahé, F. (2016). VSEARCH: a versatile open source tool for metagenomics. *PeerJ* 4, e2584. doi:10.7717/peerj.2584.
Rudel, T. K., Coomes, O. T., Moran, E., Achard, F., Angelsen, A., Xu, J., et al. (2005). Forest transitions: towards a global understanding of land use change. *Glob. Environ. Change* 15, 23–31. doi:10.1016/j.gloenvcha.2004.11.001.
Shen, J., Chen, C. R., and Lewis, T. (2016). Long term repeated fire disturbance alters soil bacterial diversity but not the abundance in an Australian wet sclerophyll forest. *Sci. Rep.* 6, 19639. doi:10.1038/srep19639.
Shi, S., Nuccio, E. E., Shi, Z. J., He, Z., Zhou, J., and Firestone, M. K. (2016). The interconnected rhizosphere: High network complexity dominates rhizosphere assemblages. *Ecol. Lett.* 19, 926–936. doi:10.1111/ele.12630.
Simon, S. A., Collins, T. K., Kauffman, G. L., McNab, W. H., and Ulrey, C. J. (2005). Ecological zones in the southern Appalachians: first approximation. Asheville, NC: USDA Forest Service.
Stempfhuber, B., Engel, M., Fischer, D., Neskovic-Prit, G., Wubet, T., Schoening, I., et al. (2015). pH as a Driver for Ammonia-Oxidizing Archaea in Forest Soils. *Microb. Ecol.* 69, 879–883. doi:10.1007/s00248-014-0548-5.
Sun, S., Li, S., Avera, B. N., Strahm, B. D., and Badgley, B. D. (2017). Soil bacterial and fungal communities show distinct recovery patterns during forest ecosystem restoration. *Appl. Environ. Microbiol.*, AEM.00966-17. doi:10.1128/AEM.00966-17.
Swank, W. T., and Vose, J. M. (1997). Long-term nitrogen dynamics of Coweeta forested watersheds in the southeastern United States of America. *Glob. Biogeochem. Cycle* 11, 657–671. doi:10.1029/97GB01752.
Veach, A. M., Stokes, C. E., Knoepp, J., Jumpponen, A., and Baird, R. (2017). Fungal Communities and Functional Guilds Shift Along an Elevational Gradient in the Southern Appalachian Mountains. *Microb. Ecol.* doi:10.1007/s00248-017-1116-6.
Vitousek, P. M., Gosz, J. R., Grier, C. C., Melillo, J. M., Reiners, W. A., and Todd, R. L. (1979). Nitrate Losses from Disturbed Ecosystems. *Science* 204, 469–474.
Vitousek, P. M., Mooney, H. A., Lubchenco, J., and Melillo, J. M. (1997). Human domination of Earth's ecosystems. *Science* 277, 494–499.
Watson, S. J., Luck, G. W., Spooner, P. G., and Watson, D. M. (2014). Land-use change: incorporating the frequency, sequence, time span, and magnitude of changes into ecological research. *Front. Ecol. Environ.* 12, 241–249. doi:10.1890/130097.
Webster, J. R., Knoepp, J. D., Swank, W. T., and Miniat, C. F. (2016). Evidence for a Regime Shift in Nitrogen Export from a Forested Watershed. *Ecosystems* 19, 881–895. doi:10.1007/s10021-016-9974-1.
Williams, R. J., Howe, A., and Hofmockel, K. S. (2014). Demonstrating microbial co-occurrence pattern analyses within and between ecosystems. *Front. Microbiol.* 5. doi:10.3389/fmicb.2014.00358.
Zhou, Z., Wang, C., and Luo, Y. (2018). Effects of forest degradation on microbial communities and soil carbon cycling: A global meta-analysis. *Global Ecol Biogeogr* 27, 110–124. doi:10.1111/geb.12663.

Figures

Figure 3.1

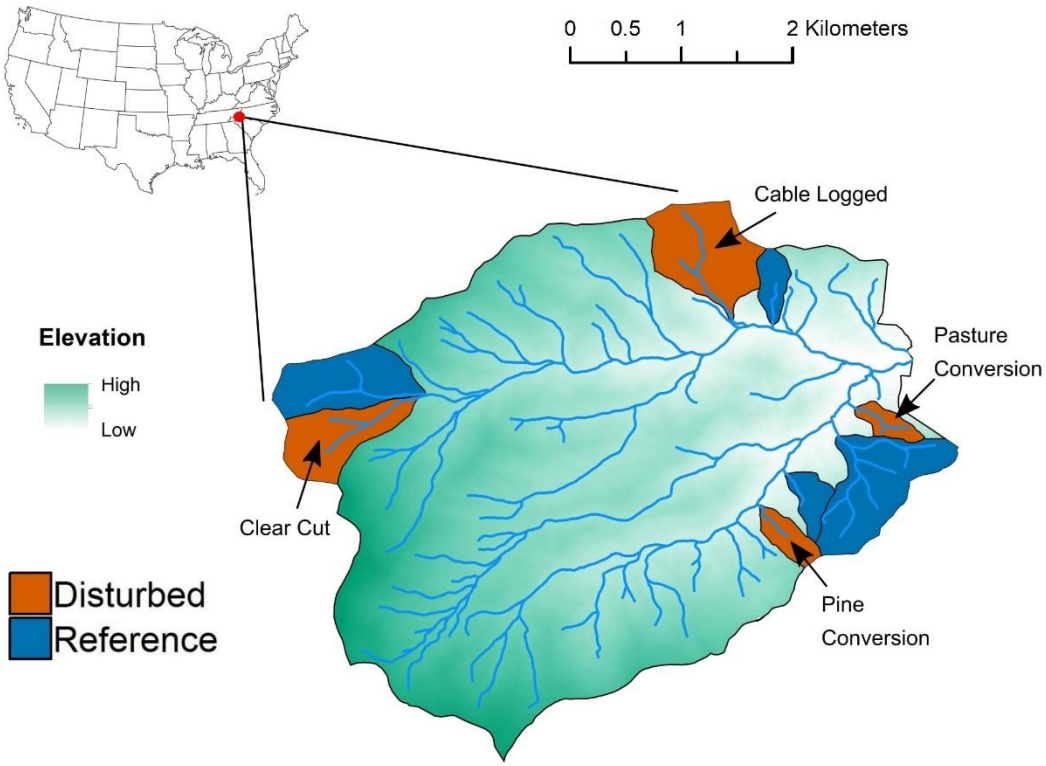

Figure 3.1: Map of disturbed-reference watershed pairs at the USDA Forest Service Coweeta Hydrologic Laboratory sampled for this study

Figure 3.2

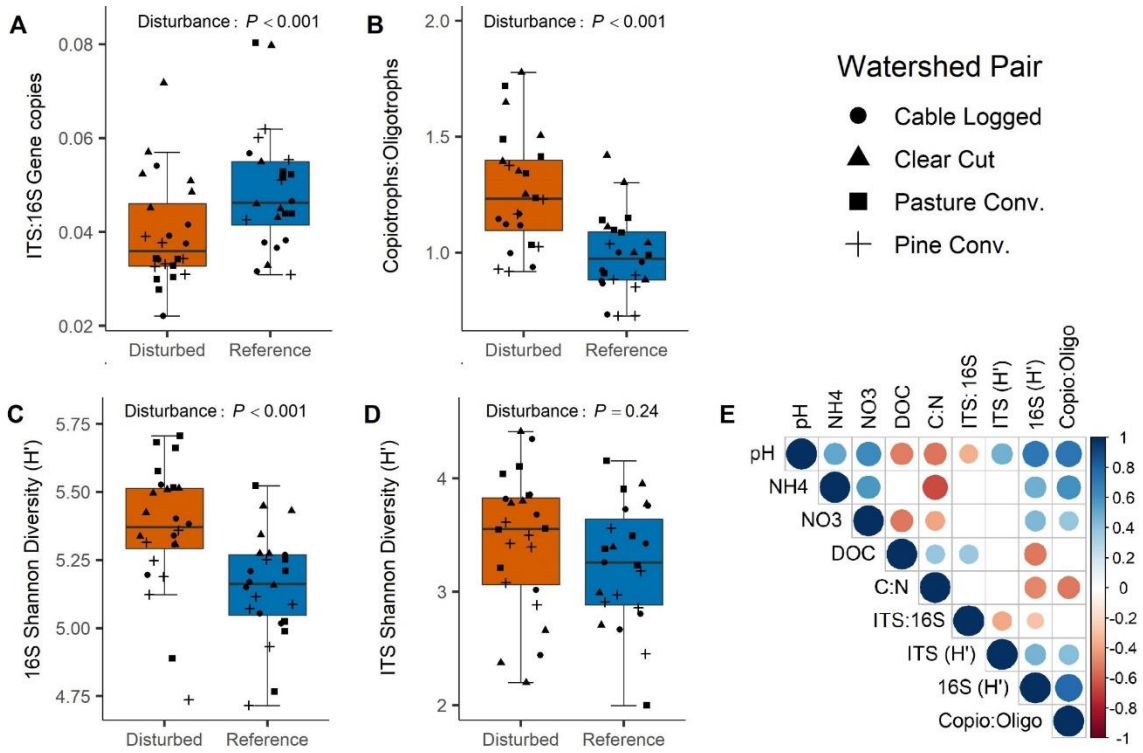

Figure 3.2: Effects of disturbance on ITS:16S gene copies (A), bacterial Copiotroph:Oligotroph ratios (B), 16S Shannon Diversity (C), and ITS Shannon Diversity (D). *P*-values are overall disturbance effects from two-way ANOVA. Correlogram (E) visualizes Spearman rank correlation coefficients between microbial variables from panels A-D and key soil variables (only statistically significant correlations shown, $P < 0.05$).

Figure 3.3

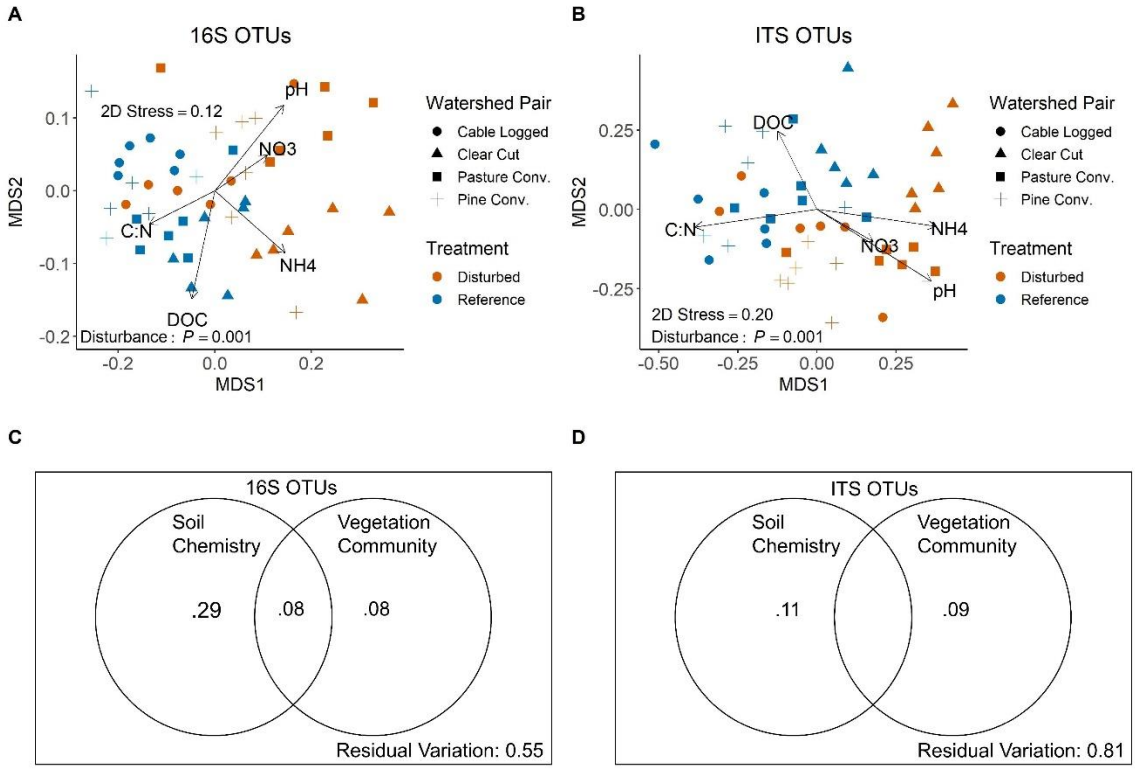

Figure 3.3: NMDS ordinations of 16S (A) and ITS (B) community structure at the OTU level. *P*-values shown are overall disturbance effects from PERMANOVA. Vectors display correlations of key soil variables with NMDS axes from envfit. Panels C and D display variation partitioning results for 16S (C) and ITS (D) communities. Values shown are adjusted R^2 values for each respective partition, and all partitions shown are statistically significant (distance-based redundancy analysis $P < 0.01$). Adjusted R^2 values < 0 not shown (i.e., middle partition on panel D).

Figure 3.4

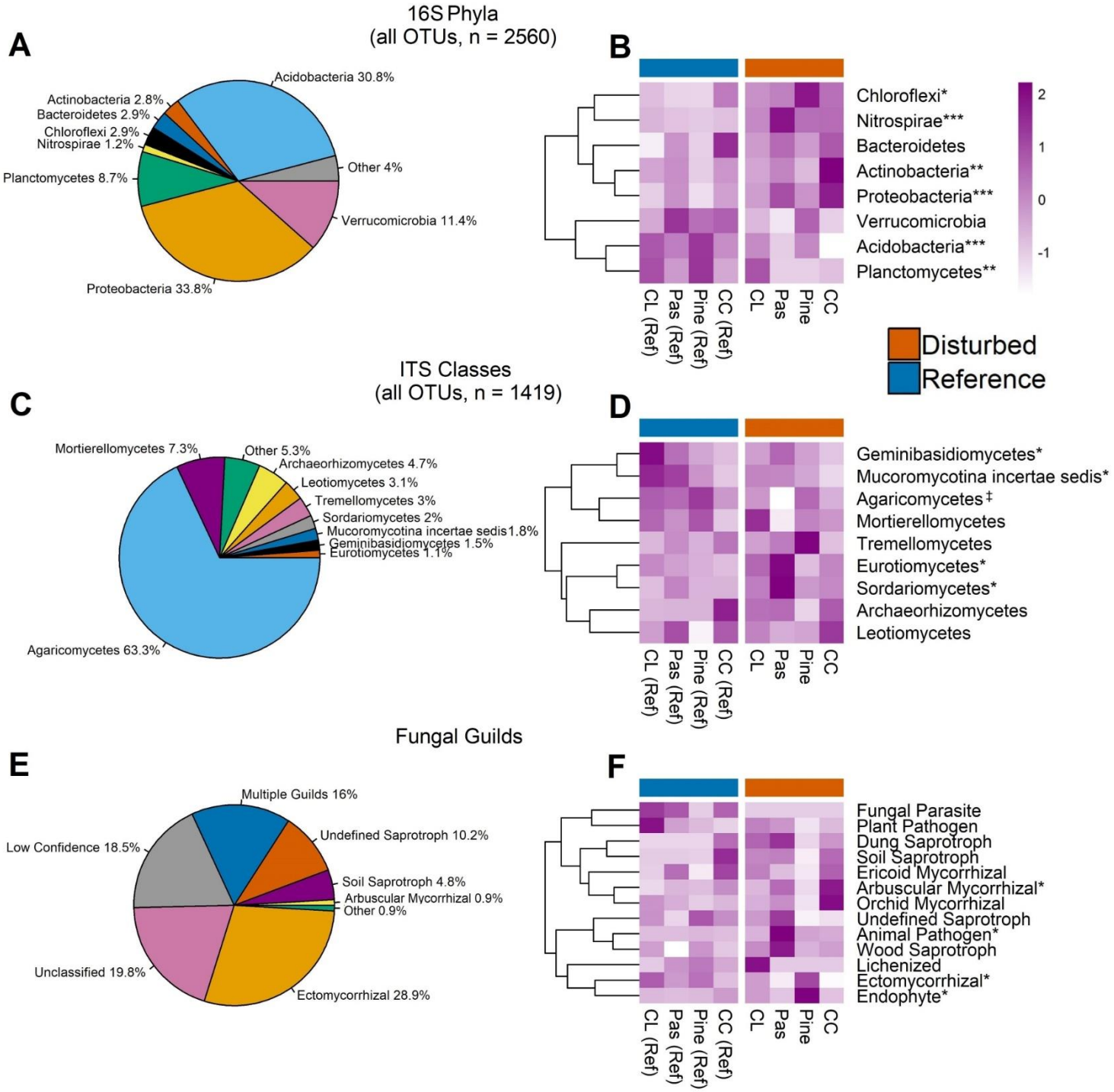
16S Phyla
(all OTUs, n = 2560)
A
Acidobacteria 30.8%
Actinobacteria 2.8%
Bacteroidetes 2.9%
Chloroflexi 2.9%
Nitrospirae 1.2%
Planctomycetes 8.7%
Other 4%
Verrucomicrobia 11.4%
Proteobacteria 33.8%
B
Chloroflexi*
Nitrospirae***
Bacteroidetes
Actinobacteria**
Proteobacteria***
Verrucomicrobia
Acidobacteria***
Planctomycetes**
2
1
0
-1
CL (Ref)
Pas (Ref)
Pine (Ref)
CC (Ref)
CL
Pas
Pine
CC
Disturbed
Reference
ITS Classes
(all OTUs, n = 1419)
C
Mortierellomycetes 7.3%
Other 5.3%
Archaeorhizomycetes 4.7%
Leotiomycetes 3.1%
Tremellomycetes 3%
Sordariomycetes 2%
Mucoromycotina incertae sedis 1.8%
Geminibasidiomycetes 1.5%
Eurotiomycetes 1.1%
Agaricomycetes 63.3%
D
Geminibasidiomycetes*
Mucoromycotina incertae sedis*
Agaricomycetes‡
Mortierellomycetes
Tremellomycetes
Eurotiomycetes*
Sordariomycetes*
Archaeorhizomycetes
Leotiomycetes
CL (Ref)
Pas (Ref)
Pine (Ref)
CC (Ref)
CL
Pas
Pine
CC
Fungal Guilds
E
Multiple Guilds 16%
Undefined Saprotroph 10.2%
Low Confidence 18.5%
Soil Saprotroph 4.8%
Arbuscular Mycorrhizal 0.9%
Other 0.9%
Unclassified 19.8%
Ectomycorrhizal 28.9%
F
Fungal Parasite
Plant Pathogen
Dung Saprotroph
Soil Saprotroph
Ericoid Mycorrhizal
Arbuscular Mycorrhizal*
Orchid Mycorrhizal
Undefined Saprotroph
Animal Pathogen*
Wood Saprotroph
Lichenized
Ectomycorrhizal*
Endophyte*
CL (Ref)
Pas (Ref)
Pine (Ref)
CC (Ref)
CL
Pas
Pine
CC

Figure 3.4: Pie charts display relative abundance of bacterial phyla (A), fungal classes (C), and fungal guilds (E) aggregated across all OTUs in all samples. Only phyla/classes comprising > 1% of sequences and guilds comprising > 0.9% of sequences are shown. Heat maps in panels B, D, and F show scaled Z-scores for relative abundances for each bacterial phylum (C), fungal class (D), and fungal guild (F) across each watershed. Abbreviations are as follows: Clear-cut (CC), cable-logged (CL), Pasture Conversion (Pas), Pine Conversion (Pine). Symbols represent statistical significance at the following levels: *** $P < 0.001$, ** $P < 0.01$, * $P < 0.05$, ‡ $P < 0.1$. *P*-values are main effects of disturbance from two-way ANOVA. Dendrograms on heat maps reflect similarity of relative abundance patterns of taxa across watersheds (complete-linkage clustering) and do not reflect phylogenetic relationships.

Figure 3.5

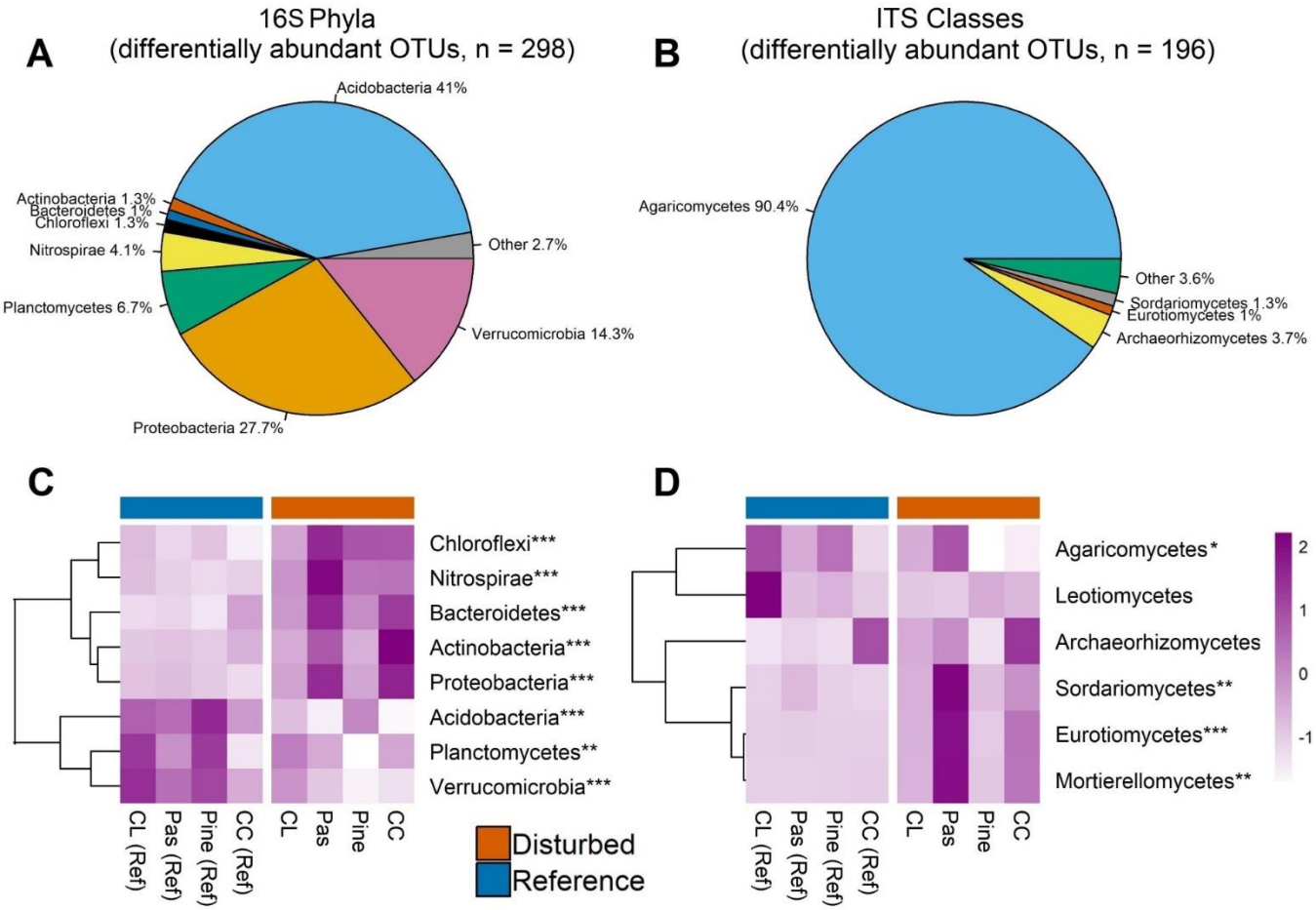

Figure 3.5: Pie charts display relative abundance of bacterial phyla (A) and fungal classes (B) aggregated across edgeR-identified differentially abundant OTUs. Only phyla/classes comprising > 1% of sequences are shown. Heat maps in panels C and D show scaled Z-scores for relative abundances for each bacterial phylum (C) and fungal class (D) for differentially abundant OTUs across each watershed. Abbreviations are as follows: Clear-cut (CC), cable-logged (CL), Pasture Conversion (Pas), Pine Conversion (Pine). Asterisks represent statistical significance at the following levels: *** $P < 0.001$, ** $P < 0.01$, * $P < 0.05$. *P*-values are main effects of disturbance from two-way ANOVA. Dendrograms on heat maps reflect similarity of relative abundance patterns of taxa across watersheds (complete-linkage clustering) and do not reflect phylogenetic relationships.

Figure 3.6

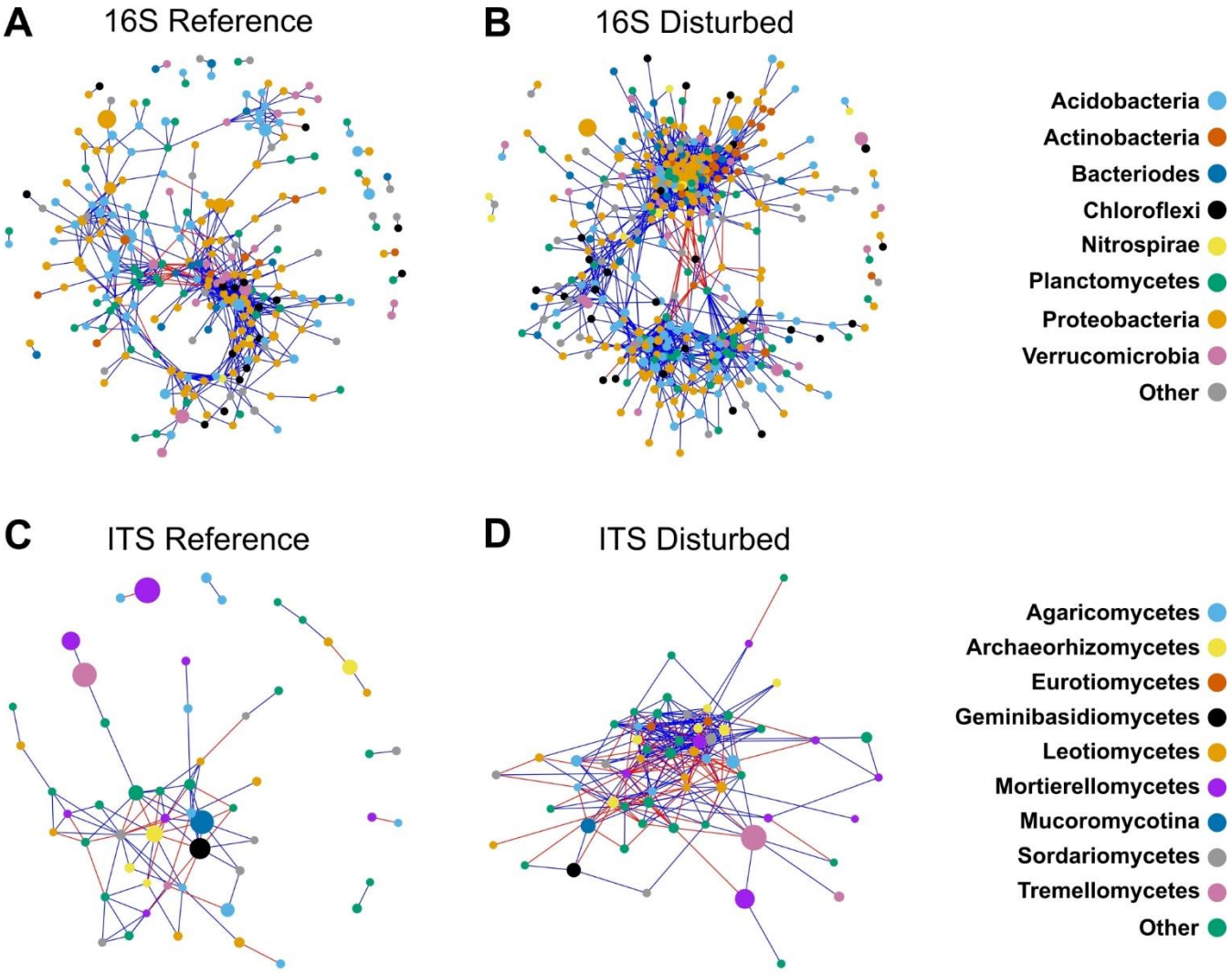

Figure 3.6: Co-occurrence networks constructed for bacterial communities in reference watersheds (A), disturbed watersheds (B) and fungal communities in reference watersheds (C), and disturbed watersheds (D). Color of nodes is indicative of bacterial phylum (A,B) or fungal class (C,D). Edge color is indicative of positive (blue), or negative (red) correlations. Size of nodes is proportional to relative abundance of the OTU represented.

Tables

Table 3.1

Name	Disturbance History
Cable Logged	Commercially clear-cut and cable-logged in 1977
Clear Cut	All woody vegetation cut in 1963, no products removed
Pasture Conversion	Clear-cut and planted to grass in 1958, limed and fertilized in 1959, fertilized in 1965, grass herbicided 1966-1967
Pine Conversion	All woody vegetation cut in 1940, re-growth cut annually until 1955, white pine planted in 1956
All References	Undisturbed since at least 1923

Table 3.1: Names and disturbance histories of watersheds sampled in this study

Table 3.2

	Network Metric	Reference	Disturbed
Bacteria	Nodes	451	546
	Edges	6,216	14,174
	Prop. Negative Edges	0.148***	0.087
	Degree Centrality	0.047 (0.066)	0.077 (0.104)***
	Betweenness Centrality	0.003 (0.004)***	0.002 (0.003)
	Closeness Centrality	0.399 (0.067)	0.441 (0.07)***
	Clustering Coefficient	0.37 (0.14)	0.45 (0.18)***
Fungi	Nodes	55	61
	Edges	95	279
	Prop. Negative Edges	0.284	0.333
	Degree Centrality	0.037 (0.074)	0.15 (0.167)***
	Betweenness Centrality	0.002 (0.029)	0.013 (0.03)*
	Closeness Centrality	0.057 (0.039)	0.441 (0.127)***
	Clustering Coefficient	0.27 (0.5)	0.43 (0.23)*

Table 3.2: Network metrics calculated for 16S and ITS co-occurrence networks constructed for reference and disturbed soils. For Degree Centrality, Betweenness Centrality, Closeness Centrality (all normalized), and Clustering Coefficient, values displayed are medians followed by interquartile ranges. Asterisks indicate significantly higher values at the following significance levels: * $P < 0.05$, *** $P < 0.001$. Proportion of Negative Edges was compared between Reference and Disturbed soils using Z-tests, while all other metrics were compared using Kruskal-Wallis tests.

Supplementary Figures

Figure 3.S1

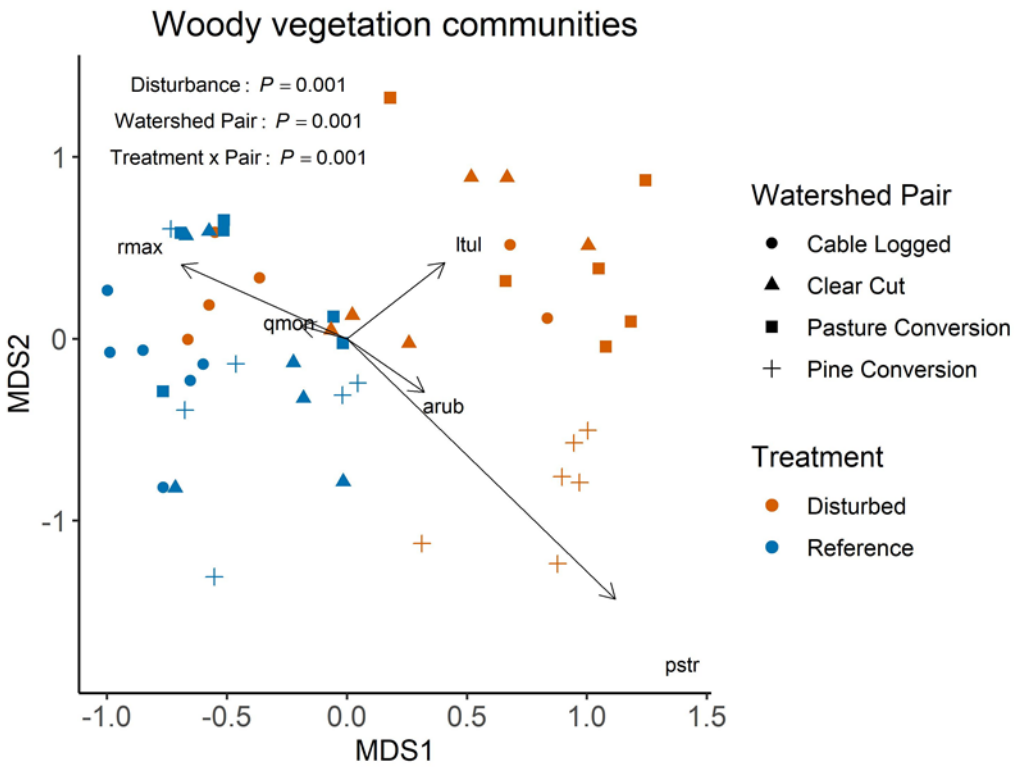

Figure 3.S1: NMDS ordination of woody vegetation community structure. P-values shown are from PERMANOVA. Vectors shown are species scores for key taxa. Abbreviations are as follows: *Rhododendron maximum* (rmax), *Quercus montana* (qmon), *Liriodendron tulipifera* (ltul), *Acer rubrum* (arub), *Pinus strobus* (pstr).

Figure 3.S2

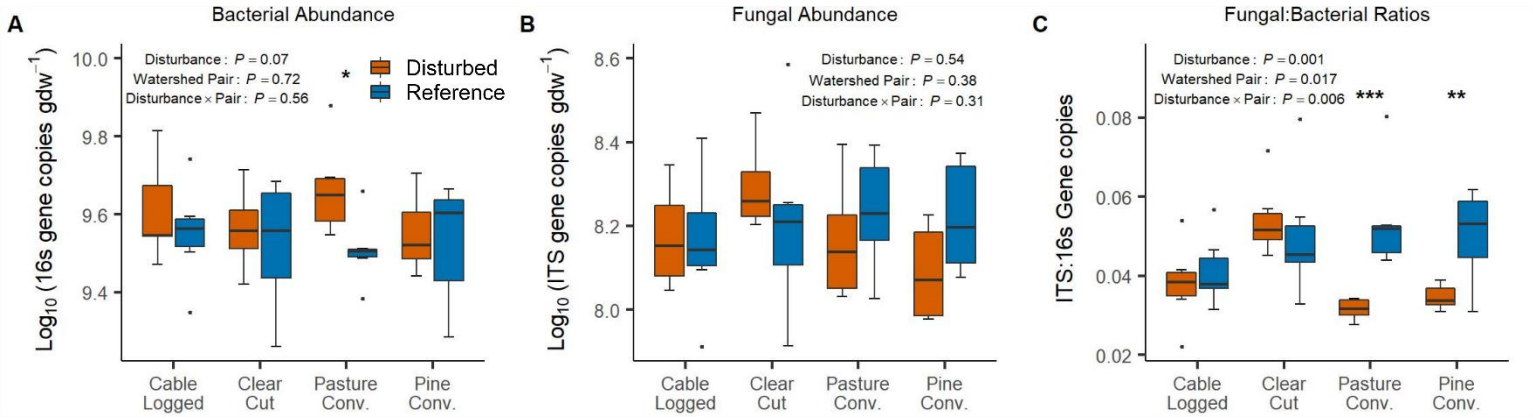

Figure 3.S2: Pairwise comparisons of watersheds within each disturbed-reference pair for 16S gene copy abundance (A), ITS gene copy abundance (B), and ITS:16S gene copy ratios (C). Asterisks represent statistical significance at the following levels: *** $P < 0.001$, ** $P < 0.01$, * $P < 0.05$.

Figure 3.S3

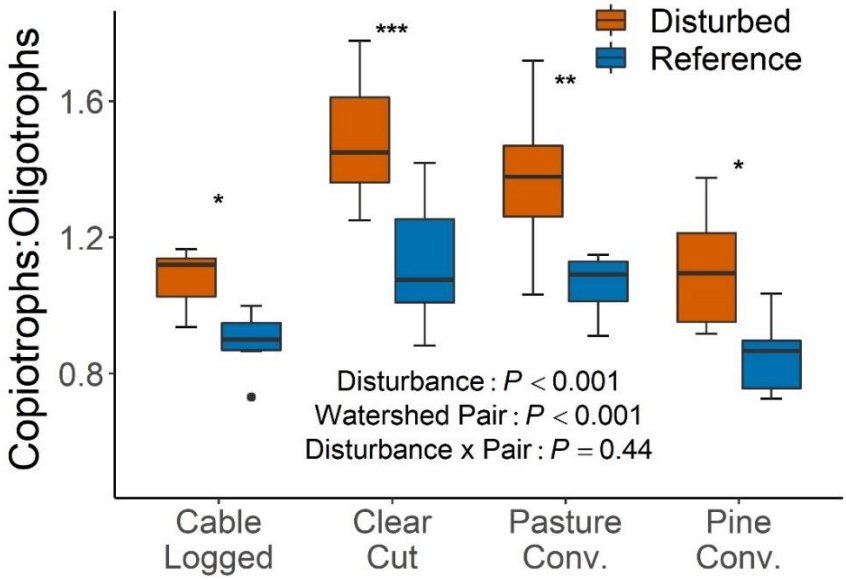

Figure 3.S3: Pairwise comparisons of watersheds within each disturbed-reference pair Copiotroph:Oligotroph ratios. Asterisks represent statistical significance at the following levels: *** $P < 0.001$, ** $P < 0.01$, * $P < 0.05$

Figure 3.S4

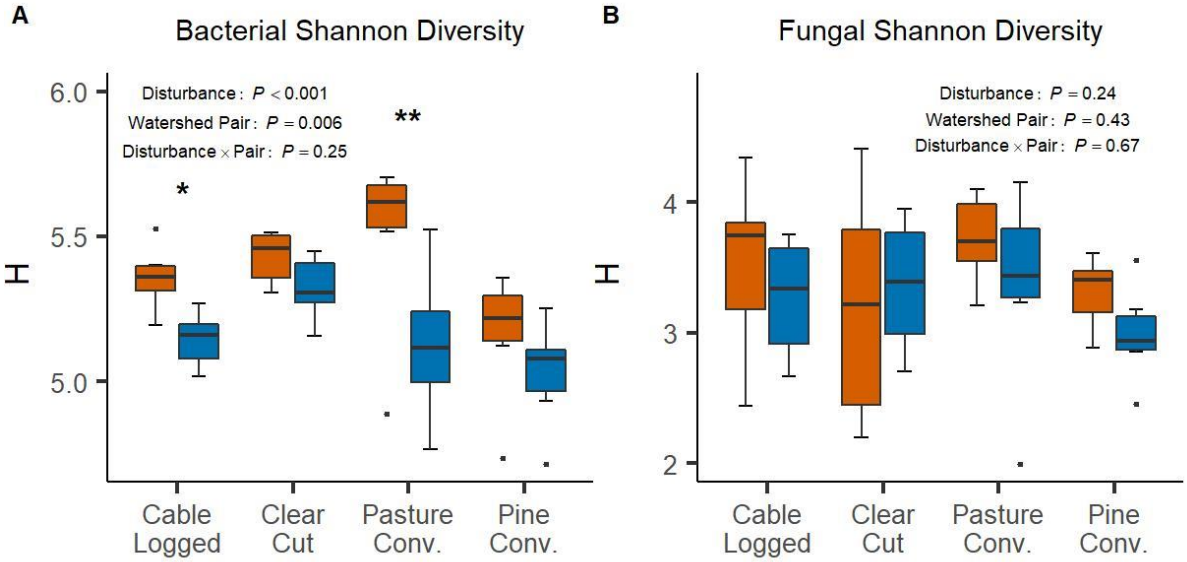

Figure 3.S4: Pairwise comparisons of watersheds within each disturbed-reference pair for 16S OTU Shannon diversity (A), ITS OTU Shannon diversity (B). Asterisks represent statistical significance at the following levels: *** $P < 0.001$, ** $P < 0.01$, * $P < 0.05$.

Figure 3.S5

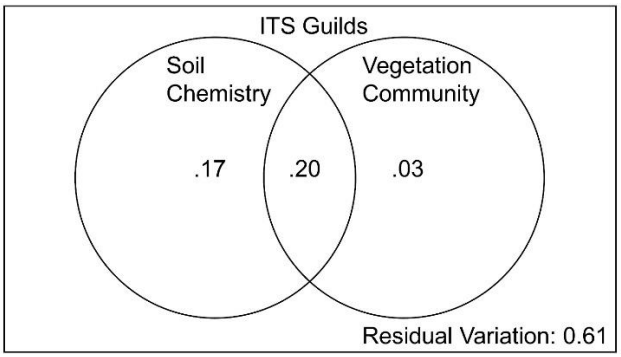

Figure 3.S5: Variation partitioning for fungal guilds. Asterisks represent statistical significance at the following levels: *** $P < 0.001$, ** $P < 0.01$, * $P < 0.05$. Values shown are adjusted R^2 values for each respective partition, and all partitions shown are statistically significant (distance-based redundancy analysis $P < 0.01$). Adjusted R^2 values < 0 not shown.

Supplementary Tables

Table 3.S1

Watershed Pair	Watershed Number	Treatment	Aspect	Elevation (m)	Area (ha)	Dominant Woody Vegetation
Cable Logged	WS2	Undisturbed since 1923	SSE	709 – 1004	12	*Rhododendron maximum, Quercus spp., Betula spp.*
	WS7	Commercially clear cut and cable logged in 1977	S	772 – 1077	59	*Rhododendron maximum, Quercus montana., Acer rubrum, Liriodendron tulipifera*
Pasture Conversion	WS14	Undisturbed since 1923	NW	707 – 992	61	*Rhododendron maximum, Liriodendron tulipifera, Betula spp.*
	WS6	Clearcut in 1958, soil scarified, planted to grass, limed and fertilized in 1959, fertilized again in 1965, grass herbicided in 1966 and 1967	NW	696 – 905	9	*Acer rubrum, Liriodendron tulipifera*
Pine Conversion	WS18	Undisturbed since 1923	NW	726 – 993	13	*Rhododendron maximum, Acer rubrum, Betula spp.*
	WS17	All woody vegetation cut annually 1940 - 1955, white pine planted in 1956	NW	760 – 1021	13	*Pinus strobus*
Clear Cut	WS36	Undisturbed since 1923	ESE	1021 – 1542	49	*Rhododendron maximum, Liriodendron tulipifera, Betula spp.*
	WS37	All woody vegetation cut in 1963, no products removed	ENE	1033 – 1592	44	*Liriodendron tulipifera, Betula spp.*

Table 3.S1: Detailed watershed information for all eight watersheds sampled in this study. Note that dominant vegetation (by density) is for study plots only and is not intended to represent watershed-scale woody vegetation communities.

Table 3.S2

Variable	Reference	Disturbed
pH	5.25 (0.038)	5.56 (0.052)***
Moisture (g H_2O g $soil^{-1}$)	0.30 (0.014)	0.294 (0.008)
NO_3 (µg N g $soil^{-1}$)	0.119 (0.040)	1.08 (0.443)***
NH_4 (µg N g $soil^{-1}$)	1.79 (0.140)	2.53 (0.187)***
DOC (µg C g $soil^{-1}$)	391.9 (13.0)***	302.7 (17.7)
TDN (µg N g $soil^{-1}$)	46.7 (2.41)	42.8 (2.59)
DOC:TDN	8.61 (0.264)*	7.22 (0.286)
DON (µg N g $soil^{-1}$)	44.7 (2.30)*	39.1 (2.50)
Microbial Biomass C (µg C g $soil^{-1}$)	207.3 (13.3)*	176.0 (15.8)
Microbial Biomass N (µg N g $soil^{-1}$)	41.5 (2.62)	40.0 (3.27)
Microbial Biomass C:N	4.85 (0.174)*	4.30 (0.115)
Total C (mg C g $soil^{-1}$)	41.3 (3.18)	45.5 (4.95)
Total N (mg N g $soil^{-1}$)	2.35 (0.203)	2.90 (0.328)*
C:N	17.9 (0.440)**	16.1 (0.354)
SIR (µg CO_2-C g $soil^{-1}$ d^{-1})	82.8 (4.13)	93.1 (7.52)*

Table 3.S2: Soil physicochemical variables aggregated across all disturbed and reference soil samples. Means ± one SE shown. Asterisks indicate significantly higher values (ANOVA) at the following significance levels: * $P < 0.05$, ** $P < 0.01$, *** $P < 0.001$.

Table 3.S3

Bacterial Phylum	Cable Logged		Pasture Conversion		Pine Conversion		Clear Cut	
	Reference	Disturbed	Reference	Disturbed	Reference	Disturbed	Reference	Disturbed
Acidobacteria	0.345 (0.012)	0.310 (0.009)	0.319** (0.013)	0.267 (0.014)	0.366** (0.012)	0.311 (0.009)	0.309*** (0.016)	0.233 (0.016)
Proteobacteria	0.310 (0.008)	0.332 (0.005)	0.337 (0.006)	0.367* (0.014)	0.303 (0.012)	0.336* (0.015)	0.331 (0.010)	0.389*** (0.006)
Nitrospirae	0.007 (0.001)	0.013 (0.005)	0.005 (0.002)	0.030*** (0.005)	0.004 (0.002)	0.017** (0.002)	0.005 (0.001)	0.017* (0.004)
Planctomycetes	0.097 (0.004)	0.097 (0.005)	0.085 (0.005)	0.077 (0.006)	0.102** (0.011)	0.076 (0.004)	0.083 (0.003)	0.079 (0.007)
Chloroflexi	0.026 (0.005)	0.029 (0.004)	0.024 (0.004)	0.03 (0.003)	0.024 (0.003)	0.038* (0.004)	0.031 (0.002)	0.031 (0.002)
Actinobacteria	0.023 (0.002)	0.024 (0.002)	0.028 (0.003)	0.030 (0.004)	0.016 (0.003)	0.019 (0.002)	0.026 (0.005)	0.056*** (0.006)

Table 3.S3: Pairwise comparisons between watersheds within disturbed-reference pairs for bacterial phyla (all OTUs) showing main effects of disturbance on relative abundance. Means ± one SE shown. Asterisks indicate significantly higher values at the following significance levels: * $P < 0.05$, ** $P < 0.01$, *** $P < 0.001$.

Table 3.S4

Fungal Class	Cable Logged		Pasture Conversion		Pine Conversion		Clear Cut	
	Reference	Disturbed	Reference	Disturbed	Reference	Disturbed	Reference	Disturbed
Agaricomycetes	0.676 (0.057)	0.619 (0.055)	0.665 (0.044)	0.516 (0.043)	0.711 (0.035)	0.666 (0.022)	0.618 (0.043)	0.595 (0.096)
Sordariomycetes	0.013 (0.003)	0.021 (0.006)	0.021 (0.006)	0.039* (0.004)	0.014 (0.003)	0.018 (0.005)	0.014 (0.002)	0.020 (0.006)
Eurotiomycetes	0.011 (0.004)	0.016 (0.004)	0.007 (0.002)	0.032*** (0.011)	0.004 (0.0004)	0.002 (0.001)	0.022 (0.0004)	0.011 (0.005)
Mucoromycotina	0.040* (0.009)	0.019 (0.004)	0.034 (0.010)	0.018 (0.009)	0.016 (0.003)	0.012 (0.002)	0.004 (0.001)	0.001 (0.0004)
Geminibasidiomycetes	0.040*** (0.011)	0.010 (0.004)	0.020 (0.004)	0.022 (0.003)	0.009 (0.001)	0.010 (0.002)	0.004 (0.001)	0.002 (0.001)

Table 3.S4: Pairwise comparisons between watersheds within disturbed-reference pairs for fungal classes (all OTUs) showing main effects of disturbance on relative abundance. Means ± one SE shown. Asterisks indicate significantly higher values at the following significance levels: * $P < 0.05$, ** $P < 0.01$, *** $P < 0.001$.

Table 3.S5

Fungal Guild	Cable Logged		Pasture Conversion		Pine Conversion		Clear Cut	
	Reference	Disturbed	Reference	Disturbed	Reference	Disturbed	Reference	Disturbed
Ectomycorrhizal	0.475* (0.082)	0.292 (0.062)	0.298** (0.066)	0.067 (0.030)	0.412 (0.084)	0.538 (0.039)	0.195 (0.069)	0.022 (0.019)
Arbuscular Myco.	0.003 (0.002)	0.006 (0.001)	0.006 (0.002)	0.013 (0.003)	0.006 (0.002)	0.003 (0.001)	0.010 (0.001)	0.021** (0.005)
Animal Pathogen	0	0.0003 (0.0003)	0	0.005*** (0.002)	0.0002 (0.0001)	0.001 (0.001)	0	0.005 (0.002)
Endophyte	0.001 (0.0005)	0.004 (0.002)	0.001 (0.001)	0.001 (0.001)	0.001 (0.0005)	0.016*** (0.005)	0.004 (0.002)	0.001 (0.001)

Table 3.S5: Pairwise comparisons between watersheds within disturbed-reference pairs for fungal guilds showing main effects of disturbance on relative abundance. Means ± one SE shown. Asterisks indicate significantly higher values at the following significance levels: * $P < 0.05$, ** $P < 0.01$, *** $P < 0.001$.

Table 3.S6

Bacterial Phylum	Cable Logged		Pasture Conversion		Pine Conversion		Clear Cut	
	Reference	Disturbed	Reference	Disturbed	Reference	Disturbed	Reference	Disturbed
Acidobacteria	0.434 (0.006)	0.405 (0.023)	0.456*** (0.015)	0.315 (0.028)	0.466 (0.023)	0.442 (0.009)	0.479*** (0.015)	0.327 (0.024)
Proteobacteria	0.226 (0.009)	0.273* (0.009)	0.250 (0.013)	0.333*** (0.019)	0.221 (0.036)	0.275* (0.006)	0.247 (0.010)	0.358*** (0.017)
Nitrospirae	0.023 (0.005)	0.040 (0.015)	0.017 (0.007)	0.089*** (0.011)	0.012 (0.005)	0.057*** (0.007)	0.019 (0.004)	0.049* (0.008)
Planctomycetes	0.089 (0.004)	0.076 (0.006)	0.071 (0.008)	0.055 (0.007)	0.088*** (0.012)	0.044 (0.007)	0.056 (0.007)	0.059 (0.004)
Chloroflexi	0.010 (0.003)	0.012 (0.003)	0.008 (0.002)	0.019** (0.004)	0.009 (0.002)	0.019** (0.002)	0.006 (0.002)	0.017** (0.002)
Actinobacteria	0.001 (0.001)	0.007 (0.003)	0.002 (0.001)	0.022*** (0.006)	0.001 (0.0003)	0.007 (0.002)	0.008 (0.002)	0.044*** (0.005)
Verrucomicrobia	0.198* (0.010)	0.153 (0.017)	0.175*** (0.014)	0.104 (0.011)	0.187*** (0.022)	0.097 (0.003)	0.155*** (0.008)	0.097 (0.010)
Bacteroidetes	0.001 (0.001)	0.010 (0.004)	0.002 (0.001)	0.021*** (0.004)	0	0.012* (0.003)	0.011 (0.006)	0.020* (0.004)

Table 3.S6: Pairwise comparisons between watersheds within disturbed-reference pairs for bacterial phyla (differentially abundant OTUs) showing main effects of disturbance on relative abundance. Means ± one SE shown. Asterisks indicate significantly higher values at the following significance levels: * $P < 0.05$, ** $P < 0.01$, *** $P < 0.001$.

Table 3.S7

Fungal Class	Cable Logged		Pasture Conversion		Pine Conversion		Clear Cut	
	Reference	Disturbed	Reference	Disturbed	Reference	Disturbed	Reference	Disturbed
Agaricomycetes	0.943 (0.031)	0.868 (0.072)	0.956 (0.018)	0.873 (0.059)	0.864 (0.088)	0.833 (0.079)	0.873* (0.059)	0.634 (0.105)
Sordariomycetes	0.001 (0.0003)	0.010 (0.008)	0.014 (0.007)	0.036 (0.009)	0.005 (0.004)	0.012 (0.006)	0.001 (0.001)	0.035** (0.016)
Eurotiomycetes	0.0001 (0.0001)	0.006 (0.003)	0.0004 (0.0003)	0.036** (0.019)	0	0.002 (0.002)	0	0.028* (0.011)
Mortierellomycetes	0	0.002 (0.001)	0	0.011** (0.005)	0.0003 (0.0003)	0.001 (0.001)	0.001 (0.001)	0.007 (0.004)

Table 3.S7: Pairwise comparisons between watersheds within disturbed-reference pairs for fungal classes (differentially abundant OTUs) showing main effects of disturbance on relative abundance. Means ± one SE shown. Asterisks indicate significantly higher values at the following significance levels: * $P < 0.05$, ** $P < 0.01$, *** $P < 0.001$.

CHAPTER 4 – Emergent properties of microbial communities drive accelerated biogeochemical cycling in disturbed temperate forests

Authors:

Ernest D Osburn, Brian D Badgley, Brian D Strahm, Frank O Aylward, J E Barrett

In review, *Ecology*

Abstract

Despite ever-increasing availability of detailed information about microbial community structure, relationships of microbial diversity with ecosystem functioning remain unclear. We investigated these relationships at the Coweeta Hydrologic Laboratory, where past forest disturbances (e.g., clear-cut) have altered both ecosystem processes (e.g., increased N export) and microbial communities (e.g., increased bacterial diversity). We sampled soils from disturbed and adjacent reference forests, characterized resident microbial communities, and measured several microbial C- and N-cycle process rates. Microbial communities from historically disturbed soils exhibited altered ecosystem functioning, including generally higher rates of C- and N-cycle processes. Disturbed soil microbial communities also exhibited altered ecosystem multifunctionality, a composite variable consisting of all measured process rates as well as extracellular enzyme activities. Though we found few relationships between ecosystem functions and microbial alpha diversity, all functions were correlated with microbial community composition metrics, particularly r:K strategist ratios of bacterial phyla. Additionally, for both ecosystem multifunctionality and specific processes (i.e., C- and N-mineralization), microbial metrics significantly improved models seeking to explain variation in process rates. Our work sheds light on the links between microbial

communities and ecosystem functioning and identifies specific microbial metrics important for modeling ecosystem responses to environmental change.

Introduction

Improving understanding of microbial biodiversity-ecosystem function (BEF) relationships remains an exceptional challenge in ecology (Hall et al. 2018). Despite three decades of BEF research spanning hundreds of studies, nearly all identified BEF relationships involve macro-organismal diversity (i.e., plants and animals, Duffy 2009; Cardinale et al. 2012; Tilman et al. 2014). These BEF relationships have been found across multiple trophic levels in marine, freshwater, and terrestrial ecosystems, and include positive effects of plant diversity on primary productivity (e.g., Tilman et al. 2001), predator diversity on plant biomass (e.g., Otto *et al.* 2008), and invertebrate decomposer diversity on litter carbon (C) and nitrogen (N) cycling (Handa et al. 2014). In contrast, few microbial BEF relationships have been identified, despite microbial facilitation of virtually all ecosystem processes, particularly biogeochemical cycling of C, N, and phosphorus (P) (Fierer 2017). Given the importance of biogeochemical functions to ecosystem services that support human well-being, including regulation of nutrient cycles and provisioning of clean drinking water (Millenium Ecosystem Assessment 2005), improved understanding of microbial BEF relationships is critical.

The exceptionally high diversity of microbial communities (Torsvik et al. 2002) has led to the prevailing paradigm that microbial-mediated processes will not show species diversity-ecosystem functioning relationships due to a high degree of functional redundancy found in microbial taxa (Schimel 1995, Nannipieri et al. 2003). Further, the degree of functional redundancy is expected to vary among different ecosystem processes

- for example, nearly all microbial taxa perform the metabolic processes that contribute to functions such as C- and N-mineralization, and therefore a high degree of functional redundancy is expected. For these 'phylogenetically broad' processes, other aspects of microbial community structure (e.g., species composition) may be more important than species diversity per se (Bardgett and van der Putten 2014). In contrast, some biogeochemical processes such as nitrification and methane cycling are facilitated by only a few groups of microorganisms, and therefore less functional redundancy and more apparent BEF relationships are expected for these 'phylogenetically narrow' functions (Schimel 1995). Regardless, microbial BEF relationships for some processes have been identified. For example, diversity of denitrifying microorganisms has been positively associated with denitrification rates in observational studies (Powell et al. 2015), which is supported by studies employing experimental manipulation of denitrifier diversity (Philippot et al. 2013). Further, ecosystem multifunctionality, a composite variable encompassing multiple ecosystem properties, has been positively correlated with microbial species diversity in both observational and experimental studies (Delgado-Baquerizo et al. 2016, 2020).

The rarity of these microbial BEF examples is surprising given the wealth of literature that has emerged in recent decades using next-generation sequencing technologies (e.g., amplicon sequencing, metagenomics) to provide in-depth characterizations of microbial taxonomic and functional diversity. These studies are often conducted under the premise that '–omics' characterizations of microbial communities will help link microorganisms to the ecosystem processes they facilitate (Hall et al. 2018). However, these microbial community-ecosystem function relationships are rarely

tested, and even when tested are often not observed (Rocca et al. 2015, Bier et al. 2015, Graham et al. 2016), leading to ambiguity regarding the generality of microbial BEF relationships. In response to this ambiguity, a conceptual framework has emerged for explicitly testing the influence of microorganisms on the ecosystems they inhabit (Hall et al. 2018). This framework argues that microbial-mediated process are acted directly upon by aggregate properties of microbial communities (i.e., biomass, functional genes), which may or may not be influenced by microbial membership, and studies should assess all of these aspects of microbial communities (Hall et al. 2018). However, rigorous evaluations of this framework are lacking in the literature. More generally, it remains unknown the extent to which microbial community information improves understanding of ecosystem processes, and therefore microbial community-ecosystem function relationships remain untested to a large degree.

Forested ecosystems provide an excellent opportunity for more rigorous testing of microbial BEF relationships, as anthropogenic forest disturbance (e.g., logging, conversion to agriculture) consistently alters the composition of soil bacterial and fungal communities (e.g., Jangid et al. 2011, Rodrigues et al. 2013, Kohout et al. 2018, Mushinski et al. 2018b, 2018a). In particular, some previous studies, including our own, show higher bacterial α diversity and higher relative abundance of r-selected bacteria in previously disturbed forest sites (Zhou et al. 2018, Osburn et al. 2019). These changes in microbial communities are associated with changes to soil properties following disturbance. Specifically, higher pH, larger NO_3^- pools, smaller organic C pools, and lower C:N ratios are commonly observed in disturbed soils (Covington 1981, Pennock and van Kessel 1997, Nave et al. 2010, Keiser et al. 2016), though in other cases organic

C and C:N have increased following disturbance (Goodale and Aber 2001, Simard et al. 2011). Forest disturbance also alters microbial-mediated ecosystem process rates, including higher decomposition rates and soil respiration rates in disturbed sites (Covington 1981, Edwards and Ross-Todd 1983, Londo et al. 1999). Common N-cycle impacts of forest disturbance include higher net nitrification rates in soil (Matson and Vitousek 1981, Waide et al. 1988, Keiser et al. 2016) and higher watershed-scale N export relative to reference sites (Vitousek et al. 1979, Swank and Vose 1997, Webster et al. 2016). However, despite these concurrent changes to soil microbial communities and ecosystem processes, relationships between soil microorganisms and the ecosystem functions they facilitate remain largely uncharacterized within the context of forest disturbance.

We evaluated microbial community-ecosystem function relationships within this forest disturbance context by sampling soils from disturbed and adjacent reference forests at the Coweeta Hydrologic Laboratory in North Carolina and measuring rates of three microbial-mediated ecosystem processes: C-mineralization, gross N-mineralization, and gross nitrification. We also assessed overall microbial C- and N-cycle multifunctionality, a composite variable that incorporates all measured C- and N-cycle process rates as well as associated extracellular enzyme activities. Then, following the Hall et al. (2018) framework, we measured several aggregate properties of microbial communities (e.g., biomass, functional gene abundances), and used an existing amplicon sequence dataset from the same soils (Osburn et al. 2019) to generate metrics of microbial community diversity and composition (e.g., bacterial/fungal α and β diversity, bacterial r:K ratios). We then tested for correlative, explanatory, and mechanistic relationships between

ecosystem functions and microbial community characteristics. Our study evaluates influences of microbial communities on ecosystem functioning across multiple biogeochemical cycles (i.e., C- and N-cycles) and in both phylogenetically broad and narrow processes (e.g., N-mineralization vs. nitrification), and seeks to identify microbial community characteristics important to understanding ecosystem responses to environmental change.

Materials and Methods

Site description, soil sampling, and soil properties

We conducted this study at the Coweeta Hydrologic Laboratory, a USDA Forest Service experimental forest in North Carolina, USA (latitude 35°03′ N, longitude 83°25′ W). Within the Coweeta basin, we selected eight forested watersheds, four of which were disturbed ~4-8 decades previously as a result of Forest Service management experiments. Disturbances included clear-cutting, conversion to pine monoculture, conversion to agriculture, and cable-logging (Fig. 4.S1, Table 4.S1). The remaining watersheds are adjacent to the disturbed watersheds and have not been manipulated by the Forest Service (i.e., reference sites, Fig. 4.S1, Table 4.S1). In June 2018, we sampled 10 cm depth mineral soil cores from six 4 m x 4 m plots evenly spaced along a 200 m transect located 5 m upslope from the main stream channel of each watershed (8 watersheds x 6 plots/watershed = 48 samples). We measured pH, moisture, ammonium (NH_4^+), nitrate (NO_3^-), total dissolved N (TDN), dissolved organic carbon (DOC), total N, and total C in all soil samples. Detailed information regarding soil sampling and measurement of soil properties can be found in Osburn et al. (2019). In general, our soils exhibit disturbance effects typical of the region (e.g., Keiser et al. 2016), where soils from historically

disturbed forests have higher pH, larger inorganic-N pools, smaller organic C pools, and lower C:N ratios compared with reference forest soils (Table 4.S2).

Ecosystem functions

To measure C-mineralization rates, we weighed 6 g fresh soil into 50 ml centrifuge tubes and sealed the tubes with lids fitted with butyl septa. We then flushed all CO_2 from the headspace, incubated the soils at 20° C, and measured accumulated CO_2 after 24 hours using an infrared gas analyzer (Li-7000; Li-Cor Biosciences, Lincoln, Nebraska, USA). Though other studies report C-mineralization over longer time periods (e.g., Fierer et al. 2007), we chose to report rates from this 24-hour incubation to reflect activity of in-situ microbial communities and to match temporal scales with N-cycle processes.

We measured gross rates of N-mineralization and nitrification using ^{15}N pool dilution incubations (Kirkham and Bartholomew 1954). For gross N-mineralization, we weighed out two replicate 20 g subsamples of each soil into 175 ml Nalgene bottles. We then added 2 - 5 µg NH_4-N in the form of $(^{15}NH_4)_2SO_4$ (99 atom% ^{15}N enrichment). We immediately extracted one of the replicates of each soil sample with 100 ml 2*M* KCl and extracted the second replicate after incubating for 24 hours at 20° C. Incubations for gross nitrification were identical, except we added 0.2 – 4 µg NO_3-N in the form of $K^{15}NO_3$ (99 atom% ^{15}N enrichment). We calculated N additions to not exceed 10% of the standing NH_4^+ and NO_3^- pools.

We recovered ^{15}N from extracts using a modified diffusion procedure described by Brooks et al. (1989). To recover $^{15}NH_4^+$, we added 50 ml of extract to 125 ml specimen containers and added ~0.2 g MgO, which facilitates conversion of NH_4^+ to

NH_3. We trapped $^{15}NH_3$ on two 6 mm Whatman no. 1 filter disks acidified with 5 µl 2.5*M* $KHSO_4$ and sealed between two strips of PTFE tape. Diffusion containers incubated for 6 days at 20° C. To recover $^{15}NO_3^-$, we first removed NH_4^+ using the procedure described above, but discarded the resulting PTFE acid traps. We then added ~0.4 g Devarda's alloy, thereby reducing NO_3^- to NH_4^+, then added an additional ~0.2 g MgO and PTFE acid trap to each container and allowed containers to incubate for 6 additional days. Following diffusion, ^{15}N atom% excess of filter disks was determined using an IsoPrime 100 IRMS interfaced with an Elementar Vario MICRO cube elemental analyzer (Elementar Americas Inc, Mt. Laurel, NJ, USA). We calculated gross N-mineralization, gross nitrification, and NH_4^+/NO_3^- consumption rates using the isotope pool dilution equations of Kirkham & Bartholomew (1954). We calculated net N-mineralization and nitrification rates as well as gross NH_4^+ and NO_3^- immobilization rates according to previously described methods (Minick et al. 2015). We express process rates in units of µg C or N g dry $soil^{-1}$ day^{-1} and for phylogenetically broad processes (i.e., C- and N-mineralization), we also adjust rates to microbial biomass to compare microbially-explicit rates of ecosystem functions across disturbed and reference sites.

As additional metrics of microbial ecosystem function, we measured activities of five extracellular enzymes, including the C-mineralization enzymes β-glucosidase (BG), β-xylosidase (XYL), and β-D-cellubiosidase (CHB) and the N-mineralization enzymes leucine aminopeptidase (LAP) and N-acetyl-β-glucosaminidase (NAG). We measured enzyme activities using fluorometric assays described in detail in Osburn et al. (2018). To assess overall C- and N-cycle functioning of microbial communities, we calculated a multifunctionality index using all five extracellular enzyme activities along with C-

mineralization rates and gross and net rates of N-mineralization and nitrification. We calculated multifunctionality by scaling each measured rate and calculating the mean scaled rate for each sample, similar to multiple recent studies (Maestre et al. 2012, Delgado-Baquerizo et al. 2016, 2020).

Microbial community characteristics

We measured microbial biomass C and C:N ratios using a modified chloroform extraction method (Fierer and Schimel 2003). After extracting DNA from ~0.25 g fresh soil using a Qiagen DNeasy PowerSoil kit (Qiagen, Valencia, CA, USA) quantifying extracts using a Qubit 2.0 fluorometer (Thermo Fisher Inc, Waltham, MA, USA), we used qPCR to measure abundances of *amoA* genes involved in nitrification from ammonia-oxidizing archaea (AOA), ammonia-oxidizing bacteria (AOB), and complete ammonia-oxidizers (CAOB). Full descriptions of *amoA* qPCR assays can be found in Osburn and Barrett (2020).

We also assessed several aspects of microbial community diversity and composition as candidate drivers of ecosystem process rates, including fungal:bacterial ratios, bacterial and fungal α and β diversity, r:K strategist ratios of bacterial phyla, and ratios of arbuscular to ectomycorrhizal fungi (AM:ECM). We estimated fungal:bacterial ratios by qPCR amplifying the 16S rRNA and ITS regions, using the primers EUB 338/515 and ITS1f/5.8s (Fierer et al. 2005). We characterized bacterial and fungal communities by amplifying and sequencing the V4 region of the 16S rRNA gene using the 515F/806R primers (Parada et al. 2016) and the ITS region using the ITS1F/ITS2 primers (Bellemain et al. 2010). Raw sequences were processed in QIIME2 (Bolyen et al. 2018) using the DADA2 pipeline (Callahan et al. 2016) and complete details regarding

sequence processing can be found in Osburn et al. (2019).We used the resulting OTU tables (defined at 97% sequence similarity) to calculate bacterial/fungal α diversity (i.e., Shannon diversity) and to quantify bacterial/fungal β diversity (i.e., compositional heterogeneity), we used principal coordinates analysis (PCoA) axis 1 scores. We conducted PCoA using Bray-Curtis distances with the vegan R package (Oksanen et al. 2019), and PCoA axis 1 accounted for 31.2% and 9.5% of the variation in bacterial and fungal communities, respectively (Fig. 4.S2, 4.S3). As an index of bacterial life-history strategies, we calculated r:K ratios of bacterial phyla for each sample according to Zhou et al. (2018). This method assigns life history categories to abundant bacterial phyla, with Proteobacteria and Bacteroidetes categorized as r-strategists while Acidobacteria and Actinobacteria are categorized as K-strategists (Zhou et al. 2018). We calculated ratios of arbuscular to ectmycorrhizal fungi (i.e., AM:ECM) for each sample by using FUNGuild (Nguyen et al. 2016) to identify mycorrhizal taxa in our ITS sequences. Raw sequence reads used to generate diversity and composition metrics are deposited in NCBI's BioProject database under accession number PRJNA548911.

Statistical analyses

All statistical analyses were performed in R (R Core Development Team 2019) using the 'lme4', 'MuMIn', 'bestglm', 'AICcmodavg', and 'lavaan' packages (Bates et al. 2019, Linden 2019, Rosseel et al. 2019, Bartoń 2019, McLeod and Lai 2020). We tested for disturbance effects on individual ecosystem processes using linear mixed-effects models ('lmer' function, lme4 package) with watershed pair as a random effect, which allowed us to account for systematic landscape variation among disturbed-reference watershed pairs (e.g., aspect, elevation). When models did not meet

assumptions of normality of residuals, we used generalized linear mixed models ('glmer' function, gamma distribution and log-link function, lme4 package). We tested for disturbance effects on C- and N-cycle multifunctionality using PERMANOVA with Euclidean distances ('adonis2' function, vegan package) and visualized patterns in multifunctionality using principal components analysis ('princomp' function, vegan package). We identified correlations between ecosystem functions and microbial community variables using Pearson correlation. For all ecosystem functions (i.e., C- and N-cycle process rates and multifunctionality), we considered biomass, diversity, and composition metrics as correlates and as candidate variables in regression models (see below). When appropriate, we also considered additional microbial variables for specific related processes, including *amoA* abundances as drivers of nitrification, extracellular enzymes as microbial drivers of C- and N-mineralization (e.g., NAG and LAP for N-mineralization), and fungal AM:ECM ratios as drivers of N-cycle processes (Phillips et al. 2013).

To determine 'importance' of soil and microbial variables for explaining variation in ecosystem functions, we used a multi-model inferencing approach (Burnham and Anderson 2002). Similar to recent studies (e.g., Powell et al. 2015; Graham et al. 2016), we generated a multiple regression model for all possible combinations of variables for each ecosystem function ('dredge' function, MuMIn package) and then selected the set of best-supported models for each function, consisting of all models within ΔAICc of 4 of the model with the lowest AICc value. We used this model set to determine standardized regression coefficients for each variable by generating a final averaged model for each ecosystem process using Aikake weights of the models ('model.avg' function, MuMIn

package). We determined importance of each candidate variable by calculating the sum of Aikake weights of all of the models in which each respective variable appeared ('importance' function, MuMIn package) (Powell et al. 2015).

To compare explanatory power of categories of variables (i.e., soil properties vs. microbial properties vs. all variables), we used best-subsets multiple regression. For each ecosystem function, we identified the regression model containing the best-supported subset of variables in each category based on AICc, resulting in three multiple regression models for each function (one for each variable category, 'bestglm' function, bestglm package). We then ranked these three best-supported models for each ecosystem function by AICc weight ('aictab' function, AICcmodavg package).

To identify mechanisms by which disturbance alters ecosystem functions, we used structural equation modeling (SEM). We included disturbance as a categorical variable in the SEM and included pH and DOC:TDN as key soil properties that respond to disturbance (Osburn et al. 2019). Candidate microbial drivers of ecosystem functions for the SEM were chosen based on correlations with functions (Fig. 4.2). To reflect mechanistic relationships, only relevant microbial variables were allowed to have direct influence on ecosystem functions (e.g., only nitrifiers directly influenced nitrification), while soil properties influenced functions indirectly through effects on microbial variables. The a-priori SEM is shown below Table 4.S3. We fit the SEM using the 'sem' function (lavaan package) and assessed SEM fit by bootstrapping estimates of comparative fit index (CFI), standardized root mean square residual (SRMR), and root mean square error of approximation (RMSEA) using the Bollen-Stine method

('bootstrapLavaan' function, lavaan package). The resulting path diagram shows standardized path coefficients ('standardizedSolution' function, lavaan package).

Results

Ecosystem functions

Measured ecosystem process rates were generally higher in disturbed sites than in reference sites, though the differences were not always statistically significant (Fig. 4.1). C-mineralization rates were not significantly different between disturbed and reference sites (Fig. 4.1A), while gross N-mineralization and nitrification rates were ~51% and ~ 143% higher in previously disturbed sites, respectively (Fig. 4.1B, C). Net N-mineralization and nitrification rates showed similar patterns compared with gross rates (Table 4.S4). Gross immobilization rates of NH_4^+ and NO_3^-, on the other hand, were not significantly different between disturbed and reference sites (Table 4.S4). When adjusted to microbial biomass, both C-mineralization and gross N-mineralization showed significant disturbance effects with ~28% and ~57% higher rates in disturbed sites, respectively (Fig 4.1D, E). Of all extracellular enzymes, only CHB showed significant disturbance effects, and was ~18% higher in disturbed sites (Table 4.S4). Finally, disturbed and reference sites were marginally different in terms of C- and N-cycle multifunctionality (PERMANOVA $P = 0.059$, Fig. 4.1F), which can be attributed to disturbed sites having generally higher C- and N-mineralization rates and enzyme activities, all of which were positively correlated with PCA axis 1 (Table 4.S4, Fig. 4.1F).

Correlations of ecosystem functions with microbial variables

C-mineralization was significantly correlated with several microbial community variables, including microbial biomass and activities of all C-cycle enzymes measured

(BG, XYL, CHB, Fig. 4.2). In terms of community composition, fungal:bacterial ratios (ITS:16S) and r:K ratios of bacterial phyla were positively correlated with C-mineralization, and bacterial and fungal β diversity (i.e., PCoA scores) also exhibited significant correlations with C-mineralization (Fig. 4.2). Similar to C-mineralization, N-mineralization was significantly correlated with several microbial community characteristics, including microbial biomass, activities of all N-acquiring enzymes measured (NAG, LAP, Fig. 4.2), bacterial r:K, bacterial and fungal β diversity, and fungal AM:ECM ratios (Fig. 4.2).

Nitrification rates were significantly positively correlated with *amoA* gene abundance of ammonia-oxidizing bacteria (AOB), complete ammonia oxidizers (CAOB), and r:K ratios of bacterial phyla (Fig. 4.2). Bacterial and fungal β diversity also exhibited significant correlations with nitrification rates (Fig. 4.2). Though community composition metrics do not directly relate to nitrification due to the phylogenetically restricted nature of nitrifying taxa, we still included the metrics as candidate variables in further analyses due to possible influence of nitrifier-heterotroph interactions on nitrification rates (Verhagen et al. 1992). Similar to specific C- and N-cycle processes, multifunctionality was significantly correlated with microbial biomass, r:K ratios of bacterial phyla, fungal AM:ECM, and bacterial and fungal β diversity (Fig 4.2). Unlike specific processes, however, multifunctionality was significantly positively correlated with bacterial α diversity (i.e., Shannon diversity, Fig. 4.2), as were activities of three enzymes: BG, CHB, and LAP (Fig. 4.S4).

Explanatory power of soil properties versus microbial properties

Multi-model inferencing showed r:K ratios of bacterial phyla and soil moisture as having the highest importance for explaining C-mineralization rates (Fig. 4.3A). Other soil properties (i.e., NO_3^-, DOC) and microbial community characteristics (i.e., biomass, XYL) were also among the most important variables (Fig 4.3A). Best-subsets multiple regression followed by model selection produced similar results, with the best-supported model for C- mineralization being the full model containing both soil and microbial properties (Table 4.1). This model had an adjusted R^2 of 0.826 (Table 4.1) and contained each of the highest importance variables (i.e., r:K, moisture, DOC, NO_3^-, XYL, biomass, Fig. 4.3A, Table 4.1) with the addition of CHB and BG enzyme activities (Table 4.1). Models for N-mineralization rates were dominated by two microbial variables, LAP enzyme activity and fungal AM:ECM, which had the highest importance values (Fig. 4.3B) and were the only variables retained in the best-supported regression model for N-mineralization (Table 4.1). This best model had an adjusted R^2 of 0.480, indicating our variables were able to explain less variation in N-mineralization relative to C-mineralization (Table 4.1).

The most important variables for explaining nitrification rates were soil NO_3^- and pH (Fig. 4.3C). CAOB abundance and 16S r:K were also among the most important variables (Fig. 4.3C). Though the full regression model containing microbial variables (i.e., CAOB abundance) explained the most variation in nitrification rates (adj. R^2 = 0.727, Table 4.1), the model containing only soil variables had the highest AICc weight (adj. R^2 = 0.713, Table 4.1). This model retained only pH and NO_3^- as predictors, suggesting microbial variables did not significantly improve explanation of nitrification

rates in our data set. The most important variables for explaining C- and N-cycle multifunctionality were r:K ratios, soil moisture, NH_4^+, and DOC (Fig. 4.3D). Each of these variables was also retained in the best-supported regression model for multifunctionality, (i.e., the full model), which had an adjusted R^2 of 0.789 (Table 4.1).

Mechanisms of disturbance effects on ecosystem functions

SEM results indicated adequate fit (CFI = 0.96, RMSEA = 0.072, and SRMR = 0.085) (Hooper et al. 2008) and the model explained 70%, 40%, and 30% of the variation in C-mineralization, N-mineralization, and nitrification, respectively. The SEM indicates significant effects of disturbance on key soil properties (i.e., increased pH, reduced DOC:TDN, Fig. 4.4). These altered soil properties affected all microbial variables, including nitrifier (i.e., CAOB) abundance, microbial biomass, and community composition (i.e., bacterial r:K, Fig 4.4). These microbial community characteristics, in turn, directly affected ecosystem functions, including CAOB effects on nitrification and effects of biomass and r:K on C-mineralization (Fig. 4.4). Bacterial r:K also indirectly affected nitrification via effects on CAOB and N-mineralization via influences on LAP, while biomass indirectly affected C-mineralization via influences on XYL (Fig. 4.4). An alternative SEM incorporating C- and N-cycle multifunctionality produced similar results, with significant effects of r:K and microbial biomass on multifunctionality (Fig. 4.S5).

Discussion

Our results revealed few microbial BEF relationships for the measured soil C- and N-cycle processes; we found no correlations of either bacterial or fungal α diversity (i.e., Shannon diversity) with rates of C-mineralization or N-mineralization (Fig. 4.2), despite

positive responses of bacterial α diversity to past forest disturbance (Osburn et al. 2019). This pattern did not change when explicitly considering species richness and evenness (Table 4.S5). In contrast, other studies involving experimental manipulation of soil bacterial α diversity have shown positive effects of diversity on processes such as denitrification (Philippot et al. 2013). This is possibly because our natural diversity gradient did not provide large enough differences in diversity to detect significant relationships. We did observe a positive correlation of bacterial α diversity with multifunctionality, similar to previous studies (Delgado-Baquerizo et al. 2016, 2020). However, α diversity was not identified by multiple regression or multi-model inferencing as an important driver of multifunctionality (Table 4.1, Fig. 4.3D), suggesting that α diversity may not be important for understanding variation in overall microbial ecosystem functioning, at least within the range of α diversity observed in our study.

In contrast to α diversity, microbial community composition metrics (e.g., bacterial r:K, β diversity, fungal AM:ECM) consistently correlated with specific ecosystem processes as well as multifunctionality (Fig. 4.2), supporting previous expectations (Bardgett and van der Putten 2014). Further, multiple regression, multi-model inferencing, and SEM indicated that bacterial r:K ratios are important for explaining variation in C-mineralization rates and C- and N-cycle multifunctionality (Table 4.1, Fig. 4.3, 4). Previous studies have also found bacterial r vs. K strategies to be important for soil C-cycling (Fierer et al. 2007). Though the r:K index for bacteria has also been recently criticized (Ho et al. 2017, Fierer 2017), in studies where environments are primarily distinguished by resource availability, as is the case for our disturbed vs. reference sites (Keiser et al. 2016, Osburn et al. 2019), the r:K index may be instructive

for elucidating microbial community-ecosystem function relationships. Multiple regression and multi-model inferencing also indicated fungal AM:ECM ratios as important for explaining variation in N-mineralization rates, which supports prior work showing that relative abundance of AM- vs. ECM-associated trees is an important indicator of terrestrial N-cycling rates (Phillips et al. 2013).

In addition to community composition, our results show several aggregate properties of microbial communities to be important for explaining variability in C- and N-mineralization rates. For example, LAP enzyme activity was an important predictor of N-mineralization (Table 4.1, Fig. 4.3A), similar to a recent study reporting strong relationships of gross N-mineralization with enzyme activities (Darby et al. 2020). Additionally, our SEM revealed XYL enzyme activity to be mechanistically important for C-mineralization and microbial biomass to be important for both C- and N-mineralization (Fig. 4.4). Overall, our multiple regression, multi-model inferencing, and SEM results suggest that studies seeking to understand overall C- and N-cycle functioning (i.e., multifunctionality) will benefit from metrics of microbial community composition (e.g., bacterial r:K), while additional measurements of microbial biomass and enzyme activities will improve understanding of specific processes (i.e., C- and N-mineralization). This is likely because these microbial community properties account for variation in ecosystem functions unaccounted for by soil properties alone. Indeed, partial correlation analyses revealed significant relationships of bacterial r:K with multifunctionality, LAP and AM:ECM with N-mineralization, and bacterial r:K and BG with C-mineralization after controlling for covariation with soil properties, while all other microbial community-ecosystem function correlations were eliminated (Fig. 4.S6). It

should be noted, however, that our models were more successful in explaining C-mineralization rates relative to N-mineralization rates, with R^2 values of 0.826 and 0.480, respectively (Table 4.1), which has also been observed in other studies (Colman and Schimel 2013, Graham et al. 2016). This difficulty in explaining N-mineralization rates may highlight the importance of soil and/or biological variables that we did not assess, such as clay mineralogy or chemical composition of organic N (Colman and Schimel 2013).

In contrast to C- and N-mineralization, multi-model inferencing and multiple regression showed microbial variables to be relatively unimportant for explaining nitrification rates (Table 4.1, Fig 4.3C). This is likely because microbial variables did not explain variation in nitrification rates unaccounted for by soil properties alone, e.g., pH, which is highly predictive of both nitrifier abundance and nitrification rates. This is supported by partial correlations, which showed no microbial variables correlated with nitrification after controlling for soil properties (Fig. 4.S6). The importance of microbial variables for explaining C-and N-mineralization and the lack thereof for nitrification appears to contradict previous expectations that microbial community information should be more valuable for phylogenetically narrow processes relative to broad processes (Schimel 1995). Though our data do not allow for rigorous tests of BEF relationships for nitrification, which would require full characterization of nitrifier diversity and community composition, it is striking that even overall abundance of these groups was relatively unimportant for explaining nitrification rates (Fig. 4.3C, Table 4.1). Similar results for other phylogenetically narrow processes (e.g., methanotrophy) may be expected if functions and the abundance of taxa responsible both strongly covary with

abiotic drivers. Our SEM results did, however, suggest important indirect effects of heterotroph-nitrifier interactions on nitrification, (Fig. 4.4), which has been previously shown in laboratory soil microcosms (Verhagen et al. 1992). Additionally, our results indicate potential mechanistic importance of newly-discovered complete ammonia-oxidizers to nitrification in forest soils (Fig. 4.4), similar to a parallel study from these sites (Osburn and Barrett 2020).

In general, our results provide strong support for including microbial community characteristics (i.e., community composition, biomass, enzyme activities) in studies seeking to understand variability in ecosystem functions such as C- and N-cycle processes. Next steps should involve elucidating links between aggregate community properties (e.g., enzyme activities) and microbial species composition (Hall et al. 2018). Though testing these links is beyond the scope of this study, our data do indicate relationships between community composition (bacterial r:K, AM:ECM, bacterial and fungal β diversity) and extracellular enzyme activities (Fig. 4.S4), which is worthy of future attention. Further, our results suggest that microbial community information may actually be more important for explaining phylogenetically broad processes (C- and N-mineralization) relative to narrow processes (nitrification), contrary to previous thinking (Schimel 1995). This is potentially because these broad processes are metabolically diverse and complex, and explicitly including microbial metabolism in models captures variation that abiotic variables cannot account for.

Overall, our study identifies long-term effects of historical forest disturbance on key ecosystem functions, as well as many notable relationships between soil microbial community properties and ecosystem functions. Specifically, previously disturbed forests

exhibited altered microbial multifunctionality, higher gross N-mineralization and nitrification rates, and higher biomass-adjusted C- and N-mineralization rates (Fig. 4.1). These higher biomass-adjusted rates (i.e., metabolic quotients) are indicative of lower microbial C- and N-use efficiencies in disturbed soil microbial communities relative to reference communities (Spohn and Chodak 2015, Li et al. 2020), which may be attributed to higher abundance of r-selected bacterial taxa in these soils (Osburn et al. 2019). Previous studies have reported similar effects on soil processes, including increased C-mineralization rates (Edwards and Ross-Todd 1983, Londo et al. 1999) and increased nitrification rates (Matson and Vitousek 1981, Waide et al. 1988, Keiser et al. 2016) in previously disturbed forests. Further, our SEM illustrates that these increased C- and N-cycle process rates are the end result of a cascade of disturbance effects, beginning with changes to soil properties such as pH and availability of C and N (Fig. 4.4), which are likely linked to distinct vegetation communities that develop in disturbed soils (Elliott and Vose 2011). These altered soil properties drive changes in key aspects of microbial communities that then have direct and indirect effects on ecosystem processes (Fig. 4.4). Importantly, the mechanisms we have described here are more precisely attributed to changes in specific soil properties, e.g., reduced C:N and increased pH, rather than to forest disturbance generally. For example, other studies have reported different effects of forest disturbance on soil properties, e.g., increased C:N, (Goodale and Aber 2001), and therefore different mechanistic influences of disturbance on microbial communities and associated ecosystem processes would be expected in such cases. However, we also expect that the microbial mechanisms that we have identified will be relevant across terrestrial ecosystems where anthropogenic activities have impacts on soil properties

similar to those we observed. For example, soil liming (i.e., increasing soil pH) increases C- and N-cycling rates in agroecosystems (Holland et al. 2018), which may involve similar microbial mechanisms to those described for our forest soils (e.g., increased bacterial r:K).

Finally, our results illustrate an apparent positive feedback in disturbed forest sites, where altered ecosystem process rates contribute to changes in soil properties (e.g., increased inorganic-N), which promote microbial community shifts that reinforce altered C- and N-cycle processes (i.e., higher r:K). This system of positive feedbacks by which soil properties, microbial communities, and ecosystem processes continually influence one another may account for the persistence of ecosystem-scale disturbance effects ~4-8 decades after disturbances occurred on our sites. In addition, this hierarchical organization of microbial influences on ecosystem functions supports several of the hypothesized linkages between microbial communities and ecosystem processes presented by the Hall et al. (2018) framework. We explicitly place the microbial and ecosystem metrics measured in this study, as well as the identified linkages between them, within the Hall et al. framework on Fig. 4.S7. Importantly, our study also illustrates the importance of incorporating anthropogenic factors, which have altered the functioning of terrestrial, freshwater, and marine ecosystems at a global scale (Millenium Ecosystem Assessment 2005). Our results demonstrate that microbial community properties (e.g., enzyme activities, bacterial r:K) play a central role in understanding these changes in ecosystem functioning and show that characterizing microbial responses to human activities will be critical for predicting ecosystem responses to future environmental change.

Acknowledgements

This work was funded by the Coweeta LTER, funded by National Science Foundation grant DEB-1637522. We thank the Coweeta Hydrologic Laboratory, Southern Research Station, USDA Forest Service for support and Angela Wiesel for assistance with field soil sampling and laboratory analyses. We also thank Bobbie Niederlehner for help with analytical chemistry and Dr. Steven McBride for his helpful comments on early versions of the manuscript. Finally, we thank two anonymous reviewers, whose insightful comments greatly improved this manuscript.

References

Bardgett, R. D., and W. H. van der Putten. 2014. Belowground biodiversity and ecosystem functioning. Nature 515:505–511.

Bartoń, K. 2019. MuMIn: Multi-Model Inference.

Bates, D., M. Maechler, B. Bolker [aut, cre, S. Walker, et al. 2019. lme4: Linear Mixed-Effects Models using "Eigen" and S4.

Bellemain, E., T. Carlsen, C. Brochmann, E. Coissac, P. Taberlet, et al. 2010. ITS as an environmental DNA barcode for fungi: an in silico approach reveals potential PCR biases. BMC Microbiology 10:189.

Bier, R. L., E. S. Bernhardt, C. M. Boot, E. B. Graham, E. K. Hall, et al. 2015. Linking microbial community structure and microbial processes: an empirical and conceptual overview. FEMS Microbiology Ecology 91.

Bolyen, E., J. R. Rideout, M. R. Dillon, N. A. Bokulich, C. Abnet, et al. 2018. QIIME 2: Reproducible, interactive, scalable, and extensible microbiome data science.

Brooks, P. D., J. M. Stark, B. B. McInteer, and T. Preston. 1989. Diffusion Method To Prepare Soil Extracts For Automated Nitrogen-15 Analysis. Soil Science Society of America Journal 53:1707–1711.

Burnham, K. P., and D. R. Anderson. 2002. Model Selection and Multimodel Inference: A Practical Information-Theoretic Approach. Springer, New York, NY.

Callahan, B. J., P. J. McMurdie, M. J. Rosen, A. W. Han, A. J. A. Johnson, et al. 2016. DADA2: High-resolution sample inference from Illumina amplicon data. Nature Methods 13:581–583.

Cardinale, B. J., J. E. Duffy, A. Gonzalez, D. U. Hooper, C. Perrings, et al. 2012. Biodiversity loss and its impact on humanity. Nature 486:59–67.

Colman, B. P., and J. P. Schimel. 2013. Drivers of microbial respiration and net N mineralization at the continental scale. Soil Biology and Biochemistry 60:65–76.

Covington, W. W. 1981. Changes in Forest Floor Organic Matter and Nutrient Content Following Clear Cutting in Northern Hardwoods. Ecology 62:41–48.

Darby, B. A., C. L. Goodale, N. A. Chin, C. B. Fuss, A. K. Lang, et al. 2020. Depth patterns and connections between gross nitrogen cycling and soil exoenzyme activities in three northern hardwood forests. Soil Biology and Biochemistry 147:107836.
Delgado-Baquerizo, M., F. T. Maestre, P. B. Reich, T. C. Jeffries, J. J. Gaitan, et al. 2016. Microbial diversity drives multifunctionality in terrestrial ecosystems. Nature Communications 7:1–8.
Delgado-Baquerizo, M., P. B. Reich, C. Trivedi, D. J. Eldridge, S. Abades, et al. 2020. Multiple elements of soil biodiversity drive ecosystem functions across biomes. Nature Ecology & Evolution 4:210–220.
Duffy, J. E. 2009. Why biodiversity is important to the functioning of real-world ecosystems. Frontiers in Ecology and the Environment 7:437–444.
Edwards, N. T., and B. M. Ross-Todd. 1983. Soil Carbon Dynamics in a Mixed Deciduous Forest Following Clear-Cutting with and without Residue Removal. Soil Science Society of America Journal 47:1014–1021.
Elliott, K. J., and J. M. Vose. 2011. The contribution of the Coweeta Hydrologic Laboratory to developing an understanding of long-term (1934-2008) changes in managed and unmanaged forests. Forest Ecology and Management 261:900–910.
Fierer, N. 2017. Embracing the unknown: disentangling the complexities of the soil microbiome. Nature Reviews Microbiology 15:579–590.
Fierer, N., M. A. Bradford, and R. B. Jackson. 2007. Toward an ecological classification of soil bacteria. Ecology 88:1354–1364.
Fierer, N., J. A. Jackson, R. Vilgalys, and R. B. Jackson. 2005. Assessment of Soil Microbial Community Structure by Use of Taxon-Specific Quantitative PCR Assays. Applied and Environmental Microbiology 71:4117–4120.
Fierer, N., and J. P. Schimel. 2003. A Proposed Mechanism for the Pulse in Carbon Dioxide Production Commonly Observed Following the Rapid Rewetting of a Dry Soil. Soil Science Society of America Journal 67:798.
Goodale, C. L., and J. D. Aber. 2001. The Long-Term Effects of Land-Use History on Nitrogen Cycling in Northern Hardwood Forests. Ecological Applications 11:253–267.
Graham, E. B., J. E. Knelman, A. Schindlbacher, S. Siciliano, M. Breulmann, et al. 2016. Microbes as Engines of Ecosystem Function: When Does Community Structure Enhance Predictions of Ecosystem Processes? Frontiers in Microbiology 7.
Hall, E. K., E. S. Bernhardt, R. L. Bier, M. A. Bradford, C. M. Boot, et al. 2018. Understanding how microbiomes influence the systems they inhabit. Nature Microbiology 3:977–982.
Handa, I. T., R. Aerts, F. Berendse, M. P. Berg, A. Bruder, et al. 2014. Consequences of biodiversity loss for litter decomposition across biomes. Nature 509:218–221.
Ho, A., D. Lonardo, D. Paolo, and P. L. E. Bodelier. 2017. Revisiting life strategy concepts in environmental microbial ecology. FEMS Microbiology Ecology 93.
Holland, J. E., A. E. Bennett, A. C. Newton, P. J. White, B. M. McKenzie, et al. 2018. Liming impacts on soils, crops and biodiversity in the UK: A review. Science of The Total Environment 610–611:316–332.

Hooper, D., J. Coughlan, and M. R. Mullen. 2008. Structural Equation Modelling: Guidelines for Determining Model Fit. Electronic Journal of Business Research Methods 6:53–60.
Jangid, K., M. A. Williams, A. J. Franzluebbers, T. M. Schmidt, D. C. Coleman, et al. 2011. Land-use history has a stronger impact on soil microbial community composition than aboveground vegetation and soil properties. Soil Biology and Biochemistry 43:2184–2193.
Keiser, A. D., J. D. Knoepp, and M. A. Bradford. 2016. Disturbance Decouples Biogeochemical Cycles Across Forests of the Southeastern US. Ecosystems 19:50–61.
Kirkham, D., and W. V. Bartholomew. 1954. Equations for Following Nutrient Transformations in Soil, Utilizing Tracer Data. Soil Science Society of America Journal 18:33–34.
Kohout, P., M. Charvátová, M. Štursová, T. Mašínová, M. Tomšovský, et al. 2018. Clearcutting alters decomposition processes and initiates complex restructuring of fungal communities in soil and tree roots. The ISME Journal 12:692–703.
Li, Z., Z. Zeng, D. Tian, J. Wang, Z. Fu, et al. 2020. The stoichiometry of soil microbial biomass determines metabolic quotient of nitrogen mineralization. Environmental Research Letters 15:034005.
Linden, M. J. M. and portions of code contributed by D. 2019. AICcmodavg: Model Selection and Multimodel Inference Based on (Q)AIC(c).
Londo, A. J., M. G. Messina, and S. H. Schoenholtz. 1999. Forest Harvesting Effects on Soil Temperature, Moisture, and Respiration in a Bottomland Hardwood Forest. Soil Science Society of America Journal 63:637–644.
Maestre, F. T., J. L. Quero, N. J. Gotelli, A. Escudero, V. Ochoa, et al. 2012. Plant Species Richness and Ecosystem Multifunctionality in Global Drylands. Science 335:214–218.
Matson, P. A., and P. M. Vitousek. 1981. Nitrogen Mineralization and Nitrification Potentials Following Clearcutting in the Hoosier National Forest, Indiana. Forest Science 27:781–791.
McLeod, A. I., and C. X. and Y. Lai. 2020. bestglm: Best Subset GLM and Regression Utilities.
Millenium Ecosystem Assessment. 2005. Ecosystems and Human Well Being: Synthesis. Island Press, Washington, DC.
Minick, K. J., B. D. Strahm, T. R. Fox, E. B. Sucre, and Z. H. Leggett. 2015. Microbial nitrogen cycling response to forest-based bioenergy production. Ecological Applications 25:2366–2381.
Mushinski, R. M., T. J. Gentry, and T. W. Boutton. 2018a. Organic matter removal associated with forest harvest leads to decade scale alterations in soil fungal communities and functional guilds. Soil Biology and Biochemistry.
Mushinski, R. M., Y. Zhou, T. J. Gentry, and T. W. Boutton. 2018b. Bacterial metataxonomic profile and putative functional behavior associated with C and N cycle processes remain altered for decades after forest harvest. Soil Biology and Biochemistry 119:184–193.

Nannipieri, P., J. Ascher, M. T. Ceccherini, L. Landi, G. Pietramellara, et al. 2003. Microbial diversity and soil functions. European Journal of Soil Science 54:655–670.
Nave, L. E., E. D. Vance, C. W. Swanston, and P. S. Curtis. 2010. Harvest impacts on soil carbon storage in temperate forests. Forest Ecology and Management 259:857–866.
Nguyen, N. H., Z. Song, S. T. Bates, S. Branco, L. Tedersoo, et al. 2016. FUNGuild: An open annotation tool for parsing fungal community datasets by ecological guild. Fungal Ecology 20:241–248.
Oksanen, J., F. G. Blanchet, M. Friendly, R. Kindt, P. Legendre, et al. 2019. vegan: Community Ecology Package.
Osburn, E. D., and J. E. Barrett. 2020. Abundance and functional importance of complete ammonia-oxidizing bacteria (comammox) versus canonical nitrifiers in temperate forest soils. Soil Biology and Biochemistry 145:107801.
Osburn, E. D., K. J. Elliottt, J. D. Knoepp, C. F. Miniat, and J. E. Barrett. 2018. Soil microbial response to Rhododendron understory removal in southern Appalachian forests: Effects on extracellular enzymes. Soil Biology and Biochemistry 127:50–59.
Osburn, E. D., S. G. McBride, F. O. Aylward, B. D. Badgley, B. D. Strahm, et al. 2019. Soil Bacterial and Fungal Communities Exhibit Distinct Long-Term Responses to Disturbance in Temperate Forests. Frontiers in Microbiology 10.
Otto, S. B., E. L. Berlow, N. E. Rank, J. Smiley, and U. Brose. 2008. Predator Diversity and Identity Drive Interaction Strength and Trophic Cascades in a Food Web. Ecology 89:134–144.
Parada, A. E., D. M. Needham, and J. A. Fuhrman. 2016. Every base matters: assessing small subunit rRNA primers for marine microbiomes with mock communities, time series and global field samples. Environmental Microbiology 18:1403–1414.
Pennock, D. J., and C. van Kessel. 1997. Clear-cut forest harvest impacts on soil quality indicators in the mixedwood forest of Saskatchewan, Canada. Geoderma 75:13–32.
Philippot, L., A. Spor, C. Hénault, D. Bru, F. Bizouard, et al. 2013. Loss in microbial diversity affects nitrogen cycling in soil. The ISME Journal 7:1609–1619.
Phillips, R. P., E. Brzostek, and M. G. Midgley. 2013. The mycorrhizal-associated nutrient economy: a new framework for predicting carbon-nutrient couplings in temperate forests. New Phytologist 199:41–51.
Powell, J. R., A. Welsh, and S. Hallin. 2015. Microbial functional diversity enhances predictive models linking environmental parameters to ecosystem properties. Ecology 96:1985–1993.
R Core Development Team. 2019. R: A Language and Environment for Statistical Computing. R Foundation for Statistical Computing, Vienna, Austria.
Rocca, J. D., E. K. Hall, J. T. Lennon, S. E. Evans, M. P. Waldrop, et al. 2015. Relationships between protein-encoding gene abundance and corresponding process are commonly assumed yet rarely observed. The ISME Journal 9:1693–1699.
Rodrigues, J. L. M., V. H. Pellizari, R. Mueller, K. Baek, E. da C. Jesus, et al. 2013. Conversion of the Amazon rainforest to agriculture results in biotic

homogenization of soil bacterial communities. Proceedings of the National Academy of Sciences 110:988–993.
Rosseel, Y., T. D. Jorgensen, D. Oberski, J. Byrnes, L. Vanbrabant, et al. 2019. lavaan: Latent Variable Analysis.
Schimel, J. 1995. Ecosystem Consequences of Microbial Diversity and Community Structure. Pages 239–254 *in* F. S. Chapin and C. Körner, editors. Arctic and Alpine Biodiversity: Patterns, Causes and Ecosystem Consequences. Springer Berlin Heidelberg, Berlin, Heidelberg.
Simard, D. G., J. W. Fyles, D. Paré, and T. Nguyen. 2011. Impacts of clearcut harvesting and wildfire on soil nutrient status in the Quebec boreal forest. Canadian Journal of Soil Science.
Spohn, M., and M. Chodak. 2015. Microbial respiration per unit biomass increases with carbon-to-nutrient ratios in forest soils. Soil Biology and Biochemistry 81:128–133.
Swank, W. T., and J. M. Vose. 1997. Long-term nitrogen dynamics of Coweeta forested watersheds in the southeastern United States of America. Global Biogeochemical Cycles 11:657–671.
Tilman, D., F. Isbell, and J. M. Cowles. 2014. Biodiversity and Ecosystem Functioning. Annual Review of Ecology, Evolution, and Systematics 45:471–493.
Tilman, D., P. B. Reich, J. Knops, D. Wedin, T. Mielke, et al. 2001. Diversity and Productivity in a Long-Term Grassland Experiment. Science 294:843–845.
Torsvik, V., L. Øvreås, and T. F. Thingstad. 2002. Prokaryotic Diversity--Magnitude, Dynamics, and Controlling Factors. Science 296:1064–1066.
Verhagen, F. J. M., H. Duyts, and H. J. Laanbroek. 1992. Competition for Ammonium between Nitrifying and Heterotrophic Bacteria in Continuously Percolated Soil Columns. Applied and Environmental Microbiology 58:3303–3311.
Vitousek, P. M., J. R. Gosz, C. C. Grier, J. M. Melillo, W. A. Reiners, et al. 1979. Nitrate Losses from Disturbed Ecosystems. Science 204:469–474.
Waide, J. B., W. H. Caskey, R. L. Todd, and L. R. Boring. 1988. Changes in Soil Nitrogen Pools and Transformations Following Forest Clearcutting. Pages 221–232 *in* W. T. Swank and D. A. Crossley, editors. Forest Hydrology and Ecology at Coweeta. Springer, New York, NY.
Webster, J. R., J. D. Knoepp, W. T. Swank, and C. F. Miniat. 2016. Evidence for a Regime Shift in Nitrogen Export from a Forested Watershed. Ecosystems 19:881–895.
Zhou, Z., C. Wang, and Y. Luo. 2018. Effects of forest degradation on microbial communities and soil carbon cycling: A global meta-analysis. Global Ecology and Biogeography 27:110–124.

Figures

Figure 4.1

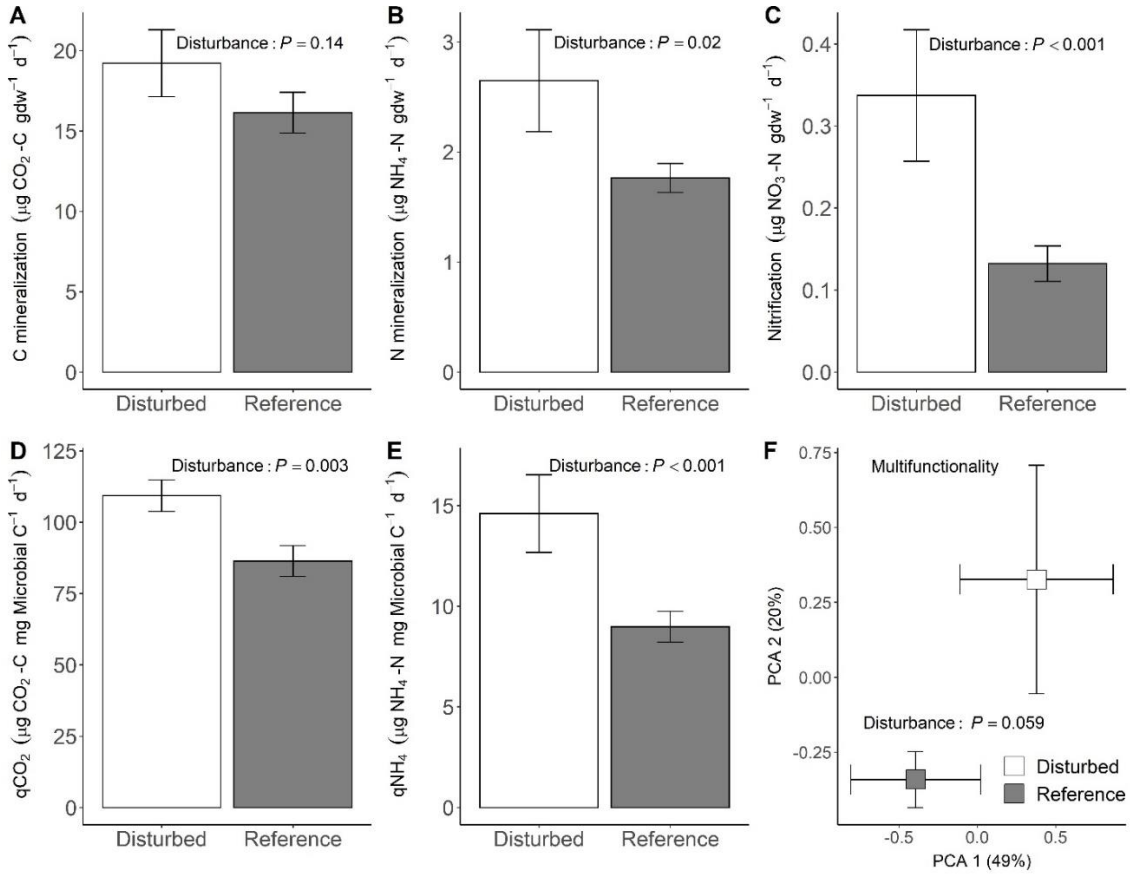

Figure 4.1: Effects of disturbance on carbon mineralization (A), gross nitrogen mineralization (B), gross nitrification (C), biomass-adjusted carbon mineralization (D), biomass-adjusted nitrogen mineralization (E), and C- and N-cycle multifunctionality (F). Error bars are ± one standard error. P-values are disturbance effects from mixed effects models (A-E) or from PERMANOVA (F). PCA in (F) represents 10 microbial C- and N-cycle functions (i.e., 'multifunctionality'): C-mineralization, net and gross N-mineralization and nitrification, and 5 enzyme activities (BG, XYL, CHB, LAP, NAG). Points in (F) are centroids of each treatment. PCA1 is positively correlated with mineralization rates and enzyme activities while PCA2 is negatively correlated with nitrification rates.

Figure 4.2

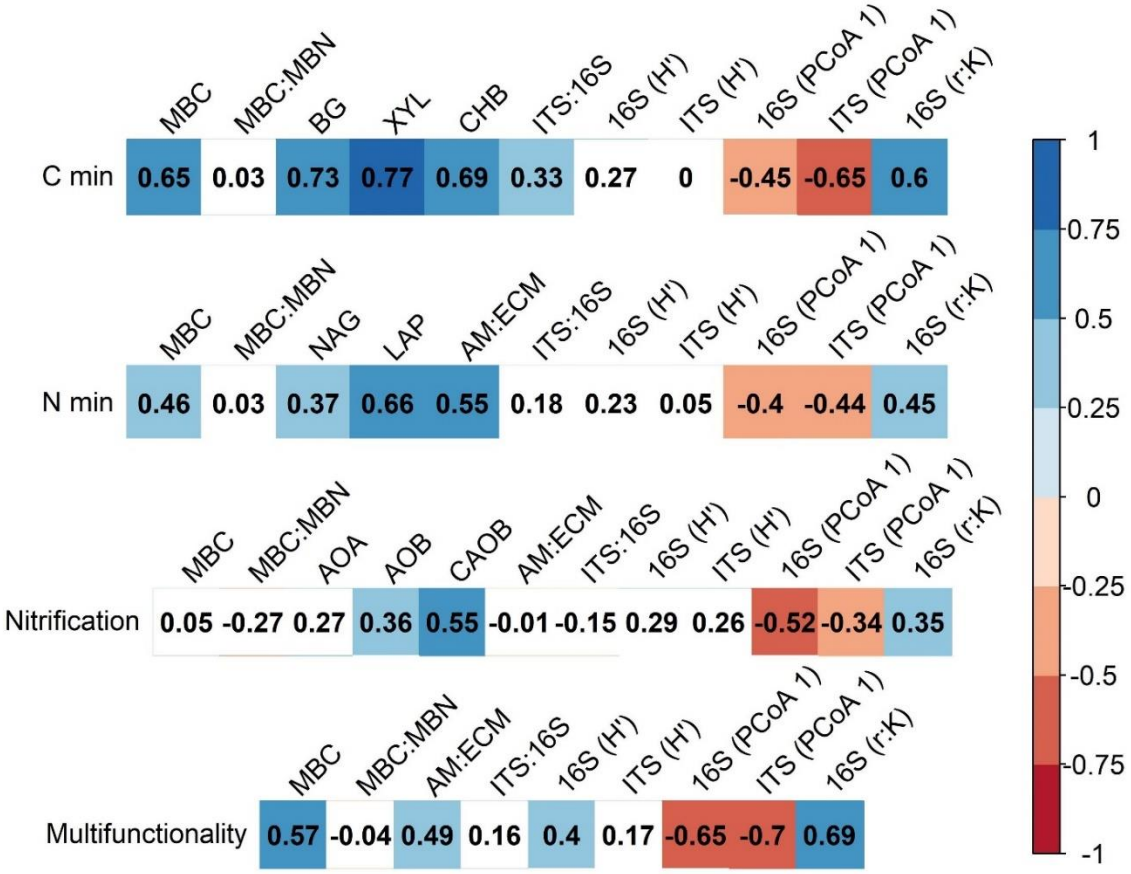

Figure 4.2: Pearson correlation coefficients between microbial properties and ecosystem functions (C-mineralization, gross N-mineralization, gross nitrification, and C- and N-cycle multifunctionality). Only statistically significant correlations are colored in ($P < 0.05$). For all ecosystem functions, we tested for correlations with microbial biomass and diversity/composition metrics. For specific C- and N-cycle processes, we also tested for correlations with appropriate extracellular enzyme activities (e.g., NAG, LAP, and N-mineralization rates) or functional genes (i.e., *amoA* genes and nitrification rates). We also included AM:ECM ratios as candidate correlates of N-cycle processes and multifunctionality. Microbial community composition (i.e., β diversity) is represented by 16S and ITS PCoA 1 scores.

Figure 4.3

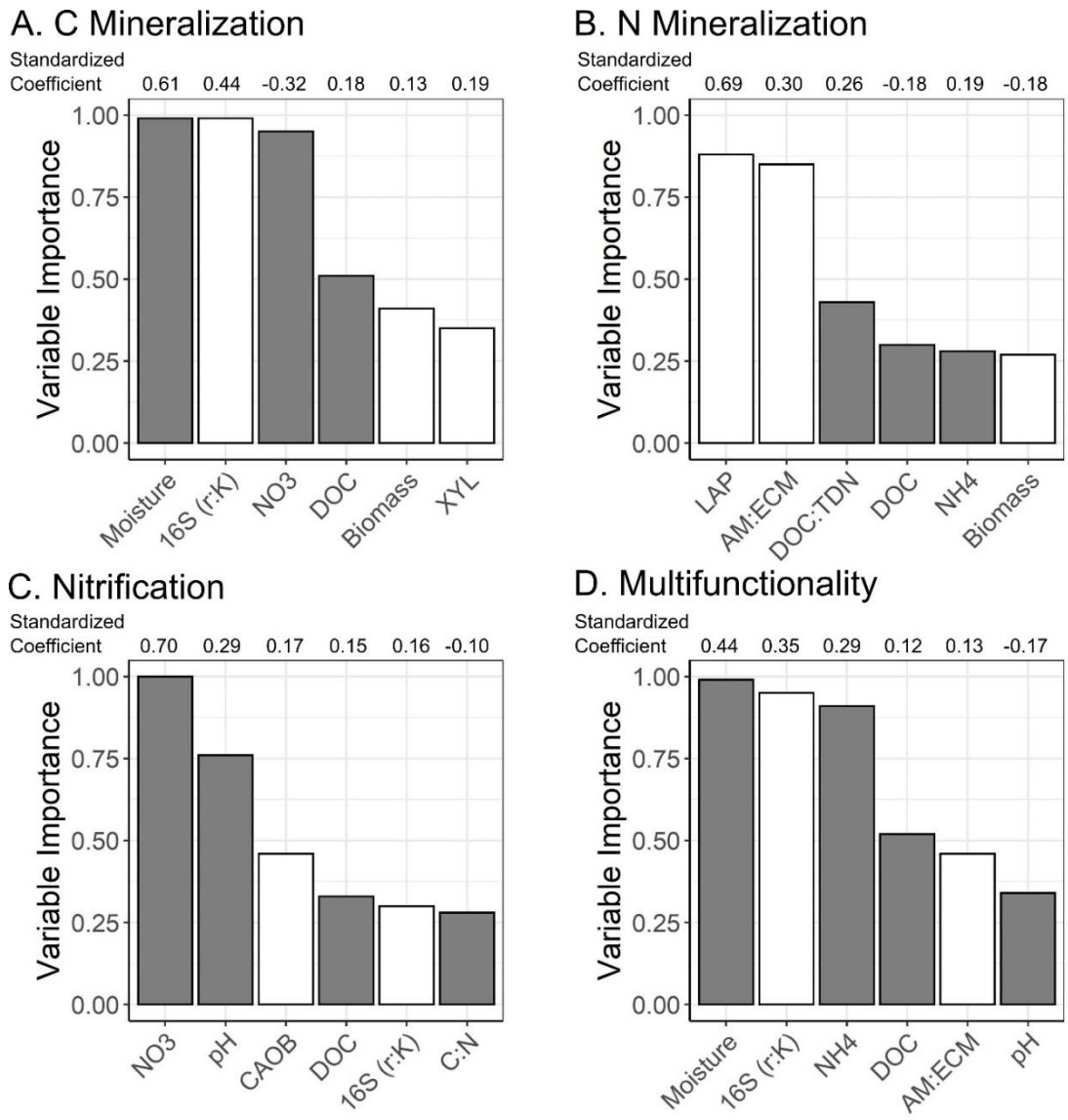

Figure 4.3: Variable importance and standardized regression coefficients from multi-model inferencing for the top predictors for each ecosystem function. Variable importance was estimated by summing Aikake weights of models containing each respective variable. Coefficients at the top of each bar are standardized regression coefficients from the final averaged model for each ecosystem function. Bar color represents variable category (grey, soil properties; white, microbial properties).

Figure 4.4

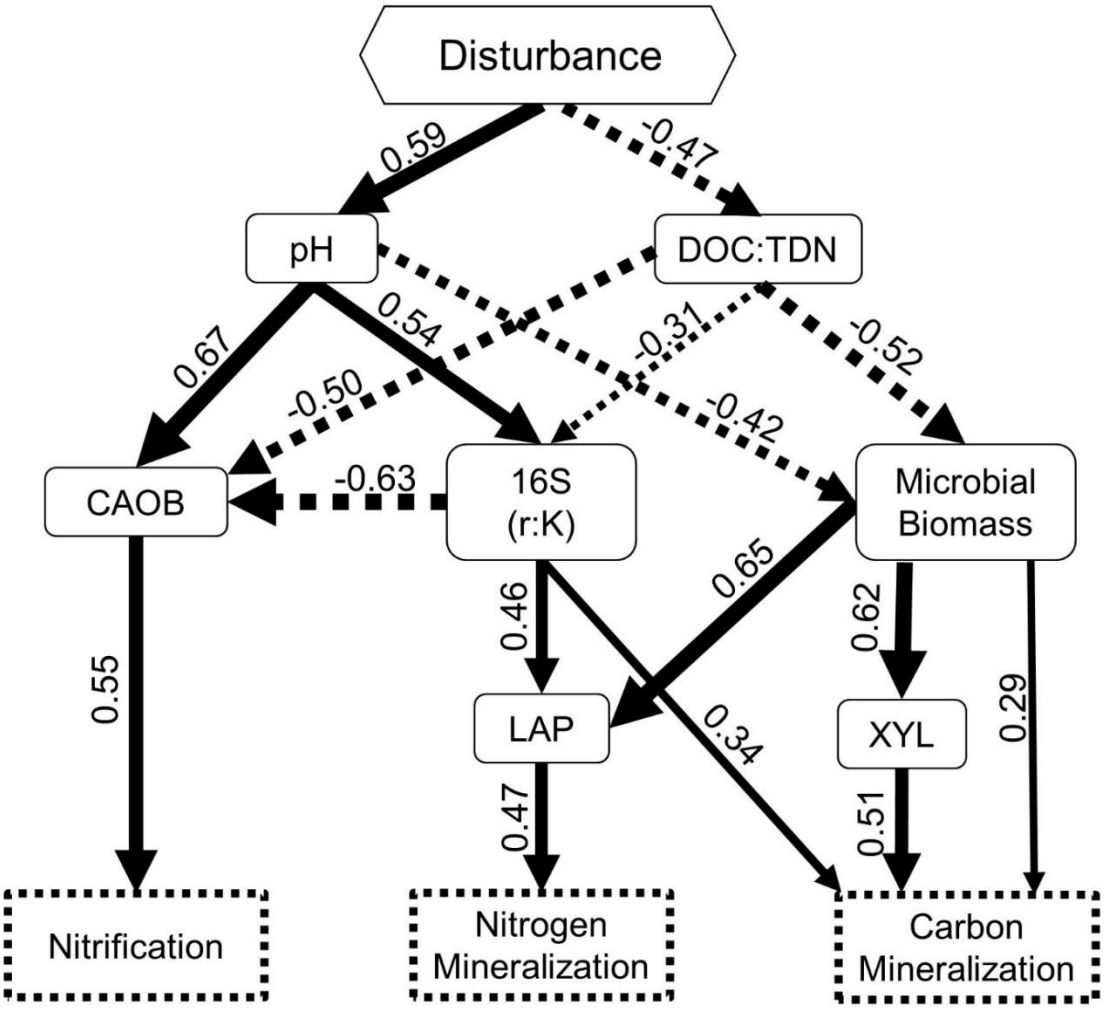

Figure 4.4: Structural equation model (SEM) of disturbance effects on soil properties, microbial communities, and C- and N-cycle processes. Values on each path are standardized path coefficients and only statistically significant paths are shown ($P < 0.05$). Solid and dashed lines represent positive and negative relationships, respectively. SEM fit was evaluated using bootstrapped values for the Comparative Fit Index (CFI = 0.96), Root Mean Square Error of Approximation (RMSEA = 0.072) and Standardized Root Mean Square Residual (SRMR = 0.085). The SEM explains 70%, 40%, and 30% of the variation in C-mineralization, N-mineralization, and nitrification rates, respectively.

Tables

Table 4.1

Process	Model	Predictor Variables Included	Adj. R^2	ΔAIC_c	AICc Wt.
C Mineralization	Full Model	16S (r:K), MBC, XYL, BG, CHB, Moisture, NO_3, DOC	0.826	0.0	1.0
	Microbial Properties	16S (r:K), MBC, XYL, BG, CHB, 16S (H'), ITS (PCoA 1)	0.772	14.88	0.0
	Soil Properties	Moisture, NH_4, NO_3	0.716	16.23	0.0
N Mineralization	Microbial Properties*	LAP, AM:ECM	0.480	0.0	0.99
	Soil Properties	Moisture	0.355	8.79	0.01
Nitrification	Soil Properties	pH, NO_3	0.713	0.0	0.56
	Full Model	CAOB, pH, NO_3, DOC	0.727	0.52	0.44
	Microbial Properties	CAOB, 16S (r:K), MBC, MBC:MBN	0.415	36.34	0.0
Multifunctionality	Full Model	Moisture, NH_4, DOC, 16S (r:K)	0.788	0.0	0.99
	Soil Properties	Moisture, NH_4, NO_3, DOC:TDN, C:N	0.749	9.56	0.01
	Microbial Properties	16S (r:K), MBC, MBC:MBN, 16S (H'), ITS (PCoA 1), AM:ECM	0.658	25.76	0

Table 4.1: Best-supported multiple regression models for each category of predictor variables for each respective ecosystem function. The three models for each ecosystem function are ranked top to bottom by AICc weight. *For N Mineralization, the best-supported ‘Microbial Properties’ and ‘Full’ models were identical.

Supplementary Figures

Figure 4.S1

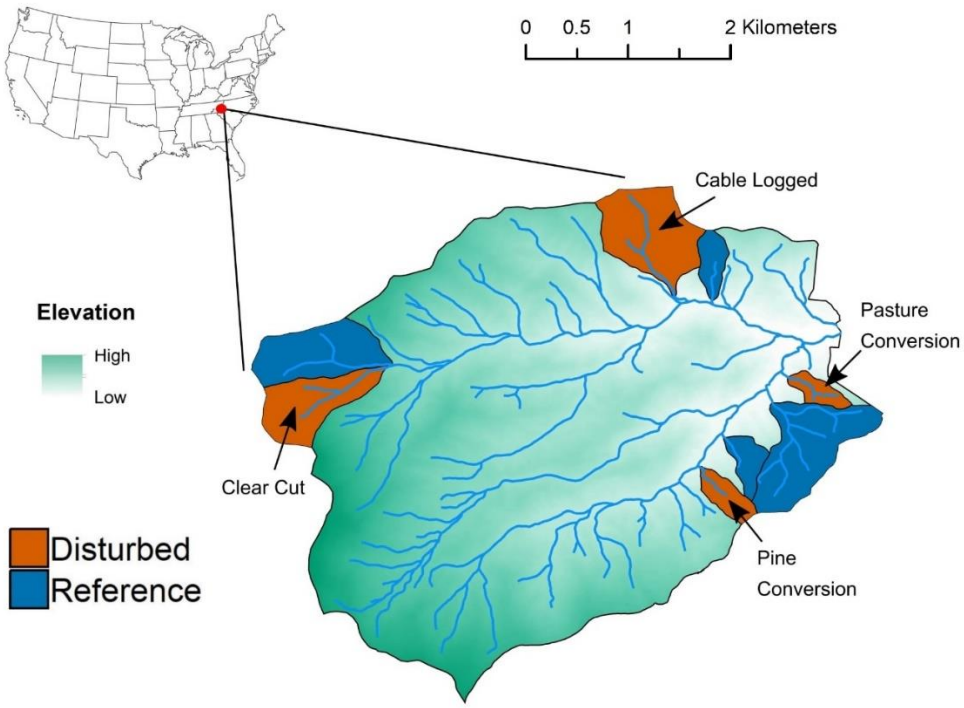

Figure 4.S1: Map of watershed pairs at the USDA Forest Service Coweeta Hydrologic Laboratory sampled for this study

Figure 4.S2

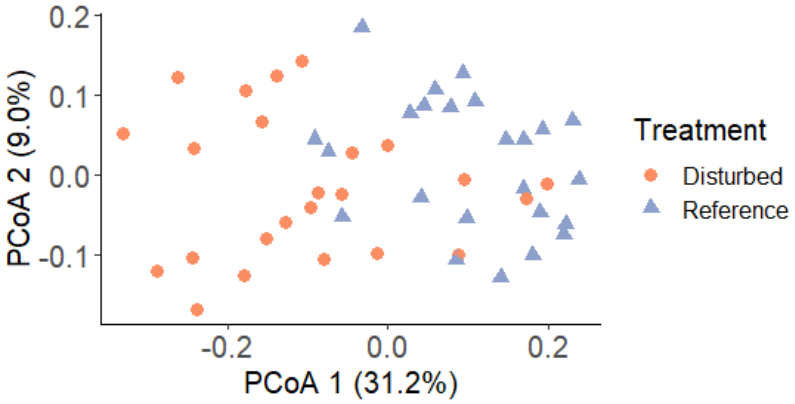

Figure 4.S2**:** Principal Coordinates Analysis (PCoA) ordination of bacterial (16S) community structure using Bray-Curtis distances. Values in parentheses represent percentage of variance explained by each respective PCoA axis.

Figure 4.S3

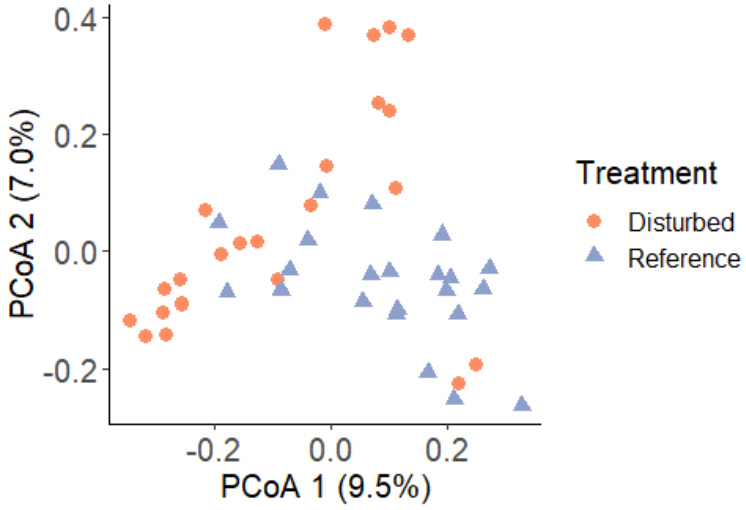

Figure 4.S3: Principal Coordinates Analysis (PCoA) ordination of fungal (ITS) community structure using Bray-Curtis distances. Values in parentheses represent percentage of variance explained by each respective PCoA axis.

Figure 4.S4

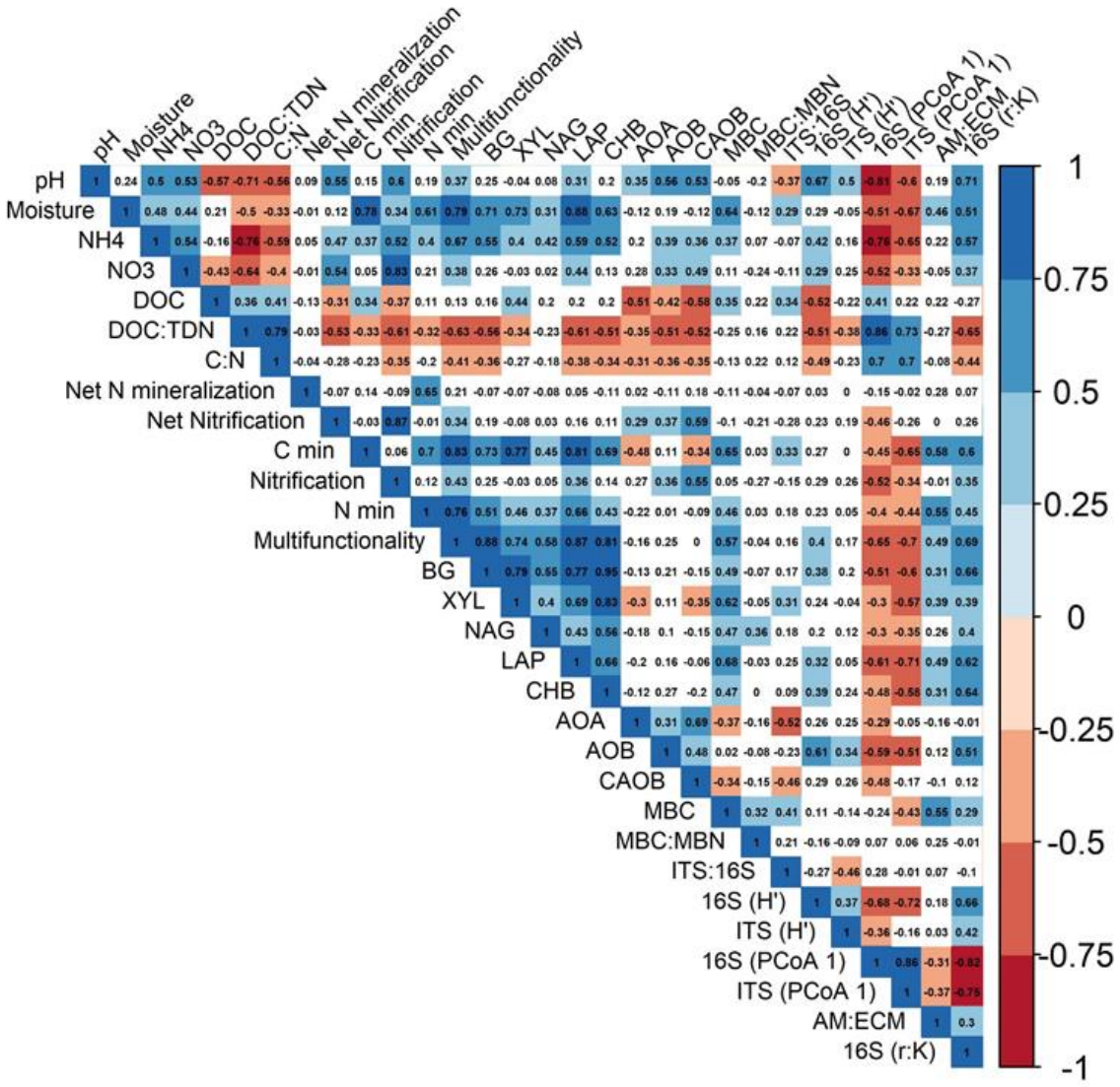

Figure 4.S4: Pearson correlations between ecosystem processes, soil variables, and microbial variables. Only significant correlations are colored in ($P < 0.05$).

Figure 4.S5

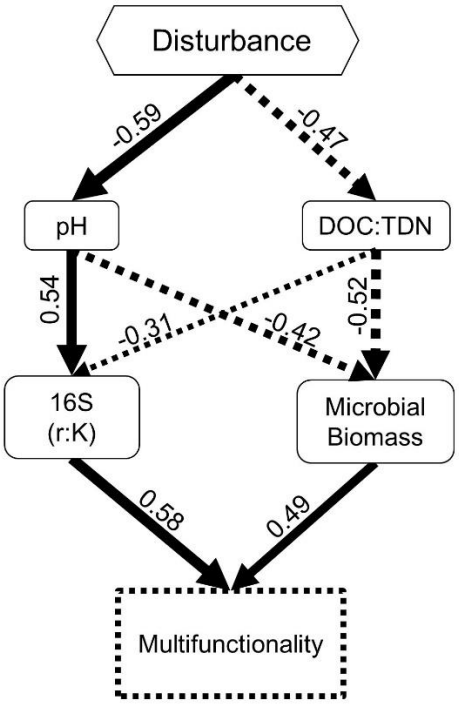

Figure 4.S5: Structural equation model (SEM) of disturbance effects on soil properties, microbial communities, and multifunctionality. Values on each path are standardized path coefficients and only statistically significant paths are shown ($P < 0.05$). Solid and dashed lines represent positive and negative relationships, respectively. SEM fit was evaluated using bootstrapped values for Comparative Fit Index (CFI = 0.98), Root Mean Square Error of Approximation (RMSEA = 0.06) and Standardized Root Mean Square Residual (SRMR = 0.06). The SEM explains 56% of the variation in microbial multifunctionality.

Figure 4.S6

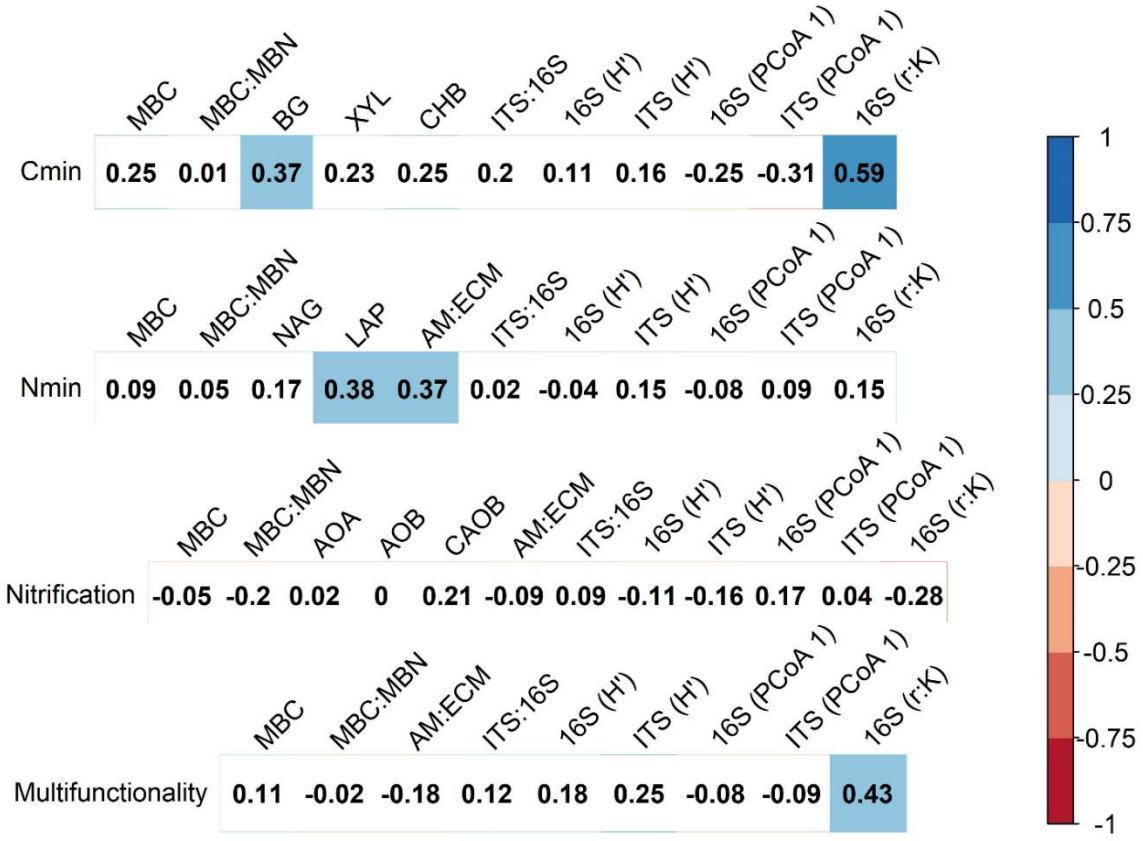

Figure 4.S6: Partial Pearson correlation coefficients between ecosystem functions and microbial variables after controlling for soil properties (pH, Moisture, DOC, DOC:TDN, C:N, NO_3, NH_4). Only significant correlations are colored in ($P < 0.05$).

Figure 4.S7

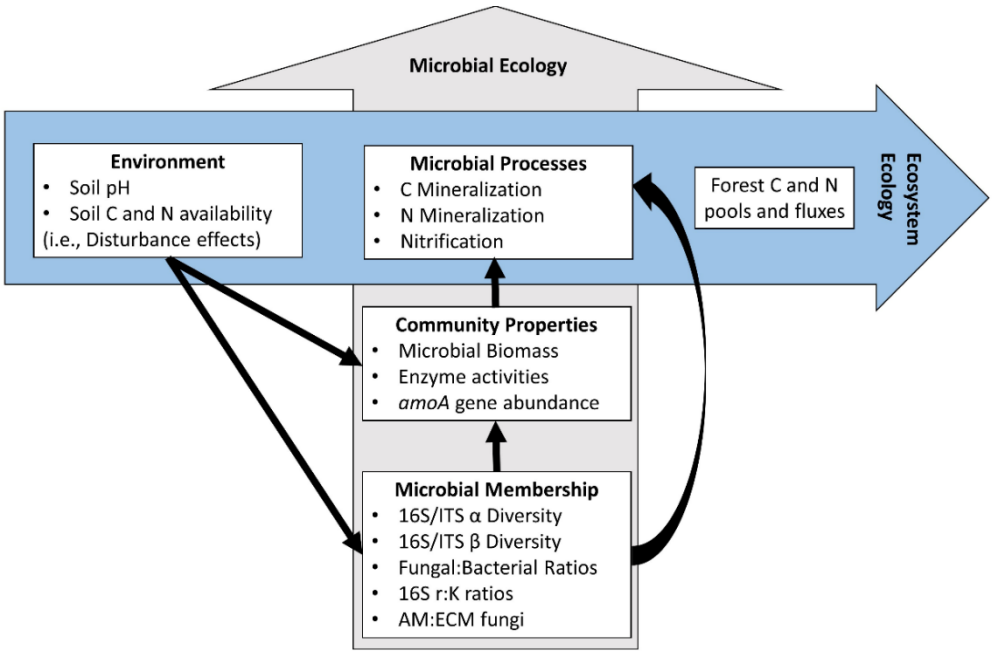

Figure 4.S7: Microbial community and process metrics from this study placed within the framework of Hall et al. (2018). Arrows represent the linkages explicitly tested in this study, i.e., Disturbance alters the soil environment, which impacts microbial membership and microbial community properties, which have direct and indirect effects on microbial process rates. These linkages correspond to arrows ‘C,’ ‘D,’ ‘E,’ ‘G,’ and ‘H’ from Figure 2 of Hall et al. (2018).

Supplementary Tables

Table 4.S1

Watershed Pair	Watershed Number	Treatment	Aspect	Elevation (m)	Area (ha)
Cable Logged	WS2	Undisturbed since 1923	SSE	709 – 1004	12
	WS7	Commercially clear cut and cable logged in 1977	S	772 – 1077	59
Pasture Conversion	WS14	Undisturbed since 1923	NW	707 – 992	61
	WS6	Clearcut in 1958, soil scarified, planted to grass, limed and fertilized in 1959, fertilized again in 1965, grass herbicided in 1966 and 1967	NW	696 – 905	9
Pine Conversion	WS18	Undisturbed since 1923	NW	726 – 993	13
	WS17	All woody vegetation cut annually 1940 - 1955, white pine planted in 1956	NW	760 – 1021	13
Clear Cut	WS36	Undisturbed since 1923	ESE	1021 – 1542	49
	WS37	All woody vegetation cut in 1963, no products removed	ENE	1033 – 1592	44

Table 4.S1: Detailed watershed information for all eight watersheds sampled in this study.

Additional watershed information can be found at:
https://coweeta.uga.edu/Watersheds.html

Table 4.S2

Variable	Reference	Disturbed
pH	5.25 (0.038)	5.56 (0.052)***
Moisture (g H_2O g $soil^{-1}$)	0.30 (0.014)	0.294 (0.008)
NO_3 (µg N g $soil^{-1}$)	0.119 (0.040)	1.08 (0.443)***
NH_4 (µg N g $soil^{-1}$)	1.79 (0.140)	2.53 (0.187)***
DOC (µg C g $soil^{-1}$)	391.9 (13.0)***	302.7 (17.7)
TDN (µg N g $soil^{-1}$)	46.7 (2.41)	42.8 (2.59)
DOC:TDN	8.61 (0.264)*	7.22 (0.286)
DON (µg N g $soil^{-1}$)	44.7 (2.30)*	39.1 (2.50)
Microbial Biomass C (µg C g $soil^{-1}$)	204.6 (13.3)*	176.0 (15.8)
Microbial Biomass N (µg N g $soil^{-1}$)	41.5 (2.62)	40.0 (3.27)
Microbial Biomass C:N	4.85 (0.174)*	4.30 (0.115)
Total C (mg C g $soil^{-1}$)	41.3 (3.18)	45.5 (4.95)
Total N (mg N g $soil^{-1}$)	2.35 (0.203)	2.90 (0.328)*
C:N	17.9 (0.440)**	16.1 (0.354)
SIR (µg CO_2-C g $soil^{-1}$ d^{-1})	82.8 (4.13)	93.1 (7.52)*

Table 4.S2: Soil physicochemical variables aggregated across disturbed and reference soil samples. Means ± one SE shown. Asterisks indicate significantly higher values (linear mixed effects models) at the following significance levels: * $P < 0.05$, ** $P < 0.01$, *** $P < 0.001$.

Table 4.S3

Regression			estimate	se	z	P value	ci.lower	ci.upper
gNmin	~	LAP	0.461	0.158	2.921	0.003	0.152	0.771
CO2	~	rK	0.318	0.083	3.84	0	0.156	0.481
CO2	~	XYL	0.508	0.093	5.475	0	0.326	0.69
CO2	~	MBC	0.303	0.098	3.085	0.002	0.111	0.496
gNit	~	logCAOB	0.549	0.1	5.466	0	0.352	0.745
LAP	~	rK	0.418	0.09	4.66	0	0.242	0.594
LAP	~	MBC	0.673	0.075	8.984	0	0.526	0.819
XYL	~	MBC	0.645	0.084	7.695	0	0.481	0.809
rK	~	pH	0.537	0.096	5.577	0	0.348	0.725
rK	~	DOC.TDN	-0.31	0.107	-2.887	0.004	-0.52	-0.099
MBC	~	DOC.TDN	-0.54	0.109	-4.973	0	-0.753	-0.327
MBC	~	pH	-0.408	0.117	-3.503	0	-0.637	-0.18
logCAOB	~	rK	-0.627	0.145	-4.335	0	-0.911	-0.344
logCAOB	~	pH	0.673	0.126	5.359	0	0.427	0.92
logCAOB	~	DOC.TDN	-0.501	0.114	-4.392	0	-0.725	-0.278
pH	~	Disturbance	0.588	0.087	6.787	0	0.419	0.758
DOC.TDN	~	Disturbance	-0.469	0.107	-4.368	0	-0.679	-0.258
gNmin	~~	gNmin	0.605	0.108	5.62	0	0.394	0.816
CO2	~~	CO2	0.297	0.071	4.19	0	0.158	0.436
gNit	~~	gNit	0.699	0.11	6.348	0	0.483	0.915
LAP	~~	LAP	0.376	0.085	4.443	0	0.21	0.542
XYL	~~	XYL	0.556	0.107	5.184	0	0.346	0.766
rK	~~	rK	0.524	0.101	5.173	0	0.326	0.723
MBC	~~	MBC	0.663	0.108	6.136	0	0.451	0.875
logCAOB	~~	logCAOB	0.529	0.105	5.062	0	0.324	0.734
pH	~~	pH	0.654	0.102	6.406	0	0.454	0.854
DOC.TDN	~~	DOC.TDN	0.78	0.101	7.749	0	0.583	0.977
gNmin	~~	CO2	0.446	0.117	3.814	0	0.217	0.675

A-priori SEM: sem <-'Nmin ~ LAP + rK + MBC + AMEM
CO2 ~rK +XYL +MBC
gNit ~ logCAOB
LAP ~ rK + MBC + AMEM
XYL ~ rK + MBC
rK ~ pH + DOC.TDN
MBC ~ DOC.TDN + pH
logCAOB ~ rK + pH + DOC.TDN + AMEM
AMEM ~ pH + DOC.TDN
pH ~ Disturbance
DOC.TDN ~ Disturbance'

Table 4.S3: Structure equation model (SEM) represented in Figure 4.4

Table 4.S4

Function	Reference	Disturbed
Net N Mineralization	-0.413 (0.305)	0.194 (0.299)**
Net Nitrification	0.041 (0.025)	0.501 (0.291)**
Gross NH_4 Immobilization	2.093 (0.170)	2.362 (0.323)
Gross NO_3 Immobilization	0.096 (0.014)	0.111 (0.023)
BG	263 (42.8)	309 (33.3)
XYL	80.1 (10.4)	72.1 (7.68)
CHB	35.5 (7.15)	41.9 (4.85)***
NAG	333 (52.9)	449 (126)
LAP	68.8 (5.14)	81.5 (9.07)

Table 4.S4: Microbial functions across disturbed and reference soil samples. Means ± one SE shown. Asterisks indicate significantly higher values (mixed effects models) at the following significance levels: * $P < 0.05$, ** $P < 0.01$, *** $P < 0.001$. Rates of N-cycle processes are in µg N per gram of dry soil per day. Rates of enzymes activities are nmoles substrate per gram of dry soil per hour.

Table 4.S5

Process	16S richness	16S evenness	ITS richness	ITS evenness
C	.20	.13	.16	-.10
mineralization	.16	.31	.29	.52
N	.20	.16	.05	.01
mineralization	.19	.32	.72	.94
Nitrification	.16	.21	.29	.20
	.28	.13	.06	.19

Table 4.S5: Pearson correlations between 16S and ITS richness and evenness and ecosystem process rates. Values are correlation coefficients (top), with *P* values listed below. Richness is estimated from observed numbers of OTUs in rarefied data sets, while evenness is estimated using the Simpson index.

Table 4.S6

Regression			est.std	se	z	P value	ci.lower	ci.upper
Multifunctionality	~	rK	0.578	0.087	6.619	0	0.407	0.749
Multifunctionality	~	MBC	0.485	0.093	5.241	0	0.304	0.666
rK	~	DOC.TDN	-0.31	0.107	-2.887	0.004	-0.52	-0.099
rK	~	pH	0.537	0.096	5.577	0	0.348	0.725
MBC	~	pH	-0.418	0.117	-3.581	0	-0.647	-0.189
MBC	~	DOC.TDN	-0.519	0.111	-4.677	0	-0.737	-0.302
DOC.TDN	~	Disturbance	-0.469	0.107	-4.368	0	-0.679	-0.258
pH	~	Disturbance	0.588	0.087	6.787	0	0.419	0.758
Multifunctionality	~~	Multifunctionality	0.443	0.094	4.729	0	0.259	0.627
rK	~~	rK	0.524	0.101	5.173	0	0.326	0.723
MBC	~~	MBC	0.675	0.108	6.251	0	0.463	0.887
DOC.TDN	~~	DOC.TDN	0.78	0.101	7.749	0	0.583	0.977
pH	~~	pH	0.654	0.102	6.406	0	0.454	0.854

```
sem2 <-
 'Multifunctionality ~  rK + MBC
rK ~ DOC.TDN + pH
MBC ~ pH+DOC.TDN
DOC.TDN ~ Disturbance
pH~Disturbance'
```

Table 4.S6: Structure equation model (SEM) represented in Figure 4.S5. A-priori model

is shown, followed by the model output table.

CHAPTER 5 - Historical forest disturbance mediates soil microbial community responses to drought

Authors

Ernest D Osburn, Brian D Badgley, Frank O Aylward, J E Barrett

Abstract

Despite the abundance of studies demonstrating effects of drought on soil microbial communities, the role of historical land use in mediating these drought effects is unclear. Because drought and land use change are common to most of earth's land surface, we conducted a drought-rewetting experiment in soils from two adjacent and currently forested watersheds with distinct land use histories: an undisturbed 'reference' site and a 'disturbed' site with a history of deforestation and conversion to agriculture. We incubated intact soil cores at either constant moisture or under a six-week drought followed by rewetting and six weeks at constant moisture. Several times throughout the experiment, we sampled soils and characterized bacterial and fungal communities using 16S and ITS amplicon sequencing. In both land uses, bacterial alpha diversity decreased following drought-rewetting while fungal diversity increased, though bacterial diversity changed less (i.e., higher resistance) and recovered more (i.e., higher resilience) compared with fungal diversity. Bacterial beta diversity also changed markedly following drought-rewetting, especially in historically disturbed soils, while fungal beta diversity exhibited little response (i.e., high resistance). Additionally, bacterial beta diversity in disturbed soils recovered less from drought-rewetting (i.e., lower resilience) compared with reference soils. Specific bacterial functional groups also exhibited drought-rewetting responses, some of which were distinct between land uses, including significant decreases in nitrifying taxa and increases in r-selected taxa in disturbed soils. Co-

occurrence networks also revealed land use influences on microbial drought responses, with large reductions in network connectivity observed in disturbed soil bacterial communities exposed to drought-rewetting. Overall, our study reveals historical land use to be important in mediating responses of soil microbial communities to drought, which will influence the ecosystem-scale trajectories of these environments under ongoing and future climate change.

Introduction

Climate change is altering precipitation patterns globally, resulting in increased frequency and duration of droughts in many regions (IPCC, 2013). These intensifying droughts will have wide-ranging impacts on biological communities and on terrestrial ecosystem processes. For example, drought is altering the diversity and species composition of plant communities in many ecosystems (e.g., Fahey et al., 2018; Liu et al., 2018) and is also altering communities of animal consumers across multiple trophic levels (e.g., Cohen et al., 2018; Eisenhauer et al., 2018; Wise & Lensing, 2019). Soil microorganisms are also impacted by drought, as desiccation and subsequent rewetting impose significant physiological stress on microbial taxa (Schimel et al., 2007). These microbial responses to drought will influence future functioning of the ecosystems they inhabit. For example, microbial taxa are the dominant drivers of carbon (C) cycling in soils (Schimel & Schaeffer, 2012), which, in turn, harbor the largest terrestrial stock of C globally (IPCC, 2013), thereby illustrating a potentially important feedback between microbial communities and climate. Overall, the sensitivity of soil microorganisms to water stress along with the central roles of microorganisms in mediating terrestrial

ecosystem processes highlight the critical importance of characterizing soil microbial responses to drought in terrestrial environments.

Some effects of drought-rewetting on soil microbial communities have long been recognized – for example, microbial activity declines as soils dry, followed by a short-lived but spectacular pulse of activity (i.e., increased repiration) following rewetting, known as the "Birch Effect" (Birch, 1958). This respiration pulse is partly driven by the rapid breakdown of microbial necromass - many microorganisms die from osmotic stress or starvation during drought periods, resulting in declines in total microbial biomass (Jansson & Hofmockel, 2019; Schimel, 2018; Zhou et al., 2018a). Though these declines in overall microbial community size are often observed, drought does not affect all microbial taxa equally – for example, fungi are thought to be more drought-tolerant than bacteria, as fungal hyphae may allow for acquisition of spatially distant resources (Schimel et al., 2007). This is supported by several lines of evidence, including studies showing increased fungal:bacterial ratios following drought (Evans & Wallenstein, 2012; Sun et al., 2020), higher drought-resistance of fungal-based food webs relative to bacterial-based food webs (De Vries et al., 2012), and greater stability of fungal co-occurrence networks under drought compared with bacterial co-occurrence networks (De Vries et al., 2018). Studies applying sequencing technologies to characterize bacterial and fungal responses to drought also support this, indicating minimal responses of fungi to drought at the community level (e.g., Barnard et al., 2013; Preece et al., 2019).

In contrast to fungi, clear responses of bacterial communities to drought-rewetting are often observed (e.g., Barnard et al., 2013; Evans et al., 2014; Evans & Wallenstein, 2014; Placella et al., 2012; Preece et al., 2019). In general, bacterial taxa that are

primarily gram-positive (e.g., Actinobacteria, Firmicutes) are expected to be more drought-tolerant than bacterial taxa that are primarily gram-negative (e.g., Proteobacteria,Verrucomicrobia) due to stronger, thicker peptidoglycan cell walls (Jansson & Hofmockel, 2019; Naylor & Coleman-Derr, 2018; Schimel et al., 2007). This is supported by multiple previous studies showing positive responses of Actinobacteria to drought (Barnard et al., 2013; Naylor & Coleman-Derr, 2018; Preece et al., 2019) as well as a recent meta-analysis showing negative drought responses of Proteobacteria and Verruomicroba (Zhou et al., 2018a). However, predicting responses of bacterial taxa is complicated by the fact that many taxa exhibit opposite responses to the distinct stresses of drying and rewetting (Barnard et al., 2013). Further, drought responses reported for bacterial phyla often differ among studies (Naylor & Coleman-Derr, 2018; Schimel, 2018), likely due compositional differences among sites at finer taxonomic scales, and can also change over time as taxa acquire drought-tolerance adaptations as a result of prior exposure to water stress (Bouskill et al., 2013; Evans & Wallenstein, 2014). Taken together, these prior studies suggest that responses of specific bacterial taxa to drought may be difficult to predict, but that community-scale impacts of drought on soil bacteria are likely to occur.

Though physiological stresses on microorganisms associated with soil drying and rewetting are significant, drought is not the only global change stressor faced by microbial communities. Indeed, global change is a multifactor phenomenon and soil communities will potentially experience drought simultaneously with multiple other environmental changes, e.g., increasing temperature, nitrogen (N) fertilization, increasing salinity, and biological invasions (Rillig et al., 2019). Here, we focus on drought in

combination with land use change, which has altered ~75% of earth's ice-free land area (Ellis, 2011) and is therefore a globally relevant driver of environmental change. These land use changes (e.g., logging, forest conversion to agriculture) have well-established impacts on the composition of soil bacterial and fungal communities (e.g., Jangid et al., 2011; Kohout et al., 2018; Mushinski, Gentry, et al., 2018; Mushinski, Zhou, et al., 2018; Rodrigues et al., 2013; Zhou et al., 2018b). However, whether land use also influences soil microbial responses to drought remains largely unknown. Though few studies have assessed microbial community drought responses across varying land uses, a previous study in forest soils suggested that current management intensity may influence how drought impacts the metabolically active portion of bacterial communities (Felsmann et al., 2015). Additional studies from forest soils have shown that current management (i.e., forest thinning) can increase the resistance and resilience of soil microbial community structure to drought (Bastida et al., 2019; Bastida et al., 2017) and that forest conversion to agriculture can influence the drought responses of some microbial taxa (Moreno et al., 2019). Together, these studies suggest that current land management is likely to influence future trajectories of soil microbial communities under intensifying droughts – however, no studies to our knowledge have addressed the potential influence of historical (i.e., multi-decadal) land use legacies on the drought responses of soil microbial communities in currently unmanaged ecosystems.

To determine how legacies of historical land use may influence drought responses of soil microbial communities, we conducted a drying-rewetting experiment using intact soil columns collected from two adjacent watersheds at the USFS Coweeta Hydrologic Lab, where droughts have increased in frequency and duration in recent decades (Burt et

al., 2018; Laseter et al., 2012). The two forested watersheds included in our study are currently forested and not actively managed; however, one experienced extensive disturbance associated with clear-cutting and conversion to agriculture ~60 years prior while the other is a minimally disturbed reference site. Our previous work from these sites and from nearby historically disturbed forests has revealed that historically disturbed sites exhibit higher bacterial α diversity and host higher abundance of nitrifying taxa and r-selected bacterial taxa relative to adjacent reference sites (Osburn et al., 2019; Osburn & Barrett, 2020). The goal of this study was to determine whether compositionally different microbial communities across these varying historical land uses would exhibit distinct responses to drought. To accomplish this goal, we addressed the following questions: 1) Do microbial taxa respond differently to drought in forests with different land use histories? 2) Do resistance and resilience of microbial diversity and community composition to drought vary between bacteria and fungi and between land uses? and 3) Do historical land use and drought interact to influence ecological interactions among bacterial and fungal taxa (i.e., altered co-occurrence network properties)?

Materials and Methods

Soil Sampling

We collected soils at the Coweeta Hydrologic Lab, a USDA Forest Service experimental forest in North Carolina, USA (latitude 35°03′ N, longitude 83°25′ W). Within the Coweeta basin, we selected two adjacent forested watersheds for soil sampling (Fig. 5.S1A). One watershed was clear cut and converted to pasture in 1958, which involved soil scarification, liming, and fertilizing. In 1967, the watershed was abandoned to forest succession. This recent history of agricultural abandonment is a

common past land use in temperate forests of the eastern US (Gragson & Bolstad, 2006) and we refer to this watershed as our 'disturbed' site, which reflects the more recent anthropogenic activity on the site. The other watershed, our 'reference' site, has been undisturbed since the period 1919-1923, when ~20% of the basal area of the Coweeta basin was cut and harvested (Elliott & Vose, 2011). Detailed information about each watershed can be found on Table 5.S1. In August 2019, we established six 1 m^2 plots within each watershed, three at low elevation near the outlet of the watershed and three at higher elevations, a total of 12 plots (Fig 5.S1A). Within each elevation, plots were located at 5 m, 25 m, and 50 m along an upslope transect starting at the stream margin (Fig 5.S1A). This sampling scheme was intended to incorporate spatial variation in soil properties and microbial communities within each watershed into our experiment. Within each plot, we sampled thirteen 10 cm depth, 3.8 cm diameter mineral soil cores using PVC corers. One core from each plot was immediately processed (sieved at 4 mm and homogenized) while the remaining twelve cores from each plot were maintained intact in the original PVC, with 25 µm nylon mesh attached to the bottom to prevent soil spillage. All soils were transported to the lab on ice and stored at 4 °C prior to measurement of soil chemical properties (processed soils) or the start of the experiment (intact cores). We measured soil pH, water content, NO_3^-, NH_4^+, extractable organic C, total extractable N, microbial biomass, and total C and N on pre-treatment soils from each plot according to previously described methods (Osburn et al., in review). Though our study only includes a single disturbed-reference watershed pair, disturbed watersheds in this region typically exhibit directionally consistent changes in soil properties across multiple distinct historical land uses (e.g., clear-cutting, conversion to agriculture, conversion to pine

monoculture) (Keiser et al., 2016; Osburn et al., 2019). Specifically, similar to nearby disturbed forests, our disturbed soils had higher pH, larger NO_3^- pools, smaller microbial biomass and organic C pools, and lower C:N ratios compared with the reference site (Table 5.S2).

Experimental Design

The twelve intact cores from each plot were incubated in the lab at 20 °C under one of two moisture conditions: a constant moisture control and a drought-rewetting treatment. Cores were incubated intact to minimize disturbances to soil communities, thereby allowing us to observe more realistic microbial responses to moisture treatments. On day 1 of the experiment, all soils were adjusted to 0.35 g H_2O g $soil^{-1}$ and constant moisture control soils were maintained at that moisture level for the duration of the experiment (Fig. 5.S1B). This control water content is equal to the long-term average summer soil moisture measured at Coweeta (Helvey & Hewlett, 1962) and is approximately equal to field capacity (i.e., -10 kPa) in our soils (Osburn et al., in review). We adjusted water content of soils by gently pipetting DI H_2O to the surface of soil cores until reaching the calculated weight of each core at 0.35 g H_2O g $soil^{-1}$. This weight was determined by weighing PVC cores before and after soil sampling and calculating the dry mass of soil in each core based on the water content of the pre-treatment soil from the same plot. We adjusted water content of control soils three times per week, which is equal to the long term average frequency of summer rainfall events at Coweeta (Burt et al., 2018).

Soil cores exposed to the drought-rewetting treatment did not receive water for six weeks, which is similar in duration to recent extreme droughts in the region (Williams et al.,

2017). After three weeks, these soils had dried to an average water potential of -1.5 mPa (equivalent to 0.12 g H_2O g $soil^{-1}$, Fig. 5.S1B), which approximates the water potential required to induce microbial stress in intact soils (Manzoni et al., 2012). At the end of the drought period, these soils had dried to ~0.04 g H_2O g $soil^{-1}$ on average (Fig. 5.S1B). After six weeks, dried soils were rewet to control moisture levels (0.35 g H_2O g $soil^{-1}$) and maintained at that water content for the remaining six weeks of the experiment. At six time points throughout the experiment, we destructively harvested one soil core from each moisture treatment from each field plot (i.e., 24 cores per time point). Cores harvested on day 1 and day 42 represent pre- and post-drought samples, respectively. Cores harvested 24 and 72 hours after rewetting (i.e., days 43 and 45) were intended to assess early microbial community responses to drought-rewetting, while cores harvested two and six weeks following rewetting (i.e., days 56 and 84) were intended to assess longer term microbial community responses. At each sampling time, soils were sieved at 4 mm, homogenized, and a subsample stored at -20 °C prior to DNA extraction.

DNA Extraction, PCR, and Amplicon Sequencing

We extracted DNA from 0.25 g soil using a Qiagen DNeasy PowerSoil kit (Qiagen, Valencia, CA, United States) and quantified extracts using a Qubit 2.0 fluorometer (Thermo Fisher Inc., Waltham, MA, United States). We characterized bacterial and fungal communities via PCR amplification and amplicon sequencing of the 16S rRNA gene and ITS1 region, respectively. For 16S amplification, we used the 515F/806R primer pair (Apprill et al., 2015; Parada et al., 2016) while for ITS we used the ITS1F/2 primer pair (Bellemain et al., 2010). Each PCR reaction contained 10 µl Thermo Fisher Platinum II Hot Start PCR Master Mix (Thermo Fisher Inc, Waltham,

MA, USA), 1 µl DNA template (~4-30 ng DNA), 0.2 µM forward and reverse primers, and nuclease-free H_2O to 25 µl. Each sample was amplified in triplicate. Thermal cycling conditions for 16S amplification were 2 min at 94°C followed by 35 cycles of 45 s at 94°C, 60 s at 50°C and 90 s at 72°C, with a 10 min final extension at 72°C while conditions for ITS were 2 min at 94°C followed by 35 cycles of 30 s at 94°C, 30 s at 52°C and 30 s at 68°C, with a 10 min final extension at 68°C. After amplification, we pooled triplicate reactions and visualized PCR products on a 1% agarose gel. We then purified amplicons using a Qiagen QIAquick PCR Purification Kit (Qiagen, Valencia, CA, USA), quantified the purified amplicons, and pooled 16S and ITS amplicons separately in equimolar ratios. Amplicons were sequenced on an Illumina MiSeq using 250 bp paired-end reads. Due to poor quality scores for the reverse reads, we only processed and analyzed the 16S and ITS forward reads. Raw sequence reads were deposited in NCBI's BioProject database under accession number PRJNA664358.

We processed raw sequence reads in QIIME2 (Bolyen et al., 2018) using the DADA2 pipeline (Callahan et al., 2016). After DADA2 processing, we retained 7,822,041 and 7,043,889 16S and ITS sequences, respectively. For downstream statistical analysis, we randomly selected 14,696 16S sequences and 9,835 ITS sequences from each sample to account for differences in sequencing depth. One sample each from the 16S and ITS sequence data sets was excluded due to insufficient sequence depth. After random sampling, we retained 11,944 16S amplicon sequence variants (ASVs) and 5,613 ITS ASVs for further analysis. We assigned taxonomy to ASVs using a naïve-bayes classifier (Pedregosa et al., 2011) trained on the Greengenes and UNITE databases for 16S and ITS, respectively (Abarenkov et al. 2010, McDonald et al. 2012). To assess

potential bacterial life history shifts induced by drought-rewetting, we categorized abundant bacterial phyla as either r-selected (i.e., Proteobacteria and Bacteroidetes) or K-selected (i.e., Acidobacteria and Verrucomicrobia), similar to the approach of Zhou et al. (2018).

Data Analysis

Statistical analyses were performed in R (R Core Development Team, 2019) using the phyloseq, lme4, vegan, and igraph packages (Bates et al., 2019; Csardi & Nepusz, 2006; McMurdie & Holmes, 2013; Oksanen et al., 2019). We measured bacterial and fungal α diversity using the Shannon index ('estimate_richness' function, phyloseq package). To determine treatment effects on bacterial and fungal β diversity (i.e., community composition), we calculated Bray-Curtis dissimilarity between drought-rewet and control soils from the same field plot at each time point. We also measured Bray-Curtis dissimilarity between each sample and the corresponding pre-drought sample on day 1 from the same field plot. These represent two complementary approaches for visualizing and statistically analyzing changes in community composition over time in our experiment. To determine effects of drought, disturbance, and drought x disturbance interactions on α diversity and Bray-Curtis dissimilarities, we used linear mixed effects models with 'Drought' and 'Disturbance' as fixed effects in the models ('lmer' function, lme4 package). We included 'Plot' as a random effect in the models, which accounts for repeated measurements of community metrics from the same field plots over time (plots being represented in the lab experiment by intact cores sampled from each respective plot). We also used mixed effects models to determine effects of experimental treatments on relative abundances of specific bacterial and fungal taxa. For all mixed effects models,

we assessed assumptions of normality of residuals by examining q-q plots and when deviations from normality were observed, we used generalized linear mixed effects models ('glmer' function, gamma distribution and log-link function, lme4 package). We also used NMDS ('metaMDS' function, vegan package) and PERMANOVA ('adonis2' function, vegan package) with Bray-Curtis dissimilarities as additional methods of visualizing and assessing effects of experimental treatments on bacterial and fungal community composition.

As additional indicators of microbial community responses to drought-rewetting, we calculated resistance and resilience indices for bacterial and fungal α and β diversity metrics. Resistance and resilience represent two distinct components of community stability (Pimm, 1984), where resistance is defined as a community's ability to remain unchanged following a disturbance while resilience is defined as the extent of a community's recovery to pre-disturbance conditions (Orwin & Wardle, 2004). We use resistance and resilience indices originally developed by Orwin & Wardle (2004) and shown in equations 1 and 2 below.

(1) $Resistance = 1 - \frac{2|D_0|}{C_0+|D_0|}$

(2) $Resilience = \frac{2|D_0|}{|D_0|+|D_x|} - 1$

These indices are bounded between -1 and 1, allowing for direct comparison of fungal and bacterial responses, where a resistance of '1' represents no change in a community metric following disturbance and a resilience of '1' represents complete recovery of a community metric. In our experiment, C_0 represents the value of diversity metrics in constant moisture control soils, D_0 represents the difference in diversity metrics between drought-rewet and control soils from each field plot after disturbance, and D_x represents

the difference between drought-rewet and control soils after the recovery period. For the purposes of this experiment, we considered drought-rewetting to be a single, integrated two-part disturbance (Schimel, 2018). Therefore, we defined 'after disturbance' (i.e., for determining D_0 and C_0) to be our second early response sampling event, i.e., the day 45 samples. For resilience, we determined 'after recovery' (i.e., for determining 'D_x') to be the final day of the experiment, i.e., the day 84 samples. For resistance and resilience of β diversity we adapted the approach used by (Shade et al., 2012) and Sorensen & Shade (2020). In this method, values are Bray-Curtis dissimilarities between each sample and the corresponding sample from the same field plot on Day 1, measured at either day 45 (for C_0 and D_0) or day 84 (for D_x). For all resistance and resilience indices, we compared taxa (i.e., bacteria vs. fungi) and land uses within taxa using ANOVA.

To investigate drought-rewetting effects on potential ecological interactions among taxa, we constructed co-occurrence networks for bacterial and fungal communities. Preliminary analyses showed qualitatively similar treatment effects on networks across all four post-rewet time points (i.e., days 43, 45, 56, 84). Therefore, we chose to aggregate samples from all post-rewet time points for each treatment, which allowed us to construct more robust networks with 24 samples representing each treatment (4 time points x 6 replicates/time point). To ensure the robustness of relationships used to construct networks, we only included ASVs that occurred in a minimum of 10 samples per treatment, similar to the approach of Shi et al. (2016). We then calculated Spearman rank correlation coefficients between taxa, corrected *P* values for false discovery rate using the Benjamini-Hochberg method (Benjamini & Hochberg, 1995) and constructed networks using only correlations with adjusted $P < 0.01$. Due to

the large number of significant correlations detected among bacterial ASVs, we were able to further improve the robustness of our bacterial networks by only including correlations with $|\rho| > 0.8$. We then used the igraph package to quantify two key network topology metrics: degree and betweenness ('degree' and 'betweenness' functions), both of which were normalized for each respective network. Degree and betweenness represent measures of the connectivity and the centrality of a co-occurrence network, respectively (De Vries et al., 2018), where degree is calculated as the number of edges per node (i.e., connections per ASV) and betweenness is calculated as the number of times a node is on the shortest path between two other nodes. We identified treatment effects on both metrics using generalized linear models ('glm' function, gamma distribution and log-link function, lme4 package). We also used Z-tests to assess effects of drought-rewetting on the proportion of negative edges in networks within each land use.

Results

Responses of bacterial and fungal α diversity

Bacterial α diversity was higher overall in soils from the historically disturbed watershed, similar to previous reports (Fig. 5.1A) (Osburn et al., 2019). Drought-rewetting also affected bacterial diversity, with a ~12% drop in Shannon diversity in drought-rewet soils observed 72 hours after rewetting (i.e., day 45, Fig. 5.1A), though diversity returned to control levels by the end of the experiment on day 84 (Fig. 5.1A). Drought effects on bacterial α diversity were essentially identical across land uses, i.e., no disturbance x drought interaction was detected (Fig. 5.1A). Fungal α diversity did not exhibit land use effects but did show significant effects of drought-rewetting, with a ~35% increase in fungal Shannon diversity in drought-rewet soils observed 72 hours after

rewetting (i.e., day 45, Fig. 5.1B). This pattern was maintained over time, with ~32% higher fungal Shannon diversity in drought-rewet soils at the end of the experiment (Fig. 5.1B). Similar to bacteria, drought-rewetting responses of fungal α diversity were the same across both land uses (Fig. 5.1B).

Resistance and resilience indices for bacterial and fungal α diversity reinforce the aforementioned patterns – bacterial diversity exhibited ~95% higher resistance and ~7-fold higher resilience to drought-rewetting compared with fungal diversity (Fig. 5.1C, D). This reflects proportionally smaller initial changes to bacterial diversity compared with fungal diversity (i.e., higher resistance) and greater recovery of bacterial diversity compared with fungal diversity by the end of the experiment (i.e., higher resilience). Within taxa, historical land use did not influence resistance or resilience of α diversity (Fig. 5.1C, D).

Responses of bacterial and fungal β diversity

Bacterial community composition (i.e., β diversity) exhibited clear differences between historical land uses, similar to previous studies (Fig. 5.2A) (Osburn et al., 2019). Bacterial community composition also exhibited clear responses to drought, with drought-rewet soils exhibiting much greater variability in community composition over time than control soils (Fig. 5.2A). PERMANOVA also detected a marginal drought x disturbance interaction ($P = 0.08$), where disturbed soil bacterial communities appear more responsive to drought-rewetting (i.e., more variable over time) than reference communities (Fig. 5.2A). This is supported by a dispersion test ('betadisper' function, vegan package), which showed disturbed-drought communities having greater multivariate dispersion than reference-drought communities ($P = 0.03$). This is also

supported by analyzing Bray-Curtis dissimilarities between drought-rewet soils and controls, with moisture treatments in soils from the disturbed site exhibiting larger community dissimilarity at most time points and 12% greater Bray-Curtis dissimilarity overall compared with moisture treatments from the reference site (Fig. 5.2C). Bray-Curtis dissimilarities from pre-drought (day 1) samples also support this, with disturbed-drought soils exhibiting larger changes relative to day 1 communities over the course of the experiment compared with reference-drought soils (Fig. 5.S2).

Fungal community composition also exhibited clear differences between historical land uses, similar to previous studies (Fig. 5.2B) (Osburn et al., 2019). However, within land uses, fungal community composition did not exhibit clear responses to drought-rewetting at the ASV level (Fig. 5.2B). This is supported by measurements of Bray-Curtis dissimilarities between drought-rewet soils and controls (Fig. 5.2D) and by Bray-Curtis dissimilarities from pre-drought samples (Fig. 5.S3), neither of which showed clear patterns over time.

Resistance of community composition reflects the clear drought-rewetting responses of bacterial communities and the lack thereof for fungal communities, with fungal communities exhibiting ~45% higher resistance than bacterial communities (Fig. 5.2E). In contrast, resilience did not vary between taxa (Fig. 5.2F), reflecting recovery of bacterial community composition despite larger initial changes. Within bacteria, we detected a marginal effect of land use on resilience (ANOVA $P = 0.06$), where reference communities exhibited ~4.7-fold higher resilience than disturbed communities (Fig. 5.2F).

Responses of bacterial and fungal taxa

Relative abundances of bacterial phyla exhibited little change over time in constant moisture control soils (Fig. 5.S4A, B), while most bacterial phyla showed clear changes over time in drought-rewet soils (Fig. 5.3A, B). In particular, the two most abundant phyla, Acidobacteria and Proteobacteria, exhibited opposite responses, with Acidobacteria relative abundance declining 52% from Day 1 to Day 45 and Proteobacteria relative abundance increasing 35% from Day 1 to Day 45 (Fig. 5.3A, B). The relative abundances of both phyla trended towards pre-drought levels by the end of the experiment (Fig. 5.3A, B). In addition, multiple distinct response trajectories were evident across bacterial phyla. For example, Actinobacteria exhibited an overall positive drought-rewetting response (i.e., 92% higher on Day 84 than Day 1), Nitrospirae exhibited an overall negative response (i.e., ~5.8-fold lower on Day 84 than Day 1), and Firmicutes exhibited an opportunistic response to drought-rewetting, with a > 100-fold increase by Day 45 followed by a return to control levels by day 84 (Fig. 5.3A, B). Some phyla also exhibited significant drought x disturbance interactions. For example, Acidobacteria exhibited larger initial declines in reference-drought soils, Actinobacteria showed larger increases in reference-drought soils, and nitrifying taxa (i.e., Nitrospirae) exhibited a distinct decline only in disturbed-drought soils where they are typically more abundant (Fig. 5.3A, B) (Osburn et al., 2019; Osburn & Barrett, 2020). Categorizing bacterial phyla as r- vs. K-selected also revealed clear patterns, where r:K ratios were ~140% higher in drought-rewet soils compared with control soils 72 hours after rewetting (i.e., day 45, Fig. 5.4). This was particularly evident in soils from disturbed sites, in which r-selected taxa outnumbered K-selected taxa 2.6 to 1 on day 45 (Fig. 5.4). r:K

ratios trended towards control levels in both land use treatments by the end of the experiment (Fig. 5.4).

Relative abundances of fungal classes exhibited some variability over time in constant moisture controls (Fig. 5.S4C, D), but drought-rewetting responses of fungal classes remained clear (Fig. 5.3C, D). Most striking was continuously increasing fungal community evenness at the class level following drought-rewetting, where the most abundant class, Agaricomycetes, declined from 71% to 22% of all sequences from day 1 to day 84, while the relative abundances of all other classes increased (Fig. 5.3C, D). Some fungal classes also exhibited drought x disturbance interactions. For example, Umbelopsidomycetes and Sordariomycetes both exhibited more distinct positive drought-rewetting responses in reference soils, while the relative abundance of Agaricoymycetes appeared to stabilize in reference-drought soils by day 56 but continued to decline through day 84 in disturbed-drought soils (Fig. 5.3C, D).

Responses of bacterial and fungal co-occurrence networks

Co-occurrence networks constructed for bacterial communities exhibited striking differences between constant moisture controls and drought-rewet soils (Fig. 5.5A-D). Specifically, drought-rewet bacterial networks had fewer nodes and edges than control networks and also had significantly lower proportions of negative edges than control networks (Fig. 5.5A-D). Network topology metrics also support this pattern - drought-rewet networks exhibited significantly lower normalized betweenness (Fig. 5.6B), indicating reduced network centrality, i.e., nodes (taxa) in drought-rewet networks were less likely to serve as links between other nodes compared with control networks. Network topologies also revealed land use influences on drought-rewetting responses of

bacterial networks. Specifically, normalized degree (i.e., network connectivity) was reduced only in drought-rewet soils from the disturbed watershed, while network connectivity was not affected by drought-rewetting in reference sites (Fig. 5.6A).

Co-occurrence networks constructed for fungal communities did not exhibit clear differences between controls and drought-rewet soils in terms of numbers of nodes and edges or proportion of negative edges (Fig. 5.5 E-H). However, network topology metrics did indicate effects of moisture treatments, where drought-rewet soils exhibited lower betweenness (i.e., reduced centrality) and lower degree (i.e., reduced connectivity) relative to control soils, though the effects were the same across both land uses (Fig. 5.6C, D).

Discussion

We observed wide-ranging impacts of drought on microbial communities in temperate forest soils. Specifically, we show that drought-rewetting altered bacterial and fungal α diversity (Fig. 5.1), bacterial β diversity (Fig. 5.2), and relative abundances of many specific bacterial and fungal taxa (Fig. 5.3, 4). Further, many of these drought responses were modulated by historical disturbance, particularly in bacterial communities. For example, disturbed soil bacteria exhibited greater β diversity responses to drought-rewetting (Fig 5.2A, C) as well as lower resilience of β diversity (Fig. 5.2E) relative to reference soil bacterial communities. These influences of past land use on drought-rewetting responses are likely attributed to disturbance selecting for taxa that appear particularly responsive to drought-rewetting. For example, nitrifying and r-selected bacterial taxa exhibited significant drought-rewetting responses (Fig. 5.3, 4), and are also typically more abundant in disturbed soils to begin with (Osburn et al., 2019),

likely contributing to the greater β diversity responses observed for bacteria in disturbed soils. The greater stability of reference soil bacterial communities may also be attributed to the higher frequency of negative interactions among taxa observed in reference communities relative to disturbed communities (Osburn et al., 2019) (Fig. 5.5A-D), which has been previously linked to microbial community stability (Coyte et al., 2015). Regardless, our results build on the growing body of literature reporting effects of drought on soil bacterial communities by suggesting that historical land use will play a role in influencing bacterial responses to future climate change.

Our results also demonstrate clear responses of soil fungal communities to drought. For example, the relative abundances of fungal classes were dramatically altered by drought-rewetting, with increasing evenness among fungal classes throughout the experiment (Fig. 5.3C, D). Drought-rewetting also increased fungal α diversity (Fig. 5.1B), contrasting with bacterial α diversity, which decreased following drought-rewetting (Fig. 5.1A). These opposite α diversity responses reflect different drought-rewetting responses of dominant bacterial and fungal taxa – the decrease in bacterial α diversity is attributable to positive drought-rewetting responses of abundant bacterial ASVs (i.e., decreased community evenness) while dominant fungal ASVs declined in relative abundance (i.e., increased evenness). Overall, however, fungal diversity was impacted more by drought (lower resistance) and recovered less (lower resilience) compared with bacterial diversity (Fig. 5.1C, D). This result challenges previous expectations that fungi will be more drought-tolerant than bacteria (e.g., Schimel et al., 2007) and suggests that some community metrics may actually be more drought-sensitive in fungi than in bacteria. Additionally, some fungal drought responses, i.e., relative

abundances of some fungal classes, were influenced by historical land use (Fig. 5.3C, D). Like bacteria, these different responses between land uses may be attributed to pre-existing compositional differences in communities. For example, relative abundances of both Agaricomycetes and Sordariomycetes exhibited disturbance x drought interactions and both have been previously shown to be differentially abundant between reference and historically disturbed forest soils (Osburn et al., 2019). Regardless, the large overall drought responses of fungi we observed may be attributed to resident fungal communities that are poorly adapted to water stress, as our sites in the Coweeta basin are historically among the wettest locations in the eastern US (~1800 mm rainfall per year) (Burt et al., 2018; Laseter et al., 2012). Indeed, previous studies have shown that prior exposure to water stress can reduce the sensitivity of microbial communities to future drought (Bouskill et al., 2013; Evans & Wallenstein, 2014; Preece et al., 2019), suggesting the possibility that drought-tolerance of fungal communities will vary among regions with differing historical hydroclimates.

In addition to changes in diversity and community composition, our network analyses suggest that ecological interactions among microbial taxa will be altered by drought in temperate forest soils (Fig. 5.5, 6). This was particularly evident in bacterial networks, which exhibited major disruptions in network structure (i.e., reduced interactions) following drought-rewetting (Fig. 5.5A-D), similar to previous reports (De Vries et al., 2018). This reduction in bacterial interactions reflects increased temporal variability in community composition following drought-rewetting (Fig. 5.2A), which reduced detection of statistical associations among taxa. Additionally, a smaller proportion of the remaining associations among bacteria were negative following

drought-rewetting (Fig. 5.5A-D), suggesting fewer antagonistic ecological interactions (e.g., competition) and greater growth among drought-responsive taxa in resource-rich post-rewet soils. Further, historical land use influenced some drought-rewetting responses of bacterial networks, with disturbed soil communities exhibiting larger reductions in network connectivity (i.e., normalized degree) compared with reference soils (Fig. 5.6A). Finally, though previous studies report greater drought-tolerance of fungal co-occurrence networks relative to bacterial networks (De Vries et al., 2018), our results show reduced network connectivity and centrality (i.e., degree and betweenness) for both bacterial and fungal communities (Fig. 5.6), suggesting ecological interactions in all microbial taxa will be impacted by drought-rewetting. Together, these results further challenge prior expectations that fungal communities will show minor responses to drought and further highlight the potential for historical land use to influence the drought responses of soil microbial communities.

The influences of historical land use on microbial drought responses we observed are likely mechanistically linked to vegetation differences between reference and disturbed forests, which, in turn, influence key soil properties. For example, forests in the southern Appalachian region are often dominated by N-fixing black locust (*Robinia pseudoacacia*) in the early decades following disturbance (Elliott & Vose, 2011), resulting in larger inorganic N pools in disturbed soils (Table 5.S1, 5.S2). The higher soil pH present in disturbed sites (Table 5.S2) is also likely linked to vegetation - historically disturbed forests host lower abundance of species with acidic leaf litter such as oaks (*Quercus spp.)* and rosebay rhododendron (*Rhododendron maximum*) and increased abundance of species with higher pH leaf litter such as red maple (*Acer rubrum*) and tulip

poplar (*Liriodendron tulipifera*) compared with reference forests (Table 5.S1) (Elliott & Vose, 2011). These vegetation-driven differences in soil properties, in turn, drive compositional differences between reference and disturbed microbial communities (Osburn et al., 2019), likely accounting for many of the land use influences on microbial drought responses we report. Overall, these results strongly suggest that any land use change that drives alterations to soils and their microbial communities will also act to constrain community responses to future perturbations such as intensifying droughts.

An additional notable result is that our data show strikingly few responses of soil microbial communities to drought alone, i.e., we observed few changes in diversity, community composition, or specific taxa between days 1 and 42 of the experiment (Fig. 5.1-4). This contrasts with multiple prior studies showing impacts of drying alone on soil microbial communities (e.g., Barnard et al., 2013; Bouskill et al., 2013; Fuchslueger et al., 2014; Naylor & Coleman-Derr, 2018; Preece et al., 2019) and may be attributed to large amounts of unmetabolized relic DNA from dead microbial cells in the dried soils on day 42 of our experiment (Carini et al., 2016). However, treating drought and rewetting as a single integrated two-part disturbance, i.e., assessing responses after rewetting, revealed numerous responses of both bacterial and fungal communities. Regardless, the land use-mediated microbial responses to drought-rewetting we observed will likely influence the ecosystem-scale responses of these forests to intensifying drought. Indeed, our previous study from these same soils showed greater respiration responses of historically disturbed soils exposed to drought-rewetting relative to reference soils (Osburn et al., in review). This may be attributed to the particularly large responses of r-selected bacteria in disturbed-drought soils (Fig. 5.4), as r-selected (i.e., copiotrophic)

bacteria have been previously linked to greater C mineralization rates (Fierer et al., 2007, Osburn et al., in review). Our previous study also observed smaller NO_3^- pools in soils exposed to drought-rewetting (Osburn et al., in review), which is consistent with the negative drought-rewetting responses of nitrifying bacteria reported here (Fig. 5.3A, B). In general, the community- and ecosystem-level drought-rewetting responses of these soils appear to be closely linked, suggesting that the distinct community-scale responses of microorganisms between land uses will drive ecosystem-scale responses to climate change that will also be influenced by long-term land use legacies.

Conclusions

We show that legacies of past land use influence responses of microbial communities to ongoing and future climate change. Though our study only explicitly addresses the influence of one type of historical land use, i.e., deforestation and conversion to agriculture, previous studies have documented remarkably consistent responses of microbial communities across multiple different historical forest disturbances, including clear-cutting, cable-logging, conversion to pine monoculture, and agricultural abandonment (Osburn et al., 2019). Therefore, we expect soil microbial communities across multiple types of forest disturbance to exhibit similar influences of past land use on drought responses to those described here. More generally, it is clear that any anthropogenic activity that alters microbial communities has the potential to influence microbial responses to climate change. Because the majority of earth's land area (~75%) has already experienced anthropogenic modification (Ellis, 2011), it is likely that these past and present land use activities will influence future trajectories of soil

microbial communities and that these differing community-scale responses will have implications for the functioning of terrestrial ecosystems at a global scale.

Acknowledgements

This work was funded by the Coweeta LTER, funded by National Science Foundation grant DEB-1637522 and by a Graduate Research Development Program (GRDP) awarded to EDO by the Virginia Tech Graduate Student Assembly. We thank the Coweeta Hydrologic Laboratory, Southern Research Station, USDA Forest Service for support, Bobbie Niederlehner for help with analytical chemistry, and Julia Simpson for help in managing the experiment.

References

Abarenkov, K., Nilsson, R. H., Larsson, K.-H., Alexander, I. J., Eberhardt, U., Erland, S., Høiland, K., Kjøller, R., Larsson, E., Pennanen, T., Sen, R., Taylor, A. F. S., Tedersoo, L., Ursing, B. M., Vrålstad, T., Liimatainen, K., Peintner, U., & Kõljalg, U. (2010). The UNITE database for molecular identification of fungi – recent updates and future perspectives. *The New Phytologist*, *186*(2), 281–285.

Apprill, A., McNally, S., Parsons, R., & Weber, L. (2015). Minor revision to V4 region SSU rRNA 806R gene primer greatly increases detection of SAR11 bacterioplankton. *Aquatic Microbial Ecology*, *75*(2), 129–137. https://doi.org/10.3354/ame01753

Barnard, R. L., Osborne, C. A., & Firestone, M. K. (2013). Responses of soil bacterial and fungal communities to extreme desiccation and rewetting. *The ISME Journal*, *7*(11), 2229–2241. https://doi.org/10.1038/ismej.2013.104

Bastida, F., López-Mondéjar, R., Baldrian, P., Andrés-Abellán, M., Jehmlich, N., Torres, I. F., García, C., & López-Serrano, F. R. (2019). When drought meets forest management: Effects on the soil microbial community of a Holm oak forest ecosystem. *Science of The Total Environment*, *662*, 276–286. https://doi.org/10.1016/j.scitotenv.2019.01.233

Bastida, Felipe, Torres, I. F., Andrés-Abellán, M., Baldrian, P., López-Mondéjar, R., Větrovský, T., Richnow, H. H., Starke, R., Ondoño, S., García, C., López-Serrano, F. R., & Jehmlich, N. (2017). Differential sensitivity of total and active soil microbial communities to drought and forest management. *Global Change Biology*, *2017*, 1–19. https://doi.org/10.1111/gcb.13790

Bates, D., Maechler, M., Bolker [aut, B., cre, Walker, S., Christensen, R. H. B., Singmann, H., Dai, B., Scheipl, F., Grothendieck, G., Green, P., & Fox, J. (2019). *lme4: Linear Mixed-Effects Models using "Eigen" and S4* (1.1-21) [Computer software]. https://CRAN.R-project.org/package=lme4

Bellemain, E., Carlsen, T., Brochmann, C., Coissac, E., Taberlet, P., & Kauserud, H. (2010). ITS as an environmental DNA barcode for fungi: An in silico approach reveals potential PCR biases. *BMC Microbiology*, *10*(1), 189. https://doi.org/10.1186/1471-2180-10-189

Benjamini, Y., & Hochberg, Y. (1995). *Controlling the False Discovery Rate: A Practical and Powerful Approach to Multiple Testing*. https://doi.org/10.1111/j.2517-6161.1995.tb02031.x

Birch, H. F. (1958). The effect of soil drying on humus decomposition and nitrogen availability. *Plant and Soil*, *10*(1), 9–31. https://doi.org/10.1007/BF01343734

Bolyen, E., Rideout, J. R., Dillon, M. R., Bokulich, N. A., Abnet, C., Al-Ghalith, G. A., Alexander, H., Alm, E. J., Arumugam, M., Asnicar, F., Bai, Y., Bisanz, J. E., Bittinger, K., Brejnrod, A., Brislawn, C. J., Brown, C. T., Callahan, B. J., Caraballo-Rodríguez, A. M., Chase, J., … Caporaso, J. G. (2018). *QIIME 2: Reproducible, interactive, scalable, and extensible microbiome data science*. https://doi.org/10.7287/peerj.preprints.27295v2

Bouskill, N. J., Lim, H. C., Borglin, S., Salve, R., Wood, T. E., Silver, W. L., & Brodie, E. L. (2013). Pre-exposure to drought increases the resistance of tropical forest soil bacterial communities to extended drought. *The ISME Journal*, *7*(2), 384–394. https://doi.org/10.1038/ismej.2012.113

Burt, T. P., Ford Miniat, C., Laseter, S. H., & Swank, W. T. (2018). Changing patterns of daily precipitation totals at the Coweeta Hydrologic Laboratory, North Carolina, USA. *International Journal of Climatology*, *38*(1), 94–104. https://doi.org/10.1002/joc.5163

Callahan, B. J., McMurdie, P. J., Rosen, M. J., Han, A. W., Johnson, A. J. A., & Holmes, S. P. (2016). DADA2: High-resolution sample inference from Illumina amplicon data. *Nature Methods*, *13*(7), 581–583. https://doi.org/10.1038/nmeth.3869

Cohen, J. M., Lajeunesse, M. J., & Rohr, J. R. (2018). A global synthesis of animal phenological responses to climate change. *Nature Climate Change*, *8*(3), 224–228. https://doi.org/10.1038/s41558-018-0067-3

Csardi, G., & Nepusz, T. (2006). The igraph software package for complex network research. *InterJournal*, *Complex Systems*, 1695. http://igraph.org

De Vries, F. T., Griffiths, R. I., Bailey, M., Craig, H., Girlanda, M., Gweon, H. S., Hallin, S., Kaisermann, A., Keith, A. M., Kretzschmar, M., Lemanceau, P., Lumini, E., Mason, K. E., Oliver, A., Ostle, N., Prosser, J. I., Thion, C., Thomson, B., & Bardgett, R. D. (2018). Soil bacterial networks are less stable under drought than fungal networks. *Nature Communications*, *9*(1), 3033. https://doi.org/10.1038/s41467-018-05516-7

De Vries, F. T., Liiri, M. E., Bjørnlund, L., Bowker, M. A., Christensen, S., Setälä, H. M., & Bardgett, R. D. (2012). Land use alters the resistance and resilience of soil food webs to drought. *Nature Climate Change; London*, *2*(4), 276–280. http://dx.doi.org.ezproxy.lib.vt.edu/10.1038/nclimate1368

Eisenhauer, N., Herrmann, S., Hines, J., Buscot, F., Siebert, J., & Thakur, M. P. (2018). The Dark Side of Animal Phenology. *Trends in Ecology & Evolution*, *33*(12), 898–901. https://doi.org/10.1016/j.tree.2018.09.010

Elliott, K. J., & Vose, J. M. (2011). The contribution of the Coweeta Hydrologic Laboratory to developing an understanding of long-term (1934-2008) changes in

managed and unmanaged forests. *Forest Ecology and Management*, *261*(5), 900–910. https://doi.org/10.1016/j.foreco.2010.03.010
Ellis, E. C. (2011). Anthropogenic transformation of the terrestrial biosphere. *Philosophical Transactions of the Royal Society A-Mathematical Physical and Engineering Sciences*, *369*(1938), 1010–1035. https://doi.org/10.1098/rsta.2010.0331
Evans, S. E., & Wallenstein, M. D. (2012). Soil microbial community response to drying and rewetting stress: Does historical precipitation regime matter? *Biogeochemistry*, *109*(1–3), 101–116. https://doi.org/10.1007/s10533-011-9638-3
Evans, S. E., & Wallenstein, M. D. (2014). Climate change alters ecological strategies of soil bacteria. *Ecology Letters*, *17*(2), 155–164. https://doi.org/10.1111/ele.12206
Evans, S. E., Wallenstein, M. D., & Burke, I. C. (2014). Is bacterial moisture niche a good predictor of shifts in community composition under long-term drought? *Ecology*, *95*(1), 110–122. https://doi.org/10.1890/13-0500.1
Fahey, C., Angelini, C., & Flory, S. L. (2018). Grass invasion and drought interact to alter the diversity and structure of native plant communities. *Ecology*, *99*(12), 2692–2702. https://doi.org/10.1002/ecy.2536
Felsmann, K., Baudis, M., Gimbel, K., Kayler, Z. E., Ellerbrock, R., Bruehlheide, H., Bruckhoff, J., Welk, E., Puhlmann, H., Weiler, M., Gessler, A., & Ulrich, A. (2015). Soil Bacterial Community Structure Responses to Precipitation Reduction and Forest Management in Forest Ecosystems across Germany. *PLOS ONE*, *10*(4), e0122539. https://doi.org/10.1371/journal.pone.0122539
Fierer, N., Bradford, M. A., & Jackson, R. B. (2007). Toward an ecological classification of soil bacteria. *Ecology*, *88*(6), 1354–1364.
Gragson, T. L., & Bolstad, P. V. (2006). Land Use Legacies and the Future of Southern Appalachia. *Society & Natural Resources*, *19*(2), 175–190. https://doi.org/10.1080/08941920500394857
Helvey, J., & Hewlett, J. D. (1962). The annual range of soil moisture under high rainfall in the southern Appalachians. *Journal of Forestry*, *60*, 485–486.
IPCC. (2013). *Climate Change 2013: The Physical Science Basis. Contribution of Working Group I to the Fifth Assessment Report of the Intergovernmental Panel on Climate Change [Stocker, T.F., D. Qin, G.-K. Plattner, M. Tignor, S.K. Allen, J. Boschung, A. Nauels, Y. Xia, V. Bex and P.M. Midgley (eds.)]*. Cambridge University Press, Cambridge, United Kingdom and New York, NY, USA.
Jangid, K., Williams, M. A., Franzluebbers, A. J., Schmidt, T. M., Coleman, D. C., & Whitman, W. B. (2011). Land-use history has a stronger impact on soil microbial community composition than aboveground vegetation and soil properties. *Soil Biology and Biochemistry*, *43*(10), 2184–2193. https://doi.org/10.1016/j.soilbio.2011.06.022
Jansson, J. K., & Hofmockel, K. S. (2019). Soil microbiomes and climate change. *Nature Reviews Microbiology*, 1–12. https://doi.org/10.1038/s41579-019-0265-7
Keiser, A. D., Knoepp, J. D., & Bradford, M. A. (2016). Disturbance Decouples Biogeochemical Cycles Across Forests of the Southeastern US. *Ecosystems*, *19*(1), 50–61. https://doi.org/10.1007/s10021-015-9917-2
Kohout, P., Charvátová, M., Štursová, M., Mašínová, T., Tomšovský, M., & Baldrian, P. (2018). Clearcutting alters decomposition processes and initiates complex

restructuring of fungal communities in soil and tree roots. *The ISME Journal*, *12*(3), 692–703. https://doi.org/10.1038/s41396-017-0027-3

Laseter, S. H., Ford, C. R., Vose, J. M., & Swift, L. W. (2012). Long-term temperature and precipitation trends at the Coweeta Hydrologic Laboratory, Otto, North Carolina, USA. *Hydrology Research*, *43*(6), 890–901. https://doi.org/10.2166/nh.2012.067

Liu, H., Mi, Z., Lin, L., Wang, Y., Zhang, Z., Zhang, F., Wang, H., Liu, L., Zhu, B., Cao, G., Zhao, X., Sanders, N. J., Classen, A. T., Reich, P. B., & He, J.-S. (2018). Shifting plant species composition in response to climate change stabilizes grassland primary production. *Proceedings of the National Academy of Sciences*, *115*(16), 4051–4056. https://doi.org/10.1073/pnas.1700299114

Manzoni, S., Schimel, J. P., & Porporato, A. (2012). Responses of soil microbial communities to water stress: Results from a meta-analysis. *Ecology*, *93*(4), 930–938. https://doi.org/10.1890/11-0026.1

McDonald, D., Price, M. N., Goodrich, J., Nawrocki, E. P., DeSantis, T. Z., Probst, A., Andersen, G. L., Knight, R., & Hugenholtz, P. (2012). An improved Greengenes taxonomy with explicit ranks for ecological and evolutionary analyses of bacteria and archaea. *The ISME Journal*, *6*(3), 610–618. https://doi.org/10.1038/ismej.2011.139

McMurdie, P. J., & Holmes, S. (2013). phyloseq: An R Package for Reproducible Interactive Analysis and Graphics of Microbiome Census Data. *PLOS ONE*, *8*(4), e61217. https://doi.org/10.1371/journal.pone.0061217

Moreno, J. L., Torres, I. F., García, C., López-Mondéjar, R., & Bastida, F. (2019). Land use shapes the resistance of the soil microbial community and the C cycling response to drought in a semi-arid area. *Science of The Total Environment*, *648*, 1018–1030. https://doi.org/10.1016/j.scitotenv.2018.08.214

Mushinski, R. M., Gentry, T. J., & Boutton, T. W. (2018). Organic matter removal associated with forest harvest leads to decade scale alterations in soil fungal communities and functional guilds. *Soil Biology and Biochemistry*. https://doi.org/10.1016/j.soilbio.2018.09.019

Mushinski, R. M., Zhou, Y., Gentry, T. J., & Boutton, T. W. (2018). Bacterial metataxonomic profile and putative functional behavior associated with C and N cycle processes remain altered for decades after forest harvest. *Soil Biology and Biochemistry*, *119*, 184–193. https://doi.org/10.1016/j.soilbio.2018.01.008

Naylor, D., & Coleman-Derr, D. (2018). Drought Stress and Root-Associated Bacterial Communities. *Frontiers in Plant Science*, *8*. https://doi.org/10.3389/fpls.2017.02223

Oksanen, J., Blanchet, F. G., Friendly, M., Kindt, R., Legendre, P., McGlinn, D., Minchin, P. R., O'Hara, R. B., Simpson, G. L., Solymos, P., Stevens, M. H. H., Szoecs, E., & Wagner, H. (2019). *vegan: Community Ecology Package* (2.5-4) [Computer software]. https://CRAN.R-project.org/package=vegan

Orwin, K. H., & Wardle, D. A. (2004). New indices for quantifying the resistance and resilience of soil biota to exogenous disturbances. *Soil Biology and Biochemistry*, *36*(11), 1907–1912. https://doi.org/10.1016/j.soilbio.2004.04.036

Osburn, E. D., & Barrett, J. E. (2020). Abundance and functional importance of complete ammonia-oxidizing bacteria (comammox) versus canonical nitrifiers in temperate

forest soils. *Soil Biology and Biochemistry*, *145*, 107801. https://doi.org/10.1016/j.soilbio.2020.107801

Osburn, E. D., McBride, S. G., Aylward, F. O., Badgley, B. D., Strahm, B. D., Knoepp, J. D., & Barrett, J. E. (2019). Soil Bacterial and Fungal Communities Exhibit Distinct Long-Term Responses to Disturbance in Temperate Forests. *Frontiers in Microbiology*, *10*. https://doi.org/10.3389/fmicb.2019.02872

Parada, A. E., Needham, D. M., & Fuhrman, J. A. (2016). Every base matters: Assessing small subunit rRNA primers for marine microbiomes with mock communities, time series and global field samples. *Environmental Microbiology*, *18*(5), 1403–1414. https://doi.org/10.1111/1462-2920.13023

Pedregosa, F., Varoquaux, G., Gramfort, A., Michel, V., Thirion, B., Grisel, O., Blondel, M., Prettenhofer, P., Weiss, R., Dubourg, V., Vanderplas, J., Passos, A., Cournapeau, D., Brucher, M., Perrot, M., & Duchesnay, É. (2011). Scikit-learn: Machine Learning in Python. *Journal of Machine Learning Research*, *12*(Oct), 2825–2830.

Pimm, S. L. (1984). The complexity and stability of ecosystems. *Nature*, *307*(5949), 321–326. https://doi.org/10.1038/307321a0

Placella, S. A., Brodie, E. L., & Firestone, M. K. (2012). Rainfall-induced carbon dioxide pulses result from sequential resuscitation of phylogenetically clustered microbial groups. *Proceedings of the National Academy of Sciences*, *109*(27), 10931–10936. https://doi.org/10.1073/pnas.1204306109

Preece, C., Verbruggen, E., Liu, L., Weedon, J. T., & Peñuelas, J. (2019). Effects of past and current drought on the composition and diversity of soil microbial communities. *Soil Biology and Biochemistry*, *131*, 28–39. https://doi.org/10.1016/j.soilbio.2018.12.022

R Core Development Team. (2019). *R: A Language and Environment for Statistical Computing*. R Foundation for Statistical Computing. http://www.R-project.org

Rillig, M. C., Ryo, M., Lehmann, A., Aguilar-Trigueros, C. A., Buchert, S., Wulf, A., Iwasaki, A., Roy, J., & Yang, G. (2019). The role of multiple global change factors in driving soil functions and microbial biodiversity. *Science*, *366*(6467), 886–890. https://doi.org/10.1126/science.aay2832

Rodrigues, J. L. M., Pellizari, V. H., Mueller, R., Baek, K., Jesus, E. da C., Paula, F. S., Mirza, B., Hamaoui, G. S., Tsai, S. M., Feigl, B., Tiedje, J. M., Bohannan, B. J. M., & Nüsslein, K. (2013). Conversion of the Amazon rainforest to agriculture results in biotic homogenization of soil bacterial communities. *Proceedings of the National Academy of Sciences*, *110*(3), 988–993. https://doi.org/10.1073/pnas.1220608110

Schimel, J., Balser, T. C., & Wallenstein, M. (2007). Microbial stress-response physiology and its implications for ecosystem function. *Ecology*, *88*(6), 1386–1394.

Schimel, J. P. (2018). Life in Dry Soils: Effects of Drought on Soil Microbial Communities and Processes. *Annual Review of Ecology, Evolution, and Systematics*, *49*(1), 409–432. https://doi.org/10.1146/annurev-ecolsys-110617-062614

Schimel, J., & Schaeffer, S. M. (2012). Microbial control over carbon cycling in soil. *Frontiers in Microbiology*, *3*. https://doi.org/10.3389/fmicb.2012.00348

Shade, A., Peter, H., Allison, S. D., Baho, D., Berga, M., Buergmann, H., Huber, D. H., Langenheder, S., Lennon, J. T., Martiny, J. B., Matulich, K. L., Schmidt, T. M., & Handelsman, J. (2012). Fundamentals of Microbial Community Resistance and Resilience. *Frontiers in Microbiology*, *3*. https://doi.org/10.3389/fmicb.2012.00417

Shi, S., Nuccio, E. E., Shi, Z. J., He, Z., Zhou, J., & Firestone, M. K. (2016). The interconnected rhizosphere: High network complexity dominates rhizosphere assemblages. *Ecology Letters*, *19*(8), 926–936. https://doi.org/10.1111/ele.12630

Sorensen, J. W., & Shade, A. (2020). Dormancy dynamics and dispersal contribute to soil microbiome resilience. *Philosophical Transactions of the Royal Society B: Biological Sciences*, *375*(1798), 20190255. https://doi.org/10.1098/rstb.2019.0255

Sun, Y., Chen, H. Y. H., Jin, L., Wang, C., Zhang, R., Ruan, H., & Yang, J. (2020). Drought stress induced increase of fungi:bacteria ratio in a poplar plantation. *CATENA*, *193*, 104607. https://doi.org/10.1016/j.catena.2020.104607

Williams, A. P., Cook, B. I., Smerdon, J. E., Bishop, D. A., Seager, R., & Mankin, J. S. (2017). The 2016 Southeastern U.S. Drought: An Extreme Departure From Centennial Wetting and Cooling. *Journal of Geophysical Research: Atmospheres*, *122*(20), 10,888-10,905. https://doi.org/10.1002/2017JD027523

Wise, D. H., & Lensing, J. R. (2019). Impacts of rainfall extremes predicted by climate-change models on major trophic groups in the leaf litter arthropod community. *Journal of Animal Ecology*, *88*(10), 1486–1497. https://doi.org/10.1111/1365-2656.13046

Zhou, Z., Wang, C., & Luo, Y. (2018a). Response of soil microbial communities to altered precipitation: A global synthesis. *Global Ecology and Biogeography*, *27*(9), 1121–1136. https://doi.org/10.1111/geb.12761

Zhou, Z., Wang, C., & Luo, Y. (2018b). Effects of forest degradation on microbial communities and soil carbon cycling: A global meta-analysis. *Global Ecology and Biogeography*, *27*(1), 110–124. https://doi.org/10.1111/geb.12663

Figures

Figure 5.1

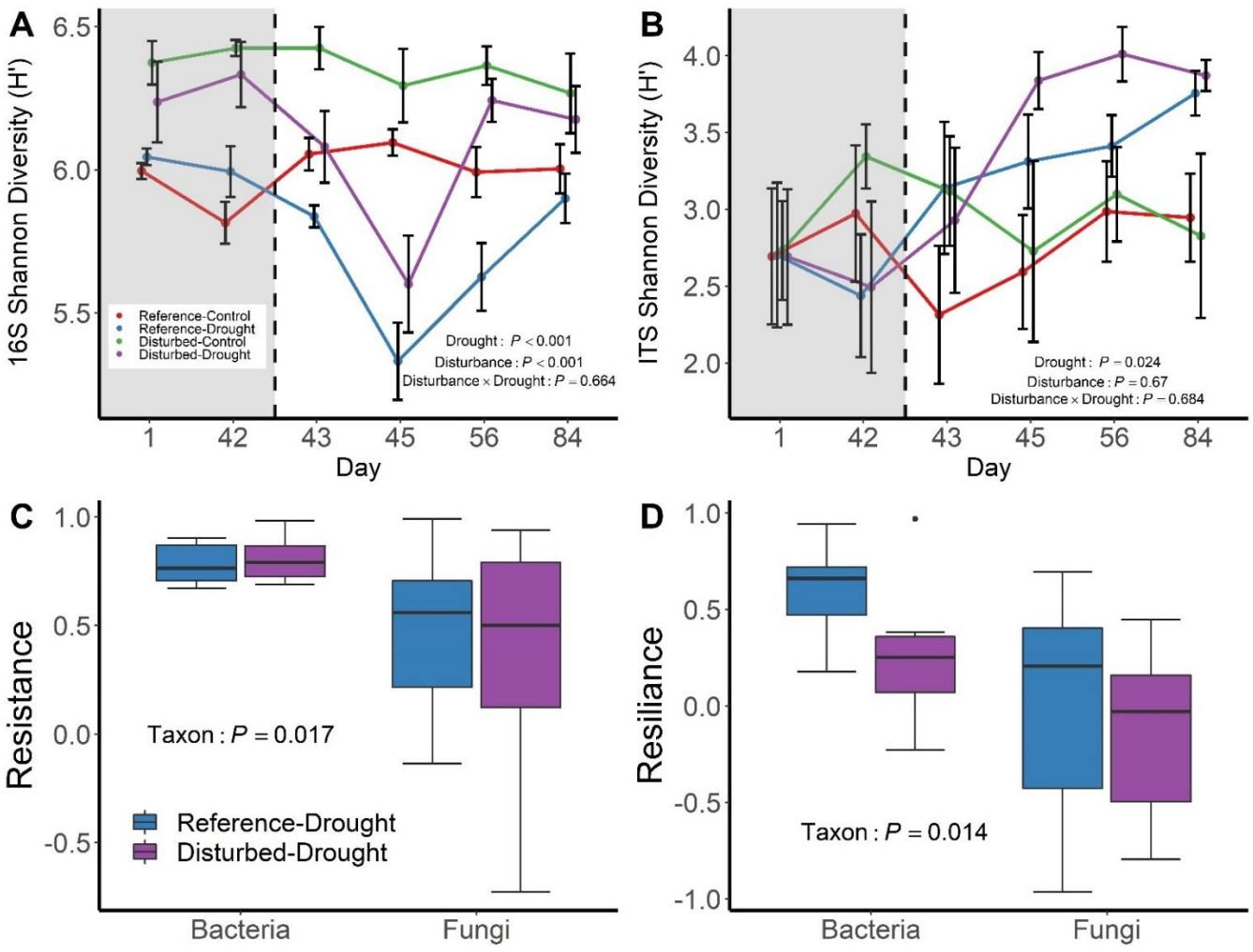

Fig. 5.1: Responses of bacterial (A) and fungal (B) alpha diversity (i.e., Shannon index) to drought-rewetting. Grey shaded areas in (A) and (B) represent the drought period, while the dashed vertical lines represent the rewetting event, which took place after collecting post-drought soils on day 42. *P* values in (A) and (B) are from mixed effects models with 'Drought' and 'Disturbance' as fixed effects and 'Plot' as a random effect. Error bars in (A) and (B) represent one SE. Resistance (C) and Resilience (D) indices for alpha diversity are shown for bacteria and fungi. Resistance (C) values are from comparisons of drought-rewet soils to control soils at day 45 (i.e., the second early response sampling) while Resilience (D) values are from comparisons of drought-rewet soils to control soils at day 84. *P* values in (C) and (D) are from ANOVA.

Figure 5.2

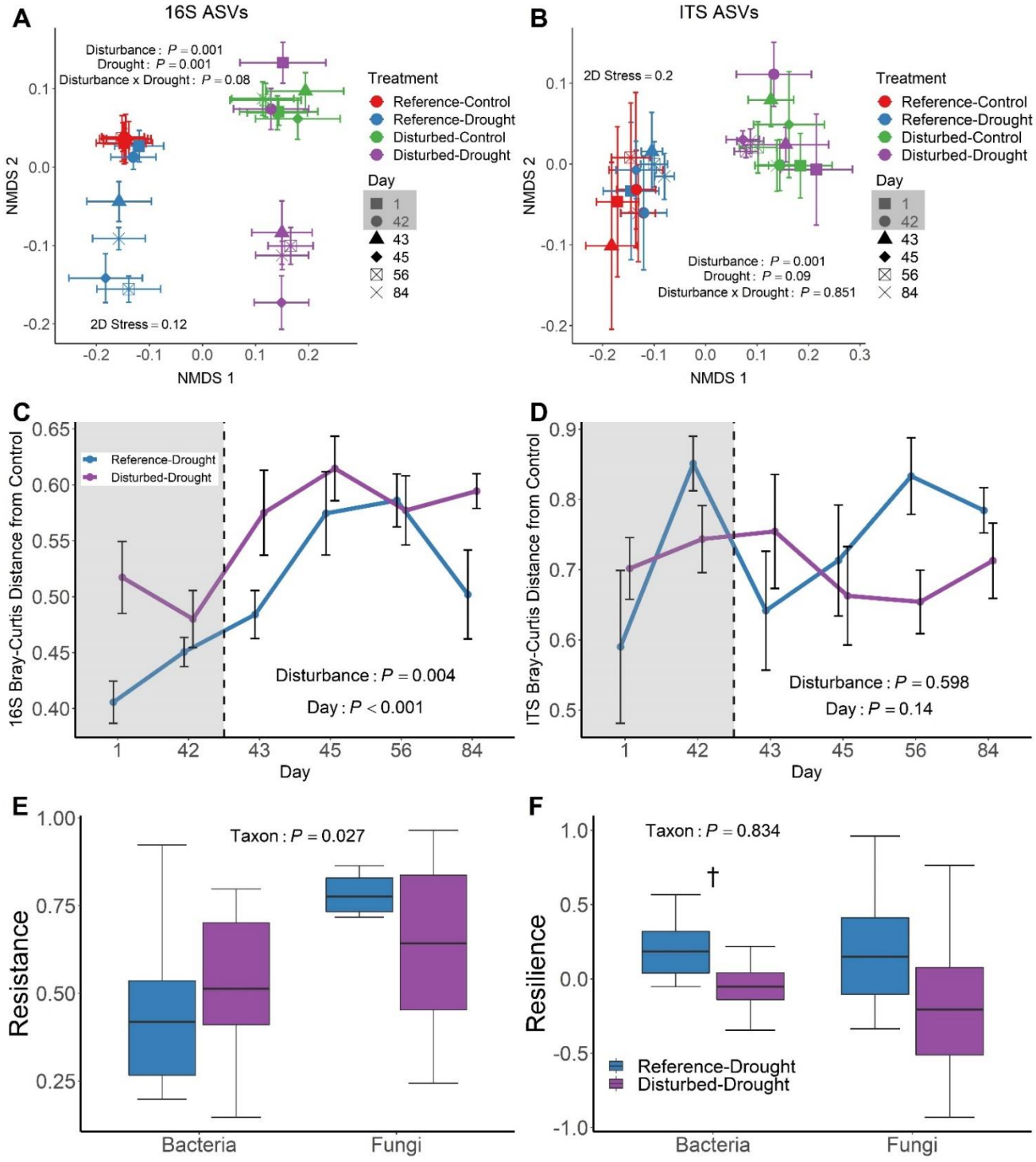
A
16S ASVs
Disturbance : P = 0.001
Drought : P = 0.001
Disturbance x Drought : P = 0.08
2D Stress = 0.12
NMDS 1
NMDS 2
B
ITS ASVs
2D Stress = 0.2
Disturbance : P = 0.001
Drought : P = 0.09
Disturbance x Drought : P = 0.851
Treatment
Reference-Control
Reference-Drought
Disturbed-Control
Disturbed-Drought
Day
1
42
43
45
56
84
C
16S Bray-Curtis Distance from Control
Disturbance : P = 0.004
Day : P < 0.001
D
ITS Bray-Curtis Distance from Control
Disturbance : P = 0.598
Day : P = 0.14
Day
E
Resistance
Taxon : P = 0.027
Bacteria
Fungi
F
Resilience
Taxon : P = 0.834
†
Reference-Drought
Disturbed-Drought

Figure 5.2: Responses of bacterial and fungal beta diversity (i.e., ASV-level community composition) to drought-rewetting. NMDS ordinations (Bray-Curtis distances) are shown for bacteria (A) and fungi (B), where each symbol represents the centroid of the six replicates of each treatment at each time point and error bars represent one SE. *P* values in (A) and (B) are from PERMANOVA. Bray-Curtis distances between drought-rewet soils and constant moisture controls are shown for bacteria (C) and fungi (D). Grey shaded areas represent the drought period, while the dashed vertical lines represent the rewetting event, which took place after collecting post-drought soils on day 42. *P* values in (C) and (D) are from mixed effects models with 'Disturbance' and 'Day' (a proxy for drought treatment) as fixed effects and 'Plot' as a random effect. Error bars in (C) and (D) represent one SE. Resistance (E) and Resilience (F) indices are shown for bacterial and fungal beta diversity. Resistance (E) values are from comparisons of drought-rewet soils to control soils at day 45 (i.e., the second early response sampling) while Resilience (F) values are from comparisons of drought-rewet soils to control soils at day 84. *P* values in (E) and (F) are from ANOVA. The † symbol in (F) represents a marginal difference in Resilience between land uses ($P = 0.06$) for bacterial beta diversity.

Figure 5.3

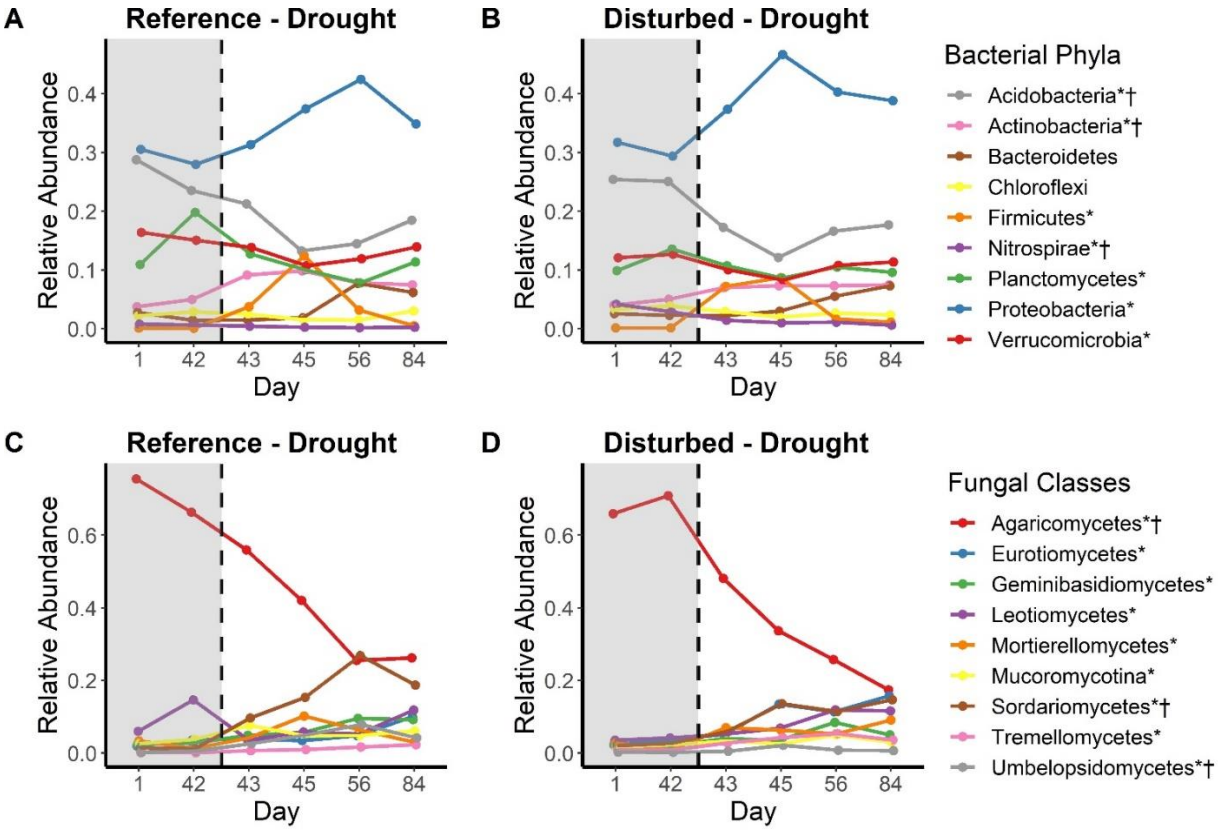

Figure 5.3: Relative abundances of bacterial phyla (A, B) and fungal classes (C, D) in drought-rewet soils at key time points in the drought-rewetting experiment. Relative abundances of each group in constant moisture control soils are shown on Figure S4. Responses are shown separately for the 'reference' soils (A, C) and the historically 'disturbed' soils (B, D). Grey shaded areas represent the drought period, while the dashed vertical lines represent the rewetting event, which took place after collecting post-drought soils on day 42. Symbols next to taxa in the legends represent significant effects from mixed effects models ($P < 0.05$), where * indicates a significant effect of drought-rewetting, while † represents a significant disturbance x drought interaction. Mixed effects models had 'Drought' and 'Disturbance' as fixed effects and 'Plot' as a random effect.

Figure 5.4

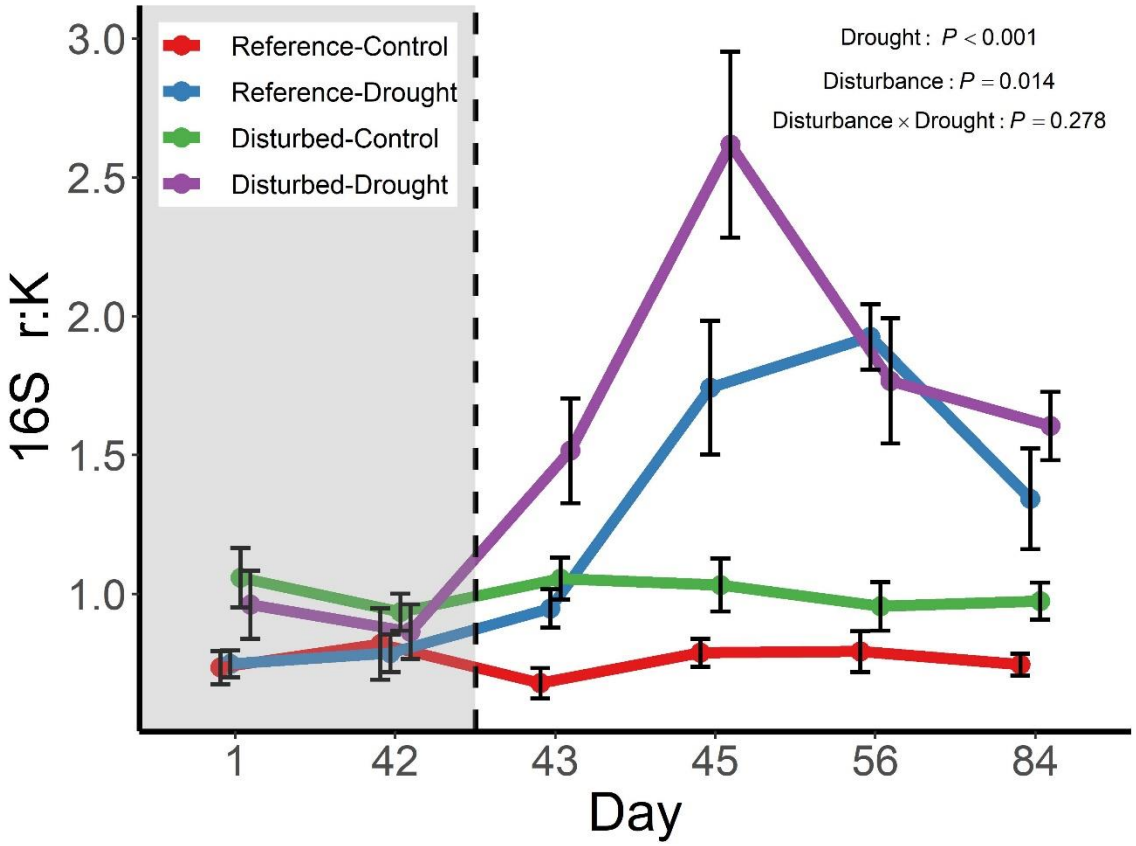

Figure 5.4: Drought-rewetting responses of r- vs. K-selected bacterial phyla. r-selected phyla are represented by Protebacteria and Bacteroidetes, while K-selected phyla are represented by Acidobacteria and Verrucomicrobia. *P* values are from mixed effects models with 'Drought' and 'Disturbance' as fixed effects and 'Plot' as a random effect. Error bars represent one SE. The grey shaded area represents the drought period, while the dashed vertical line represents the rewetting event, which took place after collecting post-drought soils on day 42.

Figure 5.5

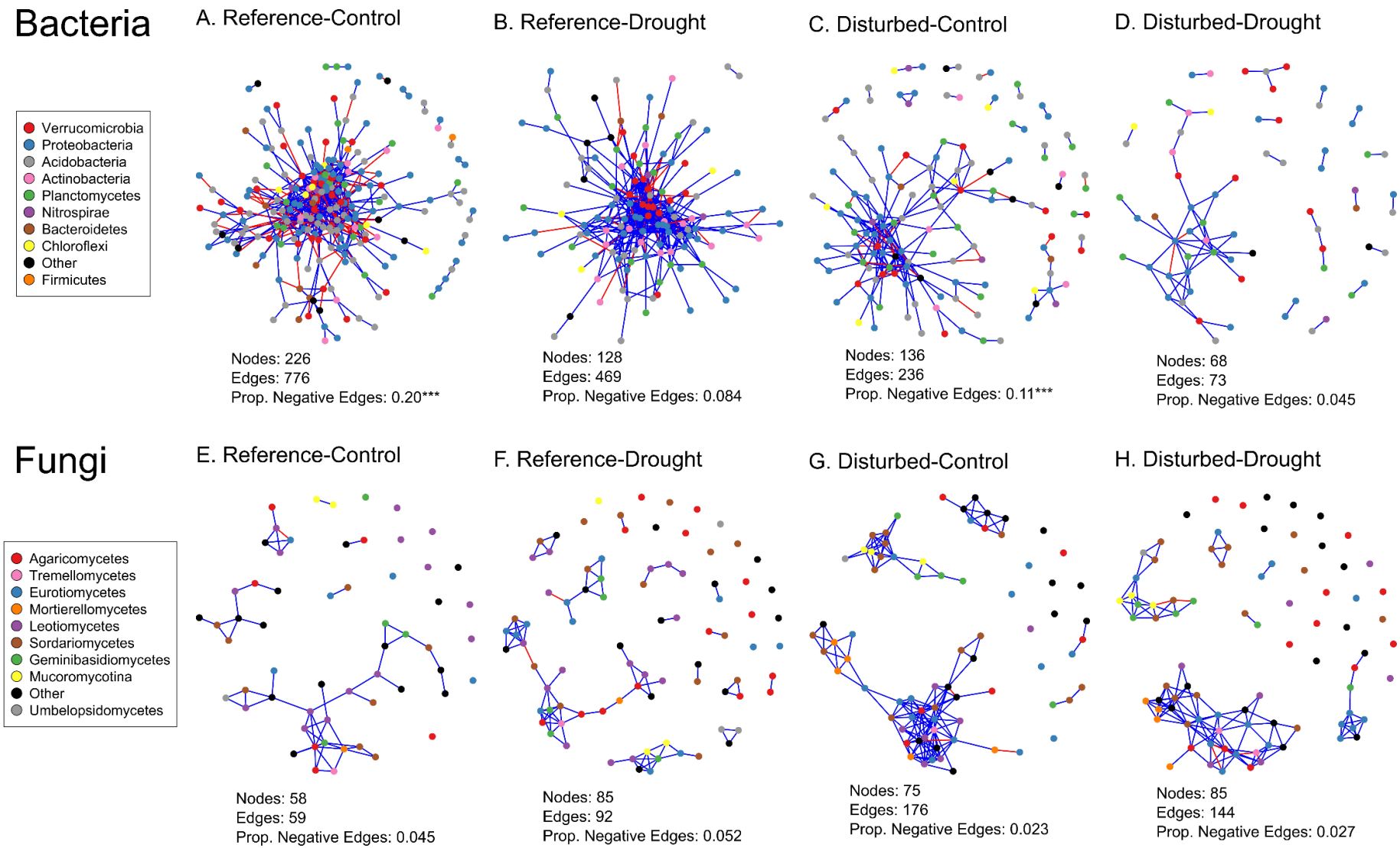
Bacteria
A. Reference-Control
B. Reference-Drought
C. Disturbed-Control
D. Disturbed-Drought
Verrucomicrobia
Proteobacteria
Acidobacteria
Actinobacteria
Planctomycetes
Nitrospirae
Bacteroidetes
Chloroflexi
Other
Firmicutes
Nodes: 226
Edges: 776
Prop. Negative Edges: 0.20***
Nodes: 128
Edges: 469
Prop. Negative Edges: 0.084
Nodes: 136
Edges: 236
Prop. Negative Edges: 0.11***
Nodes: 68
Edges: 73
Prop. Negative Edges: 0.045
Fungi
E. Reference-Control
F. Reference-Drought
G. Disturbed-Control
H. Disturbed-Drought
Agaricomycetes
Tremellomycetes
Eurotiomycetes
Mortierellomycetes
Leotiomycetes
Sordariomycetes
Geminibasidiomycetes
Mucoromycotina
Other
Umbelopsidomycetes
Nodes: 58
Edges: 59
Prop. Negative Edges: 0.045
Nodes: 85
Edges: 92
Prop. Negative Edges: 0.052
Nodes: 75
Edges: 176
Prop. Negative Edges: 0.023
Nodes: 85
Edges: 144
Prop. Negative Edges: 0.027

Figure 5.5: Co-occurrence networks for all experimental treatments for bacterial (A-D) and fungal (E-H) communities. Each network represents all post-rewetting samples (i.e., Days 43, 45, 56, 84) aggregated for each treatment (i.e., 24 samples per network). For fungi (E-H), all significant associations (adjusted $P < 0.01$) are shown, while for bacteria (A-D), only significant associations with high interactions strengths ($|\rho| > 0.8$) are shown. Blue edges represent positive associations while red edges represent negative associations. Bacterial nodes are colored based on phylum membership (A-D) while fungal nodes are colored based on class membership (E-H). In (A) and (C), *** represents significantly higher proportion of negative edges for constant moisture control soils compared with drought-rewet soils for bacterial co-occurrence networks (Z-test, $P < 0.001$).

Figure 5.6

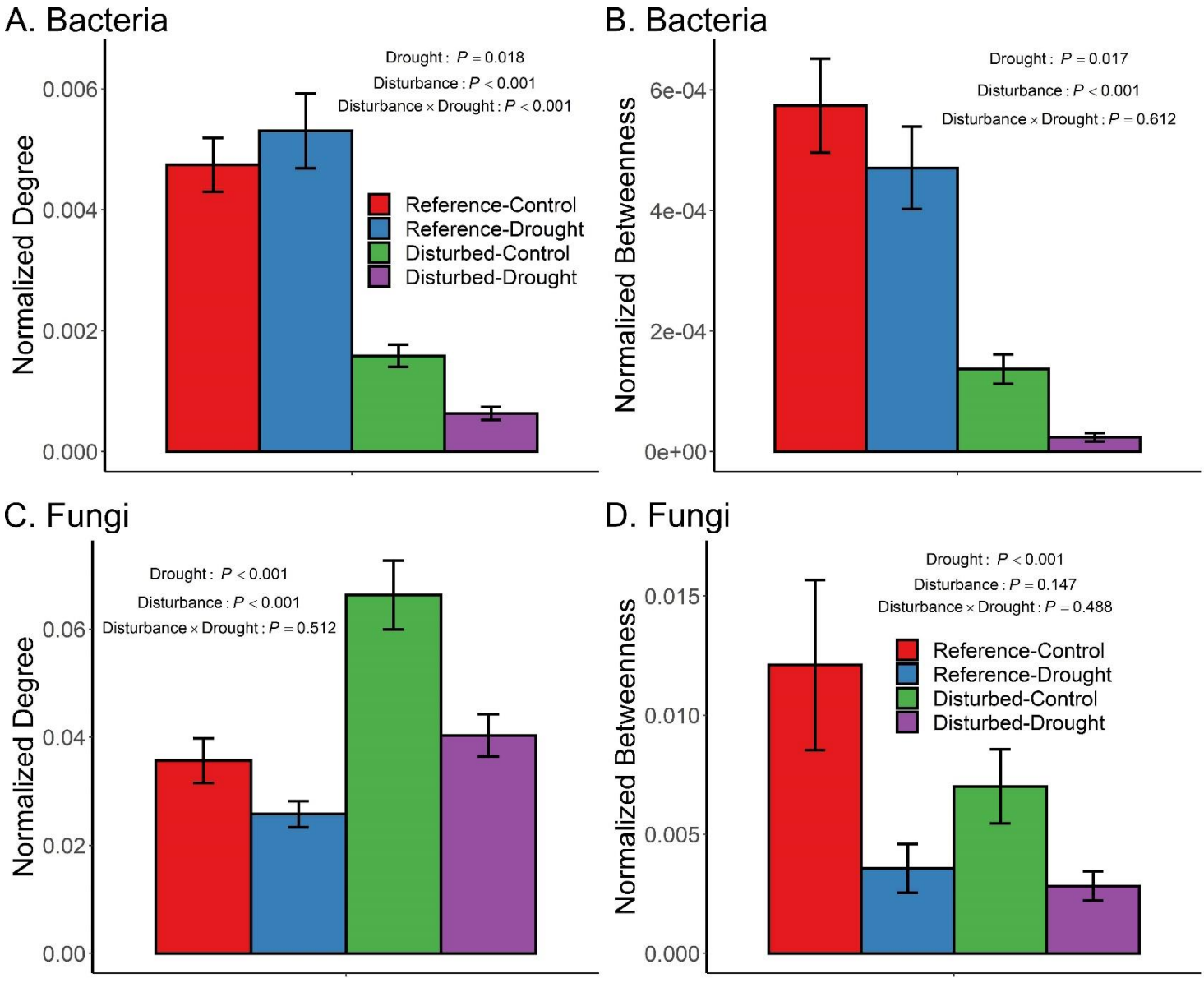

Figure 5.6: Network topology metrics for bacterial (A, B) and fungal (C, D) co-occurrence networks. Network connectivity was determined based on normalized degree scores for each node (A, C) while network centrality was determined based on normalized betweenness scores for each node (B, D). *P* values are from generalized linear models (gamma distribution, log link function), with 'Drought' and 'Disturbance' as fixed effects. Error bars represent one SE.

Supplementary Figures

Figure 5.S1

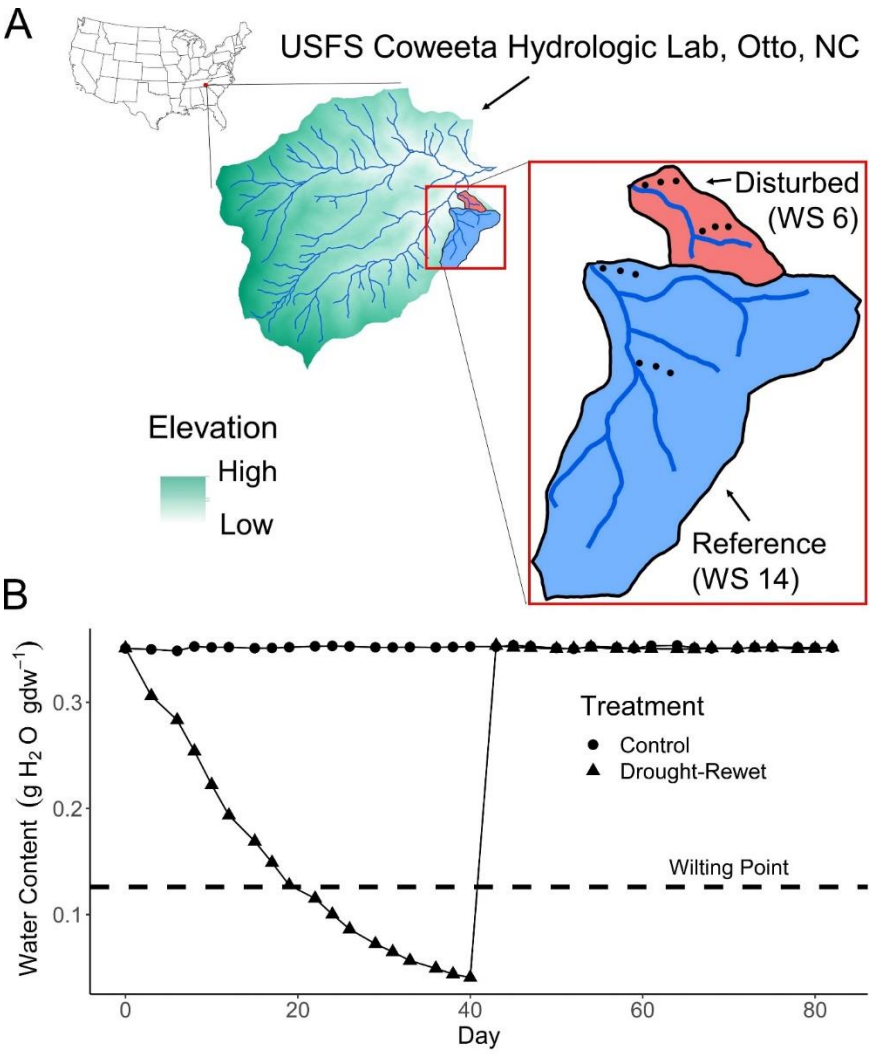

Figure 5.S1: Map of reference and disturbed watersheds sampled for this study (A). Black dots represent locations of the 6 plots within each watershed. (B) Illustrates moisture treatments applied to intact soil cores sampled from the field plots. Water content at wilting point (-1500 kPa) was estimated using a pedotransfer function based on soil texture measurements averaged across all pre-treatment soils.

Figure 5.S2

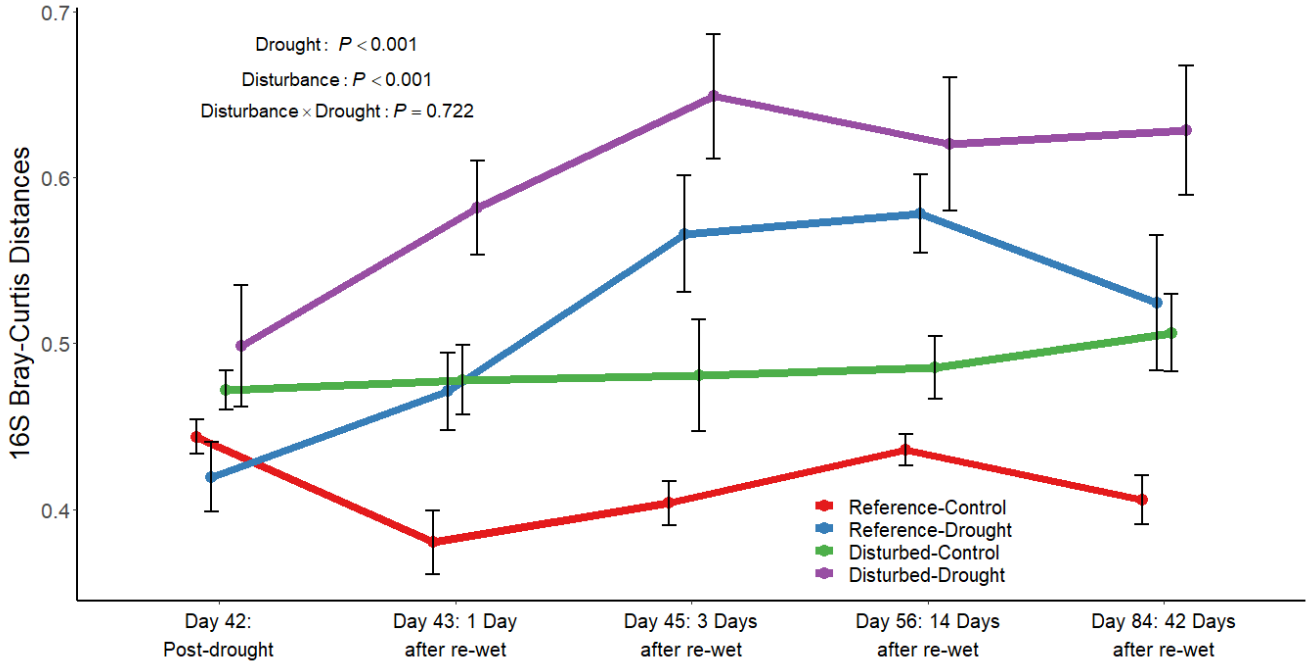

Figure 5.S2: Bray-Curtis distances from the pre-drought (Day 1) samples for bacterial communities. At each time point, Bray-Curtis distances were calculated between each sample and the corresponding sample on Day 1 from the same moisture treatment from the same plot. *P* values are from mixed effects models with 'Drought' and 'Disturbance' as fixed effects and 'Plot' as a random effect.

Figure 5.S3

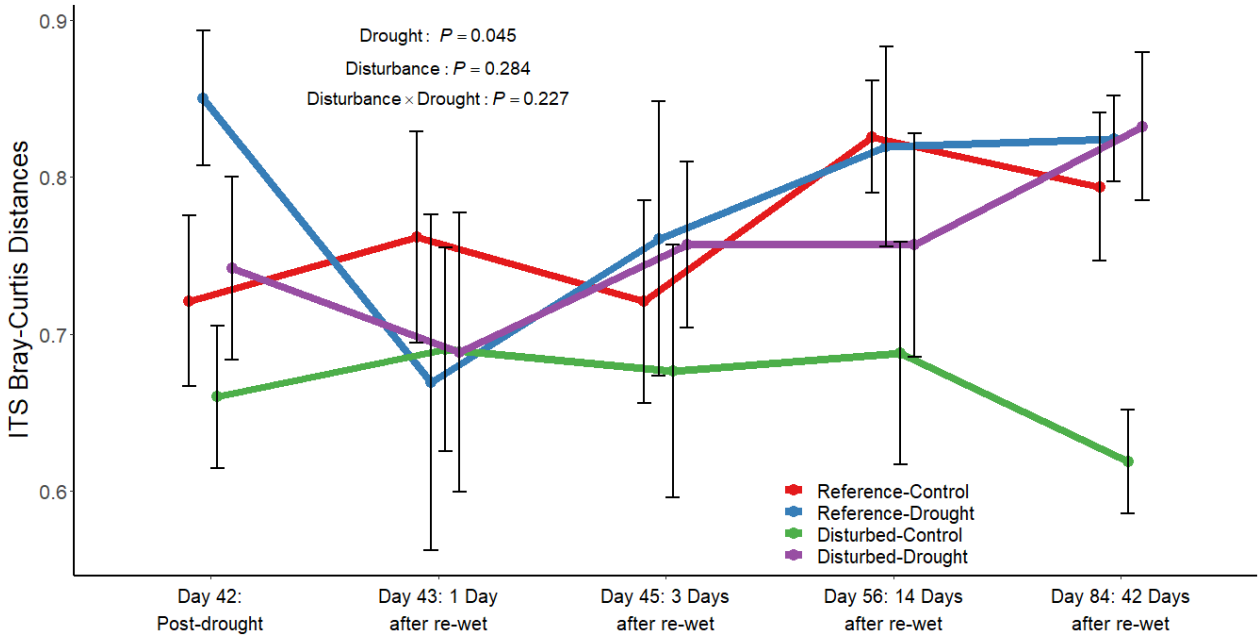

Figure 5.S3: Bray-Curtis distances from the pre-drought (Day 1) samples for fungal communities. At each time point, Bray-Curtis distances were calculated between each sample and the corresponding sample on Day 1 from the same moisture treatment from the same plot. *P* values are from mixed effects models with 'Drought' and 'Disturbance' as fixed effects and 'Plot' as a random effect.

Figure 5.S4

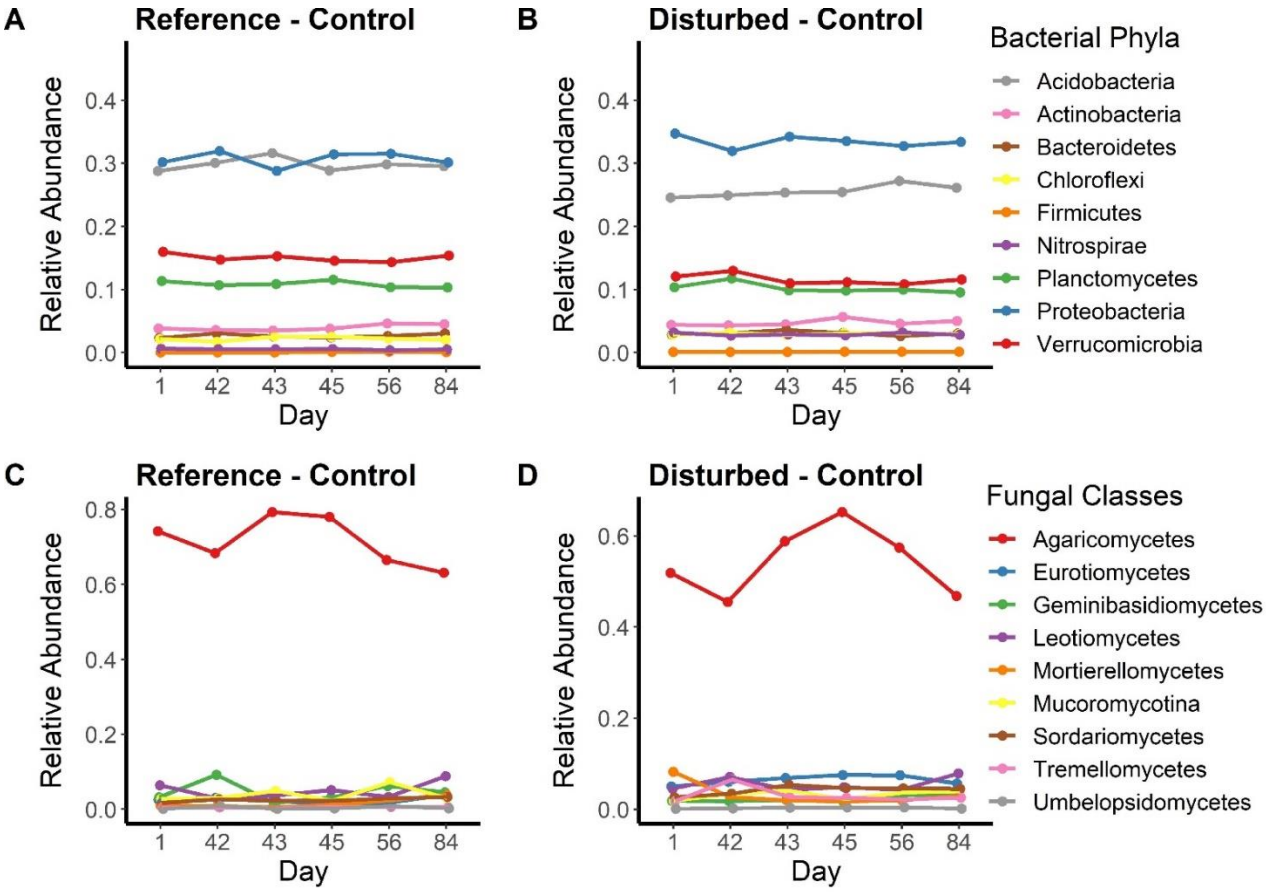

Figure 5.S4: Relative abundances of bacterial phyla (A, B) and fungal classes (C, D) in constant moisture control soils at key time points in the drought-rewetting experiment. Responses are shown separately for the 'Reference' soils (A, C) and the historically 'Disturbed' soils (B, D). Days correspond to the following experimental time points - Day 1: pre-drought, Day 42: post-drought, Day 43: 24 hours post-rewetting, Day 45: 72 hours post-rewetting, Day 56: 2 weeks post re-wetting, Day 84: 6 weeks post re-wetting.

Supplementary Tables

Table 5.S1

Watershed	History	Aspect	Elevation (m)	Area (ha)	Dominant woody vegetation
WS14	Undisturbed since 1923	NW	707 – 992	61	*Rhododendron maximum, Liriodendron tulipifera, Betula spp.*
WS6	Clearcut in 1958, soil scarified, planted to grass, limed and fertilized in 1959, fertilized again in 1965, grass herbicided in 1966 and 1967	NW	696 – 905	9	*Acer rubrum, Liriodendron tulipifera*

Table 5.S1: Detailed watershed information for the watersheds sampled in this study. Additional watershed information can be found at: https://coweeta.uga.edu/sitehistory/basin

Table 5.S2

Variable	Reference	Disturbed
pH	5.14 (0.20)	5.77 (0.06)*
NO_3^- (µg N gdw^{-1})	0.035 (0.015)	0.185 (0.080)†
NH_4^+ (µg N gdw^{-1})	0.762 (0.163)	0.923 (0.152)
Total Extractable N (µg N gdw^{-1})	40.1 (1.89)*	32.8 (1.47)
DON (µg N gdw^{-1})	39.3 (1.55)**	31.7 (1.77)
Extractable DOC (µg C gdw^{-1})	553 (36.6)***	363 (18.2)
Extractable C:N	13.8 (0.59)**	11.1 (0.44)
Microbial Biomass C (µg C gdw^{-1})	164 (24.5)*	75.9 (17.7)
Total C (mg C gdw^{-1})	44.3 (2.02)	37.1 (5.06)
Total N (mg N gdw^{-1})	2.27 (0.271)	2.31 (0.141)
Total C:N	19.9 (1.37)*	15.9 (0.41)

Table 5.S2: Pre-treatment soil variables from the reference and historically disturbed forest sites. Values are means with one SE shown in parentheses. Symbols indicate significantly higher values (ANOVA) at the following significance levels: † $P < 0.1$, * $P < 0.05$, ** $P < 0.01$, *** $P < 0.001$.

CHAPTER 6 – Land use history mediates soil biogeochemical responses to drought in temperate forest ecosystems

Authors:

Ernest D Osburn, Julia S Simpson, Brian D Strahm, J E Barrett

In review, *Ecosystems*

Abstract

Terrestrial ecosystems are experiencing increasing frequency and intensity of droughts as a result of climate change. Despite a wealth of previous studies investigating soil responses to drought, the importance of historical land use in mediating drought effects remains poorly understood. To identify interactions between drought and historical land use, we sampled soils from two adjacent forested watersheds at the USFS Coweeta Hydrologic Laboratory: a 'reference' forest that has remained undisturbed for approximately a century and a 'disturbed' forest with a history of conversion to pasture followed by abandonment to forest succession. We incubated intact soil cores in the lab under one of two moisture treatments: a constant moisture control and a drought-rewet treatment, which involved a six-week drought followed by rewetting and six additional weeks at constant moisture. We measured respiration and characterized soil C and N pools and microbial communities multiple times throughout the experiment. Soils exposed to drought-rewetting had higher cumulative respiration than control soils, which was driven by particularly strong respiration responses of disturbed soils. In addition, drought-rewetting reduced microbial biomass and increased total extractable N and NH_4^+, with greater responses in reference watershed soils. Microbial communities also exhibited responses, with increased biomass C:N, increased fungal:bacterial ratios, and decreased nitrifier abundance in response to drought-rewetting. Overall, our results show

that drought responses of forests will vary among land use histories and among soil parameters, which should be considered when seeking to predict biogeochemical responses of temperate ecosystems to climate stressors such as intensifying droughts.

Introduction

Ecosystems globally are experiencing an intensification of earth's hydrologic cycle, including increased intensity of rainfall events, but also increased frequency and duration of droughts (IPCC 2013). This intensification of drought-rewetting cycles will have far-reaching consequences for terrestrial ecosystem functioning. For example, desiccation and rewetting represent significant physiological stressors for soil microorganisms (Schimel and others 2007), which are the proximate drivers of element cycles in terrestrial environments (Falkowski and others 2008; Fierer 2017). Drought-rewetting will also alter soil physical processes such as soil organic matter (SOM) stabilization (Fierer and Schimel 2003; Schimel 2018), which has implications for the global carbon (C) cycle, as soils are the largest terrestrial stock of C (IPCC 2013). Further, these drought-sensitive elemental fluxes are key drivers of ecosystem services that support human well-being, including regulation of nutrient cycling (Millenium Ecosystem Assessment 2005), thus highlighting the need to understand effects of drought-rewetting on soil communities and processes.

Some effects of drought-rewetting cycles on soil have been long recognized – for example, drying reduces soil respiration, which is followed by a pulse of CO_2 production after rewetting (Birch 1958). This "Birch Effect" results in respiration rates that can be several times higher than basal rates. Though the mechanism of this phenomenon remains poorly understood, the CO_2 pulse likely results from mineralization of microbial

necromass and/or intracellular osmolytes by rapidly resuscitating microbial communities (Fierer and Schimel 2003; Placella and others 2012). Additional C substrates fueling the CO_2 pulse may originate from SOM that has been destabilized by rapid rewetting of dry soil (Fierer and Schimel 2003; Schimel 2018). However, the CO_2 pulse is short-lived and may not balance out reductions in CO_2 emissions during dry periods (Borken and Matzner 2009), though soil C balance in response to drought-rewetting will vary among ecosystems and will depend on soil properties such as SOM content (Canarini and others 2017; Zhang and others 2020). Drought-rewetting has similar effects on soil nitrogen (N) cycling, including reduced rates of N-cycle processes (e.g., N-mineralization, nitrification) during dry periods, followed by peaks in process rates and larger soil inorganic N pools following rewetting (Birch 1958; Fierer and Schimel 2002; Borken and Matzner 2009; Gao and others 2020). These biogeochemical drought responses are also associated with effects on microbial communities, including reduced microbial biomass, altered bacterial community structure, and increased activity of nitrifying taxa following drought-rewetting (Barnard and others 2013; Placella and Firestone 2013; Evans and Wallenstein 2014; De Vries and others 2018; Zhou and others 2018; Preece and others 2019).

Intensifying drought-rewetting cycles are not the only perturbation facing terrestrial ecosystems – these environments are also experiencing effects of historical and ongoing land use change. Indeed, land use change has modified ~75% of ice-free terrestrial ecosystems globally (Ellis 2011). Further, despite the wealth of previous studies investigating soil responses to drought-rewetting, the influence of land use change in mediating drought-rewetting responses is not well understood. Though drought-

rewetting studies across varying land uses are not common, one previous study showed that natural grasslands had more drought-resistant microbial communities and more resistant C- and N-cycle processes compared to intensively cultivated systems (De Vries and others 2012). Another grassland study showed that microbial N metabolism was more sensitive to drought in managed grasslands compared to unmanaged grasslands (Fuchslueger and others 2019). Studies in forested systems have shown that ongoing management (i.e., forest thinning) can increase the resilience of microbial community structure and function to drought (Bastida and others 2017, 2019), and that conversion of forests to cultivated or abandoned agricultural land can influence drought responses of some soil biogeochemical processes, such as microbial extracellular enzyme activities (Moreno and others 2019). Although these studies suggest that land use may play an important role in determining soil responses to drought, no studies to our knowledge have assessed the influence of long-term legacies of historical land use (i.e., several decades previous) on the drought-rewetting responses of soils from currently unmanaged terrestrial ecosystems.

To assess potential influences of historical land use on soil biogeochemical responses to drought, we conducted a drought-rewetting experiment using intact soil cores sampled from two adjacent watersheds at the USDA Forest Service Coweeta Hydrologic Lab. Though both watersheds are currently forested, they have distinct land use histories: one is an unmanaged reference site while the other experienced extensive disturbance associated with conversion to pasture in the mid-20th century. This land use history, similar to other historical disturbances in the region, has had well-documented long-term effects on various ecosystem properties, including altered vegetation (Elliott

and Vose 2011), altered soil microbial communities (Osburn and others 2019; Osburn and Barrett 2020), increased soil nitrification rates (Keiser and others 2016), and increased watershed-scale N export (Swank and Vose 1997). However, the importance of these land use legacies in influencing responses to ongoing and future stressors associated with climate change has not been assessed. The goal of this study is to address the following questions: 1) are soil C losses following drought-rewetting (i.e., the "Birch Effect") influenced by historical land use? 2) does historical land use influence responses of soil C and N pools to drought-rewetting? and 3) do key microbial functional groups (e.g., nitrifying taxa) respond differently to drought-rewetting across different historical land uses?

Materials and Methods

Soil Sampling

We sampled soils at the Coweeta Hydrologic Laboratory, a USDA Forest Service experimental forest in North Carolina, USA (latitude 35°03′ N, longitude 83°25′ W). Annual rainfall is usually high at Coweeta, averaging ~1800 mm per year, though droughts are becoming increasingly common and are increasing in duration (Laseter and others 2012; Burt and others 2018). Within the Coweeta basin, we selected two forested watersheds for soil sampling (Fig. 6.1A), one of which (watershed 6), was clear-cut and converted to pasture in 1958, which involved soil scarification, liming, and fertilizing. In 1966-67, the grass was herbicided and the watershed abandoned to forest succession. This history of agricultural abandonment is a common past land use in forested systems of the eastern US (Gragson and Bolstad 2006). The other watershed (watershed 14) is directly adjacent to watershed 6 (Fig. 6.1A). This watershed has not been manipulated by

the US Forest Service and has been undisturbed since at least 1923, when ~20% of the basal area of the Coweeta basin was cut and harvested (Elliott and Vose 2011). We refer to these alternative land use histories as 'reference' (i.e., watershed 14) vs. 'disturbed' (i.e., watershed 6), which reflects the more recent and intensive human activity that took place on the abandoned pasture site. Detailed watershed information is available on Table 6.S1. In each watershed, we established six 1 m^2 plots, three at lower elevations near the outlet of the stream and three at upper elevations closer to the source of the stream, a total of 12 plots (Fig 6.1A). The three plots at each elevation were located at 5 m, 25 m, and 50 m along a transect running upslope starting from the stream channel. This sampling scheme is similar to previous studies at Coweeta (Keiser and others 2016) and is intended to incorporate spatial variation in soil properties present in these watersheds into our experiment.

In each plot, we sampled thirteen 10 cm depth, 3.8 cm diameter mineral soil cores in PVC corers. Samples did not include O-horizon material and mineral soil samples at this depth generally include the entire A-horizon in these watersheds (Knoepp and Swank 1994). We focused on mineral soils because C and N pools are much larger in mineral layers than in organic layers at Coweeta (e.g., Knoepp and others 2018) and because organic matter is generally more stable long-term in mineral layers than in organic layers (e.g., Hemingway and others 2019). Consequently, mineral soil C and N dynamics are more relevant to the long-term C and N balance of these forests and more effectively reflect the long-term biogeochemical legacies of historical disturbance. Therefore, mineral soils are appropriate for investigating potential influences of historical disturbance on soil biogeochemical responses to climate change factors. After sampling,

one core from each plot was immediately processed for measurement of initial soil properties. We attached 25 µm nylon mesh to the bottom of the remaining cores to prevent soil spillage, transported the cores to Virginia Tech on ice, and stored them for one week at 4 °C until the start of the experiment.

Experimental Design

The twelve intact soil cores from each of the twelve field plots (144 cores total) were incubated in the original PVC corers at 20 °C under one of two moisture treatments: a constant moisture control and a drought-rewet treatment. Incubating intact cores minimized disturbances to the soil, allowing us to observe more realistic biological and chemical responses to experimental treatments. On day one of the experiment, all soil cores were adjusted to 0.35 g H_2O gdw^{-1} and soil cores assigned to the constant moisture control group were maintained at this water content throughout the duration of the twelve-week (84 day) experiment (Fig. 6.1B). This water content is equivalent to the long-term average summer soil moisture previously measured at Coweeta (Helvey and Hewlett 1962), is also similar to recent measurements of summer soil moisture at Coweeta (Keiser and others 2016; Osburn and others 2019), and has been used as a control in previous moisture experiments using Coweeta soils (Knoepp and Swank 2002). Further, this water content is approximately equal to field capacity in these soils (~ -10 kPa), which we estimated using a pedotransfer function (Saxton and others 1986) based on soil texture measurements made on the pre-treatment soils using the hydrometer method (Robertson and others 1999). To monitor water content in each core, we weighed PVC cores before and after sampling soil and calculated the dry weight of soil in each core based on initial water content, which we determined for each core based on the

water content of the pre-treatment soil sample from the same plot. We adjusted water content by gently pipetting DI H_2O evenly to the soil surface until reaching the calculated weight of the core at 0.35 g H_2O gdw^{-1}. Water additions were done three times per week, which is equal to the long-term average frequency of summer rainfall events at Coweeta (Burt et al. 2018).

Soils assigned to the drought-rewet treatment did not receive water for the first six weeks of the experiment (Fig. 6.1B), which was intended to simulate an extreme drought. Our experimental drought period was similar in duration to recent extreme droughts experienced regionally (Williams and others 2017) and at Coweeta specifically (Miniat and others 2017). By the third week of the experiment, soils in the drought-rewet treatment had reached wilting point (-1500 kPa, equivalent to ~ 0.12 g H_2O gdw^{-1}) (Fig. 6.1B). This water potential is also approximately equal to the threshold for inducing microbial osmotic stress previously reported for intact soil cores (Manzoni and others 2012). Soils in this treatment dried to 0.04 g H_2O gdw^{-1} on average by the end of the six week drought period (Fig 6.1B). At the end of the six week drought, we rewet these soils to 0.35 g H_2O gdw^{-1} and maintained them at this water content for the second six weeks of the experiment (Fig. 6.1B). At six time points throughout the experiment, we destructively harvested one control and one drought-rewet core from each field plot (24 cores per time point): after the initial adjustment to 0.35 g H_2O gdw^{-1} (day 1), at the end of the drought (day 42), 24 hours after re-wetting (day 43), 72 hours after re-wetting (day 45), two weeks after re-wetting (day 56) and six weeks after re-wetting (day 84). This sampling plan allowed us to assess both immediate and longer-term effects of drought-

rewetting on our soils. After harvesting, soils were sieved (4 mm), homogenized, and subsamples stored at -20 °C (for DNA extraction) or 4 °C (for soil properties).

Soil Respiration

We measured soil respiration by capping cores with PVC end caps with butyl septa installed, flushing CO_2 from the headspace of the cores, and measuring accumulated CO_2 after incubating for 24 hours using an infrared gas analyzer (Li-7000; Li-Cor Biosciences, Lincoln, Nebraska, USA), similar to the static incubation procedure described by Bradford and others (2008). We conducted respiration incubations twice during the first week of the experiment and twice during the week of the rewet - otherwise, respiration incubations occurred once per week. At each respiration measurement time point, we randomly selected one control and one drought-rewet core from each field plot (i.e., 24 cores measured each time) for measurement. We calculated cumulative respired C for each replicate by integrating under CO_2 evolution time series curves.

Soil Properties

We measured several chemical properties on all collected soils, including microbial biomass C and N, extractable organic C (DOC), total extractable N, NH_4^+-N, and NO_3^--N. We determined microbial biomass C and N using a modified chloroform extraction procedure (Fierer and Schimel 2003). Briefly, duplicate subsamples of each soil were extracted with 0.5 *M* K_2SO_4 (1:5 soil:solution ratio) and shaken for four hours, one with 1 ml chloroform added and one without. All extracts were analyzed for DOC and total extractable N on an Elementar vario cube TOC/TNb (Elementar Americas Inc., Mt. Laurel, NJ, United States). Extracts that did not receive chloroform were also

measured for NO_3^--N and NH_4^+-N on a Lachat QuikChem flow injection analyzer (Hach Company, Loveland, CO, United States). Extractable organic N (DON) was calculated as total extractable N - (NO_3^--N + NH_4^+-N). On pre-treatment soils, we additionally measured pH in a 1:1 soil:DI H_2O slurry (Allen and others 1974), using a Hach Sension+ pH meter (Hach company, Loveland, CO, USA) and total C and N on dried, milled samples using an Elementar vario MAX cube (Elementar Americas Inc., Mt. Laurel, NJ, United States). Gravimetric water content of all soils was measured by mass loss after drying at 105 °C for 24 hours and all soil properties are presented on an oven-dried basis.

Microbial Functional Groups

We assessed abundance of microbial functional groups using qPCR. We extracted DNA from ~0.25 g soil using the Qiagen DNeasy PowerSoil kit (Qiagen, Valencia, CA, United States) and quantified extracts using a Qubit 2.0 Fluorometer (Thermo Fisher Inc., Waltham, MA, United States). We assessed total bacterial and total fungal abundance by amplifying the 16S rRNA and ITS regions, respectively. For ITS qPCR, we used the ITS1f/5.8s primers while for 16S rRNA qPCR we used the EUB 338/515 primers (Fierer et al. 2005). We also assessed abundance of *amoA* genes involved in nitrification from ammonia-oxidizing archaea (AOA), ammonia-oxidizing bacteria (AOB), and complete ammonia-oxidizing bacteria (CAOB). For AOA we used the primer set Arch-amoAF/R (Francis et al. 2005), for AOB we used the primer set amoA-1f/2r (Rotthauwe et al. 1997), and for CAOB we used the comamoa F/R primer set (Zhao et al. 2019). All qPCR reactions contained 10 µl Quantitect SYBR master mix (Qiagen, Valencia, CA, United States), 4 µl DNA extract, 0.25 µM (*amoA* genes) or 0.5 µM (16S and ITS) forward and reverse primers, and nuclease-free H_2O to 20 µl. For *amoA* genes, we used undiluted

DNA extract (~40 – 300 ng DNA), while for 16S and ITS, we used 1:10 diluted extract (~4 – 30 ng DNA). Thermal cycling conditions for each gene are provided in Table 6.S2. Standard curves for each gene were generated by amplifying serial dilutions of the target genes. Standards for AOA, AOB, and CAOB were synthesized DNA oligonucleotides of *amoA* gene sequences from *Nitrosospira multiformis*, *Nitrosotalea devannaterra*, and *Nitrospira inopinata*, respectively. 16S and ITS gene standards were from environmental (i.e., soil) amplicons cloned into plasmids. Standard curves had amplification efficiencies of 80.5 - 97.5% and R^2 values > 0.99. Amplifications were performed in triplicate and amplification specificity was assessed using melt curves. All gene abundances were corrected for dry soil mass and were log transformed prior to analysis. Fungal:bacterial ratios (ITS:16S) were calculated by dividing ITS gene copy numbers by 16S gene copy numbers (Fierer and others 2005).

Statistical Analysis

We performed all statistical analyses in R (R Core Development Team 2019) using the 'lme4' and 'emmeans' packages (Bates and others 2019; Lenth and others 2019). To assess effects of historical land use (i.e. 'disturbance') on pre-treatment soil properties, we used one-way analysis of variance (ANOVA). For soil variables measured throughout the experiment, we assessed effects of disturbance, drought treatment, and disturbance x drought interactions using linear mixed effects models ('lmer' function, lme4 package). Our mixed effects models included 'plot' as a random effect, which allowed us to account for repeated measurements of soil and microbial variables from the same field plots over time, plots being represented in the lab experiment by the intact cores sampled from each respective plot. We assessed assumptions of normality of

residuals of our models by examining q-q plots, and when deviations from normality were observed, we used generalized linear mixed effects models ('glmer' function, gamma distribution and log-link function, lme4 package). Though we were primarily interested in effects of disturbance and drought, for variables assessed at multiple time points we also included 'day' as a categorical fixed effect in our models, which allowed us to conduct pairwise comparisons (Tukey's HSD) between all treatments within each day using the emmeans package ('emmeans' and 'contrast' functions). We identified relationships between all variables using Spearman rank correlations and we investigated potential drivers of soil NO_3^--N pools using linear regression.

For all statistical analyses, plots were treated as independent replicates, similar to other recent watershed-scale studies in the region (Keiser and others 2016). Strictly speaking, our individual plots within watersheds do not represent true replicates of the land use treatments, as land use treatments were applied at the whole-watershed scale. However, because each plot occupies a unique elevation x slope location within each watershed, and because Coweeta watersheds exhibit high spatial variability in soil properties among these different elevations and slope positions (e.g., Hawthorne and Miniat 2018; Knoepp and others 2018), our individual field plots are statistically independent.

Results

Pretreatment Soils

Pre-treatment soils collected from the reference and disturbed watersheds exhibited distinct soil properties, including significantly higher pH and ~4-fold higher NO_3^--N in the disturbed forest soils (Table 6.1). Reference forest soils, on the other hand,

had ~52% higher DOC, ~116% higher microbial biomass C, ~24% higher DON, ~24% higher extractable C:N, and ~25% higher total C:N (Table 6.1).

Soil Respiration

Respiration rates in constant moisture control soils exhibited little change over time and were not different between land uses at any measurement time point (Fig. 6.2A, Table 6.S3). In contrast, soils assigned to the drought-rewetting treatment exhibited significantly altered respiration dynamics – by week two of the drought period, these soils respired significantly less than control soils, with ~50% lower respiration rates in drought-rewet soils by the end of the drought period on day 42 (Fig. 6.2A, Table 6.S3). Drought soils peaked in respiration after being rewet, respiring ~3-fold more than control soils on day 44 (Fig. 6.2A, Table 6.S3). These soils continued respiring more than control soils for ~3 weeks following the re-wet, and then fell to levels statistically indistinct from the control soils for the final 3 weeks of the experiment (Fig. 6.2A). The peak in respiration was larger in disturbed-drought soils, which had ~40% higher respiration than reference-drought soils on day 44 (Fig. 6.2A , Table 6.S3). Integrating under time series curves showed that cumulative respiration did not differ between land uses in constant moisture control soils (Fig. 6.2B, Table 6.S4); however, we did detect a significant overall effect of drought on cumulative respiration, where soils exposed to drought-rewetting respired ~8% more C than control soils overall (Fig. 6.2B, Table 6.S4). This pattern was driven primarily by a significant pairwise difference in cumulative respiration between moisture treatments from the disturbed watershed, where drought soils had ~13% higher cumulative respiration than control soils (Fig. 6.2B, Table 6.S4).

Soil C and N pools and Microbial Functional Groups

We observed a significant overall effect of drought on microbial biomass C pools, where control soils had ~80% higher microbial biomass than drought soils at the end of the drought on day 42 (Fig. 6.3A, Table 6.S5). We also identified a significant drought x disturbance interaction, where soils from the reference watershed exhibited greater effects of drought on microbial biomass - reference-control soils had ~98% more microbial biomass than reference-drought soils on day 42 (Fig. 6.3A, Table 6.S5). This pattern held at other time points in the experiment - reference-drought soils again had significantly lower microbial biomass C than reference-control soils at day 56, while microbial biomass C in disturbed-drought soils were never significantly different from disturbed-control soils (Fig. 6.3A, Table 6.S5). Indicators of microbial community composition, i.e., microbial biomass C:N and fungal:bacterial ratios (i.e., ITS:16S), also exhibited effects of drought, though the effects were the same across both historical land uses (Fig. 6.3B, C, Table 6.S6, 6.S7). Specifically, biomass C:N was ~92% higher in drought soils at the end of the drought on day 42, though biomass C:N quickly returned to control levels within days of re-wetting (Fig. 6.3B, Table 6.S6). Similarly, fungal:bacterial ratios were ~52% higher in drought soils at the end of the drought but did not show consistent patterns between moisture treatments thereafter (Fig. 6.3C, Table 6.S7). Fungal:bacterial ratios also exhibited clear land use effects throughout the experiment, being ~67% higher in reference soils than disturbed soils overall (Fig. 6.3C, Table 6.S7).

Extractable DOC declined with microbial activity - in constant moisture control soils, DOC had significantly reduced by day 42, while DOC remained high in drought

soils at that time (Fig. 6.4A, Table 6.S8). After re-wetting, DOC rapidly declined in drought-rewet soils and reached control levels by day 56 (Fig. 6.4A, Table 6.S8). Total extractable N showed significant drought effects, with drought soils having ~75% higher N at the end of the drought on day 42, a pattern that persisted throughout the remainder of the experiment (Fig. 6.4B, Table 6.S9). Further, we identified a significant drought x disturbance interaction, where drought had particularly strong effects on extractable N in reference soils (~130% higher in drought soils, Fig. 6.4B, Table 6.S9). Because > 90% of the extractable N is organic in our samples (Table 6.1), extractable organic N exhibited nearly identical responses (Fig. 6.S1). These extractable N responses are responsible for the drought responses we observed for extractable C:N, which was overall lower in soils exposed to drought, but particularly in drought soils from the reference watershed (Fig. 6.S2). The response of NH_4^+-N was similar, though effects did not appear until the re-wet occurred on day 43, at which point drought soils had 173% higher NH_4^+-N than control soils, a pattern that persisted until the end of the experiment (Fig. 6.4C, Table 6.S10). Once again, we identified a significant drought x disturbance interaction, where reference soils showed particularly strong drought effects on NH_4^+ (~480% higher in drought soils, Fig. 6.4C, Table 6.S10).

NO_3^--N and nitrifying taxa exhibited clear land use effects throughout the experiment, where disturbed soils had ~12-fold higher NO_3^--N concentrations on average (Fig. 6.5A, Table 6.S11) and generally greater abundance of nitrifiers (Fig. 6.5B, C, 6.S3, Table 6.S12, 6.S13). NO_3^--N also showed significant drought effects, though they were opposite of NH_4^+-N; at the end of the drought on day 42, control soils had ~4-fold higher NO_3^--N than drought soils, a pattern that held at most remaining time points (Fig. 6.5A,

Table 6.S11). The NO_3^- response is likely related to the drought responses of nitrifying taxa; both AOA and CAOB had lower abundance in drought-exposed soils (Fig. 6.5B, 6.S3, Table 6.S12), indicating inhibiting effects of drought-rewetting on nitrifier activity and growth. In contrast, AOB exhibited less clear drought effects; there were no clear patterns in AOB abundance immediately post drought-rewetting (Fig. 6.5C, Table 6.S13). However, by the end of the experiment AOB appeared to be growing in the disturbed-drought treatment, which had higher AOB abundance than some other treatments on days 56 and 84 (Fig. 6.5C, Table 6.S13), which may be related to the peak in NO_3^- we observed on day 84 in disturbed-drought soils (Fig. 6.5A, Table 6.S11). Indeed, AOB abundance was a strong predictor of NO_3^- at that time point ($R^2 = 0.771$, Fig. 6.S4). Overall, across all samples, the combination of extractable C:N and AOA *amoA* gene abundance was strongly predictive of soil NO_3^- (adj. $R^2 = 0.599$, Fig. 6.6), where high soil NO_3^- was associated with the co-occurrence of low C:N and high AOA *amoA* gene abundance (Fig. 6.6, Table 6.S14).

Discussion

Forest soils of the southern Appalachian region may experience net respiratory C losses in response to drought-rewetting (Fig. 6.2B), likely associated with the C-rich nature of these soils (Canarini and others 2017). These cumulative respiratory C losses appear to be greater in soils from forests with a history of intensive land use (i.e., 'disturbed', Fig. 6.2B), which is associated with the exaggerated Birch Effect we observed in these soils (Fig. 6.2A). Several potential mechanisms may have contributed to the different respiration responses between land uses we observed. For example, increased C substrates from destabilization of SOM has been frequently proposed to be a

potential mechanism for the Birch Effect (Fierer and Schimel 2003; Borken and Matzner 2009; Zhang and others 2020), and this destabilization effect may vary among land uses due to differences in soil physical properties (e.g., aggregation) leading to differences in soil C protection in soils with distinct disturbance histories. SOM pool sizes also differ among land uses (i.e., larger in reference watershed soils) (Keiser and others 2016), which may further contribute to SOM-related mechanisms that differ among historical land uses. However, SOM destabilization is thought to play a larger role when multiple repeated cycles of drought-rewetting take place (Miller and others 2005; Xiang and others 2008; Schimel 2018) and SOM destabilization is therefore a less likely source of C in our single drought-rewetting event.

Differences in resident microbial communities between historical land uses may also have contributed to the distinct respiration responses we observed; disturbed soils at Coweeta host higher relative abundance of r-selected bacterial taxa and higher microbial activity (i.e., higher substrate-induced respiration) (Osburn and others 2019), both of which may have contributed to the amplified respiration response. In addition, the apparently greater drought-tolerance of microbial biomass in disturbed soils (Fig. 6.3A) may have resulted in a larger active community in disturbed soils following drought, potentially contributing to the larger respiration responses we observed. The differences in drought-tolerance of microbial biomass between historical land uses may also be attributed to compositional differences in microbial communities. For example, reference soils from Coweeta have higher relative abundance of Acidobacteria (Osburn and others 2019), which have been previously shown to decline in abundance following drought (Barnard and others 2013), while disturbed soils host higher relative abundance of

Actinobacteria (Osburn and others 2019), which have been shown to respond positively to drought (Barnard and others 2013; Preece and others 2019). Regardless, the reductions in biomass suggest that labile C from lysed microbial cells is a likely source of C fueling the CO_2 pulse we observed after rewetting. Rapid mineralization of intracellular osmolytes as microorganisms adapted to changing water potentials also likely played a role (Fierer and Schimel 2003; Schimel 2018).

Our results also illustrate effects of drought on broad indicators of microbial community composition. For example, we observed increased microbial biomass C:N in response to drought (Fig. 6.3B), which has also been previously observed (Evans and Wallenstein 2012; Sun and others 2020b). This increased biomass C:N may be due in part to microbial physiological responses to drought. For example, fungal taxa accumulate polyol osmolytes (e.g., glycerol, mannitol) in response to water stress, which do not contain N and might increase overall biomass C:N (Schimel and others 2007). Another potential mechanism is greater dominance of fungi, which have higher biomass C:N than bacteria (Cleveland and Liptzin 2007). This is supported by fungal:bacterial ratios, which were higher in soils exposed to drought at the end of the drought period (Fig. 6.3C), a pattern that has also been observed in other studies (Evans and Wallenstein 2012; Preece and others 2019; Sun and others 2020a). Indeed, in general, fungi are thought to be better adapted to water stress than bacteria (Schimel and others 2007) and previous studies have shown fungal communities to be more drought-tolerant relative to bacterial communities (De Vries and others 2012, 2018; Barnard and others 2013; Preece and others 2019). Nevertheless, more sophisticated molecular techniques (e.g., amplicon

sequencing) should be used in future studies to assess influences of past land use on drought responses on soil microorganisms at the community scale.

Because our experiment did not involve C additions, the reductions in DOC we observed over the course of the experiment (Fig. 6.4A) were expected. C additions to mineral soil from O-horizon leachate and root exudates would likely influence drought responses, highlighting the need to perform additional studies under field conditions. The increases in NH_4^+ pools we observed following re-wetting (Fig. 6.4C) are a common result in drought-rewetting experiments, and are the product of a peak in N-mineralization rates after rewetting, i.e., the N-cycle manifestation of the Birch Effect (Birch 1958; Borken and Matzner 2009; Gao and others 2020). However, the larger N-mineralization responses of reference soils was surprising, given the greater N-mineralization potential we have previously observed in disturbed soils from Coweeta (Osburn and others, unpublished manuscript). We considered the possibility that higher nitrification rates in disturbed soils may be responsible for the smaller apparent responses of NH_4^+ pools. However, examining total DIN (i.e., $NH_4^+ + NO_3^-$) reveals that this is not the case – the DIN response of reference soils still appears larger (Fig. 6.S5). Instead, the larger NH_4^+ response of reference soils may be attributed to differences in microbial community structure – reference soils exhibit higher fungal:bacterial ratios (Fig. 6.3C), and because fungi have lower N demands than bacteria (Cleveland and Liptzin 2007), lower microbial N uptake in fungal-dominated reference soils may explain the larger net increase in NH_4^+. The large NH_4^+ response of reference soils is also likely attributed to the large flush of mineralizable organic N that occurred in these soils after drought (Fig. 6.4B, 6.S1) and NH_4^+ pools were indeed strongly correlated with DON availability (Fig.

6.S6). Approximately half of the ~50 µg N increase in DON that occurred in reference-drought soils can be accounted for by lysed microbial biomass N entering the DON pools (Fig. 6.S1, 6.S7). After accounting for low extraction efficiency of microbial biomass N using chloroform-based methods (~50%, Joergensen and Mueller 1996), it is likely that the majority of the DON increase can be explained by lysed biomass N. Though less likely in our single drought-rewetting event, it is also possible that N from destabilized SOM contributed to the DON increase.

Multiple previous studies have documented rapid increases in activity of nitrifying taxa and increases in soil NO_3^- pools immediately after drought-rewetting (Fierer and Schimel 2002; Placella and Firestone 2013; Gao and others 2020). However, our experiment yielded different results – we observed reduced abundance of AOA and CAOB up to six weeks following re-wetting (Fig. 6.5B, 6.S3) and smaller NO_3^- pools in drought-rewet soils compared to control soils at most time points (Fig. 6.5A). This result may reflect small resident populations of nitrifiers or poor drought-tolerance of nitrifying taxa in soils from this normally high-rainfall ecosystem. Indeed, a previous study from high-rainfall ecosystems also reported reduced nitrifer abundance after repeated drought and rewetting (Zhou and others 2016). Regardless, the inhibiting effects of drought-rewetting on nitrifying taxa may be short lived – AOB appeared to be growing in disturbed-drought soils by days 56 and 84 of the experiment (Fig. 6.5C), and NO_3^- pools had peaked in those soils by day 84 (Fig. 6.5A). Further, long-term effects of drought-rewetting on nitrifiers and NO_3^- pools will likely be mediated by effects of drought on soil C:N, which will alter competitive dynamics for NH_4^+ between heterotrophic microorganisms and autotrophic nitrifiers (Verhagen and others 1992; Booth and others

2005). Indeed, our results show that large soil NO_3^- pools are associated with the co-occurrence of low soil C:N and high nitrifier abundance (Fig. 6.6), likely because C-limiting conditions promote increased nitrifier activity as a result of reduced heterotrophic N-demand (Booth and others 2005; Keiser and others 2016). This C:N – NO_3^- relationship is similar to previous reports (Taylor and Townsend 2010) and has implications for the long-term N-balance of these ecosystems, as NO_3^- is the dominant form of N loss from watersheds in the region (Webster and others 2016).

In addition to documenting influences of historical land use on effects of drought-rewetting, our study is somewhat unique in that the Coweeta basin is historically among the wettest locations in the eastern US (Laseter and others 2012). While many previous drought-rewetting studies have taken place in semi-arid environments with soils presumably pre-adapted to water stress (e.g., Fierer and Schimel 2002; Placella and others 2012; Barnard and others 2013; Bastida and others 2017; Guillot and others 2019; Moreno and others 2019), our results show that drought responses may be different in humid, historically high rainfall ecosystems. For example, though previous work has suggested that the Birch Effect generally does not make up for reduced respiration during dry periods (Borken and Matzner 2009), we documented larger respiratory C loss in drought-rewetting soils compared with control soils (Fig. 6.2B). This is potentially due to the C-rich nature of our soils (Canarini and others 2017) or to resident microbial communities poorly adapted to stress associated with drought-rewetting cycles. Similarly, we observed N-cycle responses different from those reported from semi-arid environments (i.e., reduced nitrification, Fig. 6.5A) (Fierer and Schimel 2002; Placella and Firestone 2013). Our study also highlights opportunities for future work –for

example, future studies should incorporate different drought durations, as different C and N dynamics may be observed under more moderate drought conditions that induce less extreme microbial water stress. Future investigations should also focus on identifying causal links among soil properties, microbial communities, and biogeochemical process rates in the context of drought and rewetting. Though our results show many strong correlations between variables (Fig. 6.S6) and suggest clear mechanistic links between soil C:N, nitrifier abundance, and soil NO_3^- pools (Fig. 6.6, 6.S4), our experiment does not directly assess causal mechanisms. Future studies should attempt to elucidate these mechanisms, potentially by employing ^{15}N and ^{13}C isotopes to track movement of C and N between various soil pools throughout the drought-rewetting process.

Finally, it should be noted that our study only explicitly addresses the influence of one type of historical land use, i.e., forest conversion to agriculture, on drought responses of forest soils. However, the differences in soil properties we observed between land uses (Table 6.1) are similar to those reported from nearby sites across multiple different types of historical disturbance, including clear-cutting, cable logging, and conversion to pine monoculture (Keiser and others 2016; Osburn and others 2019). Further, microbial communities and biogeochemical cycles respond similarly to multiple different historical disturbance types in the region (Swank and Vose 1997; Keiser and others 2016; Osburn and others 2019). Therefore, not only do reference and disturbed soils exhibit distinct drought responses, but we also expect soils across multiple disturbance types to exhibit similar disturbance x drought interactions to those described here, at least within the context of forested ecosystems of the southern Appalachian region.

Conclusions

Responses of terrestrial ecosystems to drought will depend on the drought-tolerance of microbial communities, which are the proximate drivers of all soil biogeochemical processes. We observed greater drought-tolerance of microbial biomass in soils from historically disturbed forests, likely due to existing compositional differences in the communities as a result of past land use activities. This drought-tolerant microbial biomass contributed to an amplified Birch Effect and higher cumulative respiratory C loss following rewetting in disturbed soils. However, greater drought-tolerance of microbial biomass also appears to have resulted in less responsive soil N pools in disturbed soils relative to soils from reference forests following drought-rewetting. The complexity of these responses illustrates the possibility of alternative trajectories of different soil pools and processes, even when these parameters have common microbial drivers. Regardless, our results show that intensifying drought-rewetting cycles are likely to alter the C and N balance of temperate forest ecosystems. Additionally, our results illustrate that drought responses will likely vary among terrestrial environments with different historical land uses, which will be a critical consideration when assessing potential threats to ecosystem services due to climate change in ecosystems of the eastern US.

Acknowledgements

This work was funded by the Coweeta LTER, funded by National Science Foundation grant DEB-1637522 and by a Graduate Research Development Program (GRDP) awarded to EDO by the Virginia Tech Graduate Student Assembly. We thank the Coweeta Hydrologic Laboratory, Southern Research Station, USDA Forest Service for

support and Bobbie Niederlehner for help with analytical chemistry. Finally, we thank two anonymous reviewers, whose helpful comments greatly improved this manuscript.

References

Allen SE, Grimshaw HM, Parkinson JA, Quarmby C. 1974. Chemical analysis of ecological materials. Chemical analysis of ecological materials. https://www.cabdirect.org/cabdirect/abstract/19751431633. Last accessed 20/10/2020

Barnard RL, Osborne CA, Firestone MK. 2013. Responses of soil bacterial and fungal communities to extreme desiccation and rewetting. ISME J 7:2229–41.

Bastida F, López-Mondéjar R, Baldrian P, Andrés-Abellán M, Jehmlich N, Torres IF, García C, López-Serrano FR. 2019. When drought meets forest management: Effects on the soil microbial community of a Holm oak forest ecosystem. Science of The Total Environment 662:276–86.

Bastida F, Torres IF, Andrés-Abellán M, Baldrian P, López-Mondéjar R, Větrovský T, Richnow HH, Starke R, Ondoño S, García C, López-Serrano FR, Jehmlich N. 2017. Differential sensitivity of total and active soil microbial communities to drought and forest management. Glob Change Biol:1–19.

Bates D, Maechler M, Bolker [aut B, cre, Walker S, Christensen RHB, Singmann H, Dai B, Scheipl F, Grothendieck G, Green P, Fox J. 2019. lme4: Linear Mixed-Effects Models using 'Eigen' and S4. https://CRAN.R-project.org/package=lme4. Last accessed 08/11/2019

Birch HF. 1958. The effect of soil drying on humus decomposition and nitrogen availability. Plant Soil 10:9–31.

Booth MS, Stark JM, Rastetter E. 2005. Controls on Nitrogen Cycling in Terrestrial Ecosystems: A Synthetic Analysis of Literature Data. Ecological Monographs 75:139–57.

Borken W, Matzner E. 2009. Reappraisal of drying and wetting effects on C and N mineralization and fluxes in soils. Glob Change Biol 15:808–24.

Bradford MA, Fierer N, Reynolds JF. 2008. Soil carbon stocks in experimental mesocosms are dependent on the rate of labile carbon, nitrogen and phosphorus inputs to soils. Funct Ecol 22:964–74.

Burt TP, Ford Miniat C, Laseter SH, Swank WT. 2018. Changing patterns of daily precipitation totals at the Coweeta Hydrologic Laboratory, North Carolina, USA. Int J Climatol 38:94–104.

Canarini A, Kiær LP, Dijkstra FA. 2017. Soil carbon loss regulated by drought intensity and available substrate: A meta-analysis. Soil Biol Biochem 112:90–9.

Cleveland CC, Liptzin D. 2007. C:N:P stoichiometry in soil: is there a "Redfield ratio" for the microbial biomass? Biogeochemistry 85:235–52.

De Vries FT, Griffiths RI, Bailey M, Craig H, Girlanda M, Gweon HS, Hallin S, Kaisermann A, Keith AM, Kretzschmar M, Lemanceau P, Lumini E, Mason KE, Oliver A, Ostle N, Prosser JI, Thion C, Thomson B, Bardgett RD. 2018. Soil bacterial networks are less stable under drought than fungal networks. Nat Commun 9:3033.

De Vries FT, Liiri ME, Bjørnlund L, Bowker MA, Christensen S, Setälä HM, Bardgett RD. 2012. Land use alters the resistance and resilience of soil food webs to drought. Nature Climate Change; London 2:276–80.
Elliott KJ, Vose JM. 2011. The contribution of the Coweeta Hydrologic Laboratory to developing an understanding of long-term (1934-2008) changes in managed and unmanaged forests. For Ecol Manag 261:900–10.
Ellis EC. 2011. Anthropogenic transformation of the terrestrial biosphere. Philos Trans R Soc A-Math Phys Eng Sci 369:1010–35.
Evans SE, Wallenstein MD. 2012. Soil microbial community response to drying and rewetting stress: does historical precipitation regime matter? Biogeochemistry 109:101–16.
Evans SE, Wallenstein MD. 2014. Climate change alters ecological strategies of soil bacteria. Ecol Lett 17:155–64.
Falkowski PG, Fenchel T, Delong EF. 2008. The Microbial Engines That Drive Earth's Biogeochemical Cycles. Science 320:1034–9.
Fierer N. 2017. Embracing the unknown: disentangling the complexities of the soil microbiome. Nat Rev Microbiol 15:579–90.
Fierer N, Jackson JA, Vilgalys R, Jackson RB. 2005. Assessment of Soil Microbial Community Structure by Use of Taxon-Specific Quantitative PCR Assays. Appl Environ Microbiol 71:4117–20.
Fierer N, Schimel JP. 2002. Effects of drying–rewetting frequency on soil carbon and nitrogen transformations. Soil Biol Biochem 34:777–87.
Fierer N, Schimel JP. 2003. A Proposed Mechanism for the Pulse in Carbon Dioxide Production Commonly Observed Following the Rapid Rewetting of a Dry Soil. Soil Sci Soc Am J 67:798.
Francis CA, Roberts KJ, Beman JM, Santoro AE, Oakley BB. 2005. Ubiquity and diversity of ammonia-oxidizing archaea in water columns and sediments of the ocean. Proc Natl Acad Sci USA 102:14683–8.
Fuchslueger L, Wild B, Mooshammer M, Takriti M, Kienzl S, Knoltsch A, Hofhansl F, Bahn M, Richter A. 2019. Microbial carbon and nitrogen cycling responses to drought and temperature in differently managed mountain grasslands. Soil Biology and Biochemistry 135:144–53.
Gao D, Bai E, Li M, Zhao C, Yu K, Hagedorn F. 2020. Responses of soil nitrogen and phosphorus cycling to drying and rewetting cycles: A meta-analysis. Soil Biology and Biochemistry 148:107896.
Gragson TL, Bolstad PV. 2006. Land Use Legacies and the Future of Southern Appalachia. Soc Nat Resour 19:175–90.
Guillot E, Hinsinger P, Dufour L, Roy J, Bertrand I. 2019. With or without trees: Resistance and resilience of soil microbial communities to drought and heat stress in a Mediterranean agroforestry system. Soil Biology and Biochemistry 129:122–35.
Hawthorne S, Miniat CF. 2018. Topography may mitigate drought effects on vegetation along a hillslope gradient. Ecohydrology 11:e1825.
Helvey J, Hewlett JD. 1962. The annual range of soil moisture under high rainfall in the southern Appalachians. Journal of Forestry 60:485–6.

Hemingway JD, Rothman DH, Grant KE, Rosengard SZ, Eglinton TI, Derry LA, Galy VV. 2019. Mineral protection regulates long-term global preservation of natural organic carbon. Nature 570:228–31.

IPCC. 2013. Climate Change 2013: The Physical Science Basis. Contribution of Working Group I to the Fifth Assessment Report of the Intergovernmental Panel on Climate Change [Stocker, T.F., D. Qin, G.-K. Plattner, M. Tignor, S.K. Allen, J. Boschung, A. Nauels, Y. Xia, V. Bex and P.M. Midgley (eds.)]. Cambridge University Press, Cambridge, United Kingdom and New York, NY, USA

Joergensen RG, Mueller T. 1996. The fumigation-extraction method to estimate soil microbial biomass: Calibration of the kEN value. Soil Biology and Biochemistry 28:33–7.

Keiser AD, Knoepp JD, Bradford MA. 2016. Disturbance Decouples Biogeochemical Cycles Across Forests of the Southeastern US. Ecosystems 19:50–61.

Knoepp JD, See CR, Vose JM, Miniat CF, Clark JS. 2018. Total C and N Pools and Fluxes Vary with Time, Soil Temperature, and Moisture Along an Elevation, Precipitation, and Vegetation Gradient in Southern Appalachian Forests. Ecosystems 21:1623–38.

Knoepp JD, Swank WT. 1994. Long-Term Soil Chemistry Changes in Aggrading Forest Ecosystems. Soil Sci Soc Am J 58:325.

Knoepp JD, Swank WT. 2002. Using soil temperature and moisture to predict forest soil nitrogen mineralization. Biol Fertil Soils 36:177–82.

Laseter SH, Ford CR, Vose JM, Swift LW. 2012. Long-term temperature and precipitation trends at the Coweeta Hydrologic Laboratory, Otto, North Carolina, USA. Hydrol Res 43:890–901.

Lenth R, Singmann H, Love J, Buerkner P, Herve M. 2019. emmeans: Estimated Marginal Means, aka Least-Squares Means. https://CRAN.R-project.org/package=emmeans. Last accessed 03/05/2019

Manzoni S, Schimel JP, Porporato A. 2012. Responses of soil microbial communities to water stress: results from a meta-analysis. Ecology 93:930–8.

Millenium Ecosystem Assessment. 2005. Ecosystems and Human Well Being: Synthesis. Washington, DC: Island Press

Miller AE, Schimel JP, Meixner T, Sickman JO, Melack JM. 2005. Episodic rewetting enhances carbon and nitrogen release from chaparral soils. Soil Biology and Biochemistry 37:2195–204.

Miniat CF, Laseter SH, Swank WT, Swift LWJr. 2017. Daily precipitation data from recording rain gages (RRG) at Coweeta Hydrologic Lab, North Carolina. https://www.fs.usda.gov/rds/archive/Catalog/RDS-2017-0031. Last accessed 09/02/2021

Moreno JL, Torres IF, García C, López-Mondéjar R, Bastida F. 2019. Land use shapes the resistance of the soil microbial community and the C cycling response to drought in a semi-arid area. Science of The Total Environment 648:1018–30.

Osburn ED, Barrett JE. 2020. Abundance and functional importance of complete ammonia-oxidizing bacteria (comammox) versus canonical nitrifiers in temperate forest soils. Soil Biol Biochem 145:107801.

Osburn ED, McBride SG, Aylward FO, Badgley BD, Strahm BD, Knoepp JD, Barrett JE. 2019. Soil Bacterial and Fungal Communities Exhibit Distinct Long-Term Responses to Disturbance in Temperate Forests. Front Microbiol 10.
Placella SA, Brodie EL, Firestone MK. 2012. Rainfall-induced carbon dioxide pulses result from sequential resuscitation of phylogenetically clustered microbial groups. Proc Natl Acad Sci USA 109:10931–6.
Placella SA, Firestone MK. 2013. Transcriptional Response of Nitrifying Communities to Wetting of Dry Soil. Appl Environ Microbiol 79:3294–302.
Preece C, Verbruggen E, Liu L, Weedon JT, Peñuelas J. 2019. Effects of past and current drought on the composition and diversity of soil microbial communities. Soil Biology and Biochemistry 131:28–39.
R Core Development Team. 2019. R: A Language and Environment for Statistical Computing. Vienna, Austria: R Foundation for Statistical Computing http://www.R-project.org
Robertson GP, Robertson P of C and SSGP, Coleman DC, Sollins P, Bledsoe CS, Bledsoe P of SE in the D of LA and WRCS, Sollins P of FE and S in the FSDP. 1999. Standard Soil Methods for Long-term Ecological Research. Oxford University Press
Rotthauwe JH, Witzel KP, Liesack W. 1997. The ammonia monooxygenase structural gene amoA as a functional marker: molecular fine-scale analysis of natural ammonia-oxidizing populations. Appl Environ Microbiol 63:4704–12.
Saxton KE, Rawls WJ, Romberger JS, Papendick RI. 1986. Estimating Generalized Soil-water Characteristics from Texture 1. Soil Sci Soc Am J 50:1031–6.
Schimel J, Balser TC, Wallenstein M. 2007. Microbial stress-response physiology and its implications for ecosystem function. Ecology 88:1386–94.
Schimel JP. 2018. Life in Dry Soils: Effects of Drought on Soil Microbial Communities and Processes. Annu Rev Ecol Evol Syst 49:409–32.
Sun Y, Chen HYH, Jin L, Wang C, Zhang R, Ruan H, Yang J. 2020a. Drought stress induced increase of fungi:bacteria ratio in a poplar plantation. CATENA 193:104607.
Sun Y, Liao J, Zou X, Xu X, Yang J, Chen HYH, Ruan H. 2020b. Coherent responses of terrestrial C:N stoichiometry to drought across plants, soil, and microorganisms in forests and grasslands. Agricultural and Forest Meteorology 292–293:108104.
Swank WT, Vose JM. 1997. Long-term nitrogen dynamics of Coweeta forested watersheds in the southeastern United States of America. Glob Biogeochem Cycle 11:657–71.
Taylor PG, Townsend AR. 2010. Stoichiometric control of organic carbon–nitrate relationships from soils to the sea. Nature 464:1178–81.
Verhagen FJM, Duyts H, Laanbroek HJ. 1992. Competition for Ammonium between Nitrifying and Heterotrophic Bacteria in Continuously Percolated Soil Columns. Appl Environ Microbiol 58:3303–11.
Webster JR, Knoepp JD, Swank WT, Miniat CF. 2016. Evidence for a Regime Shift in Nitrogen Export from a Forested Watershed. Ecosystems 19:881–95.
Williams AP, Cook BI, Smerdon JE, Bishop DA, Seager R, Mankin JS. 2017. The 2016 Southeastern U.S. Drought: An Extreme Departure From Centennial Wetting and Cooling. Journal of Geophysical Research: Atmospheres 122:10,888-10,905.

Xiang S-R, Doyle A, Holden PA, Schimel JP. 2008. Drying and rewetting effects on C and N mineralization and microbial activity in surface and subsurface California grassland soils. Soil Biology and Biochemistry 40:2281–9.
Zhang S, Yu Z, Lin J, Zhu B. 2020. Responses of soil carbon decomposition to drying-rewetting cycles: A meta-analysis. Geoderma 361:114069.
Zhao Z, Huang G, He S, Zhou N, Wang M, Dang C, Wang J, Zheng M. 2019. Abundance and community composition of comammox bacteria in different ecosystems by a universal primer set. Sci Total Environ 691:146–55.
Zhou X, Fornara D, Ikenaga M, Akagi I, Zhang R, Jia Z. 2016. The Resilience of Microbial Community under Drying and Rewetting Cycles of Three Forest Soils. Front Microbiol 7.
Zhou Z, Wang C, Luo Y. 2018. Response of soil microbial communities to altered precipitation: A global synthesis. Global Ecology and Biogeography 27:1121–36.

Figures

Figure 6.1

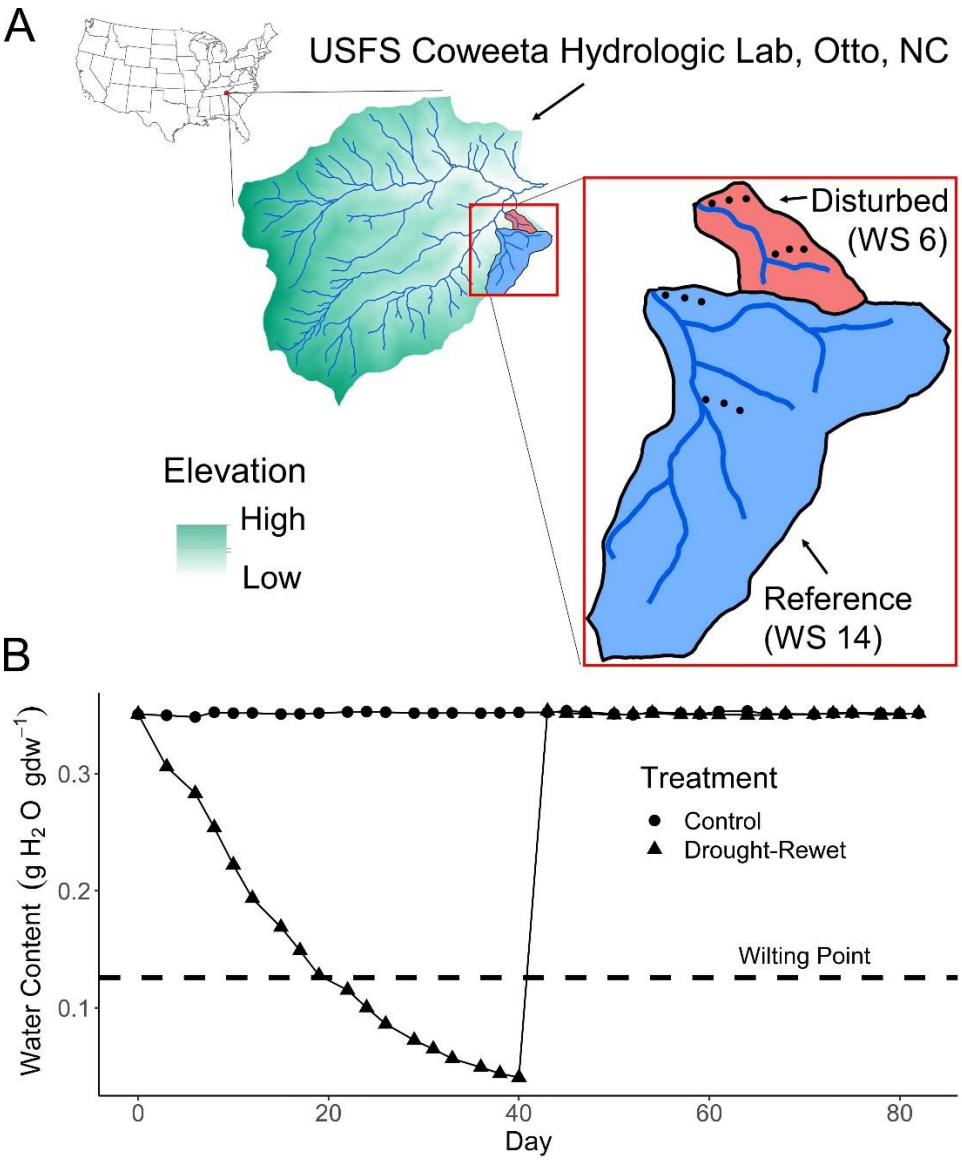

Figure 6.1: Map of reference and disturbed watersheds sampled for this study (A). Black dots represent locations of the 6 plots within each watershed. (B) Illustrates moisture treatments applied to intact soil cores sampled from the field plots. Water content at wilting point (-1500 kPa) was estimated using a pedotransfer function based on soil texture measurements averaged across all pre-treatment soils.

Figure 6.2

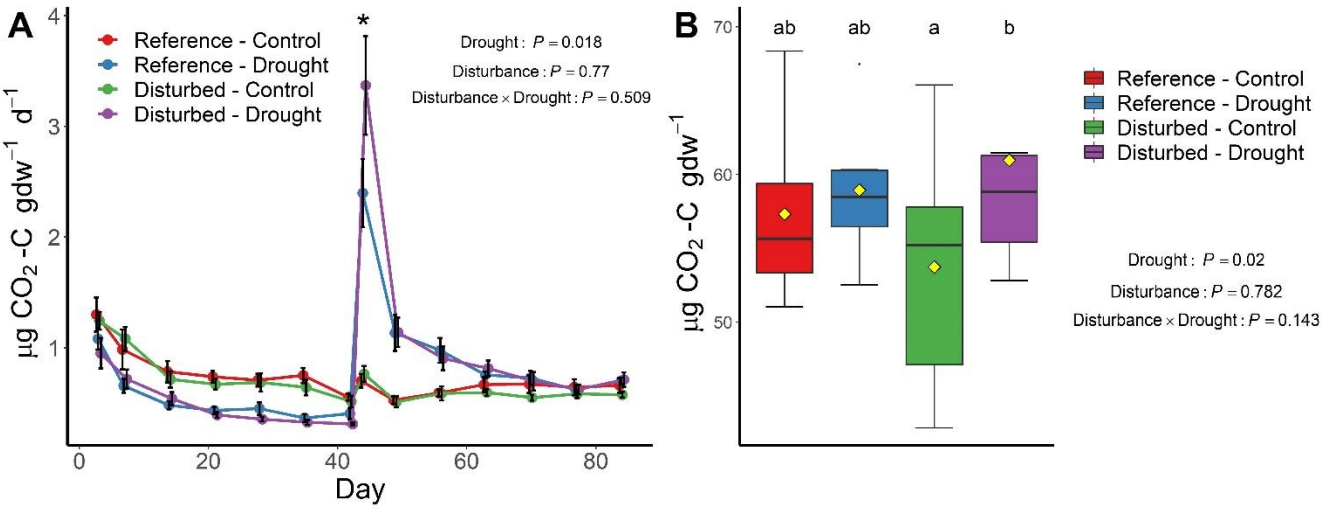

Figure 6.2: Respiration dynamics during the drought-rewetting experiment (A) and cumulative respiration integrated over the entire 84-day experiment (B). *P* values are from mixed effects models. The asterisk in (A) indicates significantly higher respiration in the Disturbed-Drought soil cores relative to the Reference-Drought soil cores immediately after the re-wet occurred. Yellow diamonds in (B) represent mean cumulative respiration for each treatment. Different letters in (B) represent significant pairwise differences between treatments (Tukey's HSD $P < 0.05$). Full statistical tables for mixed effects models and post-hoc tests are shown for respiration dynamics and cumulative respiration in Tables 6.S3 and 6.S4, respectively.

Figure 6.3

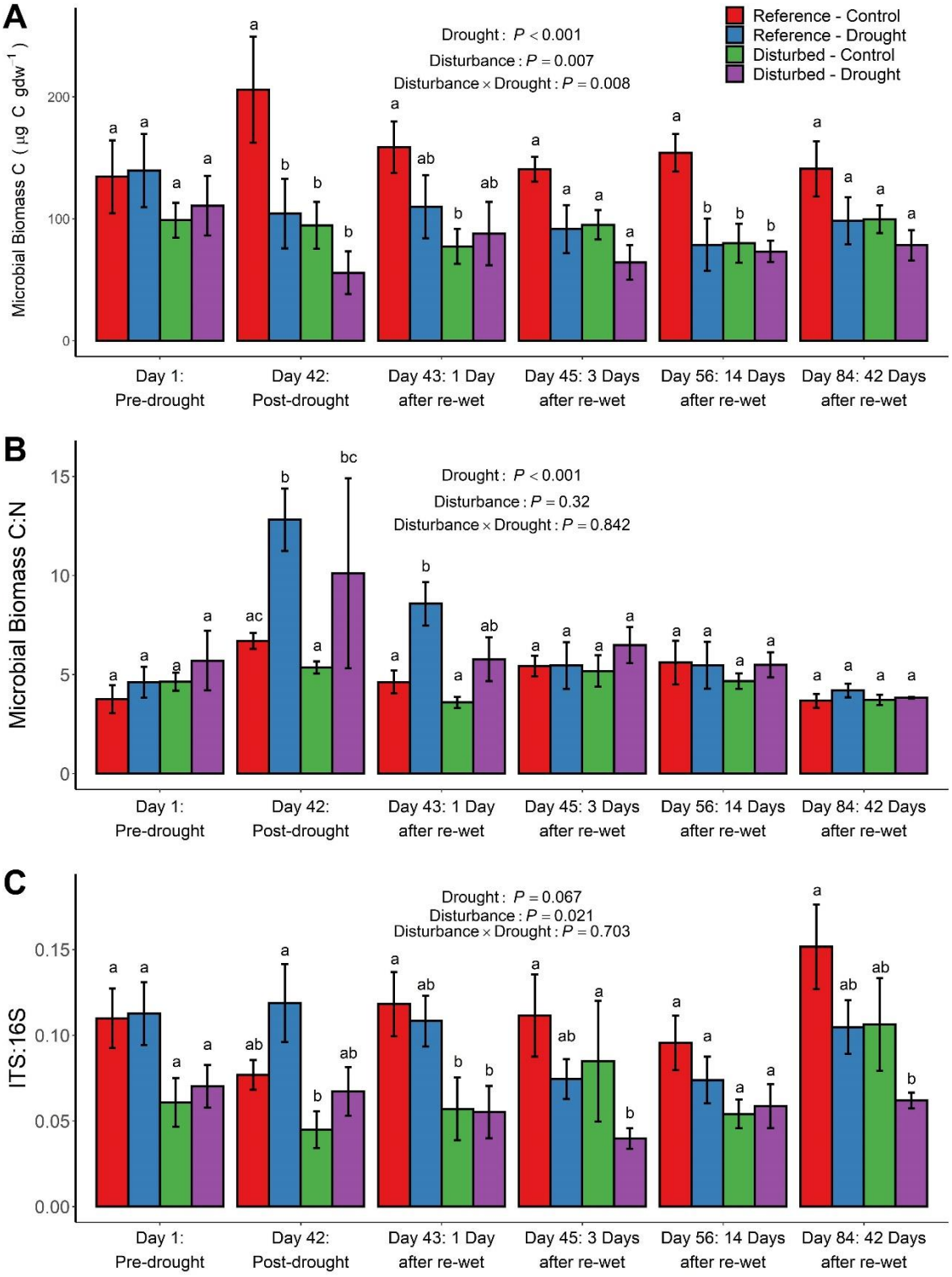
A
Microbial Biomass C (μg C gdw⁻¹)
Drought : P < 0.001
Disturbance : P = 0.007
Disturbance × Drought : P = 0.008
Reference - Control
Reference - Drought
Disturbed - Control
Disturbed - Drought
B
Microbial Biomass C:N
Drought : P < 0.001
Disturbance : P = 0.32
Disturbance × Drought : P = 0.842
C
ITS:16S
Drought : P = 0.067
Disturbance : P = 0.021
Disturbance × Drought : P = 0.703
Day 1: Pre-drought
Day 42: Post-drought
Day 43: 1 Day after re-wet
Day 45: 3 Days after re-wet
Day 56: 14 Days after re-wet
Day 84: 42 Days after re-wet

Figure 6.3: Microbial biomass C (A), Microbial Biomass C:N (B), and fungal:bacterial (ITS:16S) ratios (C) at key time points in the drought-rewetting experiment. *P* values are from mixed effects models while different letters represent significant pairwise differences between treatments within each day (Tukey's HSD $P < 0.05$). Error bars represent ± one SE. Complete statistical tables for mixed effects models and post-hoc tests are shown for Microbial biomass C, biomass C:N, and ITS:16S in Tables 6.S5, and 6.S6, and 6.S7, respectively.

Figure 6.4

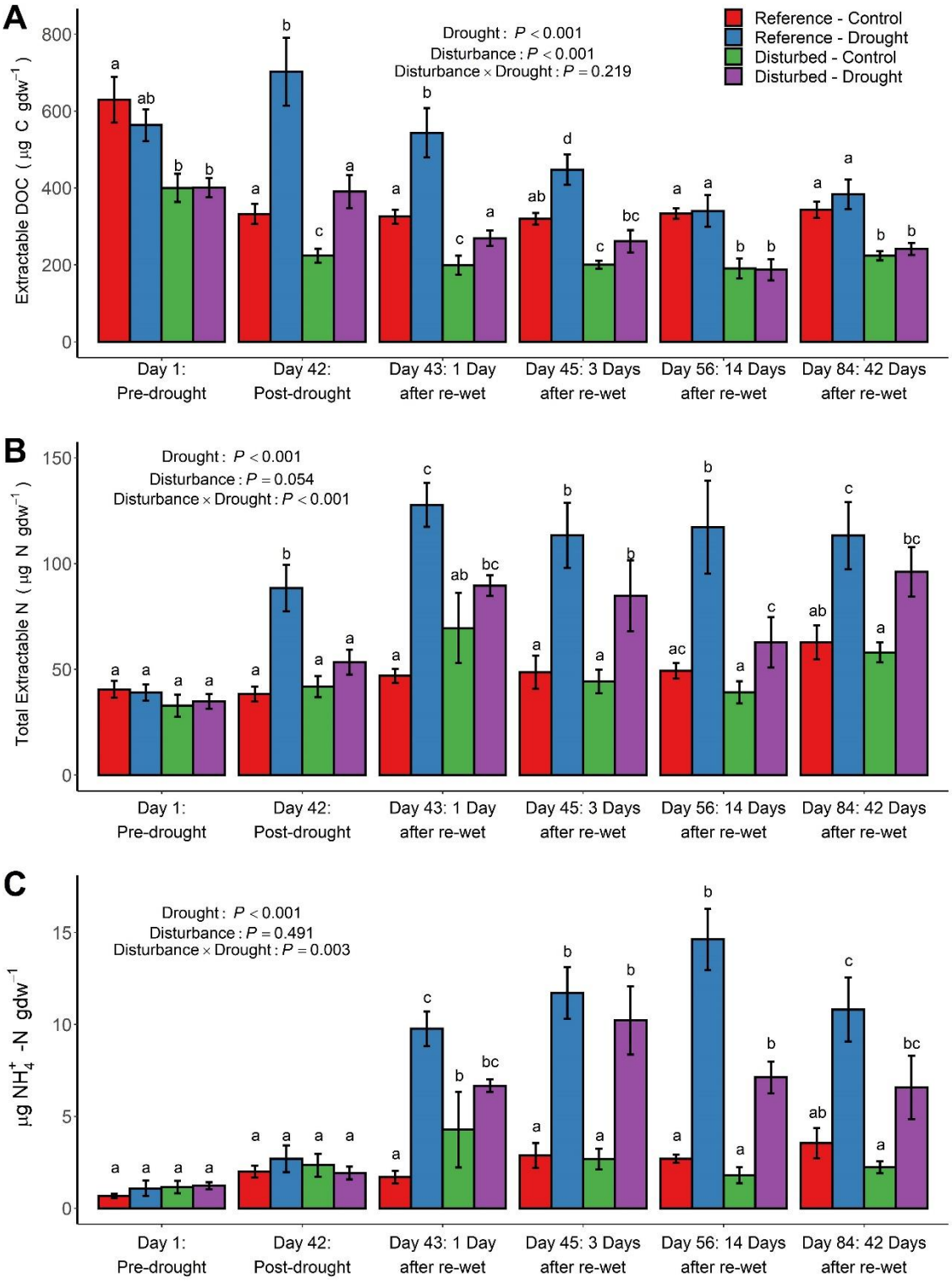
A
Extractable DOC (µg C gdw^{-1})
Drought : $P < 0.001$
Disturbance : $P < 0.001$
Disturbance × Drought : $P = 0.219$
Reference - Control
Reference - Drought
Disturbed - Control
Disturbed - Drought
B
Total Extractable N (µg N gdw^{-1})
Drought : $P < 0.001$
Disturbance : $P = 0.054$
Disturbance × Drought : $P < 0.001$
C
µg NH_4^+ -N gdw^{-1}
Drought : $P < 0.001$
Disturbance : $P = 0.491$
Disturbance × Drought : $P = 0.003$
Day 1: Pre-drought
Day 42: Post-drought
Day 43: 1 Day after re-wet
Day 45: 3 Days after re-wet
Day 56: 14 Days after re-wet
Day 84: 42 Days after re-wet

Figure 6.S4: Soil extractable DOC (A) total extractable N (B) and NH_4^+-N (C) pools at key time points in the drought-rewetting experiment. *P* values are from mixed effects models while different letters represent significant pairwise differences between treatments within each day (Tukey's HSD $P < 0.05$). Error bars represent ± one SE. Complete statistical tables for mixed effects models and post-hoc tests are shown for DOC, total extractable N, and NH_4^+ in Tables 6.S8, 6.S9, and 6.S10, respectively.

Figure 6.5

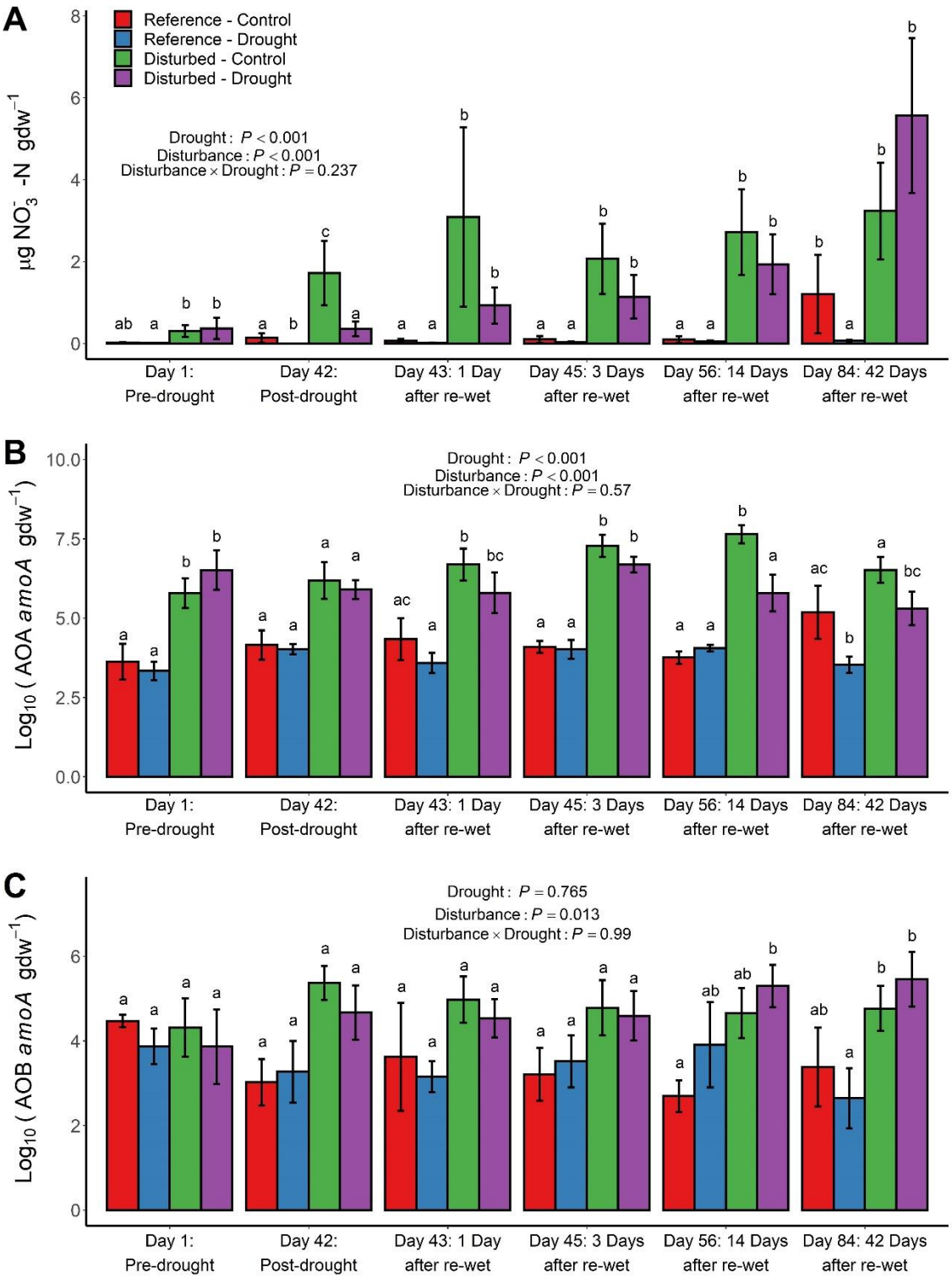
A
Reference - Control
Reference - Drought
Disturbed - Control
Disturbed - Drought
Drought : P < 0.001
Disturbance : P < 0.001
Disturbance × Drought : P = 0.237
μg NO3- -N gdw-1
B
Drought : P < 0.001
Disturbance : P < 0.001
Disturbance × Drought : P = 0.57
Log10 (AOA amoA gdw-1)
C
Drought : P = 0.765
Disturbance : P = 0.013
Disturbance × Drought : P = 0.99
Log10 (AOB amoA gdw-1)
Day 1: Pre-drought
Day 42: Post-drought
Day 43: 1 Day after re-wet
Day 45: 3 Days after re-wet
Day 56: 14 Days after re-wet
Day 84: 42 Days after re-wet

Figure 6.S5: Soil NO_3^- (A), AOA *amoA* (B), and AOB *amoA* (C) at key time points in the drought-rewetting experiment. *P* values are from mixed effects models while different letters represent significant pairwise differences between treatments within each day (Tukey's HSD $P < 0.05$). Error bars represent ± one SE. Complete statistical tables for mixed effects model and post-hoc tests are shown for NO_3^-, AOA *amoA*, and AOB *amoA* in Tables 6.S11, 6.S12, and 6.S13, respectively.

Figure 6.6

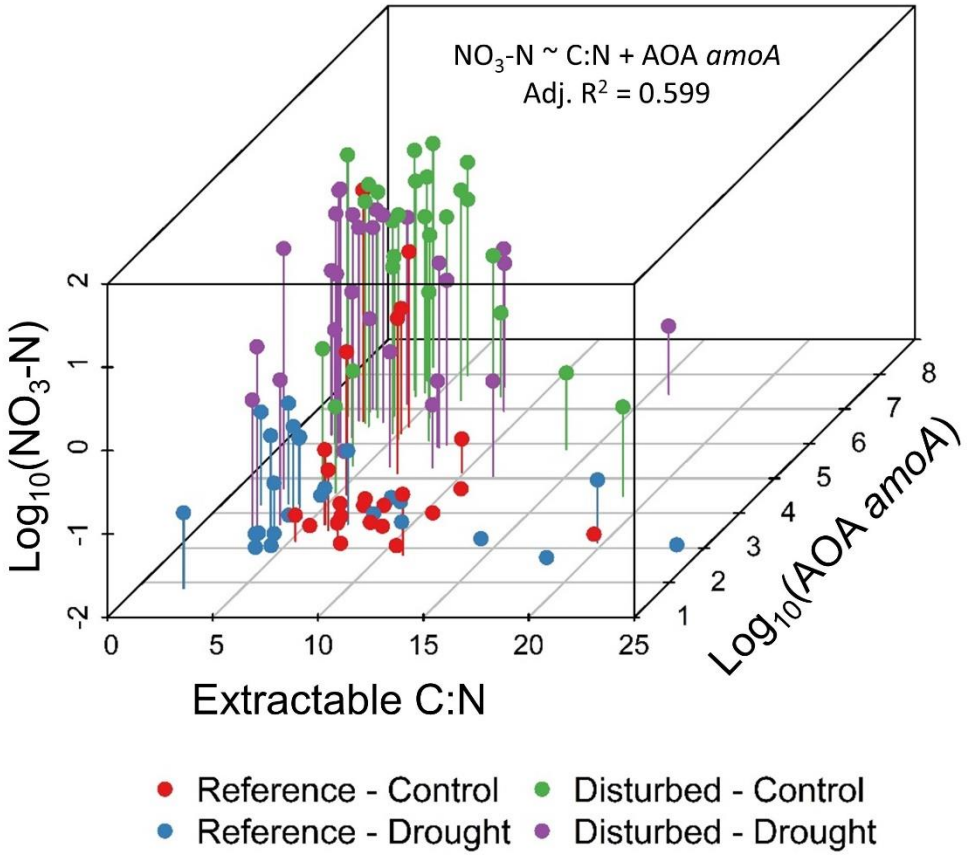

Figure 6.6: Relationships among soil extractable C:N, AOA *amoA* gene abundances, and soil NO_3-N concentrations. NO_3^- is in units of µg N and both NO_3-N and AOA *amoA* are expressed per gram of dry soil. The adjusted R^2 listed is for the multiple regression shown, predicting NO_3-N from extractable C:N and AOA *amoA* abundance. Table 6.S14 shows complete statistical results for the multiple regression model shown.

Tables

Table 6.1

Variable	Reference	Disturbed
pH	5.14 (0.20)	5.77 (0.06)*
NO_3^- (µg N gdw^{-1})	0.035 (0.015)	0.185 (0.080)†
NH_4^+ (µg N gdw^{-1})	0.762 (0.163)	0.923 (0.152)
Total Extractable N (µg N gdw^{-1})	40.1 (1.89)*	32.8 (1.47)
DON (µg N gdw^{-1})	39.3 (1.55)**	31.7 (1.77)
Extractable DOC (µg C gdw^{-1})	553 (36.6)***	363 (18.2)
Extractable C:N	13.8 (0.59)**	11.1 (0.44)
Microbial Biomass C (µg C gdw^{-1})	164 (24.5)*	75.9 (17.7)
Total C (mg C gdw^{-1})	44.3 (2.02)	37.1 (5.06)
Total N (mg N gdw^{-1})	2.27 (0.271)	2.31 (0.141)
Total C:N	19.9 (1.37)*	15.9 (0.41)

Table 6.1: Pre-treatment soil variables from Watershed 14 (Reference) and Watershed 6 (Disturbed). Values are means with one SE shown in parentheses. Symbols indicate significantly higher values (ANOVA) at the following significance levels: † $P < 0.1$, * $P < 0.05$, ** $P < 0.01$, *** $P < 0.001$.

Supplementary Figures

Figure 6.S1

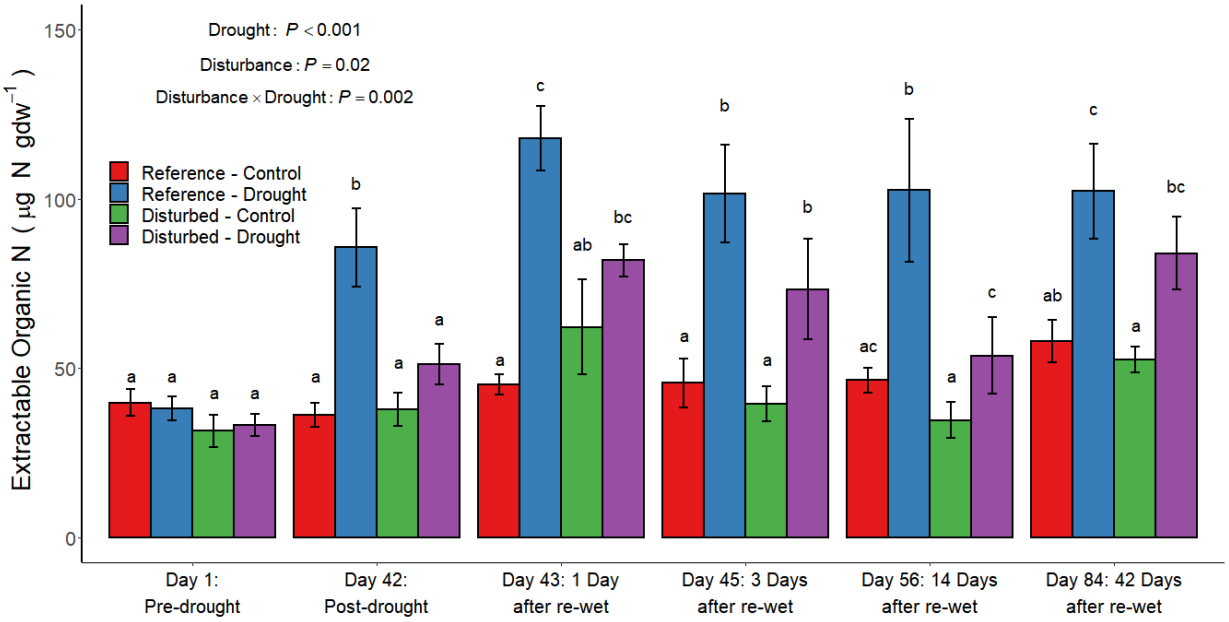

Figure 6.S1: Soil extractable organic N at key time points in the drought-rewetting experiment. Error bars represent ± one SE. *P* values are from mixed effects models while different letters represent significant pairwise differences between treatments within time points ($P < 0.05$).

Figure 6.S2

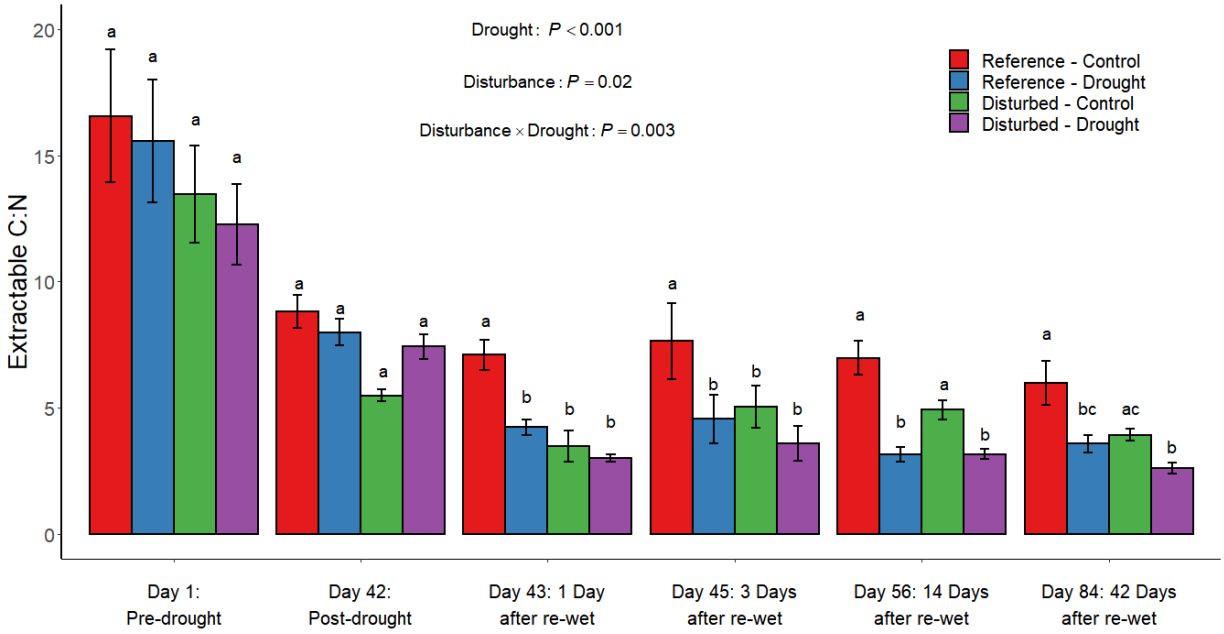

Figure 6.S2: Soil extractable C:N at key time points in the drought-rewetting experiment. Error bars represent ± one SE. *P* values are from mixed effects models while different letters represent significant pairwise differences between treatments within time points ($P < 0.05$).

Figure 6.S3

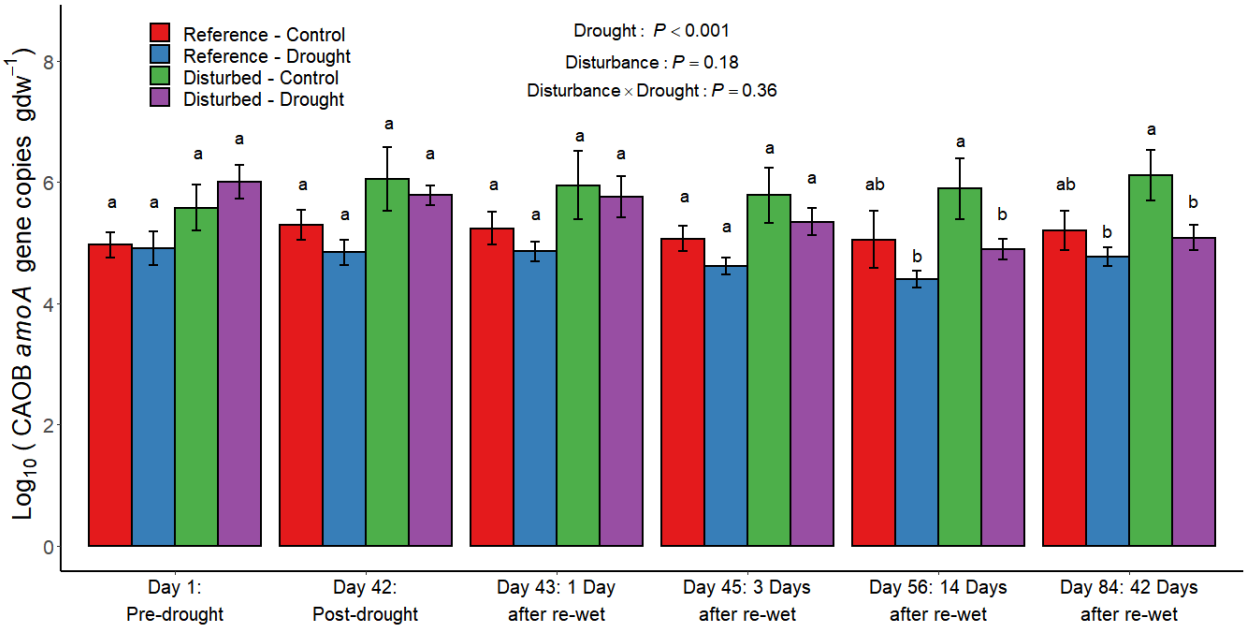

Figure 6.S3: CAOB *amoA* at key time points in the drought-rewetting experiment. Error bars represent ± one SE. *P* values are from mixed effects models while different letters represent significant pairwise differences between treatments within time points ($P < 0.05$).

Figure 6.S4

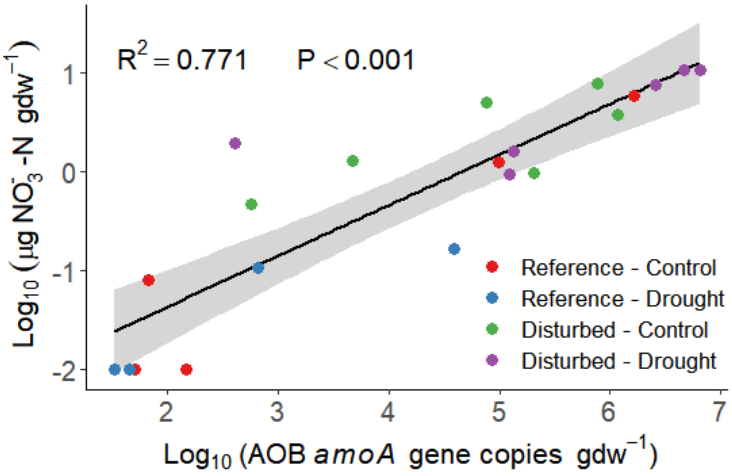

Figure 6.S4: Regression of soil NO_3-N as a function of AOB *amoA* abundance on day 84 of the experiment.

Figure 6.S5

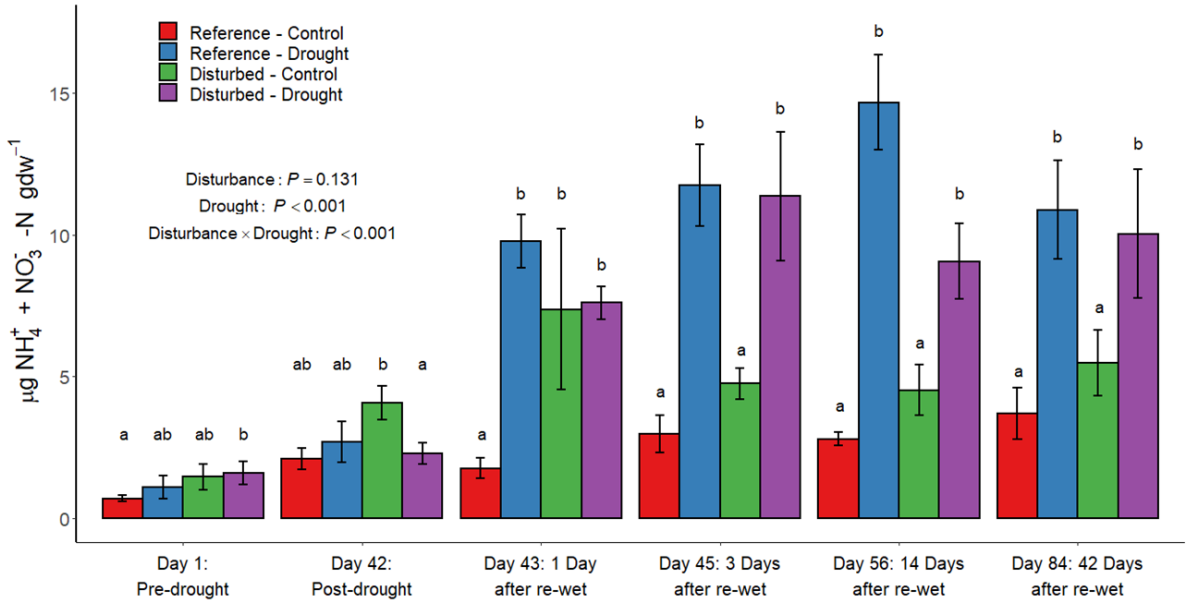

Figure 6.S5: DIN (NH_4^+-N + NO_3-N) at key time points in the drought-rewetting experiment. Error bars represent ± one SE. *P* values are from mixed effects models while different letters represent significant pairwise differences between treatments within time points ($P < 0.05$).

Figure 6.S6

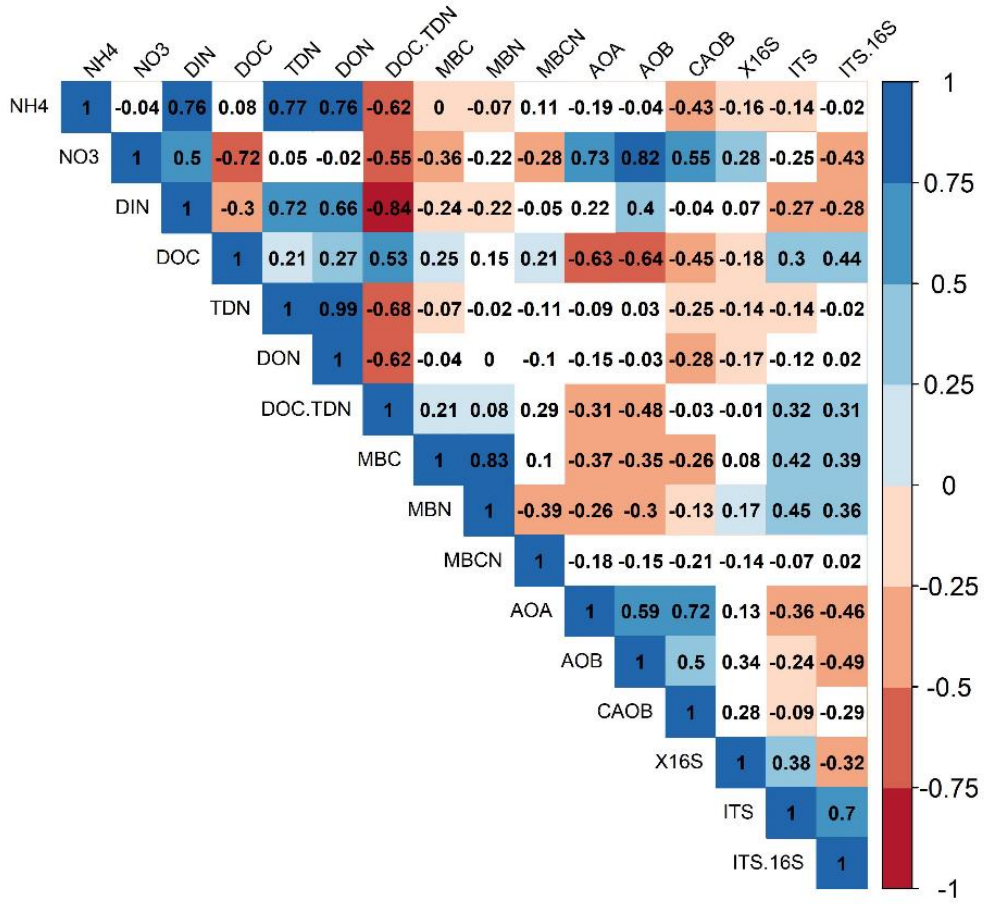

Figure 6.S6: Spearman rank correlations among all soil variables. Numbers represent correlation coefficients. Only significant correlations are colored in ($P < 0.05$).

Figure 6.S7

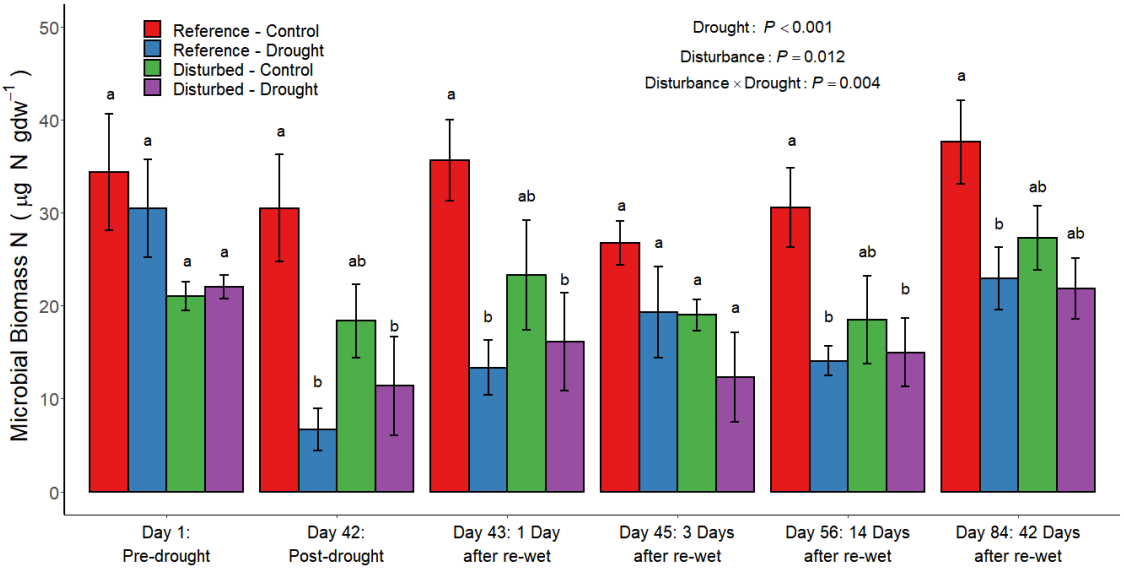

Figure 6.S7: Microbial biomass N at key time points in the drought-rewetting experiment. Error bars represent ± one SE. *P* values are from mixed effects models while different letters represent significant pairwise differences between treatments within time points ($P < 0.05$).

Supplementary Tables

Table 6.S1

Watershed	History	Aspect	Elevation (m)	Area (ha)
WS14	Undisturbed since 1923	NW	707 – 992	61
WS6	Clearcut in 1958, soil scarified, planted to grass, limed and fertilized in 1959, fertilized again in 1965, grass herbicided in 1966 and 1967	NW	696 – 905	9

Table 6.S1: Detailed watershed information for the watersheds sampled in this study.

Additional watershed information can be found at:
https://coweeta.uga.edu/Watersheds.html

Table 6.S2

Gene target	Primer Pair	Thermal cycling protocol
16S	EUB 338/515 (Fierer et al. 2005)	15 min at 95 °C, 40 cycles of 15 s at 94 °C, 30 s at 55 °C, and 30 s at 72 °C.
ITS	ITS1F/5.8s(Fierer et al. 2005)	15 min at 95 °C, 40 cycles of 15 s at 94 °C, 30 s at 55 °C, and 30 s at 72 °C.
AOA *amoA*	Arch-amoAF/R (Francis et al. 2005)	15 min at 95 °C, 40 cycles of 15 s at 94 °C, 30 s at 53 °C, and 60 s at 72 °C.
AOB *amoA*	amoA-1f/2r (Rotthauwe et al. 1997)	15 min at 95 °C, 40 cycles of 15 s at 94 °C, 30 s at 55 °C, 60 s at 72 °C, and 5s at 78 °C (plate read step).
CAOB *amoA*	comamoa F/R (Zhao et al. 2019)	15 min at 95 °C, 40 cycles of 30 s at 94 °C, 30 s at 53 °C, and 60 s at 72 °C.

Table 6.S2: Thermal cycling conditions for 16S rRNA, ITS, and *amoA* genes quantified for this study.

Table 6.S3

Factor	**χ^2 Test Statistic**	**Df**	***P* value**
Land Use	0.0857	1	0.77
Drought	5.61	1	0.018
Drought x Land Use	.436	1	0.51
Day	128.0116	13	< 0.001
Day x Land Use	5.94	13	0.95
Day x Drought	359	13	< 0.001
Drought x Land Use x Day	9.83	13	0.71

Day	**contrast**	**estimate**	**SE**	**z.ratio**	**p.value**
3	Disturbed Control - Reference Control	-0.03594	0.122769	-0.29278	0.99127
	Disturbed Control - Disturbed Drought	0.27875	0.117714	2.368031	0.083313
	Disturbed Control - Reference Drought	0.132908	0.122769	1.082585	0.700207
	Reference Control - Disturbed Drought	0.314694	0.122769	2.563306	0.050765
	Reference Control - Reference Drought	0.168852	0.117714	1.434434	0.477737
	Disturbed Drought - Reference Drought	-0.14584	0.122769	-1.18794	0.634489
7	Disturbed Control - Reference Control	0.080742	0.122769	0.657678	0.912878
	Disturbed Control - Disturbed Drought	0.39664	0.117714	3.369536	0.004192
	Disturbed Control - Reference Drought	0.482626	0.122769	3.931173	0.00049
	Reference Control - Disturbed Drought	0.315898	0.122769	2.573111	0.049461
	Reference Control - Reference Drought	0.401883	0.117714	3.414077	0.003579
	Disturbed Drought - Reference Drought	0.085985	0.122769	0.700384	0.89696
14	Disturbed Control - Reference Control	-0.10795	0.122769	-0.87931	0.815614
	Disturbed Control - Disturbed Drought	0.268734	0.117714	2.282948	0.101976
	Disturbed Control - Reference Drought	0.384287	0.122769	3.130169	0.009463
	Reference Control - Disturbed Drought	0.376686	0.122769	3.06825	0.011565
	Reference Control - Reference Drought	0.492239	0.117714	4.181664	0.00017
	Disturbed Drought - Reference Drought	0.115553	0.122769	0.941225	0.782603
21	Disturbed Control - Reference Control	-0.10474	0.122769	-0.85318	0.828857
	Disturbed Control - Disturbed Drought	0.529215	0.117714	4.495779	4.10E-05
	Disturbed Control - Reference Drought	0.433331	0.122769	3.529651	0.002351
	Reference Control - Disturbed Drought	0.633959	0.122769	5.16384	1.45E-06
	Reference Control - Reference Drought	0.538076	0.117714	4.571056	2.88E-05
	Disturbed Drought - Reference Drought	-0.09588	0.122769	-0.78101	0.863111
28	Disturbed Control - Reference Control	-0.03443	0.122769	-0.28043	0.992309
	Disturbed Control - Disturbed Drought	0.653499	0.117714	5.551602	1.70E-07
	Disturbed Control - Reference Drought	0.417854	0.122769	3.403584	0.003716
	Reference Control - Disturbed Drought	0.687927	0.122769	5.60343	1.26E-07
	Reference Control - Reference Drought	0.452282	0.117714	3.842222	0.000704
	Disturbed Drought - Reference Drought	-0.23565	0.122769	-1.91942	0.219786
35	Disturbed Control - Reference Control	-0.15558	0.122769	-1.26726	0.583865
	Disturbed Control - Disturbed Drought	0.67086	0.117714	5.69908	7.22E-08

	Disturbed Control - Reference Drought	0.552015	0.122769	4.496376	4.09E-05
	Reference Control - Disturbed Drought	0.82644	0.122769	6.73167	1.01E-10
	Reference Control - Reference Drought	0.707595	0.117714	6.011158	1.10E-08
	Disturbed Drought - Reference Drought	-0.11884	0.122769	-0.96803	0.767662
42	Disturbed Control - Reference Control	-0.07434	0.122769	-0.60554	0.930355
	Disturbed Control - Disturbed Drought	0.496409	0.117714	4.217092	0.000145
	Disturbed Control - Reference Drought	0.236038	0.122769	1.922618	0.218456
	Reference Control - Disturbed Drought	0.57075	0.122769	4.648982	1.98E-05
	Reference Control - Reference Drought	0.310379	0.117714	2.636727	0.041668
	Disturbed Drought - Reference Drought	-0.26037	0.122769	-2.12083	0.146426
44	Disturbed Control - Reference Control	0.07206	0.122769	0.58696	0.936056
	Disturbed Control - Disturbed Drought	-1.49472	0.117714	-12.6979	0
	Disturbed Control - Reference Drought	-1.16029	0.122769	-9.45099	3.50E-14
	Reference Control - Disturbed Drought	-1.56678	0.122769	-12.762	0
	Reference Control - Reference Drought	-1.23235	0.117714	-10.469	3.73E-14
	Disturbed Drought - Reference Drought	0.334429	0.122769	2.72405	0.032687
49	Disturbed Control - Reference Control	-0.03992	0.122769	-0.32517	0.988129
	Disturbed Control - Disturbed Drought	-0.8142	0.117714	-6.9168	2.77E-11
	Disturbed Control - Reference Drought	-0.79673	0.122769	-6.48969	5.16E-10
	Reference Control - Disturbed Drought	-0.77428	0.122769	-6.30682	1.71E-09
	Reference Control - Reference Drought	-0.75681	0.117714	-6.42925	7.69E-10
	Disturbed Drought - Reference Drought	0.01747	0.122769	0.142298	0.998973
56	Disturbed Control - Reference Control	-0.01714	0.122769	-0.13961	0.99903
	Disturbed Control - Disturbed Drought	-0.42608	0.117714	-3.61967	0.001679
	Disturbed Control - Reference Drought	-0.5096	0.122769	-4.15085	0.000194
	Reference Control - Disturbed Drought	-0.40894	0.122769	-3.33101	0.004799
	Reference Control - Reference Drought	-0.49246	0.117714	-4.1835	0.000168
	Disturbed Drought - Reference Drought	-0.08351	0.122769	-0.68023	0.904651
63	Disturbed Control - Reference Control	-0.11085	0.122769	-0.90293	0.803279
	Disturbed Control - Disturbed Drought	-0.30628	0.117714	-2.60194	0.045789
	Disturbed Control - Reference Drought	-0.23998	0.122769	-1.9547	0.205411
	Reference Control - Disturbed Drought	-0.19543	0.122769	-1.59187	0.383221
	Reference Control - Reference Drought	-0.12912	0.117714	-1.09694	0.691417
	Disturbed Drought - Reference Drought	0.066308	0.122769	0.540104	0.949209
70	Disturbed Control - Reference Control	-0.19983	0.122769	-1.62769	0.362923
	Disturbed Control - Disturbed Drought	-0.22977	0.117714	-1.9519	0.206528
	Disturbed Control - Reference Drought	-0.28263	0.122769	-2.30216	0.097498
	Reference Control - Disturbed Drought	-0.02994	0.122769	-0.24383	0.994908
	Reference Control - Reference Drought	-0.0828	0.117714	-0.70343	0.895771
	Disturbed Drought - Reference Drought	-0.05287	0.122769	-0.43063	0.97323
77	Disturbed Control - Reference Control	-0.09432	0.122769	-0.76829	0.868768
	Disturbed Control - Disturbed Drought	-0.06254	0.117714	-0.53126	0.951495
	Disturbed Control - Reference Drought	-0.0602	0.122769	-0.49034	0.961272

	Reference Control - Disturbed Drought	0.031786	0.122769	0.25891	0.993921
	Reference Control - Reference Drought	0.034124	0.117714	0.289889	0.991521
	Disturbed Drought - Reference Drought	0.002338	0.122769	0.019042	0.999998
84	Disturbed Control - Reference Control	-0.13458	0.122769	-1.09623	0.691853
	Disturbed Control - Disturbed Drought	-0.20484	0.117714	-1.74018	0.302801
	Disturbed Control - Reference Drought	-0.19734	0.122769	-1.60738	0.374371
	Reference Control - Disturbed Drought	-0.07026	0.122769	-0.5723	0.94036
	Reference Control - Reference Drought	-0.06275	0.117714	-0.5331	0.951024
	Disturbed Drought - Reference Drought	0.007507	0.122769	0.061147	0.999918

Table 6.S3: Mixed effects model results for C mineralization over time in the drought-rewetting experiment. The model has ‘Drought’, ‘Disturbance’, and ‘Day’ as fixed effects, and ‘Plot’ as a random effect, which accounts for repeated measurements from soil cores representing each plot over time in the experiment. Shown below are ost-hoc tests (Tukey’s HSD) for C mineralization. All pairwise comparisons are shown between all treatments within each day.

Table 6.S4

Factor	**χ^2 Test Statistic**	**Degrees of freedom**	***P* value**
Land Use	0.077	1	0.782
Drought	5.43	1	0.02
Drought x Land Use	2.14	1	0.143

contrast	**estimate**	**SE**	**z.ratio**	**p.value**
Disturbed Control - Reference Control	-0.0705	0.0837	-0.843	0.8339
Disturbed Control - Disturbed Drought	-0.1279	0.0477	-2.683	0.0367
Disturbed Control - Reference Drought	-0.0998	0.0837	1.193	0.6313
Reference Control - Disturbed Drought	-0.0574	0.0836	-0.686	0.9025
Reference Control - Reference Drought	-0.0293	0.0476	-0.615	0.9273
Disturbed Drought - Reference Drought	0.0281	0.0836	0.336	0.9870

Table 6.S4: Model results for cumulative C mineralization in the drought-rewetting experiment. Shown below are post-hoc tests for cumulative C mineralization. All pairwise comparisons are shown between all treatments.

Table 6.S5

Factor	**χ^2 Test Statistic**	**Df**	**P value**
LandUse	7.263217	1	0.007038
Drought	19.21406	1	1.17E-05
Day	5.038159	5	0.411241
LandUse:Drought	6.961705	1	0.008327
LandUse:Day	5.830253	5	0.323088
Drought:Day	11.10383	5	0.04936
LandUse:Drought:Day	3.29248	5	0.654993

Day	**contrast**	**estimate**	**SE**	**t.ratio**	**p.value**
1	Disturbed Control - Reference Control	-28.6758	30.63919	-0.93592	0.785669
	Disturbed Control - Disturbed Drought	-11.0415	28.55977	-0.38661	0.980261
	Disturbed Control - Reference Drought	-40.8462	29.47758	-1.38567	0.512655
	Reference Control - Disturbed Drought	17.63429	33.34978	0.528768	0.951871
	Reference Control - Reference Drought	-12.1704	26.68418	-0.45609	0.968303
	Disturbed Drought - Reference Drought	-29.8047	32.28584	-0.92315	0.792553
42	Disturbed Control - Reference Control	-111.432	29.47758	-3.78021	0.001867
	Disturbed Control - Disturbed Drought	38.78338	25.34192	1.530404	0.42315
	Disturbed Control - Reference Drought	-9.64428	29.47758	-0.32717	0.987801
	Reference Control - Disturbed Drought	150.215	29.47758	5.095905	1.78E-05
	Reference Control - Reference Drought	101.7873	25.34192	4.016558	0.000635
	Disturbed Drought - Reference Drought	-48.4277	29.47758	-1.64286	0.362018
43	Disturbed Control - Reference Control	-81.3017	29.47758	-2.75808	0.036714

	Disturbed Control - Disturbed Drought	-10.4327	25.34192	-0.41168	0.976347
	Disturbed Control - Reference Drought	-35.9043	30.6324	-1.1721	0.646258
	Reference Control - Disturbed Drought	70.86892	29.47758	2.404163	0.086033
	Reference Control - Reference Drought	45.39739	26.67638	1.701782	0.327922
	Disturbed Drought - Reference Drought	-25.4715	30.6324	-0.83152	0.839316
45	Disturbed Control - Reference Control	-45.5358	29.47758	-1.54476	0.417012
	Disturbed Control - Disturbed Drought	30.81373	25.34192	1.215919	0.618185
	Disturbed Control - Reference Drought	3.492986	29.47758	0.118496	0.999399
	Reference Control - Disturbed Drought	76.34949	29.47758	2.590087	0.055732
	Reference Control - Reference Drought	49.02874	25.34192	1.934689	0.219967
	Disturbed Drought - Reference Drought	-27.3207	29.47758	-0.92683	0.790594
56	Disturbed Control - Reference Control	-74.2439	29.47758	-2.51866	0.066082
	Disturbed Control - Disturbed Drought	6.748129	25.34192	0.266283	0.993354
	Disturbed Control - Reference Drought	8.333082	30.63919	0.271975	0.992907
	Reference Control - Disturbed Drought	80.99205	29.47758	2.747581	0.03771
	Reference Control - Reference Drought	82.577	26.68418	3.094605	0.013268
	Disturbed Drought - Reference Drought	1.584953	30.63919	0.05173	0.99995
84	Disturbed Control - Reference Control	-41.2867	29.47758	-1.40061	0.50342
	Disturbed Control - Disturbed Drought	21.26943	25.34192	0.839298	0.835599
	Disturbed Control - Reference Drought	1.15331	29.47758	0.039125	0.999978
	Reference Control - Disturbed Drought	62.55615	29.47758	2.12216	0.156616
	Reference Control - Reference Drought	42.44004	25.34192	1.674697	0.342181
	Disturbed Drought - Reference Drought	-20.1161	29.47758	-0.68242	0.903434

Table 6.S5: Mixed effects model results for Microbial Biomass C over time in the drought-rewetting experiment. The model has 'Drought', 'Disturbance', and 'Day' as fixed effects, and 'Plot' as a random effect, which accounts for repeated measurements from soil cores representing each plot over time in the experiment. Shown below are post-hoc tests (Tukey's HSD) for Microbial biomass C. All pairwise comparisons between treatments within each day are shown.

Table 6.S6

Factor	**χ^2 Test Statistic**	**Df**	**P value**
LandUse	0.987365	1	0.320387
Drought	20.72819	1	5.29E-06
Day	49.9961	5	1.39E-09
LandUse:Drought	0.03983	1	0.841814
LandUse:Day	8.110449	5	0.150253

Drought:Day	25.13064	5	0.000131		
LandUse:Drought:Day	2.588462	5	0.763118		
Day	**contrast**	**estimate**	**SE**	**t.ratio**	**p.value**
1	Disturbed Control - Reference Control	0.847445	1.251037	0.677394	0.905444
	Disturbed Control - Disturbed Drought	-0.893	1.419291	-0.62919	0.922431
	Disturbed Control - Reference Drought	0.029753	1.193612	0.024927	0.999994
	Reference Control - Disturbed Drought	-1.74044	1.505479	-1.15607	0.655727
	Reference Control - Reference Drought	-0.81769	1.205569	-0.67826	0.905109
	Disturbed Drought - Reference Drought	0.922752	1.45811	0.632842	0.92122
42	Disturbed Control - Reference Control	-1.34321	1.193612	-1.12533	0.674825
	Disturbed Control - Disturbed Drought	-4.70297	1.419291	-3.31361	0.006941
	Disturbed Control - Reference Drought	-7.69949	1.457878	-5.2813	4.16E-06
	Reference Control - Disturbed Drought	-3.35976	1.45811	-2.30419	0.103628
	Reference Control - Reference Drought	-6.35627	1.419053	-4.47924	0.000117
	Disturbed Drought - Reference Drought	-2.99651	1.681303	-1.78226	0.287582
43	Disturbed Control - Reference Control	-1.02666	1.193612	-0.86013	0.825292
	Disturbed Control - Disturbed Drought	-2.29585	1.205442	-1.90457	0.232931
	Disturbed Control - Reference Drought	-4.97555	1.251011	-3.97723	0.000745
	Reference Control - Disturbed Drought	-1.26919	1.250914	-1.01461	0.741279
	Reference Control - Reference Drought	-3.94889	1.205543	-3.27561	0.007854
	Disturbed Drought - Reference Drought	-2.6797	1.305797	-2.05216	0.175998
45	Disturbed Control - Reference Control	-0.25078	1.193612	-0.2101	0.996701
	Disturbed Control - Disturbed Drought	-1.31603	1.145868	-1.1485	0.660537
	Disturbed Control - Reference Drought	-0.27865	1.193612	-0.23345	0.995492
	Reference Control - Disturbed Drought	-1.06525	1.193612	-0.89246	0.808773
	Reference Control - Reference Drought	-0.02788	1.145868	-0.02433	0.999995
	Disturbed Drought - Reference Drought	1.037378	1.193612	0.869108	0.820768
56	Disturbed Control - Reference Control	-0.93795	1.193612	-0.78581	0.86074
	Disturbed Control - Disturbed Drought	-0.82111	1.145868	-0.71658	0.890285
	Disturbed Control - Reference Drought	-0.83211	1.251037	-0.66513	0.909938
	Reference Control - Disturbed Drought	0.116841	1.193612	0.097889	0.999662
	Reference Control - Reference Drought	0.105842	1.205569	0.087795	0.999756
	Disturbed Drought - Reference Drought	-0.011	1.251037	-0.00879	1
84	Disturbed Control - Reference Control	0.042858	1.193612	0.035906	0.999983
	Disturbed Control - Disturbed Drought	-0.1114	1.205701	-0.0924	0.999715
	Disturbed Control - Reference Drought	-0.47812	1.193612	-0.40057	0.97813
	Reference Control - Disturbed Drought	-0.15426	1.251164	-0.12329	0.999326
	Reference Control - Reference Drought	-0.52098	1.145868	-0.45466	0.96857
	Disturbed Drought - Reference Drought	-0.36672	1.251164	-0.2931	0.991185

Table 6.S6: Mixed effects model results for Microbial Biomass C:N ratios over time in the drought-rewetting experiment. The model has ‘Drought’, ‘Disturbance’, and ‘Day’ as

fixed effects, and 'Plot' as a random effect, which accounts for repeated measurements from soil cores representing each plot over time in the experiment. Shown below are post-hoc tests (Tukey's HSD) for Microbial Biomass C:N over time. All pairwise comparisons between treatments within each day are shown.

Table 6.S7

Factor	**χ^2 Test Statistic**	**Df**	**P value**
LandUse	5.300684	1	0.021317
Drought	3.366062	1	0.066553
Day	27.6331	5	4.29E-05
LandUse:Drought	0.145345	1	0.703024
LandUse:Day	5.49554	5	0.358435
Drought:Day	31.04227	5	9.19E-06
LandUse:Drought:Day	3.042177	5	0.693483

Day	**contrast**	**estimate**	**SE**	**z.ratio**	**p.value**
1	Disturbed Control - Reference Control	-0.64569	0.293921	-2.1968	0.124066
	Disturbed Control - Disturbed Drought	-0.18428	0.192391	-0.95782	0.773395
	Disturbed Control - Reference Drought	-0.66917	0.294054	-2.27567	0.103714
	Reference Control - Disturbed Drought	0.461409	0.293972	1.569571	0.396111
	Reference Control - Reference Drought	-0.02349	0.191361	-0.12273	0.99934
	Disturbed Drought - Reference Drought	-0.4849	0.294106	-1.64871	0.351261
42	Disturbed Control - Reference Control	-0.59263	0.29398	-2.0159	0.182025
	Disturbed Control - Disturbed Drought	-0.39528	0.192091	-2.05778	0.167144
	Disturbed Control - Reference Drought	-0.97972	0.294155	-3.33062	0.004805
	Reference Control - Disturbed Drought	0.197354	0.294073	0.671105	0.908027
	Reference Control - Reference Drought	-0.38709	0.191563	-2.02067	0.180283
	Disturbed Drought - Reference Drought	-0.58444	0.294245	-1.98624	0.193114
43	Disturbed Control - Reference Control	-0.85456	0.294394	-2.90279	0.019369
	Disturbed Control - Disturbed Drought	-0.05678	0.194299	-0.29222	0.991319
	Disturbed Control - Reference Drought	-0.74091	0.294214	-2.51829	0.057127
	Reference Control - Disturbed Drought	0.797786	0.294601	2.708017	0.034199
	Reference Control - Reference Drought	0.11365	0.191867	0.592337	0.934434
	Disturbed Drought - Reference Drought	-0.68414	0.294428	-2.32361	0.092683
45	Disturbed Control - Reference Control	-0.28478	0.29494	-0.96556	0.769059
	Disturbed Control - Disturbed Drought	0.693918	0.193116	3.593267	0.001855
	Disturbed Control - Reference Drought	0.094873	0.294837	0.321781	0.988487
	Reference Control - Disturbed Drought	0.978699	0.293894	3.330112	0.004814
	Reference Control - Reference Drought	0.379654	0.191418	1.983374	0.19421
	Disturbed Drought - Reference Drought	-0.59905	0.293785	-2.03906	0.173682
56	Disturbed Control - Reference Control	-0.54493	0.293884	-1.85424	0.248062

	Disturbed Control - Disturbed Drought	-0.02094	0.192087	-0.10899	0.999537
	Disturbed Control - Reference Drought	-0.28426	0.293829	-0.96743	0.768001
	Reference Control - Disturbed Drought	0.523995	0.293901	1.782899	0.281532
	Reference Control - Reference Drought	0.260671	0.191673	1.359978	0.524616
	Disturbed Drought - Reference Drought	-0.26332	0.293848	-0.89613	0.806866
84	Disturbed Control - Reference Control	-0.37532	0.294419	-1.27477	0.579051
	Disturbed Control - Disturbed Drought	0.442499	0.193233	2.289973	0.10032
	Disturbed Control - Reference Drought	0.014651	0.294265	0.049788	0.999956
	Reference Control - Disturbed Drought	0.817818	0.294089	2.780851	0.027785
	Reference Control - Reference Drought	0.389969	0.191812	2.033082	0.175809
	Disturbed Drought - Reference Drought	-0.42785	0.29394	-1.45556	0.464634

Table 6.S7: Mixed effects model results for ITS:16S ratios over time in the drought-rewetting experiment. The model has 'Drought', 'Disturbance', and 'Day' as fixed effects, and 'Plot' as a random effect, which accounts for repeated measurements from soil cores representing each plot over time in the experiment. Shown below are post-hoc tests (Tukey's HSD) for ITS:16S ratios over time. All pairwise comparisons between all treatments within each day are shown.

Table 6.S8

Factor	**χ^2 Test Statistic**	**Df**	**P value**
LandUse	21.3679	1	3.79E-06
Drought	65.36951	1	6.21E-16
Day	217.2349	5	5.81E-45
LandUse:Drought	1.508052	1	0.219437
LandUse:Day	6.988897	5	0.221467
Drought:Day	72.57544	5	2.98E-14
LandUse:Drought:Day	3.382847	5	0.641184

Day	**contrast**	**estimate**	**SE**	**z.ratio**	**p.value**
1	Disturbed Control - Reference Control	-0.45524	0.144734	-3.14537	0.009002
	Disturbed Control - Disturbed Drought	-0.0141	0.099178	-0.14215	0.998976
	Disturbed Control - Reference Drought	-0.34667	0.144723	-2.3954	0.077929
	Reference Control - Disturbed Drought	0.441145	0.144728	3.048101	0.012334
	Reference Control - Reference Drought	0.108574	0.099163	1.094905	0.692664
	Disturbed Drought - Reference Drought	-0.33257	0.144716	-2.2981	0.098432
42	Disturbed Control - Reference Control	-0.39129	0.144732	-2.70357	0.034628
	Disturbed Control - Disturbed Drought	-0.54913	0.099183	-5.53651	1.85E-07
	Disturbed Control - Reference Drought	-1.13064	0.144784	-7.80916	5.72E-14

	Reference Control - Disturbed Drought	-0.15783	0.14474	-1.09046	0.695388
	Reference Control - Reference Drought	-0.73935	0.09923	-7.45085	5.83E-13
	Disturbed Drought - Reference Drought	-0.58151	0.144791	-4.01622	0.000344
43	Disturbed Control - Reference Control	-0.51234	0.14477	-3.539	0.002271
	Disturbed Control - Disturbed Drought	-0.32393	0.099227	-3.26454	0.006037
	Disturbed Control - Reference Drought	-1.02164	0.144824	-7.05438	1.04E-11
	Reference Control - Disturbed Drought	0.18841	0.144722	1.301873	0.561697
	Reference Control - Reference Drought	-0.5093	0.099211	-5.13352	1.70E-06
	Disturbed Drought - Reference Drought	-0.69771	0.144777	-4.81921	8.58E-06
45	Disturbed Control - Reference Control	-0.46296	0.144718	-3.19902	0.007534
	Disturbed Control - Disturbed Drought	-0.24254	0.09928	-2.44303	0.069234
	Disturbed Control - Reference Drought	-0.78669	0.144734	-5.43543	3.27E-07
	Reference Control - Disturbed Drought	0.220413	0.144746	1.522761	0.42375
	Reference Control - Reference Drought	-0.32374	0.099172	-3.26439	0.00604
	Disturbed Drought - Reference Drought	-0.54415	0.144757	-3.75905	0.00098
56	Disturbed Control - Reference Control	-0.56822	0.144791	-3.92442	0.000504
	Disturbed Control - Disturbed Drought	0.023881	0.09924	0.240639	0.995102
	Disturbed Control - Reference Drought	-0.59805	0.144876	-4.12798	0.000214
	Reference Control - Disturbed Drought	0.592102	0.144808	4.088876	0.000253
	Reference Control - Reference Drought	-0.02983	0.099238	-0.30054	0.990573
	Disturbed Drought - Reference Drought	-0.62193	0.144894	-4.29229	0.000104
84	Disturbed Control - Reference Control	-0.42794	0.144705	-2.95735	0.016394
	Disturbed Control - Disturbed Drought	-0.07243	0.099147	-0.73048	0.884893
	Disturbed Control - Reference Drought	-0.53461	0.144738	-3.69362	0.001265
	Reference Control - Disturbed Drought	0.355517	0.144711	2.456736	0.066885
	Reference Control - Reference Drought	-0.10666	0.099196	-1.07527	0.704662
	Disturbed Drought - Reference Drought	-0.46218	0.144744	-3.19309	0.007685

Table 6.S8: Mixed effects model results for DOC over time in the drought-rewetting experiment. The model has ‘Drought’, ‘Disturbance’, and ‘Day’ as fixed effects, and ‘Plot’ as a random effect, which accounts for repeated measurements from soil cores representing each plot over time in the experiment. Shown below are post-hoc tests (Tukey’s HSD) for DOC over time. All pairwise comparisons between all treatments within each day are shown.

Table 6.S9

Factor	χ^2 Test Statistic	Df	P value
LandUse	3.709118	1	0.054116
Drought	127.0189	1	1.84E-29
Day	130.1038	5	2.26E-26
LandUse:Drought	12.30105	1	0.000453
LandUse:Day	8.688918	5	0.122134
Drought:Day	26.00033	5	8.92E-05
LandUse:Drought:Day	9.407749	5	0.093865

Day	contrast	estimate	SE	z.ratio	p.value
1	Disturbed Control - Reference Control	-0.21773	0.183629	-1.18572	0.635895
	Disturbed Control - Disturbed Drought	-0.06645	0.16005	-0.41519	0.975892
	Disturbed Control - Reference Drought	-0.18121	0.183624	-0.98687	0.756952
	Reference Control - Disturbed Drought	0.151283	0.183435	0.824721	0.842787
	Reference Control - Reference Drought	0.036521	0.159917	0.228373	0.995805
	Disturbed Drought - Reference Drought	-0.11476	0.183434	-0.62563	0.923877
42	Disturbed Control - Reference Control	0.094623	0.183553	0.515505	0.955415
	Disturbed Control - Disturbed Drought	-0.2355	0.160053	-1.47137	0.454902
	Disturbed Control - Reference Drought	-0.74385	0.183635	-4.05072	0.000298
	Reference Control - Disturbed Drought	-0.33012	0.183458	-1.79944	0.273542
	Reference Control - Reference Drought	-0.83847	0.160014	-5.24002	9.60E-07
	Disturbed Drought - Reference Drought	-0.50835	0.183542	-2.76968	0.028695
43	Disturbed Control - Reference Control	0.356401	0.184007	1.936887	0.212587
	Disturbed Control - Disturbed Drought	-0.28887	0.160577	-1.79894	0.273781
	Disturbed Control - Reference Drought	-0.64904	0.184044	-3.52655	0.002378
	Reference Control - Disturbed Drought	-0.64527	0.18334	-3.51953	0.002441
	Reference Control - Reference Drought	-1.00544	0.159919	-6.28717	1.94E-09
	Disturbed Drought - Reference Drought	-0.36017	0.183363	-1.96426	0.20163
45	Disturbed Control - Reference Control	-0.07733	0.183768	-0.42077	0.974949
	Disturbed Control - Disturbed Drought	-0.60574	0.160402	-3.77638	0.000915
	Disturbed Control - Reference Drought	-0.92362	0.183668	-5.02871	2.95E-06
	Reference Control - Disturbed Drought	-0.52842	0.183828	-2.87451	0.02109
	Reference Control - Reference Drought	-0.84629	0.160149	-5.2844	7.54E-07
	Disturbed Drought - Reference Drought	-0.31787	0.18373	-1.73012	0.307941
56	Disturbed Control - Reference Control	-0.26021	0.183495	-1.41808	0.487948
	Disturbed Control - Disturbed Drought	-0.45616	0.159953	-2.85184	0.022565
	Disturbed Control - Reference Drought	-1.11437	0.183763	-6.06414	7.95E-09
	Reference Control - Disturbed Drought	-0.19595	0.183765	-1.06631	0.710098
	Reference Control - Reference Drought	-0.85416	0.160234	-5.33067	5.85E-07
	Disturbed Drought - Reference Drought	-0.65821	0.184007	-3.57707	0.001971
84	Disturbed Control - Reference Control	-0.09005	0.183471	-0.49082	0.961165
	Disturbed Control - Disturbed Drought	-0.50076	0.160004	-3.12967	0.009478

	Disturbed Control - Reference Drought	-0.67961	0.183482	-3.70397	0.001215
	Reference Control - Disturbed Drought	-0.41071	0.18354	-2.23771	0.113158
	Reference Control - Reference Drought	-0.58956	0.160514	-3.67297	0.00137
	Disturbed Drought - Reference Drought	-0.17885	0.183552	-0.9744	0.764063

Table 6.S9: Mixed effects model results for Total Extractable N over time in the drought-rewetting experiment. The model has 'Drought', 'Disturbance', and 'Day' as fixed effects, and 'Plot' as a random effect, which accounts for repeated measurements from soil cores representing each plot over time in the experiment. Shown below are post-hoc tests (Tukey's HSD) for Total Extractable N over time. All pairwise comparisons between all treatments within each day are shown.

Table 6.S10

Factor	**χ^2 Test Statistic**	**Df**	**P value**
LandUse	0.474782	1	0.490795
Drought	159.6701	1	1.34E-36
Day	273.1016	5	6.04E-57
LandUse:Drought	8.569488	1	0.003418
LandUse:Day	26.08655	5	8.59E-05
Drought:Day	62.90016	5	3.05E-12
LandUse:Drought:Day	7.076116	5	0.215041

Day	**contrast**	**estimate**	**SE**	**z.ratio**	**p.value**
1	Disturbed Control - Reference Control	0.692663	0.295059	2.347543	0.087535
	Disturbed Control - Disturbed Drought	0.027213	0.252104	0.107943	0.99955
	Disturbed Control - Reference Drought	0.244161	0.296736	0.822821	0.843697
	Reference Control - Disturbed Drought	-0.66545	0.291796	-2.28054	0.102549
	Reference Control - Reference Drought	-0.4485	0.252324	-1.77749	0.284175
	Disturbed Drought - Reference Drought	0.216948	0.293352	0.739547	0.881125
42	Disturbed Control - Reference Control	0.12983	0.292249	0.444244	0.970739
	Disturbed Control - Disturbed Drought	0.182932	0.250649	0.729834	0.885161
	Disturbed Control - Reference Drought	-0.147	0.292893	-0.50189	0.958645
	Reference Control - Disturbed Drought	0.053102	0.291377	0.182245	0.997853
	Reference Control - Reference Drought	-0.27683	0.250296	-1.10601	0.685827
	Disturbed Drought - Reference Drought	-0.32993	0.29206	-1.12967	0.67115
43	Disturbed Control - Reference Control	0.813164	0.29508	2.75574	0.029868
	Disturbed Control - Disturbed Drought	-0.57678	0.253666	-2.27379	0.104167
	Disturbed Control - Reference Drought	-0.96857	0.294785	-3.28568	0.005615
	Reference Control - Disturbed Drought	-1.38995	0.291381	-4.7702	1.09E-05

	Reference Control - Reference Drought	-1.78173	0.249178	-7.15045	5.22E-12
	Disturbed Drought - Reference Drought	-0.39179	0.290832	-1.34712	0.532795
45	Disturbed Control - Reference Control	-0.11359	0.292417	-0.38846	0.980097
	Disturbed Control - Disturbed Drought	-1.35672	0.250501	-5.41603	3.65E-07
	Disturbed Control - Reference Drought	-1.52178	0.291602	-5.21869	1.08E-06
	Reference Control - Disturbed Drought	-1.24313	0.291997	-4.25733	0.000122
	Reference Control - Reference Drought	-1.40819	0.250061	-5.63137	1.07E-07
	Disturbed Drought - Reference Drought	-0.16506	0.291164	-0.56689	0.941904
56	Disturbed Control - Reference Control	-0.47298	0.291941	-1.62013	0.367166
	Disturbed Control - Disturbed Drought	-1.41797	0.250595	-5.6584	9.15E-08
	Disturbed Control - Reference Drought	-2.14122	0.291886	-7.33581	1.35E-12
	Reference Control - Disturbed Drought	-0.94498	0.290896	-3.24853	0.006375
	Reference Control - Reference Drought	-1.66824	0.249193	-6.69457	1.30E-10
	Disturbed Drought - Reference Drought	-0.72325	0.290936	-2.48596	0.062094
84	Disturbed Control - Reference Control	-0.47077	0.291797	-1.61335	0.370986
	Disturbed Control - Disturbed Drought	-1.08067	0.249752	-4.32699	8.91E-05
	Disturbed Control - Reference Drought	-1.65211	0.291688	-5.66399	8.86E-08
	Reference Control - Disturbed Drought	-0.6099	0.292268	-2.08679	0.15736
	Reference Control - Reference Drought	-1.18134	0.250777	-4.71073	1.47E-05
	Disturbed Drought - Reference Drought	-0.57144	0.29213	-1.95612	0.204848

Table 6.S10: Mixed effects model results for NH_4 over time in the drought-rewetting experiment. The model has 'Drought', 'Disturbance', and 'Day' as fixed effects, and 'Plot' as a random effect, which accounts for repeated measurements from soil cores representing each plot over time in the experiment. Shown below are post-hoc tests (Tukey's HSD) for NH_4 over time. All pairwise comparisons between all treatments within each day are shown.

Table 6.S11

Factor	**χ^2 Test Statistic**	**Df**	**P value**
LandUse	28.82948	1	7.90E-08
Drought	15.22811	1	9.53E-05
Day	113.0312	5	9.37E-23
LandUse:Drought	1.400205	1	0.236689
LandUse:Day	13.64283	5	0.018045
Drought:Day	11.56583	5	0.041246
LandUse:Drought:Day	14.26371	5	0.014018

Day	contrast	estimate	SE	z.ratio	p.value
1	Disturbed Control - Reference Control	1.705887	0.735337	2.31987	0.093508
	Disturbed Control - Disturbed Drought	0.122194	0.515279	0.237142	0.99531
	Disturbed Control - Reference Drought	2.304964	0.73149	3.151055	0.008835
	Reference Control - Disturbed Drought	-1.58369	0.73748	-2.14744	0.138276
	Reference Control - Reference Drought	0.599077	0.537094	1.115404	0.680019
	Disturbed Drought - Reference Drought	2.18277	0.733641	2.975255	0.01551
42	Disturbed Control - Reference Control	2.634657	0.737032	3.574685	0.001989
	Disturbed Control - Disturbed Drought	1.626184	0.512512	3.172969	0.008218
	Disturbed Control - Reference Drought	4.287675	0.729869	5.87458	2.54E-08
	Reference Control - Disturbed Drought	-1.00847	0.736943	-1.36845	0.519234
	Reference Control - Reference Drought	1.653018	0.535083	3.089272	0.010808
	Disturbed Drought - Reference Drought	2.661492	0.729895	3.646401	0.001516
43	Disturbed Control - Reference Control	3.69082	0.735087	5.020927	3.07E-06
	Disturbed Control - Disturbed Drought	0.91275	0.51659	1.766875	0.289404
	Disturbed Control - Reference Drought	4.148643	0.736436	5.633405	1.06E-07
	Reference Control - Disturbed Drought	-2.77807	0.734245	-3.78357	0.00089
	Reference Control - Reference Drought	0.457823	0.538078	0.85085	0.830019
	Disturbed Drought - Reference Drought	3.235893	0.735325	4.400629	6.37E-05
45	Disturbed Control - Reference Control	3.228641	0.735702	4.388518	6.74E-05
	Disturbed Control - Disturbed Drought	0.18647	0.556514	0.335067	0.987043
	Disturbed Control - Reference Drought	3.808459	0.731605	5.205622	1.16E-06
	Reference Control - Disturbed Drought	-3.04217	0.754901	-4.02989	0.000325
	Reference Control - Reference Drought	0.579818	0.531259	1.091404	0.694812
	Disturbed Drought - Reference Drought	3.621989	0.750422	4.826601	8.27E-06
56	Disturbed Control - Reference Control	3.810279	0.733883	5.191945	1.24E-06
	Disturbed Control - Disturbed Drought	0.402031	0.521226	0.771317	0.867433
	Disturbed Control - Reference Drought	3.383335	0.740201	4.57083	2.88E-05
	Reference Control - Disturbed Drought	-3.40825	0.734929	-4.63752	2.09E-05
	Reference Control - Reference Drought	-0.42694	0.545935	-0.78204	0.862644
	Disturbed Drought - Reference Drought	2.981304	0.741497	4.020653	0.000338
84	Disturbed Control - Reference Control	0.98165	0.767025	1.279815	0.575823
	Disturbed Control - Disturbed Drought	-0.50468	0.513119	-0.98356	0.758847
	Disturbed Control - Reference Drought	3.25324	0.731921	4.4448	5.20E-05
	Reference Control - Disturbed Drought	-1.48633	0.766276	-1.93968	0.21145
	Reference Control - Reference Drought	2.27159	0.563225	4.033183	0.000321
	Disturbed Drought - Reference Drought	3.757922	0.731268	5.138915	1.65E-06

Table 6.S11: Mixed effects model results for NO_3 over time in the drought-rewetting experiment. The model has ‘Drought’, ‘Disturbance’, and ‘Day’ as fixed effects, and ‘Plot’ as a random effect, which accounts for repeated measurements from soil cores

representing each plot over time in the experiment. Shown below are post-hoc tests (Tukey's HSD) for NO_3 over time. All pairwise comparisons between all treatments within each day are shown.

Table 6.S12

Factor	**χ^2 Test Statistic**	**Df**	**P value**
LandUse	17.93352	1	2.29E-05
Drought	15.84008	1	6.89E-05
Day	7.032554	5	0.21823
LandUse:Drought	0.322109	1	0.570343
LandUse:Day	7.238148	5	0.203523
Drought:Day	15.13182	5	0.009814
LandUse:Drought:Day	6.144207	5	0.292439

Day	**contrast**	**estimate**	**SE**	**t.ratio**	**p.value**
1	Disturbed Control - Reference Control	2.112641	0.721878	2.926588	0.027011
	Disturbed Control - Disturbed Drought	-0.38204	0.522073	-0.73177	0.884007
	Disturbed Control - Reference Drought	2.237246	0.663181	3.373507	0.009598
	Reference Control - Disturbed Drought	-2.49468	0.722975	-3.45057	0.006707
	Reference Control - Reference Drought	0.124605	0.550541	0.226332	0.995875
	Disturbed Drought - Reference Drought	2.619283	0.664375	3.942477	0.002051
42	Disturbed Control - Reference Control	1.492102	0.665691	2.241431	0.132416
	Disturbed Control - Disturbed Drought	0.01076	0.491114	0.02191	0.999996
	Disturbed Control - Reference Drought	1.690065	0.722803	2.33821	0.105259
	Reference Control - Disturbed Drought	-1.48134	0.642373	-2.30605	0.118632
	Reference Control - Reference Drought	0.197963	0.538567	0.367574	0.982893
	Disturbed Drought - Reference Drought	1.679304	0.701386	2.394267	0.094676
43	Disturbed Control - Reference Control	1.849153	0.688931	2.684089	0.050405
	Disturbed Control - Disturbed Drought	0.504593	0.496349	1.016611	0.740293
	Disturbed Control - Reference Drought	2.586138	0.68709	3.763901	0.003077
	Reference Control - Disturbed Drought	-1.34456	0.663836	-2.02544	0.198611
	Reference Control - Reference Drought	0.736985	0.525698	1.401917	0.502404
	Disturbed Drought - Reference Drought	2.081545	0.661925	3.144684	0.017206
45	Disturbed Control - Reference Control	2.673905	0.688931	3.881237	0.002201
	Disturbed Control - Disturbed Drought	0.588313	0.512474	1.147986	0.661304
	Disturbed Control - Reference Drought	2.754685	0.688931	3.998491	0.00157
	Reference Control - Disturbed Drought	-2.08559	0.688931	-3.02729	0.022055
	Reference Control - Reference Drought	0.08078	0.512474	0.157627	0.998592
	Disturbed Drought - Reference Drought	2.166372	0.688931	3.144541	0.016382
45	Disturbed Control - Reference Control	3.185838	0.687297	4.635317	0.000238
	Disturbed Control - Disturbed Drought	1.577019	0.491114	3.211103	0.010554
	Disturbed Control - Reference Drought	3.113748	0.686768	4.533917	0.000323

	Reference Control - Disturbed Drought	-1.60882	0.664736	-2.42024	0.092175
	Reference Control - Reference Drought	-0.07209	0.53258	-0.13536	0.999106
	Disturbed Drought - Reference Drought	1.536729	0.66419	2.31369	0.114744
84	Disturbed Control - Reference Control	1.386494	0.647851	2.140144	0.1623
	Disturbed Control - Disturbed Drought	1.491697	0.446654	3.339712	0.007184
	Disturbed Control - Reference Drought	3.050138	0.621462	4.908008	0.000192
	Reference Control - Disturbed Drought	0.105203	0.666426	0.157862	0.998571
	Reference Control - Reference Drought	1.663644	0.502001	3.314028	0.007755
	Disturbed Drought - Reference Drought	1.558441	0.640803	2.432014	0.091999

Table 6.S12: Mixed effects model results for AOA *amoA* over time in the drought-rewetting experiment. The model has 'Drought', 'Disturbance', and 'Day' as fixed effects, and 'Plot' as a random effect, which accounts for repeated measurements from soil cores representing each plot over time in the experiment. Shown below are post-hoc tests (Tukey's HSD) for AOA *amoA* over time. All pairwise comparisons between all treatments within each day are shown.

Table 6.13

Factor	**χ^2 Test Statistic**	**Df**	**P value**
LandUse	6.144456	1	0.013182
Drought	0.089189	1	0.76521
Day	6.508187	5	0.25986
LandUse:Drought	1.07E-07	1	0.999738
LandUse:Day	8.297326	5	0.140593
Drought:Day	3.664713	5	0.598624
LandUse:Drought:Day	5.53385	5	0.354248

Day	**contrast**	**estimate**	**SE**	**t.ratio**	**p.value**
1	Disturbed Control - Reference Control	0.472314	1.030038	0.45854	0.967608
	Disturbed Control - Disturbed Drought	0.452732	0.588981	0.76867	0.868336
	Disturbed Control - Reference Drought	0.715434	1.02927	0.695089	0.898434
	Reference Control - Disturbed Drought	-0.01958	1.030038	-0.01901	0.999997
	Reference Control - Reference Drought	0.24312	0.953788	0.2549	0.994147
	Disturbed Drought - Reference Drought	0.262702	1.02927	0.255231	0.994085
42	Disturbed Control - Reference Control	2.001321	0.856726	2.33601	0.116152
	Disturbed Control - Disturbed Drought	0.699977	0.588981	1.188454	0.635817
	Disturbed Control - Reference Drought	1.756328	0.856726	2.050046	0.196602
	Reference Control - Disturbed Drought	-1.30134	0.856726	-1.51897	0.441322

	Reference Control - Reference Drought	-0.24499	0.537664	-0.45566	0.968346
	Disturbed Drought - Reference Drought	1.056351	0.856726	1.233009	0.612241
43	Disturbed Control - Reference Control	1.95443	0.932697	2.09546	0.175249
	Disturbed Control - Disturbed Drought	0.439767	0.537664	0.817922	0.845841
	Disturbed Control - Reference Drought	2.076045	0.887211	2.339967	0.112507
	Reference Control - Disturbed Drought	-1.51466	0.932697	-1.62396	0.379277
	Reference Control - Reference Drought	0.121615	0.720392	0.168818	0.998276
	Disturbed Drought - Reference Drought	1.636278	0.887211	1.844293	0.274177
45	Disturbed Control - Reference Control	1.57375	0.837627	1.87882	0.263765
	Disturbed Control - Disturbed Drought	0.190681	0.537664	0.354648	0.984601
	Disturbed Control - Reference Drought	1.572612	0.887781	1.771396	0.307341
	Reference Control - Disturbed Drought	-1.38307	0.837627	-1.65117	0.370745
	Reference Control - Reference Drought	-0.00114	0.612878	-0.00186	1
	Disturbed Drought - Reference Drought	1.381931	0.887781	1.556611	0.41846
56	Disturbed Control - Reference Control	2.016723	0.885931	2.276388	0.127478
	Disturbed Control - Disturbed Drought	-0.64172	0.537664	-1.19353	0.632638
	Disturbed Control - Reference Drought	1.343125	0.932697	1.440044	0.484049
	Reference Control - Disturbed Drought	-2.65844	0.885931	-3.00073	0.026817
	Reference Control - Reference Drought	-0.6736	0.735934	-0.9153	0.79675
	Disturbed Drought - Reference Drought	1.984843	0.932697	2.128067	0.164956
84	Disturbed Control - Reference Control	1.474261	0.858637	1.716979	0.335798
	Disturbed Control - Disturbed Drought	-0.68901	0.537664	-1.2815	0.577221
	Disturbed Control - Reference Drought	2.425652	0.887781	2.732263	0.04934
	Reference Control - Disturbed Drought	-2.16328	0.858637	-2.51943	0.08052
	Reference Control - Reference Drought	0.951391	0.631158	1.507375	0.43773
	Disturbed Drought - Reference Drought	3.114666	0.887781	3.508371	0.007759

Table 6.S13: Mixed effects model results for AOB *amoA* over time in the drought-rewetting experiment. The model has ‘Drought’, ‘Disturbance’, and ‘Day’ as fixed effects, and ‘Plot’ as a random effect, which accounts for repeated measurements from soil cores representing each plot over time in the experiment. Shown below are post-hoc tests (Tukey’s HSD) for AOB *amoA* over time. All pairwise comparisons between all treatments within each day are shown.

Table 6.S14

Factor	**Sum Sq**	**Df**	**F value**	**P value**
DOC:TDN	5.409831	1	12.72485	0.000556
AOA *amoA*	45.01788	1	105.8898	2.29E-17
Residuals	42.51391	100	NA	NA

Table 6.S14: Results of the multiple regression model predicting soil NO_3 pools from DOC:TDN ratios and AOA *amoA* abundance (NO_3 ~ DOC:TDN + AOA *amoA*). The model explains 59.9% of the observed variation in NO_3 pools (adjusted $R^2 = 0.599$).

CHAPTER 7 – CONCLUSIONS

Summary and Conclusions

The influences of land use on soil microbial community structure are wide-ranging and well-established (e.g., Jangid et al. 2011, Rodrigues et al. 2013, Kohout et al. 2018, Mushinski et al. 2018b, 2018a). In particular, forest conversion (e.g., to agriculture) is known to favor specific microbial functional groups in soil, such as rapidly growing r-selected bacterial taxa (e.g., Zhou et al. 2018). These land use-driven changes in microbial communities are also associated with altered microbial ecosystem functioning, including changes in nitrogen (N) cycling and organic matter decomposition gene abundances (Cardenas et al. 2015, Hermans et al. 2020). This dissertation attempts to advance these lines of investigation by characterizing long-term effects of historical land use on the structure and ecosystem functions of microbial communities in currently unmanaged forests. Further, this dissertation attempts to identify influences of historical land use on the responses of soil microbial communities to climate change. Finally, this dissertation attempts to inform current forest management by determining soil microbial responses to a new management practice, *Rhododendron* removal.

Chapter 2 demonstrated that microbial functional responses to *Rhododendron* understory removal were largely dependent on community size, i.e., total microbial biomass. Specifically, plots receiving removal treatments exhibited generally greater carbon (C) and nutrient-acquiring extracellular enzyme activities, which was attributed to greater microbial biomass in these removal plots. The greater microbial biomass in these plots is likely due to larger soil C and N pools present following *Rhododendron* removal treatments. This work highlights the key role of aggregate properties of microbial

communities in driving ecosystem process rates and also challenges the resource allocation framework commonly invoked to predict and explain microbial extracellular enzyme production. The resource allocation framework argues that microbial enzyme production is nutrient demand-driven, where microorganisms increase production of enzymes for acquiring scare resources (Allison et al. 2010). In contrast, my results support resource supply-driven enzyme production, where enzyme production generally increases where greater soil resources promote higher microbial biomass. This work is also directly relevant to forest management – a parallel study from these same plots demonstrated greater recruitment of hardwood tree seedlings in removal plots (Elliott and Miniat 2018), which is likely linked to the larger pools and faster cycling rates of soil nutrients we observed. Together, these studies suggest that *Rhododendron* understory removal may be successful for achieving management goals, at least in the short term.

Chapter 3 demonstrated that currently unmanaged forests exhibit persistently altered microbial communities ~4-8 decades after anthropogenic disturbances occurred. This was true for both bacterial and fungal communities and the community differences were directionally consistent across many different historical land use changes. Further, several specific microbial functional groups were consistently more abundant in disturbed soils, including nitrifying bacteria, r-selected bacteria, and arbuscular mycorrhizal fungi. Changes in microbial communities were strongly associated with changes to specific soil properties following disturbance (e.g., higher pH, lower C:N), which, in turn, are likely linked to vegetation changes as a result of disturbance. This supports prior work demonstrating the importance of soil properties, especially pH, in structuring microbial communities (e.g., Fierer and Jackson 2006, Lauber et al. 2008) and also casts new light

on the ecosystem-scale responses to forest disturbance in the southern Appalachian region. Specifically, historically disturbed forests exhibit greater nitrification rates in soil (Keiser et al. 2016) as well as greater watershed-scale N export (Webster et al. 2016), which is consistent with the microbial functional group shifts we observed (i.e., more nitrifiers and arbuscular mycorrhizae in disturbed sites). Overall, this chapter highlights the importance of legacy effects of historical land use in structuring microbial communities and also suggests several links between microbial communities and ecosystem-scale processes in disturbed forests.

Chapter 4 demonstrated that microbial-mediated ecosystem process rates are also different between reference and historically disturbed forest soils. In general, historically disturbed soils exhibited higher rates of C mineralization, N mineralization, and nitrification. All ecosystem functions exhibited several correlations with properties of microbial communities, including microbial compositional metrics (e.g., β diversity, bacterial r:K) and aggregate microbial community properties (e.g., biomass, enzyme activities). Further, microbial community properties were among the strongest predictor variables for explaining variation in some ecosystem process rates. Interestingly, my results did not reveal strong alpha diversity – ecosystem function (i.e., BEF) relationships, but did show relationships between community composition and functions, which supports prior expectations (e.g., Bardgett and van der Putten 2014). My results also showed stronger community – function relationships for phylogenetically broad processes (i.e., C and N mineralization) vs. narrow processes (i.e., nitrification), which contrasts with prior expectations (Schimel 1995). Overall, this chapter shows that microbial community characteristics are key for understanding variation in ecosystem

process rates and identifies specific microbial properties important for modeling ecosystem responses to environmental change.

Chapter 5 used an intact soil core lab experiment to demonstrate that microbial community responses to drought differ between bacteria and fungi and also differ between historical land uses. Alpha diversity responded to drought-rewetting in both bacteria and fungi and the clear fungal diversity response challenges prior expectations that fungi will be drought-tolerant (e.g., Schimel et al. 2007). However, only bacterial communities exhibited detectable β-diversity responses to drought-rewetting. Further, bacterial communities from historically disturbed soils exhibited larger responses than communities from reference sites. Finally, specific bacterial functional groups exhibited drought-rewetting responses, particularly in disturbed soils, including negative responses of nitrifiers and positive responses of r-selected taxa. Overall, this chapter demonstrates that legacies of historical land use will also influence responses of soil communities to ongoing and future climate change. Further, the different responses of specific bacterial functional groups between land uses suggests that ecosystem responses to intensifying drought may also be influenced by historical land use.

Chapter 6 built upon the experiment performed for Chapter 5, demonstrating that soil respiration and N pools also exhibit clear responses to drought-rewetting, some of which were distinct between historical land uses. For example, more C was respired in total from soils exposed to drought-rewetting, which was driven by particularly large drought-rewetting responses in disturbed soils, which, in turn, may be attributed to the large positive response of r-selected bacteria observed in those soils. NO_3^- pools were smaller overall in soils exposed to drought-rewetting compared with control soils,

consistent with the negative drought-rewetting responses of nitrifiers observed in chapter 5. Total N pools, however, greatly increased in all drought-rewetting soils, likely due to widespread lysing of microbial cells as a result of the osmotic stresses of drying and wetting. Overall, this chapter demonstrates that soil ecosystem properties will likely exhibit different responses to climate change depending on past land use.

Future Directions

The work contained herein represents significant contributions to the ecological literature, adopting a microbial perspective to cast new light on biodiversity-ecosystem function relationships and disturbance ecology. This work also informs forest management, illustrating both long-term impacts of historical management on soil microorganisms as well as short-term effects of newer forest management practices currently being developed. However, several questions remain unanswered. For example, the qPCR and amplicon sequencing approaches used here to characterize microbial communities do not provide information on what portions of those communities are actually active. This could potentially be addressed by sequencing 16S rRNA itself, and if this were done across land uses and across seasons, greater insight into the spatial and temporal variability in active microbial communities would be gained. Metatranscriptomics and/or metaproteomics approaches could provide additional information on the active functions of those communities and may help to directly link variability in communities to variability in ecosystem processes.

More work also needs to be done on soil and microbial responses to drought, which would build upon my lab experiment. This could involve field experiments that employ gutter systems or rain-out shelters to simulate drought. In particular, it should be

noted that effects of drought and effects of land use are likely not actually independent factors in the way I treated them in my lab experiment. Specifically, many of the land use effects on microbial communities can be attributed to past and present vegetation differences between land uses, and intensifying drought will almost certainly influence those vegetation differences. For example, some studies predict that drought-tolerant tree species that such as oaks and hickories (currently characteristic of reference watersheds) will become increasingly abundant in the southern Appalachians as droughts increase in frequency. Other work suggests that continued fire suppression may promote mesic species such as red maple and tulip poplar that currently characterize disturbed forests (Abrams 1998). Therefore, a field drought experiment should also incorporate these future forest composition scenarios in addition to historical land use treatments. Nevertheless, characterization of microbial communities and the ecosystem functions they facilitate should remain a central focus of research in the southern Appalachian region. The forests of this region provide numerous services that support the ever-expanding human population of the southern US, which highlights the need to continually improve our understanding and management of these critically important ecosystems.

References

Abrams, M. D. 1998. The Red Maple Paradox. BioScience 48:355–364.

Allison, S. D., M. N. Weintraub, T. B. Gartner, and M. P. Waldrop. 2010. Evolutionary-Economic Principles as Regulators of Soil Enzyme Production and Ecosystem Function. Pages 229–243 Soil Enzymology. Springer, Berlin, Heidelberg.

Bardgett, R. D., and W. H. van der Putten. 2014. Belowground biodiversity and ecosystem functioning. Nature 515:505–511.

Cardenas, E., J. M. Kranabetter, G. Hope, K. R. Maas, S. Hallam, et al. 2015. Forest harvesting reduces the soil metagenomic potential for biomass decomposition. The ISME Journal 9:2465–2476.

Elliott, K. J., and C. F. Miniat. 2018. Herbaceous-layer diversity and tree seedling recruitment are enhanced following Rhododendron maximum shrub removal. Forest Ecology and Management 430:403–412.

Fierer, N., and R. B. Jackson. 2006. The diversity and biogeography of soil bacterial communities. Proceedings of the National Academy of Sciences of the United States of America 103:626–631.

Hermans, S. M., M. Taylor, G. Grelet, F. Curran-Cournane, H. L. Buckley, et al. 2020. From pine to pasture: land use history has long-term impacts on soil bacterial community composition and functional potential. FEMS Microbiology Ecology 96.

Jangid, K., M. A. Williams, A. J. Franzluebbers, T. M. Schmidt, D. C. Coleman, et al. 2011. Land-use history has a stronger impact on soil microbial community composition than aboveground vegetation and soil properties. Soil Biology and Biochemistry 43:2184–2193.

Keiser, A. D., J. D. Knoepp, and M. A. Bradford. 2016. Disturbance Decouples Biogeochemical Cycles Across Forests of the Southeastern US. Ecosystems 19:50–61.

Kohout, P., M. Charvátová, M. Štursová, T. Mašínová, M. Tomšovský, et al. 2018. Clearcutting alters decomposition processes and initiates complex restructuring of fungal communities in soil and tree roots. The ISME Journal 12:692–703.

Lauber, C. L., M. S. Strickland, M. A. Bradford, and N. Fierer. 2008. The influence of soil properties on the structure of bacterial and fungal communities across land-use types. Soil Biology and Biochemistry 40:2407–2415.

Mushinski, R. M., T. J. Gentry, and T. W. Boutton. 2018a. Organic matter removal associated with forest harvest leads to decade scale alterations in soil fungal communities and functional guilds. Soil Biology and Biochemistry.

Mushinski, R. M., Y. Zhou, T. J. Gentry, and T. W. Boutton. 2018b. Bacterial metataxonomic profile and putative functional behavior associated with C and N cycle processes remain altered for decades after forest harvest. Soil Biology and Biochemistry 119:184–193.

Rodrigues, J. L. M., V. H. Pellizari, R. Mueller, K. Baek, E. da C. Jesus, et al. 2013. Conversion of the Amazon rainforest to agriculture results in biotic homogenization of soil bacterial communities. Proceedings of the National Academy of Sciences 110:988–993.

Schimel, J. 1995. Ecosystem Consequences of Microbial Diversity and Community Structure. Pages 239–254 *in* F. S. Chapin and C. Körner, editors. Arctic and Alpine Biodiversity: Patterns, Causes and Ecosystem Consequences. Springer Berlin Heidelberg, Berlin, Heidelberg.

Schimel, J., T. C. Balser, and M. Wallenstein. 2007. Microbial stress-response physiology and its implications for ecosystem function. Ecology 88:1386–1394.

Webster, J. R., J. D. Knoepp, W. T. Swank, and C. F. Miniat. 2016. Evidence for a Regime Shift in Nitrogen Export from a Forested Watershed. Ecosystems 19:881–895.

Zhou, Z., C. Wang, and Y. Luo. 2018. Effects of forest degradation on microbial communities and soil carbon cycling: A global meta-analysis. Global Ecology and Biogeography 27:110–124.